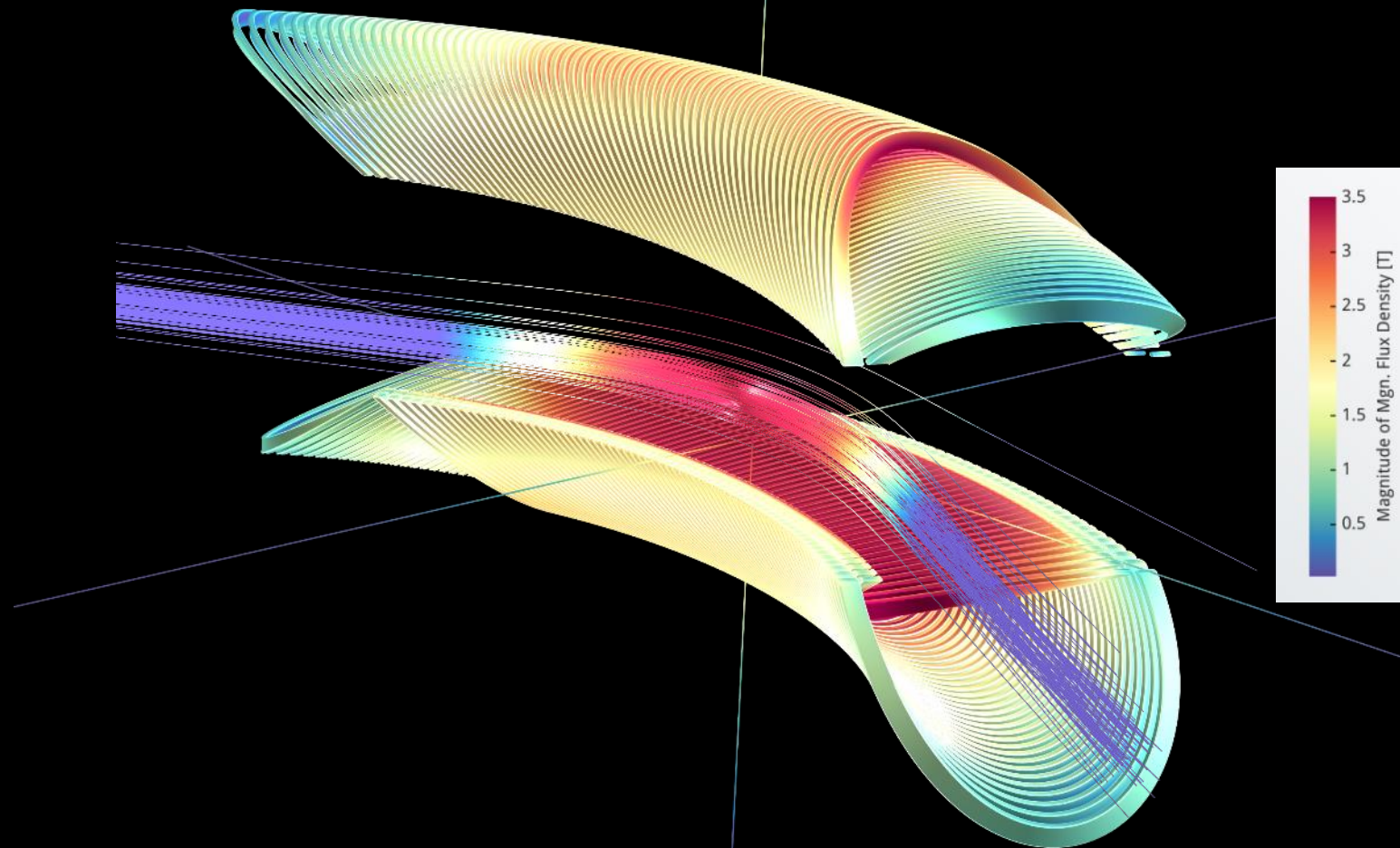


The State of The Art Canted Cosine Theta (CCT) magnets

Glyn Kirby

May 19th 2022



Beam tracking in curved CCT field on magnet coil and beam Rat output

Talk Overview

- CCT history
 - What are CCT's
 - Some of the magnets built and under construction.
 - A look at CCT designs features and idea's 2014 to today
-



1st CCT to go into LHC MCBRD CCT at CERN

HISTORY First CCT papers in the late 1960's

D. I. Meyer and R. Flasck, "A new configuration for a dipole magnet for use in high energy physics applications," Nucl. Instrum. Method, vol. 80, no. 2, pp. 339-341, Apr. 1970.

NUCLEAR INSTRUMENTS AND METHODS 80 (1970) 339-341; © NORTH-HOLLAND PUBLISHING CO.

A NEW CONFIGURATION FOR A DIPOLE MAGNET FOR USE IN HIGH ENERGY PHYSICS APPLICATIONS*

D. I. MEYER and R. FLASCK
Physics Department, University of Michigan, Ann Arbor, Michigan 48104, U.S.A.
Received 16 December 1969

The magnetic field configuration obtained when an ordinary circular solenoid is skewed looks very promising for use as a dipole magnet. The field inside is uniform and $\int B dl$ including end effect is independent of position across the magnet.

At the high fields now attainable with superconducting materials the support of the long narrow coils which are needed in bending magnets for high energies becomes a problem. In addition considerable rather difficult coil placement must be done to attain uniform fields. I suggest here a configuration which eliminates both of these problems.

Consider a long circular solenoid skewed at an angle θ as shown in fig. 1. On analysis of the field pattern it is found that the field inside such a configuration is completely uniform and makes an angle of $\theta/2$ with the z' axis. Details of this analysis are given in the appendix. The magnitude of the z' component of the magnetic field is the same as that of an unskewed solenoid with the same current and turn spacing in the z direction.

If we now send a beam of particles through along the skewed axis they will be bent perpendicular to the plane of the paper by the component B_y of the field. Thus the effective bending will be $B \sin \frac{1}{2} \theta$. We may however improve on this configuration by the method illustrated in fig. 2. Place two skewed solenoid windings on top of each other but skewed in opposite direction. Then by applying currents as shown the z' field components cancel but the x' components add. Thus we have ellipsoidal cross sections with a completely uniform field perpendicular to the axis in the x' direction.

Clearly since we are cancelling one field component there is some effective loss of ampere turns. Approximately twice as much wire is needed as in a standard cosine dipole for a given field. However for a superconducting magnet this is not too serious and is compensated for by four factors.

1. The field is completely uniform and the $\int B \cdot dl$ of lateral position.
2. The field volume is used very effectively. The aperture viewed along the beam line is elliptical with the long axis of the ellipse in the direction of bend. For 60° skew for example the aperture for 10 cm diameter rings would be 10 cm in the direction of bend and 5 cm perpendicular to this direction.
3. A uniform field of elliptic cross section can be generated by the proper distribution of current ($J \cos \varphi / a$) in wires run along the x' direction however the end effects are not so neatly handled.
4. The mechanical construction is much simplified over that of a cosine dipole from the standpoint of properly placing the wires. The circular coils and compact structure simplify the handling of magnetic stresses.

The configuration lends itself very well to being made in modules which can then be stacked end to end to provide any desired bending. This could add

Fig. 1. Diagram for calculating the magnetic field at the point x_0, y_0 .

Fig. 2. Two superimposed coils with opposite skew.

339

MEYER AND R. FLASCK

must equal the overshoot at A due to the solid coil. This same argument can be used for $x' = 0$ even for a single coil or for many coils of different radii. For $x' = 0$ the symmetry argument fails if the coils of different skew have different radii. However by alternating the skew of the coil layers the $\int B_y dz'$ is constant over the entire solenoid area to a very high order.

A model was made using 4 coils, the innermost being 10 cm in diameter. These were skewed at 70° angles on an elliptic tube. Field measurements show a field uniformity across the aperture (centered in the z' direction) better than 1%. (This was also verified the accuracy of the measurements.) They also verified the end effects which we calculated. No great care was taken in making a true ellipse was as large as 1 mm. deviation from a true ellipse was taken to accurately set skew angle of all coils the same. Thus as might be expected mechanical tolerances do not seem very critical.

Because of the uniformity of the field and of the end effects, magnets with this design should be valuable not only in beam lines but also as spectrometer magnets and in storage rings.

in analyzing the field of a skewed two coordinate systems as shown in fig. 1. We will use x, y, z for the unskewed system and x', y', z' for the skewed system. The angle between the z and z' axes is θ . Since the field inside the solenoid is uniform and makes an angle of $\theta/2$ with the z' axis, the field components are $B_x = B \sin \frac{1}{2} \theta$ and $B_z = B \cos \frac{1}{2} \theta$. The magnitude of the field is $B = \mu_0 J n \cos \frac{1}{2} \theta$.

One may still integrate over φ but now the elliptic integral expression no longer appears. The expression to be integrated is not a standard form that can be found in integral tables. A hint as to how φ proceed comes from the fact that we do not expect B_z to have a simple dependence outside the solenoid region. Note that the denominator becomes 0 for some value of φ when $(x^2 + y^2)/a^2 = 1$. A contour integral is indicated the solution to which is applicable only inside the solenoid. Therefore a substitute $\delta = \varphi - \theta$ in the expression for δB , above. The integral of φ from 0 to 2π then becomes an integral around a contour C of unit radius

$$B_z = \frac{\mu_0 J}{2\pi} \sin \theta \cos \theta \int_C \frac{a \cos \varphi (a \cos \varphi - x_0) d\varphi}{\cos^2 \theta (a \cos \varphi - x_0)^2 + (a \sin \varphi - y_0)^2}$$

This expression has simple poles within the contour at $\delta = 0$ and $\delta = \pi$ and

$$\delta = \frac{x_0 \cos \theta - i y_0 \sin \theta}{a} \pm \left(\frac{x_0 \cos \theta - i y_0 \sin \theta}{a} \right)^2 + \sin^2 \theta$$

The evaluation of the residues of these poles proceeds in a straightforward but tedious manner. Taking the sum of the residues gives

$$B_z = \mu_0 J \cos \theta \tan \frac{1}{2} \theta = \mu_0 J n \tan \frac{1}{2} \theta$$

Thus B_z is independent of position inside the solenoid and is equal to $B_z \tan \frac{1}{2} \theta$. A little trigonometry then shows that $B_x = B_z \cos \theta$, $B_y = B_z \sin \theta$.

The field in the solenoid is uniform and makes an angle of $\theta/2$ with the solenoid axis. A computer sum of the elliptic integrals of individual circular loops gives the same result. By the curl and divergence theorems $B_r = B_z = 0$.

Then replace the individual turns by an equivalent current per unit length $J = In$ and integrate over dz from $-\infty$ to $+\infty$. This integral when evaluated gives

Fig. 3. End effect of magnet on center line.

Fig. 4. Detail of overshoot in fig. 3 as a function of position inside coil.

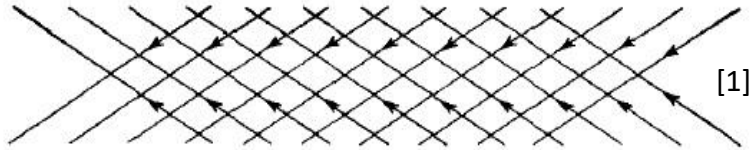
Fig. 5. The symmetry of two coils joined together.



1970, I was playing football

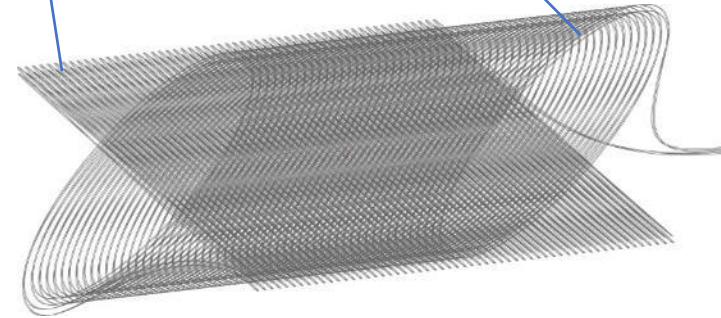
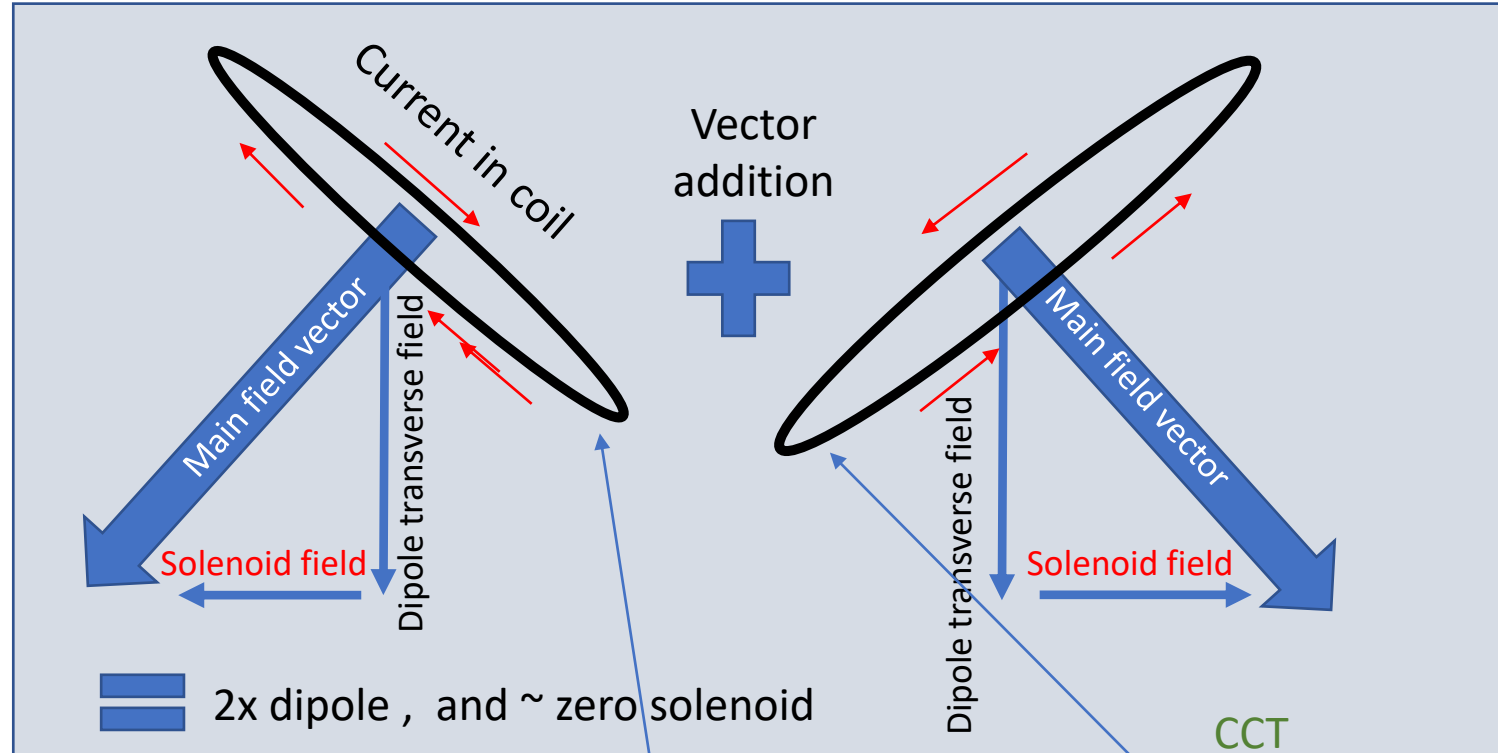
A bit of Background

- Idea originates from 1960's [1]
- Two nested canted solenoids



- Axial field components **cancel**
- Dipolar field components **add up**
- Visit Shlomo Caspi LBNL before Christmas
- Sparked renewed interest in CCT design

- Why now?
 - Advancements in Rapid Prototyping
 - Advancements in Computing



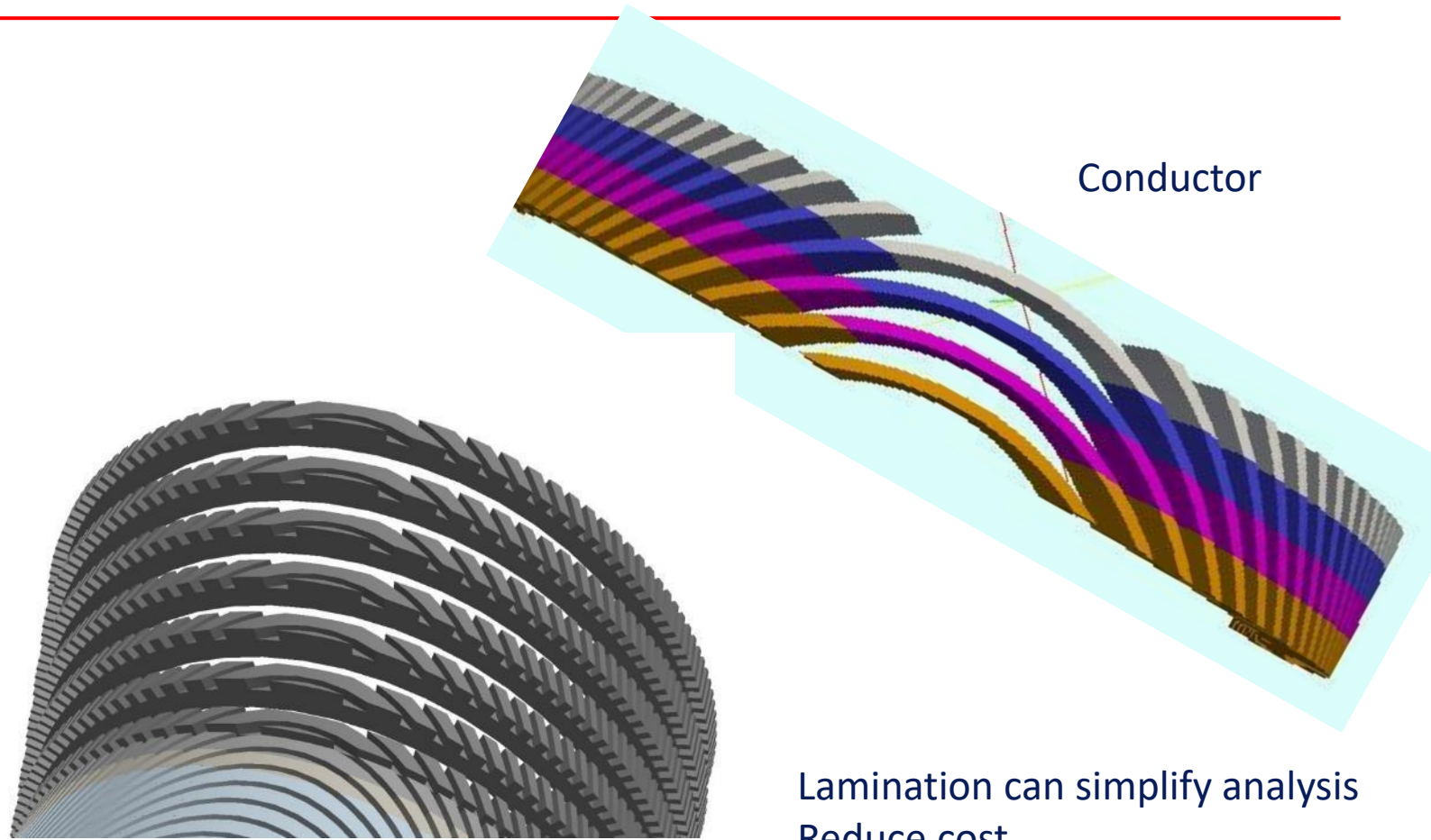
[1] D. Meyer and R. Flasck, A new configuration for a dipole magnet for use in high energy physics applications, Nuclear Instruments and Methods, no. 80, pp. 339-341, 1970.



Repeating geometry



Shlomo Caspi led the CCT program in LBNL and lit my interests in CCT's



Lamination can simplify analysis
Reduce cost
Reduce losses



2LPC-02

Compact Superconducting High Gradient Quadrupole Magnets for the Interaction Regions of High Luminosity Colliders

Filippo Bosi, Pasquale Fabbriatore, Stefania Farinon, Umberto Gambardella, Riccardo Musenich, Roberto Marabotto, Eugenio Paoloni

Abstract—Recent developments in the high luminosity e^+e^- colliders are based on a collision scheme with a large Piwinski angle, a vertical beta function β_y much smaller than the bunch length and a crab waist transformation. This scheme is being adopted in the SuperB asymmetric collider, to be built in Italy, with a design peak luminosity of 10^{36} cm⁻²sec⁻¹. A crucial role is played by the quadrupole doublets (QD/QF) which are placed close to the interaction point and generate gradients close to 100 T/m. The available space for the doublets is very small, causing the magnets to be operated with a high engineering current density (2000 A/cm²). Starting from the helical coil concept, an advanced design of the quadrupole has been developed. The paper discusses the basic design concepts and the development of a coil model aimed at assessing the design criteria and demonstrating the feasibility of the quadrupole. The successful test of the coil model opens the way to new compact superconducting high gradient quadrupole magnets for the interaction regions of high luminosity colliders.

Index Terms—Superconducting quadrupole, helical coils.

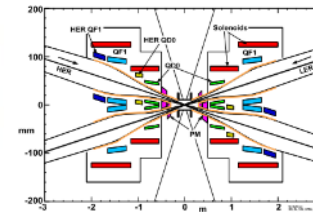


Fig. 1. Top view of the IR layout. The PM and the cold masses of the SC magnets are represented together with the horizontal LER and HER beam stay clear.

This article has been accepted for publication in a future issue of this journal, but has not been fully edited. Content may change prior to final publication.

1A0-1

Design, Construction and Test of a Model Superconducting Quadrupole for the Interaction Region of SuperB Factory

Filippo Bosi, Eugenio Paoloni, Pasquale Fabbriatore, Stefania Farinon, Riccardo Musenich, Roberto Marabotto, Davide Nardelli

Abstract—SuperB is an asymmetric energy e^+e^- collider operating at the $\Upsilon(4S)$ peak ($\sqrt{s} \sim 10.58$ GeV) to be built in Italy, with a design peak luminosity of 10^{36} Hz/cm². In order to get the required high luminosity, a novel collision scheme, the so called “large Piwinski angle and crab waist”, has been designed. This scheme requires that two doublets of high gradient superconducting quadrupoles (denominated in the SuperB naming scheme as QD and QF) are placed as close as possible to the interaction point. This layout is critical because the space allowed to the doublets is very small. An advanced design of the quadrupole has been developed, based on the so-called helical coil concept. The paper discusses the design and construction concept of a model of the superconducting quadrupole based on NbTi technology.

Index Terms—Helical coils, Superconducting coils, Quadru-

showed that it is reasonable to revise the *Snowmass Year* definition to $1.5 \cdot 10^{36}$ s.

II. THE COLLIDER AND ITS INTERACTION REGION (IR)

SuperB is designed as an High Energy Ring (HER) and a Low Energy Ring (LER) storing respectively positrons at 6.7 GeV and electrons at 4.18 GeV injected at nominal energy by a linac. The SuperB collision scheme requires a short focus final doublet to reduce the vertical beta function down to $\beta_y^* = 0.2$ mm at the Interaction Point (IP). The final doublet (see Fig. 1) will be composed by a set of permanent samarium cobalt magnets (PM) and superconducting (SC) quadrupoles.

IOP PUBLISHING
Supercond. Sci. Technol. 25 (2012) 065006 (10pp)

SUPERCONDUCTOR SCIENCE AND TECHNOLOGY
doi:10.1088/0951-2041/25/6/065006

Refined modeling of superconducting double helical coils using finite element analyses

S Farinon and P Fabbriatore

INFN Sezione di Genova, Via Dodecaneso, 33, 16146 Genova, Italy

E-mail: stefania.farinon@ge.infn.it

Received 24 January 2012, in final form 1 March 2012

Published 12 April 2012

Online at stacks.iop.org/SUST/25/065006

Abstract

Double helical coils are becoming more and more attractive for accelerator magnets and other applications. Conceptually, a sinusoidal modulation of the longitudinal position of the turns allows virtually any multipolar field to be produced and maximizes the effectiveness of the supplied ampere turns. Being intrinsically three-dimensional, the modeling of such structures is very complicated, and several approaches, with different degrees of complexity, can be used. In this paper we present various possibilities for solving the magnetostatic problem of a double helical coil, through both finite element analyses and direct integration of the Biot-Savart law, showing the limits and advantages of each solution and the corresponding information which can be derived.

(Some figures may appear in colour only in the online journal)

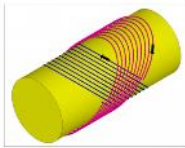


Figure 2. Two layers of the helical coil wound on a cylindrical mandrel with opposite tilt angles with respect to the central axis, showing the current flow directions.



fig. 1. Top: winding of a double helical coil for generating a quadrupole magnetic field. Bottom: a winding test with a dummy wire.

Supercond. Sci. Technol. 25 (2012) 065006

S Farinon and P Fabbriatore

References

- [1] Meinke R B, Ball M J and Goodzeit C L 2003 Superconducting double helix accelerator magnets *Proc. 2003 Particle Accelerator Conf. (Portland, OR, May 2003)* pp 1996–8 <http://accelconf.web.cern.ch/accelconf/p03/PAPERS/NIPAPERS/P03>
- [2] Goodzeit C L, Ball M J and Meinke R B 2003 The double-helix dipole—a novel approach to accelerator magnet design *IEEE Trans. Appl. Supercond.* **13** 1365–8
- [3] Meinke R B, Goodzeit C L and Ball M J 2003 Modulated double helix quadrupole magnets *IEEE Trans. Appl. Supercond.* **13** 1369–72
- [4] Goodzeit C, Meinke R and Ball M 2007 Combined function magnets using double helix coils *Proc. 2007 Particle Accelerator Conf. (Albuquerque, NM, June 2007)* pp 560–2 <http://accelconf.web.cern.ch/accelconf/p07/PAPERS/MOPAS055.PDF>
- [5] Meinke R B, Lammers J, Masson P J and Stelzer G 2009 Direct double-helix magnet technology *Proc. 2009 Particle Accelerator Conf. (Vancouver, May 2009)* pp 229–31 <http://accelconf.web.cern.ch/accelconf/p09/PAPERS/MOPAS055.PDF>
- [6] Paoloni E, Bertoni S, Biagini M E and Raimondi P 2009 Magnetic design studies for the final focus quadrupoles of the super B large crossing angle collision scheme *Proc. 2009 Particle Accelerator Conf. (Genoa, June 2009)* pp 2401–3 <http://accelconf.web.cern.ch/accelconf/p09/PAPERS/wcpd002.pdf>
- [7] ANSYS Multiphysics Release 11, ANSYS Inc.
- [8] Paoloni E, Bertoni S, Biagini M E, Raimondi P and Sullivan M 2009 Advances in the studies of the magnetic design for the final focus quadrupoles of the superB *Proc. 2009 Particle Accelerator Conf. (Vancouver, May 2009)* pp 238–40 <http://accelconf.web.cern.ch/accelconf/p09/PAPERS/wcpd004.pdf>
- [9] Paoloni E et al 2011 Advances in the design of the superB final doublets *Proc. 2011 Int. Particle Accelerator Conf. (New York, May 2011)* pp 2454–6 <http://accelconf.web.cern.ch/accelconf/p11/PAPERS/wcpd026.pdf>
- [10] Jain A K 1998 Basic theory of magnets *CERN Yellow Report* 98-05 <http://cdsweb.cern.ch/record/1246515/files/p1.pdf>

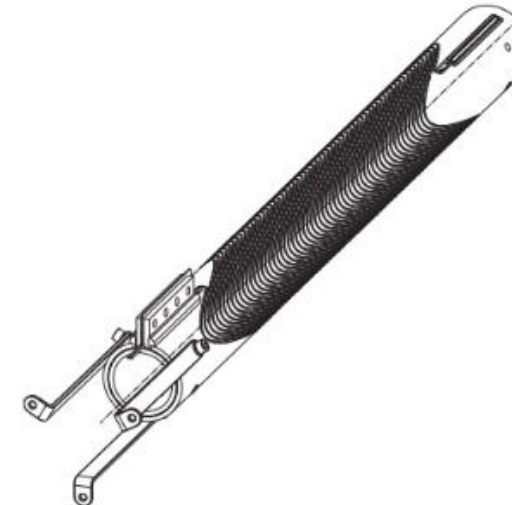
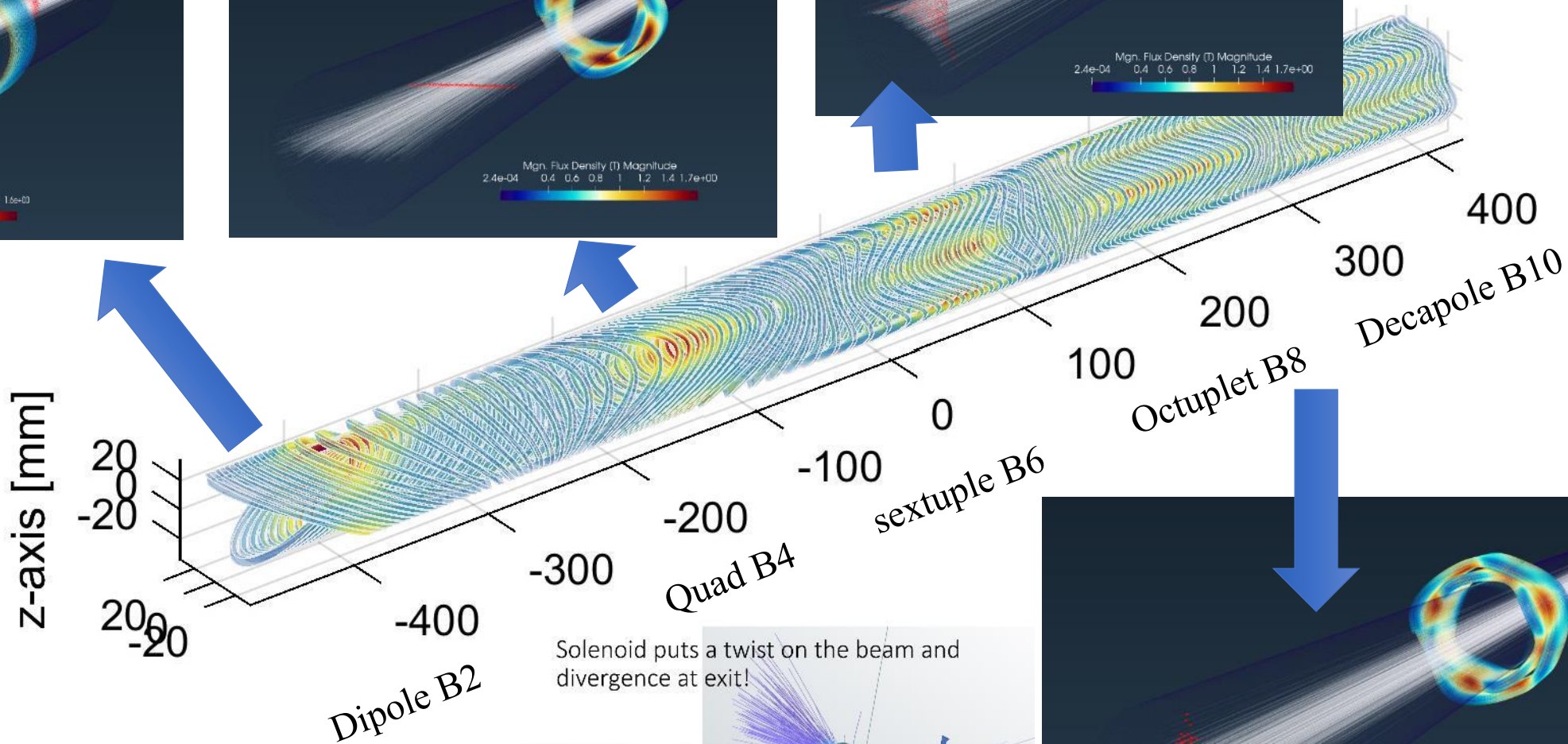
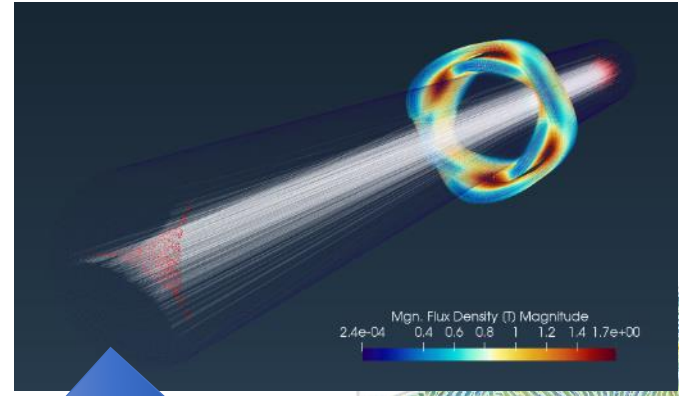
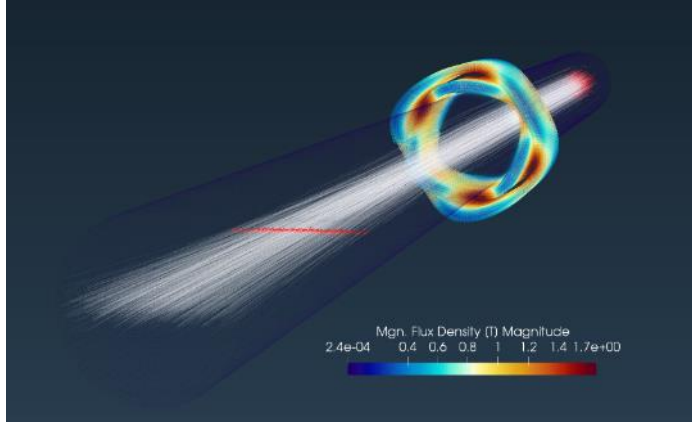
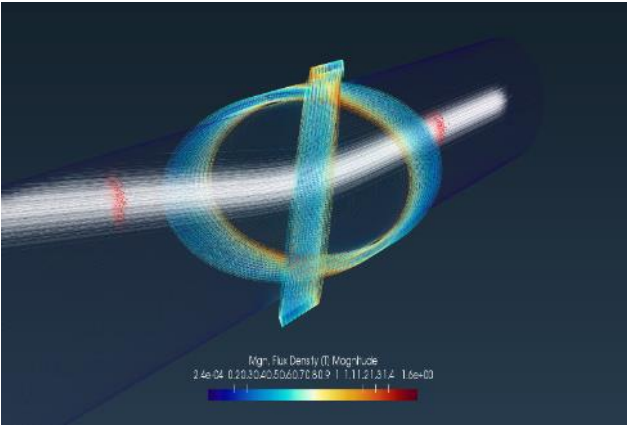
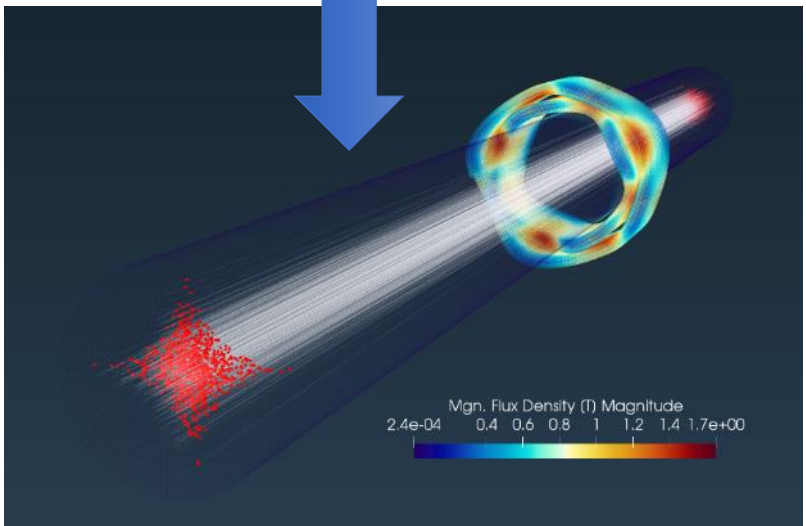
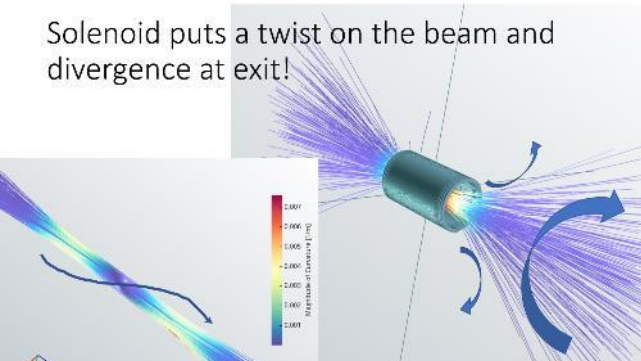


Fig. 3. Assembly view of the SC quadrupole prototype. The current feeders and the mechanical fixture are on the bottom left side and the junction is on the top right side.

CCT coil possibilities



Its even possible to combine the coil shapes to have multi function

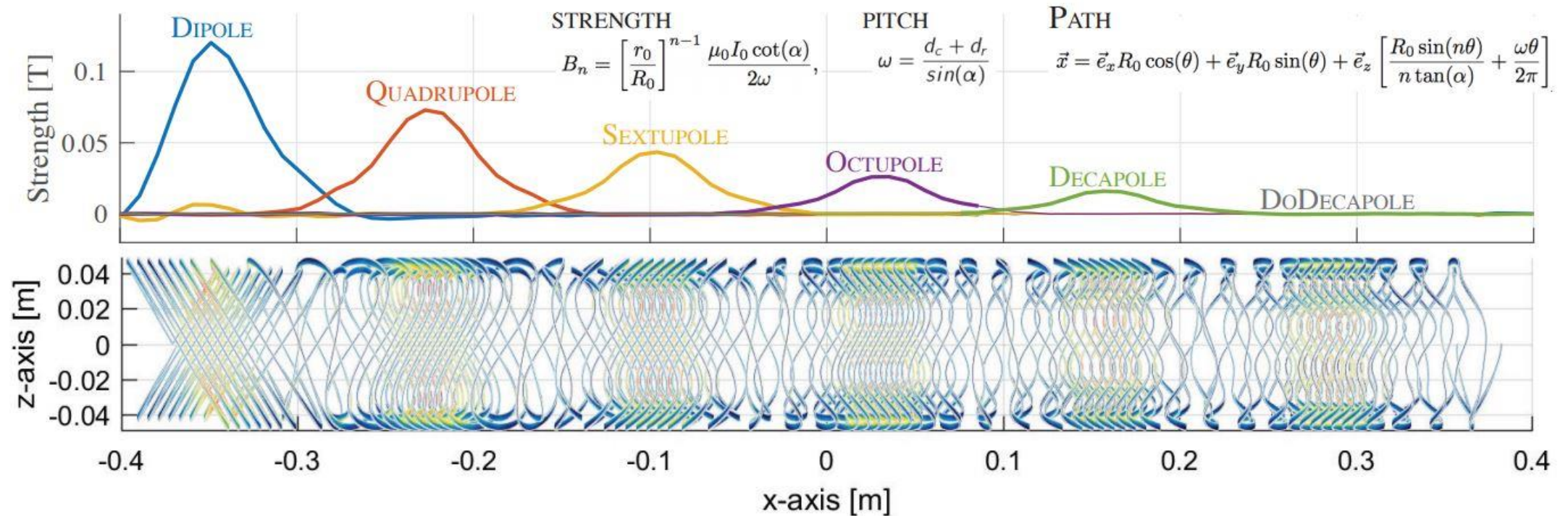
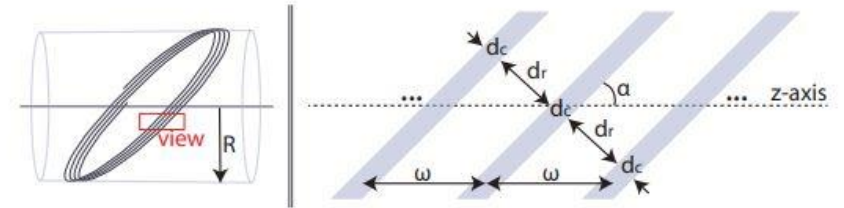


Thanks to JvN

A few CCT Harmonic Coil Layouts

II. CCT IS A UNIQUE MAGNET LAYOUT

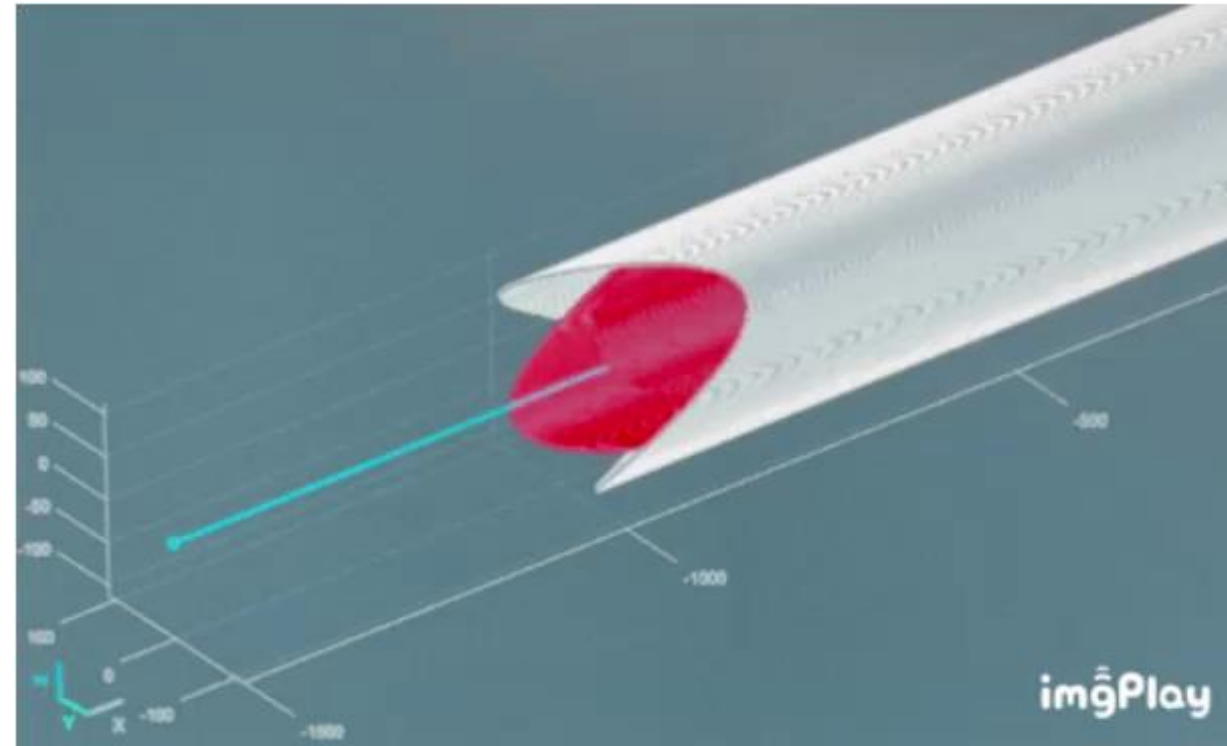
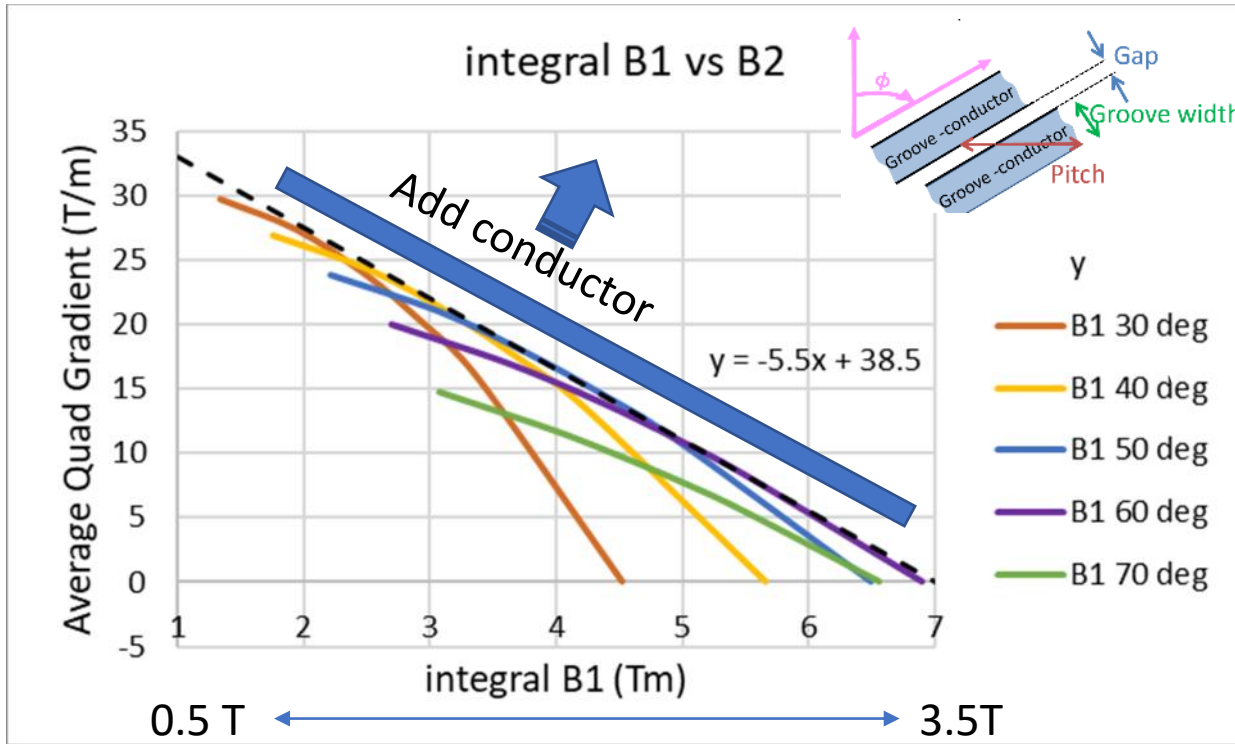
IT CAN GENERATE ANY REQUIRED HARMONIC AND ANY SUPERPOSITION OF MULTIPLE HARMONICS WITHOUT INTEGRATED FIELD ERRORS



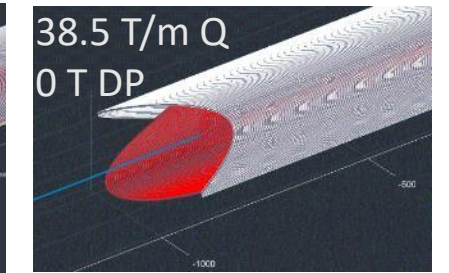
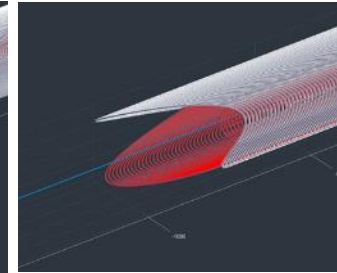
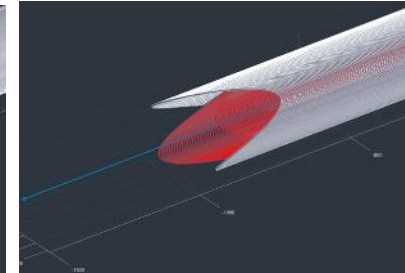
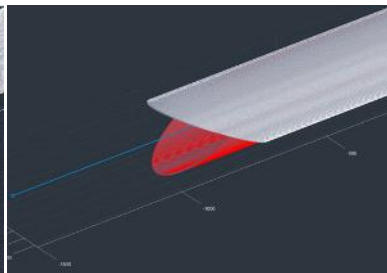
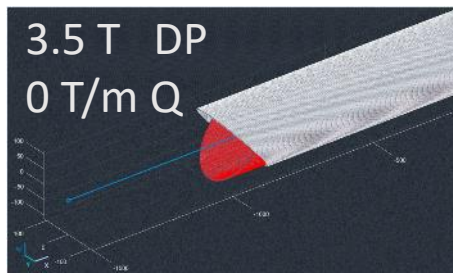
Morphing between Dipole and Quad Combined function strengths

Thanks to Mike K & JvN's & his Field program

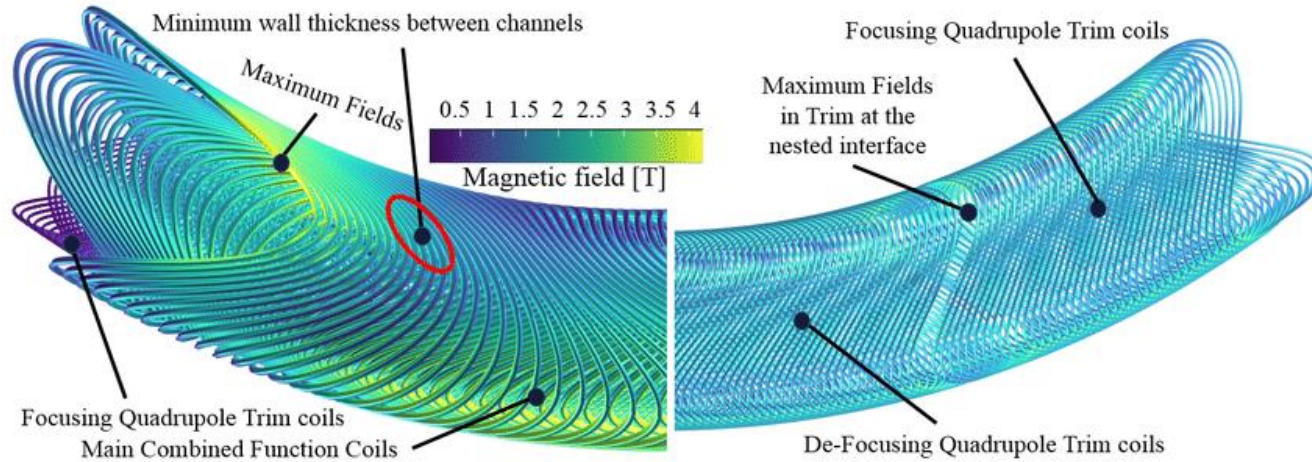
We can also set all the other harmonics if needed



200 mm aperture
2 m long
Two layers
2x10 mm channel
95 A/mm



Multi harmonic coil adds all functions together



Superconducting Curved Canted-Cosine-Theta (CCT) for the HIF-ISOLDE Recoil Separator Ring at CERN

Abstract

The ISOLDE facility at CERN delivers the largest range of low energy ion beams, produced by several distinct species. To investigate nuclear properties from the stable isotopes to the very most exotic close to the neutron or proton drip lines, these beams can reach kinetic energies of a few MeV. To produce such beams, one needs a special superconducting ISOL ring, the first superconducting beam-circulator (SBC) in the world. The ring will operate as an injection accelerator. Several alternative injection schemes are being studied. The field distribution of the SBC is being optimized. The field distribution of the SBC is being optimized. The field distribution of the SBC is being optimized.

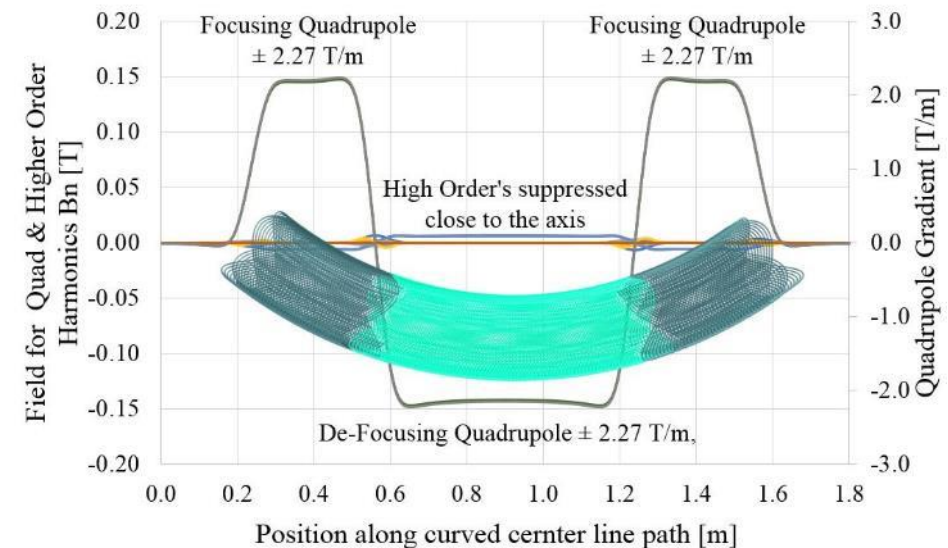
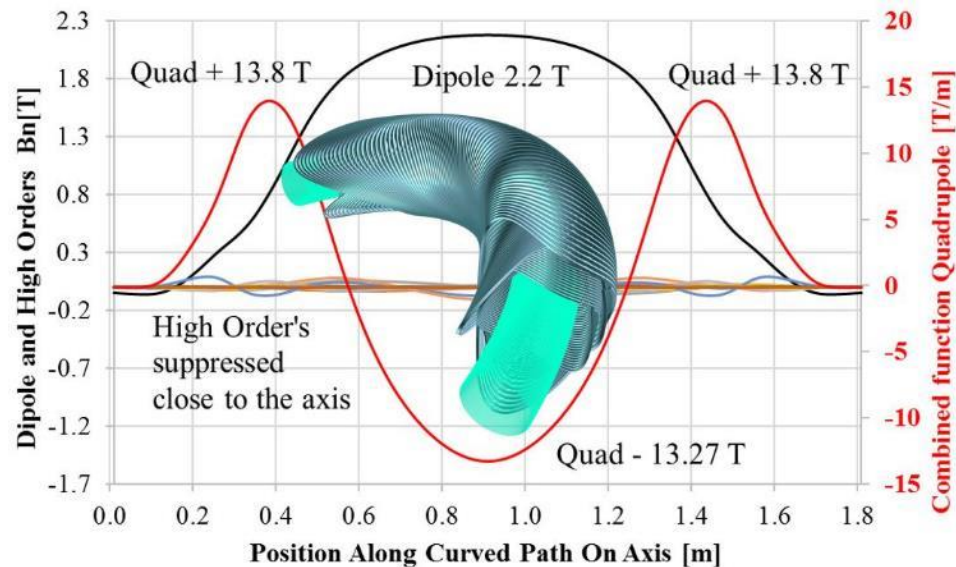
Parameter	Value
Ring radius	200 m
Ring length	1000 m
Ring circumference	6283 m
Ring cross-section	100 m x 100 m
Ring current	100 A
Ring energy	10 MeV
Ring magnetic field	10 T
Ring temperature	4.2 K
Ring material	Superconducting
Ring design	Superconducting
Ring construction	Superconducting
Ring operation	Superconducting
Ring maintenance	Superconducting
Ring safety	Superconducting
Ring cost	Superconducting
Ring schedule	Superconducting
Ring status	Superconducting

HIF-ISOLDE Ring curved CCT conceptual design development.

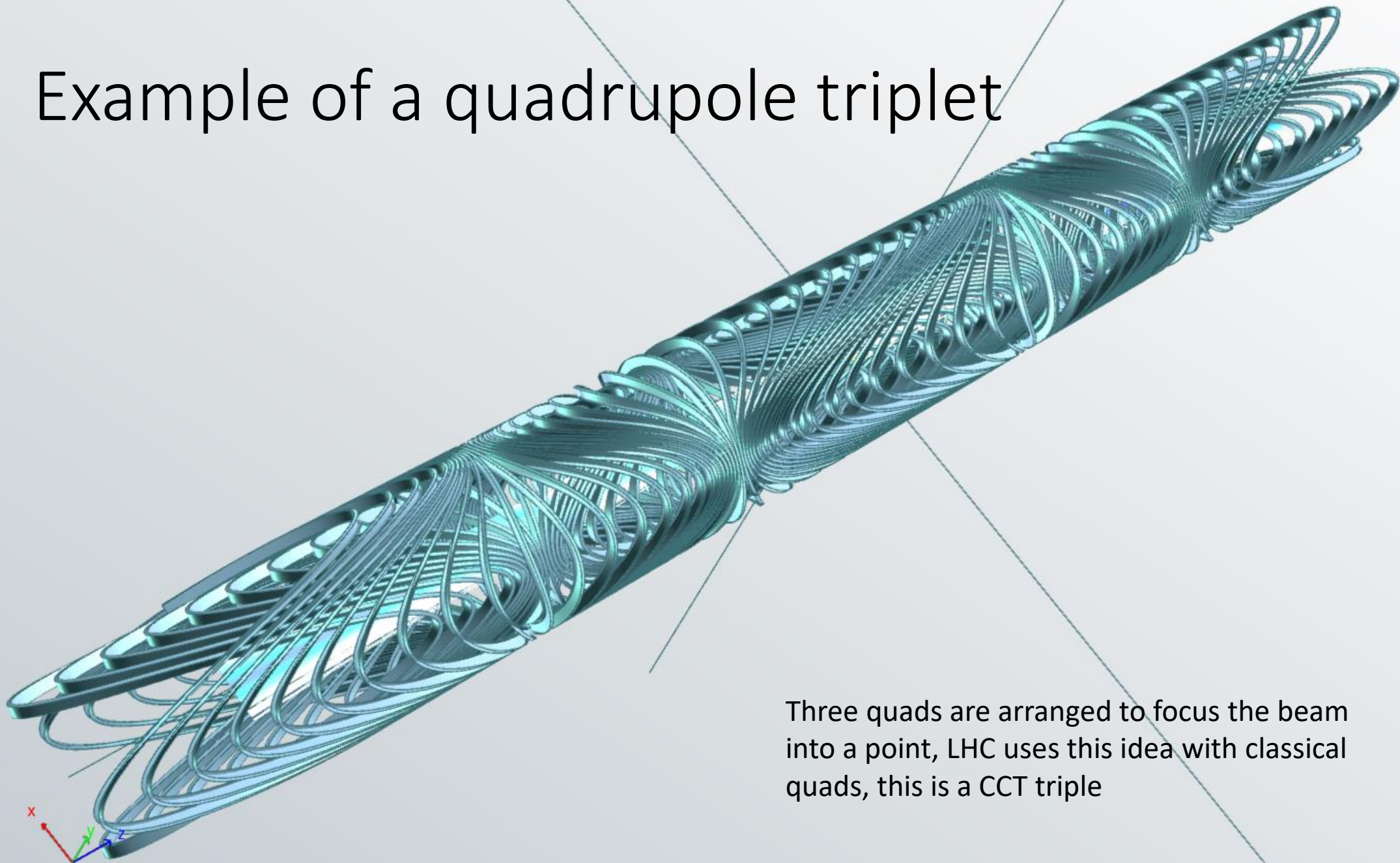
Active dry field shimming

High Order's suppressed close to the axis

Quadrupole Gradient [T/m]



Example of a quadrupole triplet



Three quads are arranged to focus the beam into a point, LHC uses this idea with classical quads, this is a CCT triple

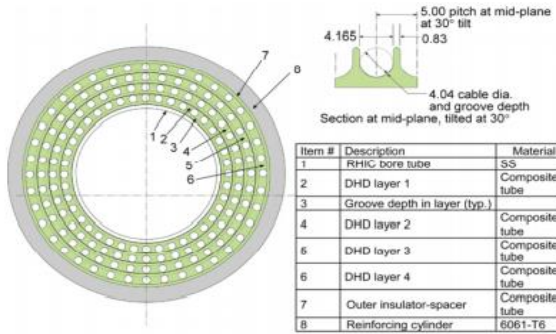
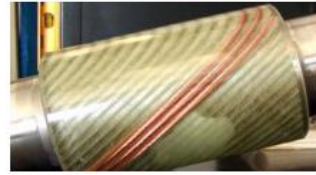


Figure 5: A few turns of epoxy impregnated coil, with a Lexan cover, show typical turn geometry. Insulation is provided by the web of the coil support grooves and the epoxy impregnation.



SUPERCONDUCTING DOUBLE-HELIX ACCELERATOR MAGNETS*

R. B. Meinke², M. J. Ball, C. L. Goodzeit, Advanced Magnet Laboratory, Palm Bay, FL, USA

Abstract

We describe an important contribution to accelerator magnet technology based on the concept of modulating the helical turns of solenoid coils to produce pure multipole fields of any order. Calculations show that these configurations inherently produce virtually error free fields of the desired multipole order in a large fraction of the aperture in the two dimensional cross section without the presence of iron. The characteristics of one such configuration, the double-helix dipole (DHD), are described. It is also explained how the novel geometry of the double-helix coils simplifies the manufacturing, eliminates complex coil parts, and thus significantly reduces the cost of the magnets in comparison to the conventional cosine theta (racetrack design) coils. This has been demonstrated by the design and construction of a prototype dipole that produces a 4T field in an 80 mm aperture (without iron).

modulating the conductor path at 2 frequencies. For example, $z = h + A_0 (\sin\theta + 0.01 \sin 3\theta)$ will produce a dipole with a small amount of sextupole.

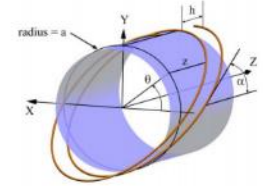


Figure 1: For the case of the dipole, the z coordinate of the conductor path is given by $z = h + A_0 \sin\theta$ with $A_0 = a / \tan\alpha$, where a is the radius of the coil aperture, α is the tilt angle of the winding with respect to the horizontal axis, and h is the helical advance per turn.

FOREWORD

The double helix coil configuration represents a significant advance in accelerator magnet technology over the conventional cosine theta type (racetrack design) coils. The performance of virtually any type of accelerator magnet is improved while the cost of manufacture is substantially reduced with this magnet configuration.

The double-helix dipole and higher multipole magnets have been previously described [1,2,3]. They achieve pure multipole fields by the sinusoidal modulation of the axial position of the turns of a solenoid wound coil. For example, in the case of the dipole, the axial position of the conductor path is described as shown in Figure 1 and Figure 2 shows a 2-layer double helix dipole magnet (DHD).

Each turn of the coil can be well approximated as an ellipse tilted at an angle α with respect to the axis of the coil. This produces a transverse field component superimposed on a solenoid field component. When pairs

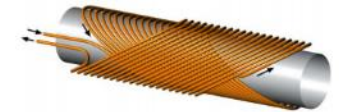


Figure 2: Double helix dipole (DHD) concept uses pairs of layers with opposite tilt and current direction. Aperture may be circular or elliptical. High field values can be obtained by using multiple pairs of layers with the transition between layers as shown.

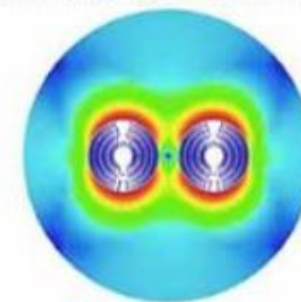
USA company specializing in CCT's
 AMLSuperconductivity.com



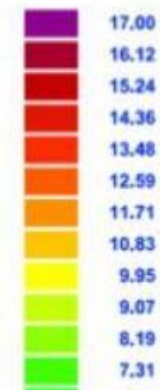
Nb3Sn dipole development at PSI

Bernhard Auchmann & team at (PSI)

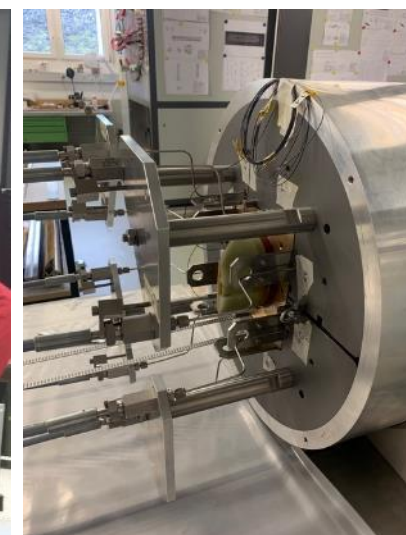
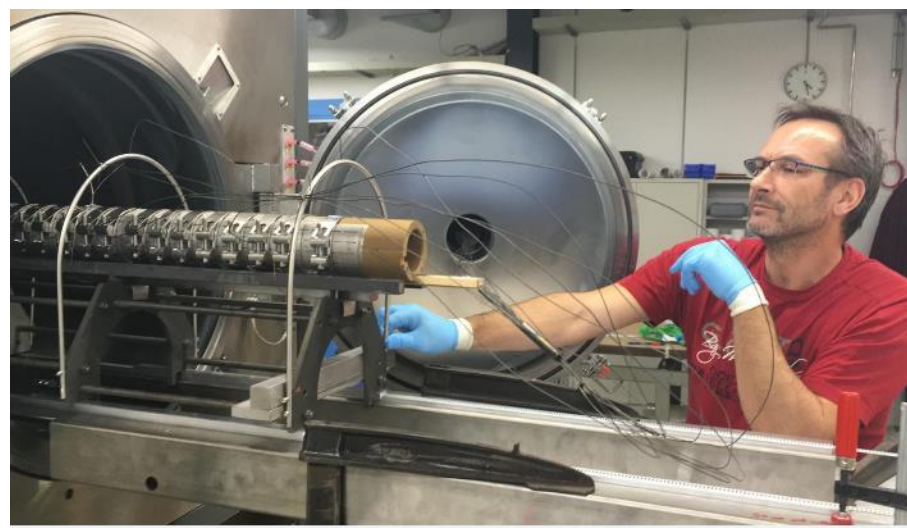
Canted Cosine Theta



|B| flux density (T)

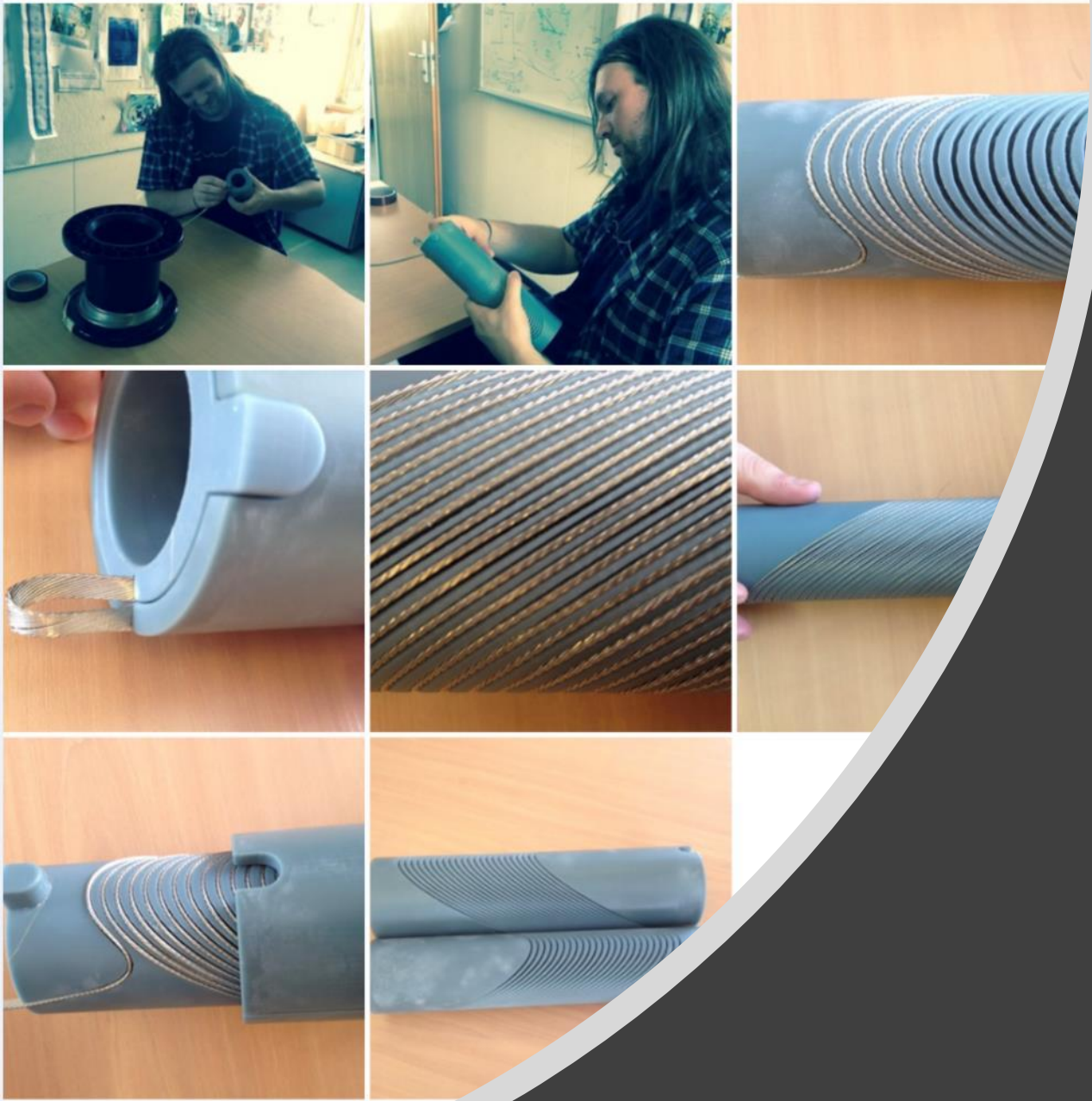


Test halted due to liquefier problem at LBNL ! So far One quench, at 62% SS, 11 KA, ~6T.....




Large Hadron Collider

18 Sep 2014 · Large Hadron Collider



Our first CCT dipole 2014.

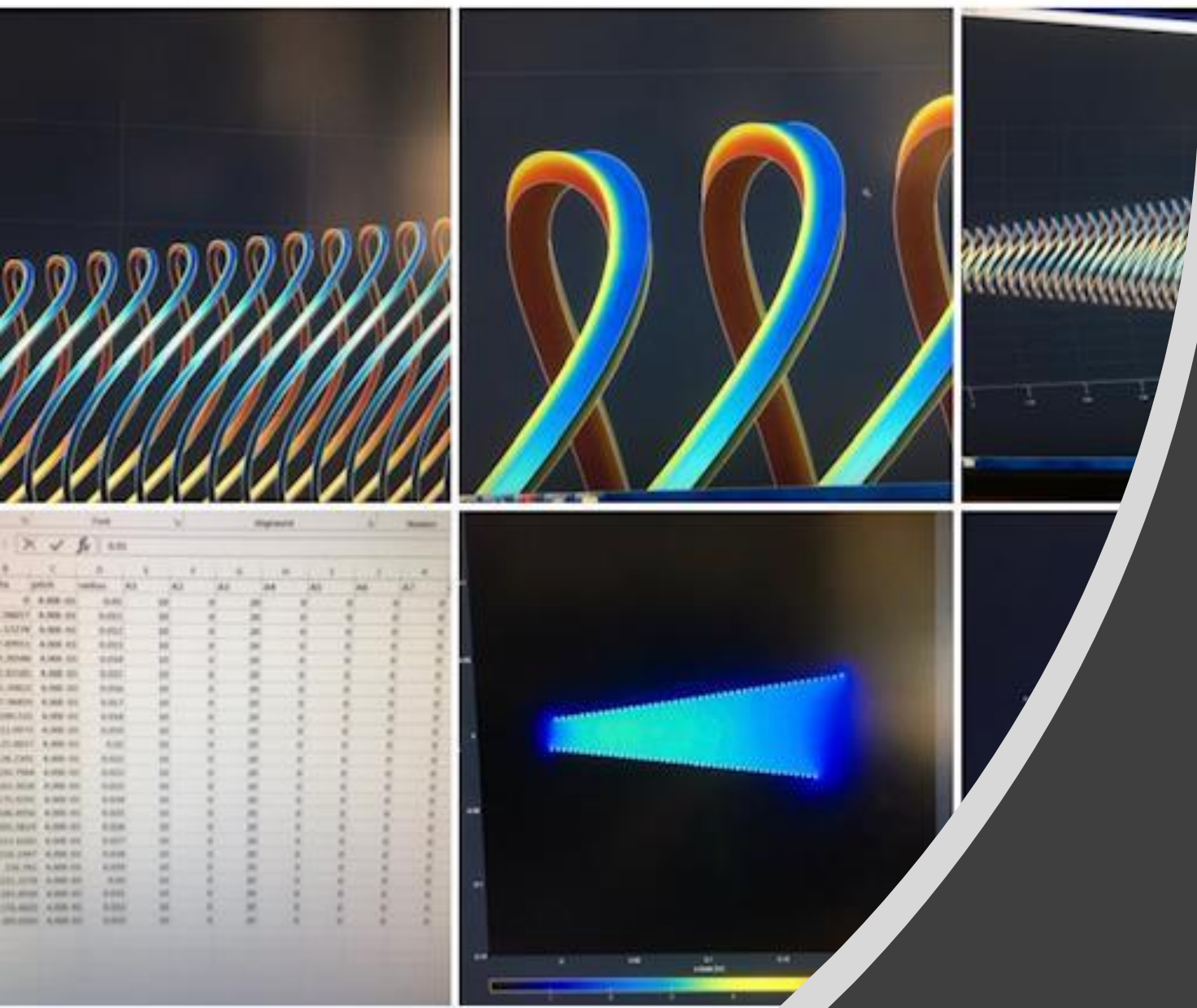
Built in my office.
Sadly, we never tested it.



One of the first ideas wind on inside and outside of former.

Large Hadron Collider

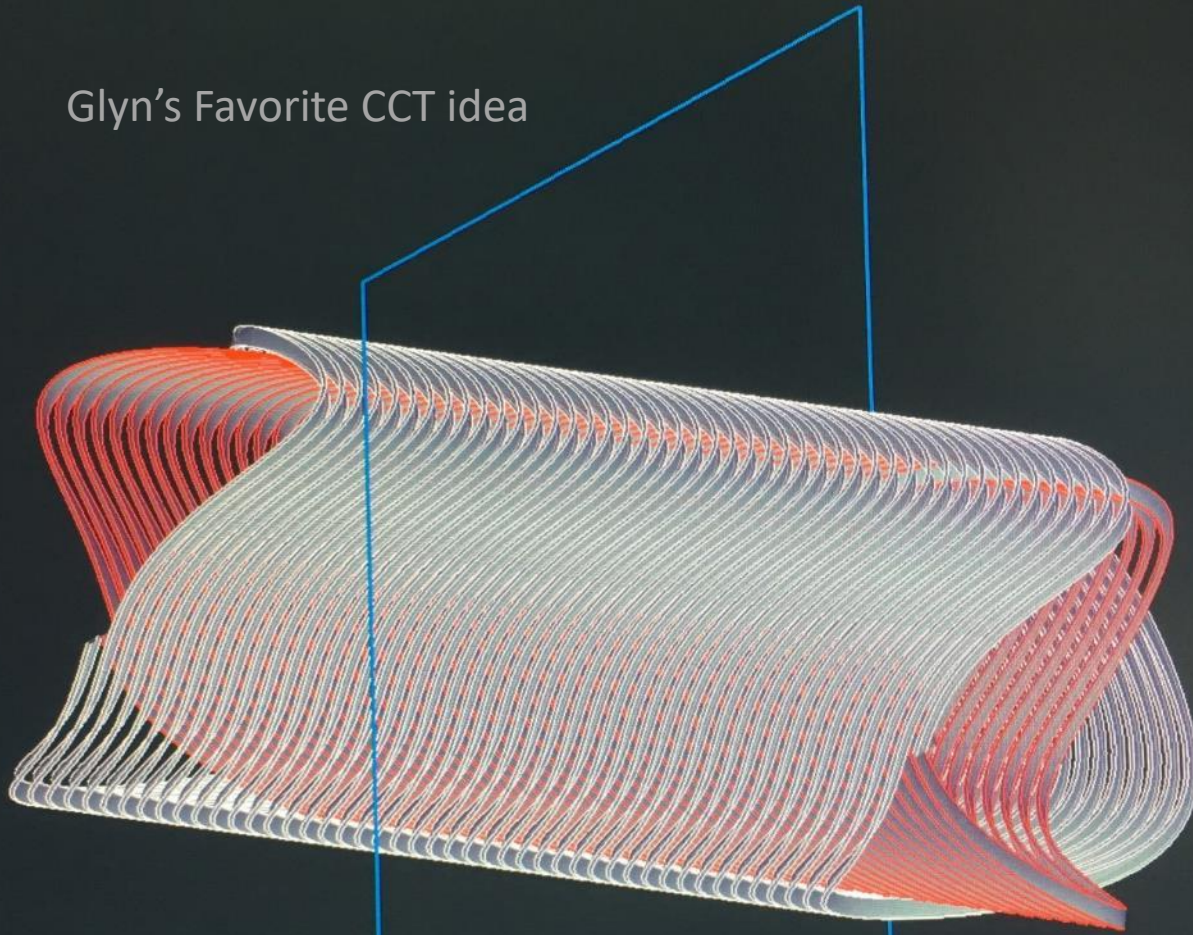
15 Mar 2017 · Large Hadron Collider



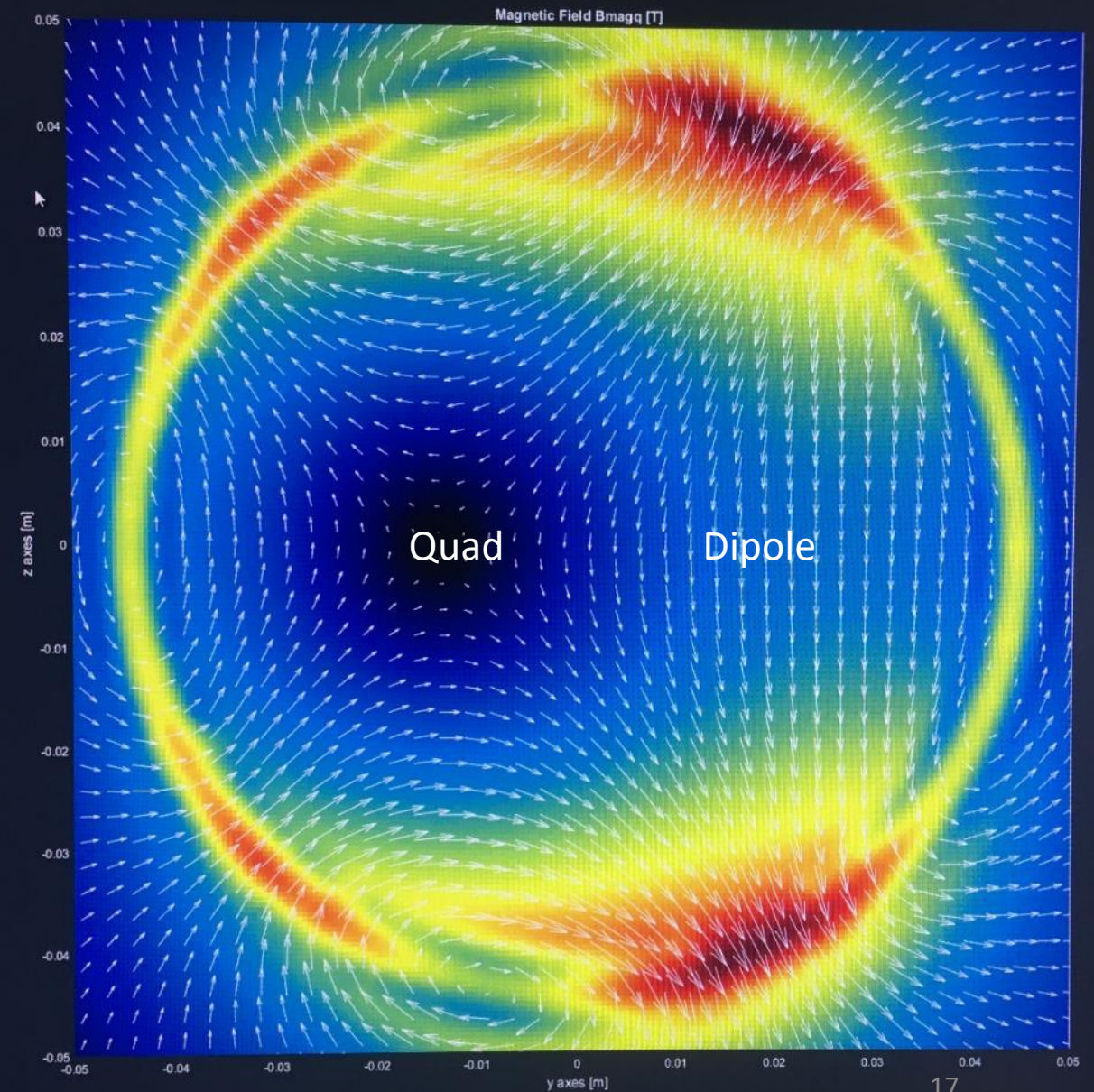
JvN's field program advances Cone Quad

Flexibility of CCT designs combined function off axis

Glyn's Favorite CCT idea

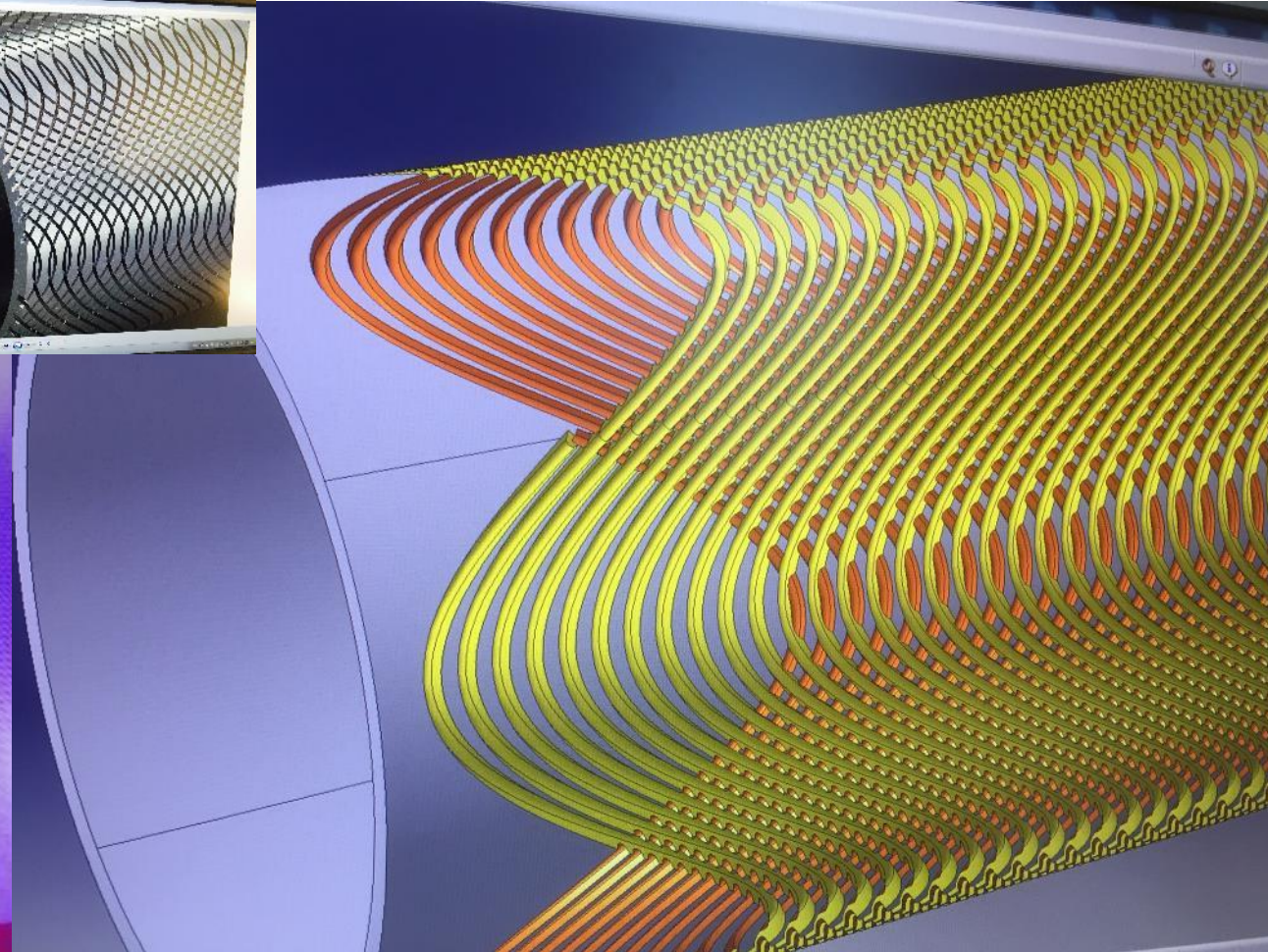
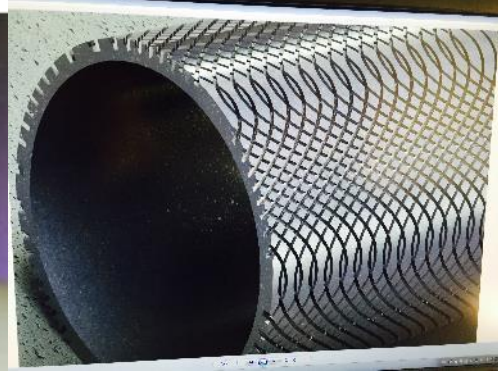
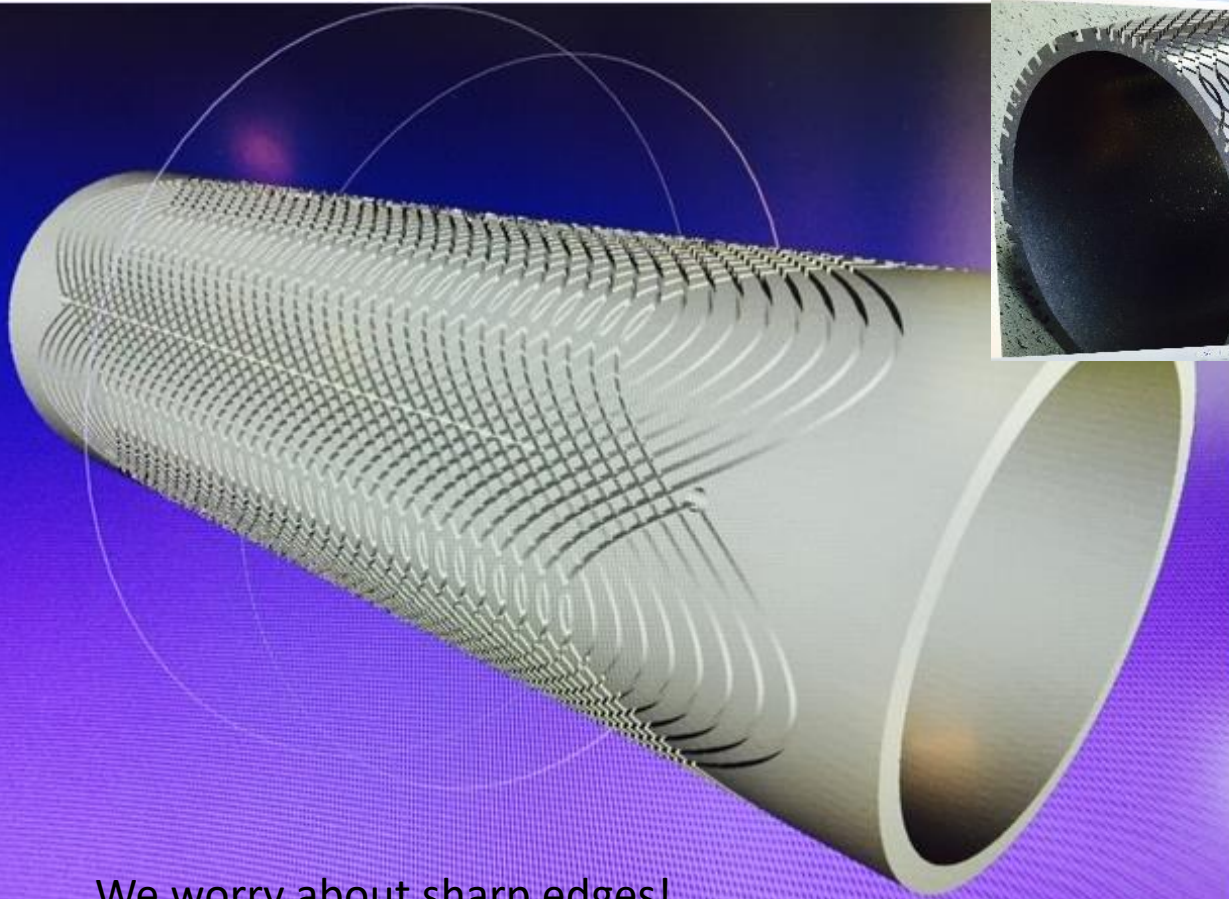


Courtesy of JvN



Former ideas

two layers wound onto a single tube
two channel depths in the single tube



We worry about sharp edges!

Possible PhD idea

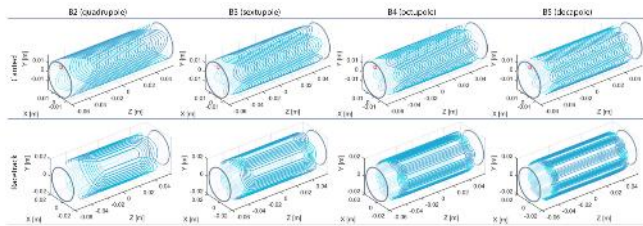
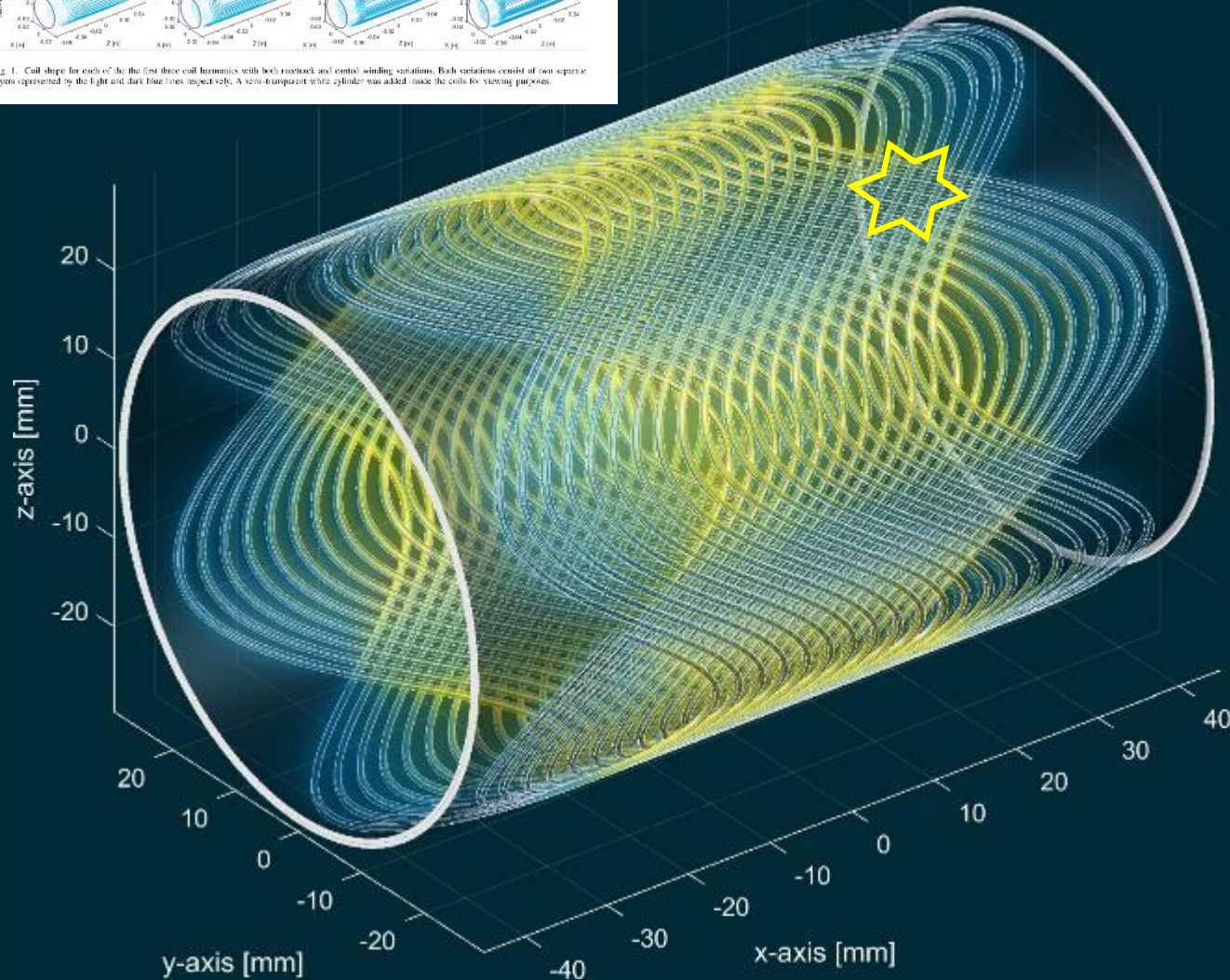


Fig. 1. Coil shape for each of the first three coil harmonics with both track and control winding variations. Both variations consist of two separate layers represented by the light and dark blue lines respectively. A zero-invariant white cylinder was added inside the coils for viewing purposes.



One more technology that
may prove to be necessary for
HTS

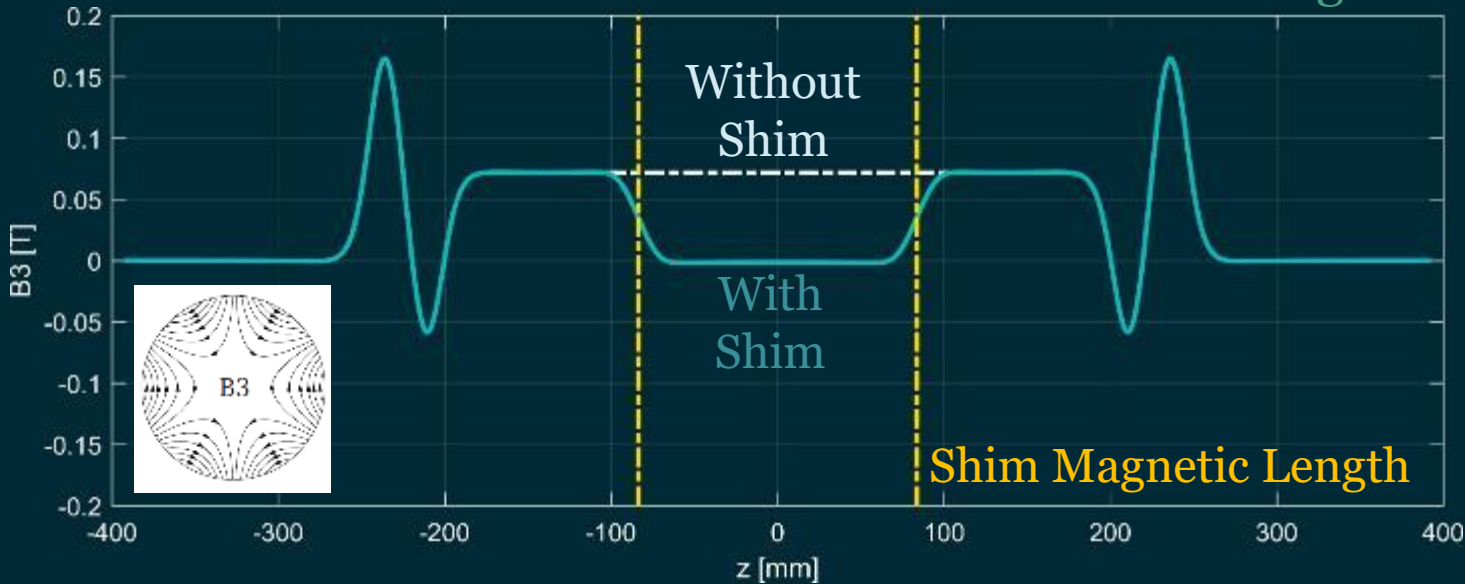
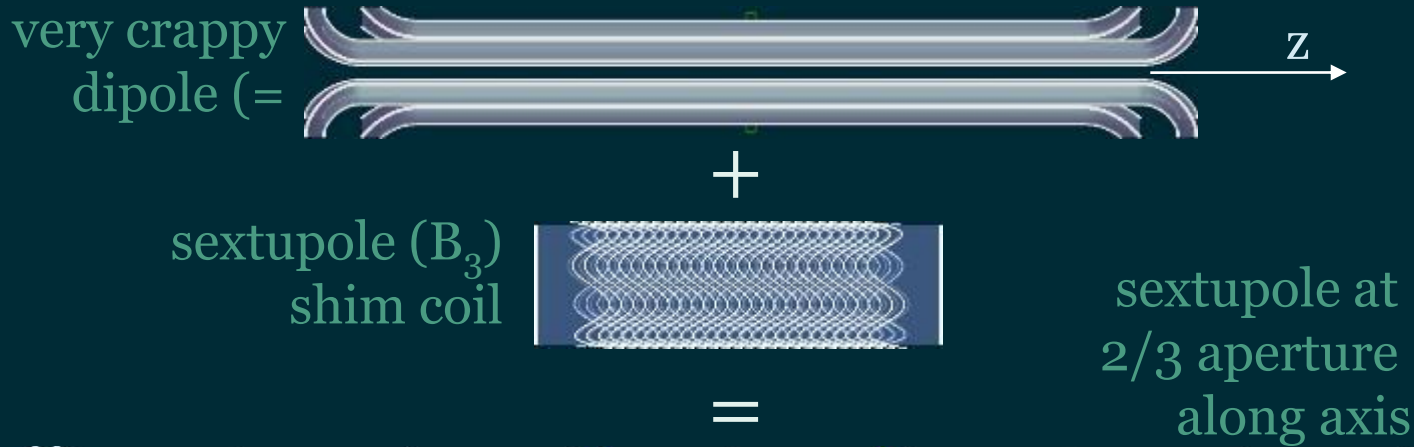
Persistent Current Shim Coils for Accelerator Magnets

-The Magic Magnet-

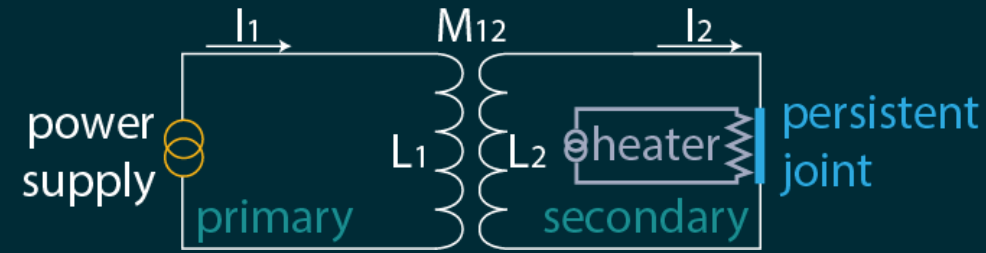
- [1] J. van Nugteren et. Al. "Persistent Current Shim Coils for Accelerator Magnets", *Technical Report, CERN, 2016*
- [2] J. van Nugteren, "High Temperature Superconductor Accelerator Magnets", *PhD Thesis, University of Twente, 2016*
- [3] A. Dael et. Al., "Auto Correction des Harmoniques du champ Magnetique d'un multipole pulse par enroulements supraconducteurs," *Particle Accelerators, vol. 4, pp. 145-150, 1973, in French.*

Shim Coil Numerical Analysis

- Shim corrects its integrated harmonic exactly over its **magnetic length**, local errors remain.
- Here is demonstrated on static field, but concept also works for dynamic

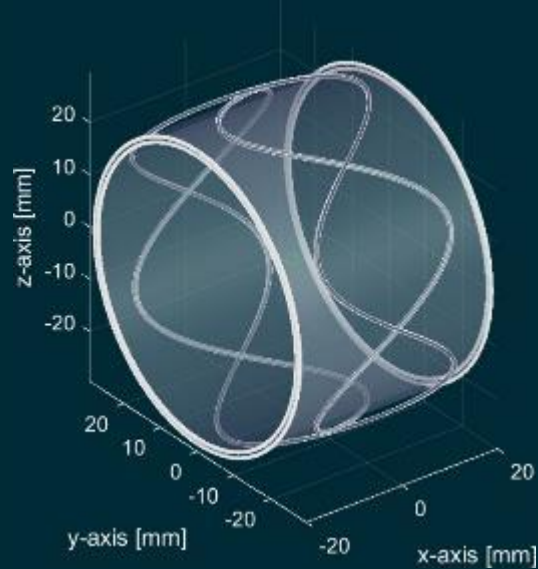


- The current in the shim can be calculated using the mutual inductance matrix of the system (as a transformer)



$$\frac{I_2}{dt} = \frac{M_{12}}{L_2} \frac{I_1}{dt}$$

- Where M_{12} and L_2 are calculated using *Field 2017* code



- A repeated pattern of single lanes also works due to mutual coupling
- Layers are not electrically connected
- Vapour deposition ReBCO on tube?



DESIGN STUDY OF A NOVEL AIR-COIL CCT HIGH-LUMI ORBIT CORRECTOR

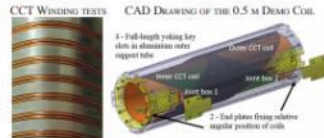
Magnet Technology Conference, Amsterdam, 2017

J. van Nugteren, G. Kirby, G. de Rijk,

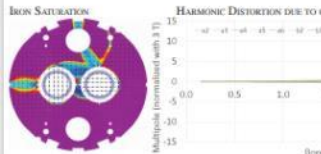


I. INTRODUCTION TO THE D1 ORBITAL CORRECTOR PROBLEM

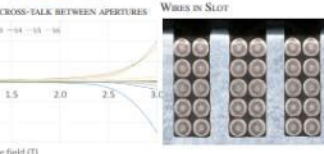
The D1 is an orbital corrector required for the High Luminosity Upgrade of the LHC at CERN. Required is a 5 Tm dipole field integral with less than 10 units field error and an operating current less than 600 A. The CCT allows winding of single wires in the slots making the operating current possible. Aperture separation distance is fixed at 188 mm. The magnetic field is limited at 2.6T by the saturation of the iron. This results in a design which is 2.2 m long. Space is limited and a much shorter magnet option would be preferable.



IRON SATURATION

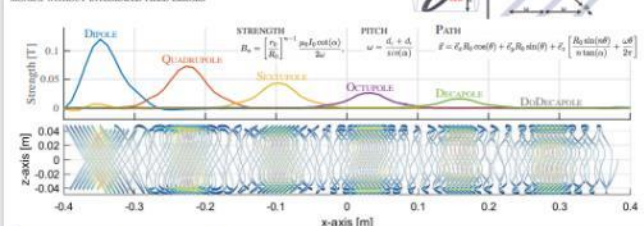


WIRES IN SLOT



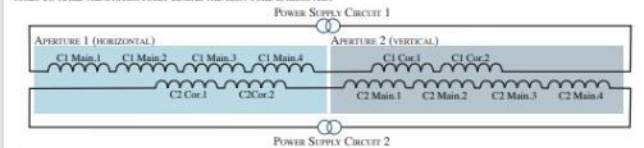
II. CCT IS A UNIQUE MAGNET LAYOUT

IT CAN GENERATE ANY REQUIRED HARMONIC AND ANY SUPERPOSITION OF MULTIPLE HARMONICS WITHOUT INTEGRATED FIELD ERRORS



III. PROPOSED SOLUTION AND APPROACH

The coil is made as short as possible by increasing the number of layers from 2 to 4 (skew angle increased to 40 deg). The magnetic field is increased to 4 T resulting in a coil length of approximately 1.4m. To avoid cross-talk between the coils 2 additional correction coil layers are added. These correction coils are connected in series with the main coil of the other aperture. To make the system fully linear the iron yoke is removed.



IV. THE SKEW ANGLES OF EACH HARMONIC IN ALL COILS NEED TO BE SOLVED

THE SOLUTION IS FOUND SEPARATELY FOR EACH CIRCUIT

- Circuit 1 (generates horizontal field in aperture 1)**
- VARIABLES** - The skew angles of the main and correction coils except for the main harmonic A1, which is fixed at 40 deg, resulting in 39 variables total.
 - TARGETS** - Minimization of the integrated harmonics A2 to A10 and B1 to B10 in aperture 1 (19 targets), as well as the integrated harmonics A1 to A10 and B1 to B10 in aperture 2 (20 targets). Resulting in a total of 39 targets.
- Circuit 2 (generates vertical field in aperture 2)**
- VARIABLES** - The skew angles of the main and correction coils except for the main harmonic B1, which is fixed at 40 deg, resulting in 39 variables total.
 - TARGETS** - Minimization of the integrated harmonics A1 to A10 and B1 to B10 in aperture 1 (20 targets), as well as the integrated harmonics A1 to A10 and B2 to B10 in aperture 2 (19 targets). Resulting in a total of 39 targets.

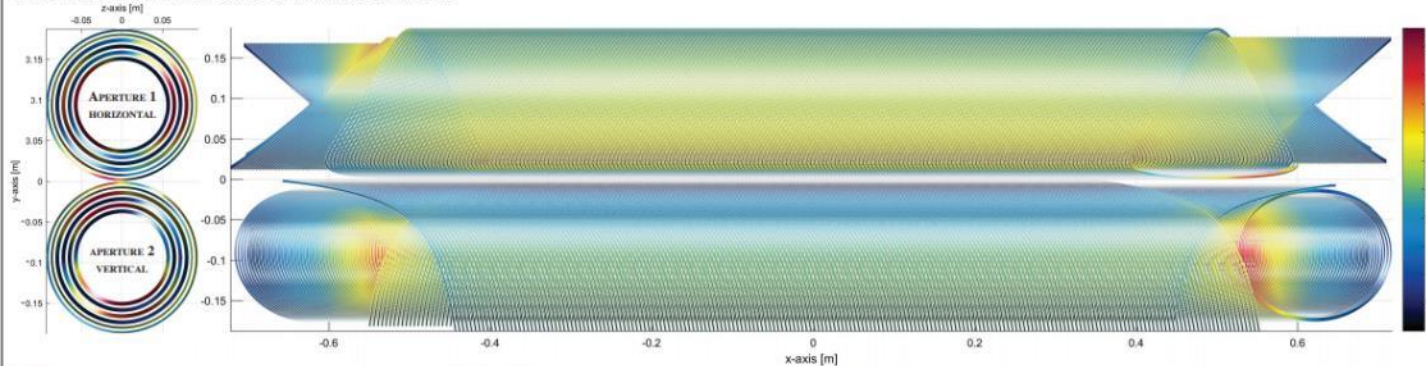
TABLE I
THE SOLVED SKEW ANGLES USED FOR THE DESIGN OF THE CCT MAGNET.

Coil	Aperture	unit	A1	A2	A3	A4	A5	A6	A7	A8	A9	A10
main C1	1 (horz)	[deg]	+40.0	+3.27	+2.25	+1.35	+0.75	+0.39	+0.20	+0.097	+0.05	+0.03
	corrector C1	2 (vert)	+40.8	+0.00	-31.3	+0.00	+13.4	-0.00	-4.55	-0.00	+1.43	+0.02
main C2	2 (vert)	[deg]	+40.0	-3.33	+0.00	+1.35	+0.00	-0.39	+0.00	+0.09	+0.00	-0.02
	corrector C2	1 (horz)	+40.0	+0.00	+0.00	+0.00	-0.00	-0.00	+0.00	+0.01	+0.03	-0.02

Coil	Aperture	unit	B1	B2	B3	B4	B5	B6	B7	B8	B9	B10
main C1	1 (horz)	[deg]	+40.0	+0.00	+0.00	+0.00	+0.00	+0.00	+0.00	+0.00	+0.00	-0.00
	corrector C1	2 (vert)	+40.0	+0.00	-21.4	+0.00	+7.93	-0.00	-2.56	-0.01	+0.79	-0.00
main C2	2 (vert)	[deg]	+40.0	+0.00	-2.36	+0.00	+0.75	+0.00	-0.19	+0.00	+0.04	-0.00
	corrector C2	1 (horz)	+44.3	+40.1	+31.3	+21.4	+13.40	+7.93	+4.55	+2.55	+1.42	+0.81

* VARIABLES CIRCUIT 1 OPTIMISATION * VARIABLES CIRCUIT 2 OPTIMISATION

THE OPTIMIZED COIL GEOMETRY WITH MAGNETIC FIELD SHOWN ON THE SURFACE OF THE CONDUCTOR



V. THE DISTORTION ON THE INTEGRATED HARMONICS CAUSED BY THE OTHER APERTURE IS NOW FULLY CANCELLED AT ANY CURRENT IN EITHER CIRCUIT

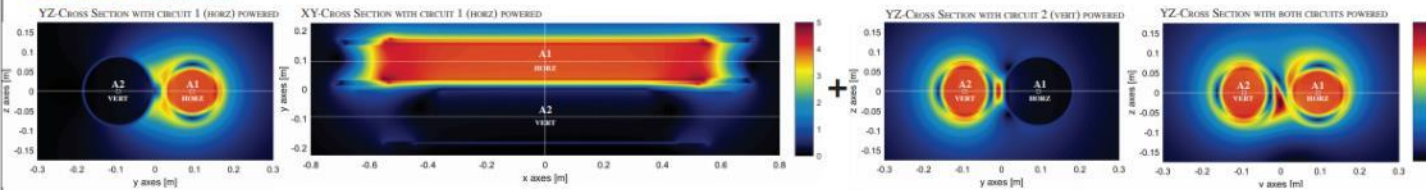
TABLE II
INTEGRATED HARMONICS IN APERTURE 1 GIVEN PER COIL SET AT THE FULL CURRENT OF 550 A.

Coil	unit	A1	A2	A3	A4	A5	A6	A7	A8	A9	A10
C1 Main	[Tm]	+7.32E-01	+2.74E-01	+7.80E-02	+1.98E-02	+4.73E-03	+1.09E-03	+2.45E-04	+5.43E-05	+1.18E-05	+2.51E-06
C1 Correction	[Tm]	-7.32E-01	-2.74E-01	-7.80E-02	-1.98E-02	-4.73E-03	-1.09E-03	-2.45E-04	-5.43E-05	-1.17E-05	-2.27E-06
C2 Main	[Tm]	-5.99E-07	+1.04E-06	+2.59E-07	-3.98E-07	-3.65E-07	+9.80E-07	+1.17E-06	-1.56E-06	-6.60E-07	+4.92E-07
C2 Correction	[Tm]	+1.19E-06	-3.79E-07	-2.98E-07	1.86E-07	-9.76E-08	-6.53E-08	-5.27E-08	-4.18E-08	-4.85E-08	-6.99E-08
total integrated	[Tm]	-1.06E-05	-3.53E-07	-2.04E-08	-5.43E-07	-8.66E-07	+6.02E-07	+7.49E-07	-1.63E-06	-6.29E-07	+6.57E-07
reduced harmonics	[units]	+0.021	+0.001	+0.000	-0.001	-0.002	+0.001	+0.001	-0.003	-0.001	+0.001

TABLE III
INTEGRATED HARMONICS IN APERTURE 2 GIVEN PER COIL SET AT THE FULL CURRENT OF 550 A.

Coil	unit	B1	B2	B3	B4	B5	B6	B7	B8	B9	B10
C1 Main	[Tm]	+2.39E-07	-1.24E-07	+1.82E-08	-3.13E-08	-5.77E-08	5.68E-08	-7.43E-08	-4.58E-08	+2.47E-08	-2.53E-08
C1 Correction	[Tm]	+1.63E-10	+1.59E-07	+3.17E-07	-6.47E-07	-9.02E-07	-7.34E-07	-2.20E-07	+1.18E-07	+3.97E-07	-4.80E-08
C2 Main	[Tm]	+5.28E+00	+1.32E-01	+4.78E-02	+1.54E-02	+4.66E-03	+1.36E-03	+3.81E-04	+1.08E-04	+2.96E-05	+8.77E-06
C2 Correction	[Tm]	-2.71E-01	-3.72E-01	-4.78E-02	-1.56E-02	-4.67E-03	-1.35E-03	-3.82E-04	-1.08E-04	-2.96E-05	-7.69E-06
total integrated	[Tm]	+5.01E+00	+1.51E-07	-1.53E-06	-1.10E-06	-1.91E-06	+4.86E-07	-1.38E-06	+6.33E-07	+1.42E-06	+1.06E-06
reduced harmonics	[units]	+10000	+0.000	-0.003	-0.002	-0.004	+0.001	-0.003	+0.001	+0.003	+0.002

* VARIABLES HARMONICS * COMPARISON PLAN



VI. COMPARISON TO ORIGINAL D1

THE AIR-COIL CORRECTOR HAS AN INDUCTANCE OF 1440 mH COMPARED TO 820 mH ON THE ORIGINAL DESIGN. ALSO IT HAS ABOUT TWICE THE WIRE LENGTH, 96m VS 44.6m.

TABLE IV - COIL DISTANCE

Coil	unit	dist	dist	dist
C1m	[mm]	1544.178	-87.4815	-0.15322
C1c	[mm]	-87.4815	112.2948	0.18977
C2m	[mm]	-0.15322	-0.18977	1545.297
C2c	[mm]	-0.18977	0.15322	-88.995
C1c2	[mm]	-0.10366	0.04944	-48.953
C2c1	[mm]	48.953	-0.10366	113.874

TABLE V - WIRE LENGTHS

Coil	unit	dist	dist	dist	wire length
layer 1	[mm]	148.5	2	5	1484.7
layer 2	[mm]	167.8	2	5	1682.6
layer 3	[mm]	181.1	2	5	1805.5
layer 4	[mm]	207.8	2	5	2078.5
C1c	[mm]	166.7	2	3	880.2
layer 2	[mm]	156.2	2	3	937.3
C2c	[mm]	168.0	2	5	1480.3
layer 1	[mm]	167.8	2	5	1677.9
layer 3	[mm]	187.5	2	5	1875.3
layer 4	[mm]	207.8	2	5	2072.7
C1c2	[mm]	167.3	2	3	853.7
layer 2	[mm]	153.2	2	3	907.0

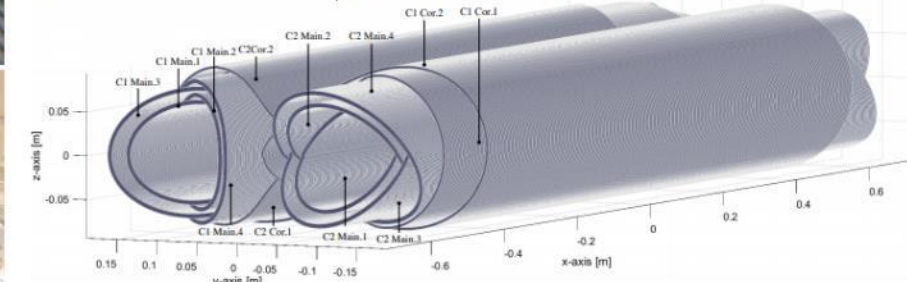
VII. DEALING WITH TORQUE AND FORCES

PROPOSAL FOR DEALING WITH TORQUE IN HORIZONTAL VERTICAL SKEWED CIRCUIT CORRECTORS. 3D PRINTED DEMO SHOWING CASTELLATIONS THAT BLOCK ROTATION.



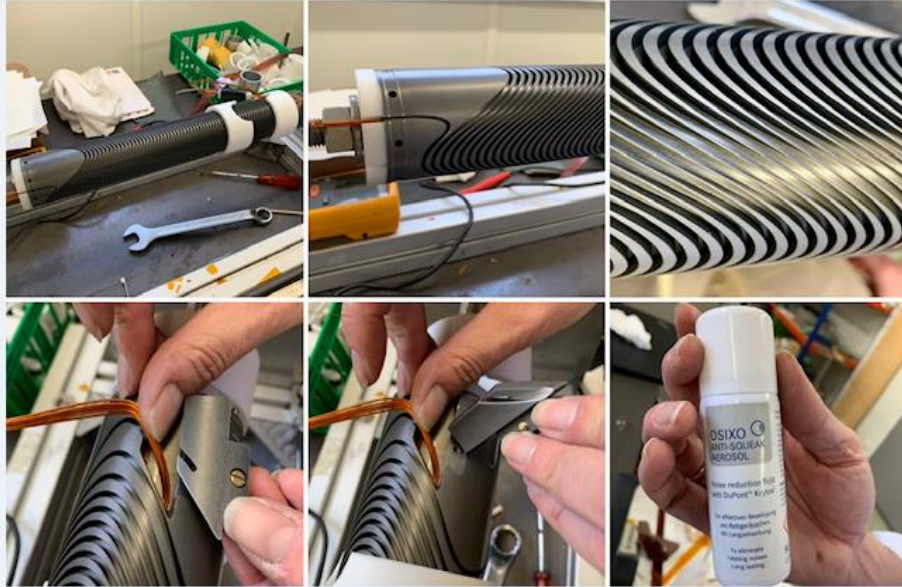
VIII. CONCLUSION

- A NOVEL AIR-COIL TYPE LAYOUT HAS BEEN PROPOSED FOR THE D1 ORBITAL CORRECTOR FOR THE HIGH LUMINOSITY UPGRADE.
- MANAGED TO REDUCE THE OVERALL LENGTH OF THE MAGNET FROM 2.2 TO 1.4 m, A 37% REDUCTION.
- THIS IS ACHIEVED BY USING A SET OF CCT SHIELD COILS THAT CANCEL THE CROSS-TALK BETWEEN THE APERTURES. TO AVOID NON-LINEARITY, THE IRON YOKE HAS BEEN REMOVED RESULTING IN A SO-CALLED AIR-COIL.
- THIS COMES AT THE COST OF APPROXIMATELY TWICE QUANTITY OF CONDUCTOR, AND TWICE THE COIL INDUCTANCE.
- THE CCT IS A VERY FLEXIBLE DESIGN THAT CAN GENERATE ANY COMBINATION OF HARMONICS AND IS FULLY CAPABLE OF CANCELING ANY TRANSVERSE FIELDS.
- THE PRESENTED DESIGN IS A DEMONSTRATION OF WHAT IS POSSIBLE USING CCT.

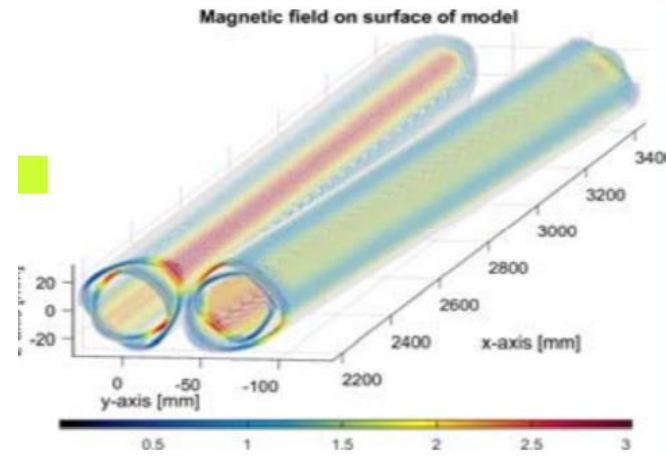


- FCC quad CCT
- Low-Cost Project 17 CHF

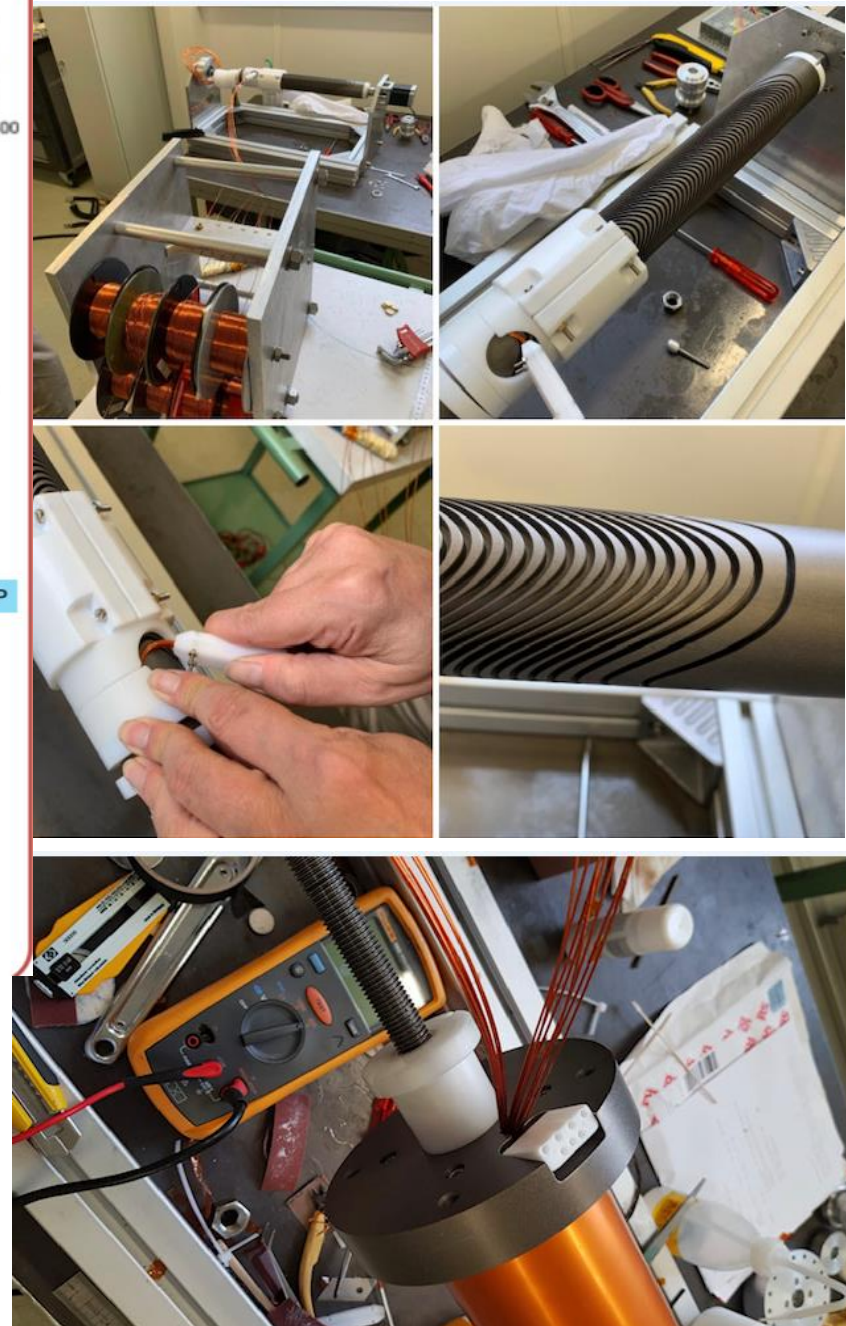
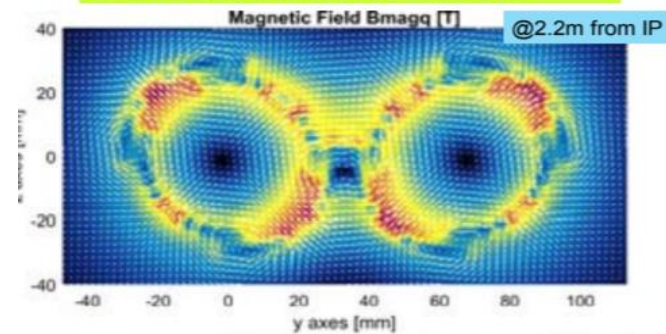
Large Hadron Collider
3 Dec 2019 · Large Hadron Collider



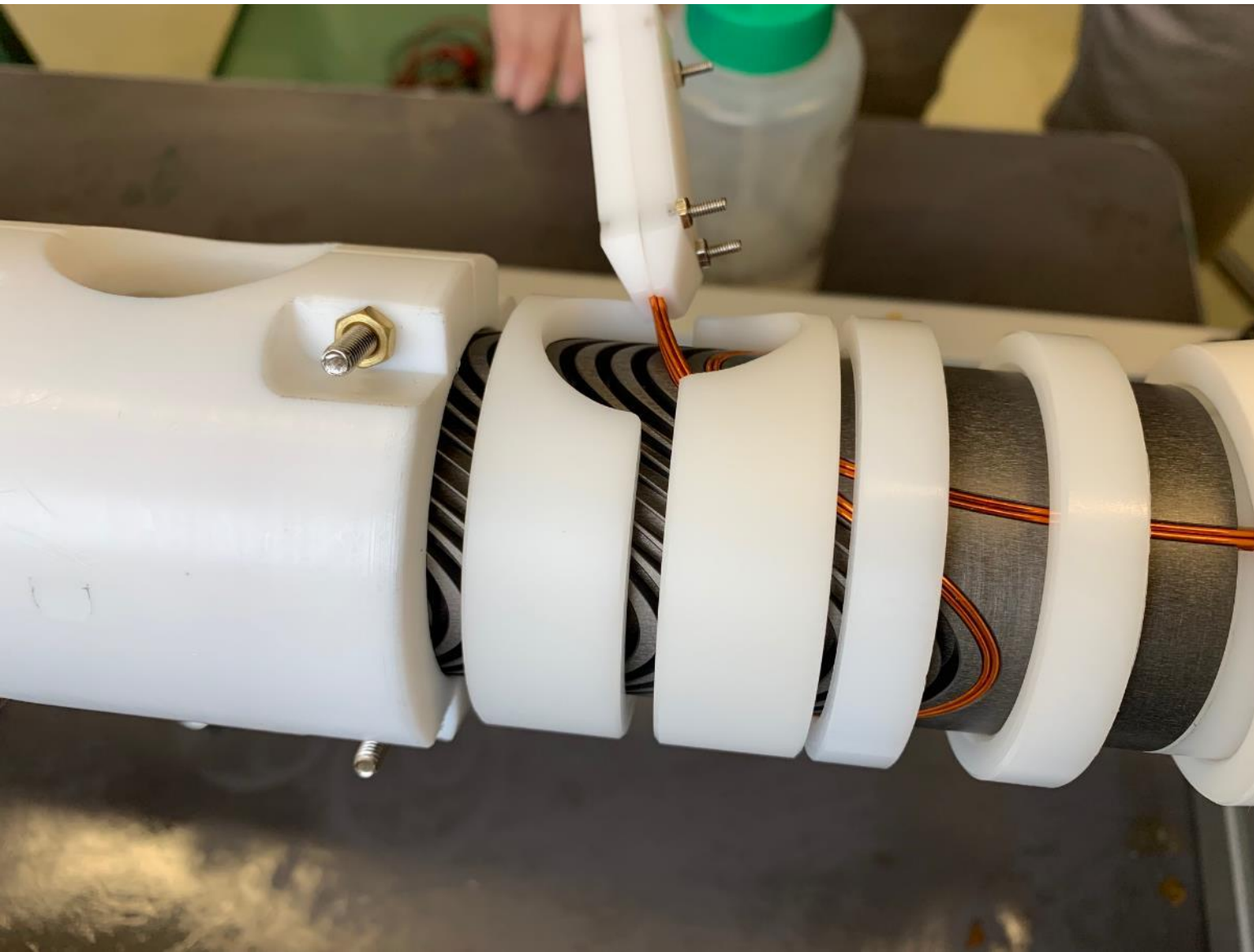
Design to CNC !!
How to transfer the
geometry is important !!



Looking from the beam side

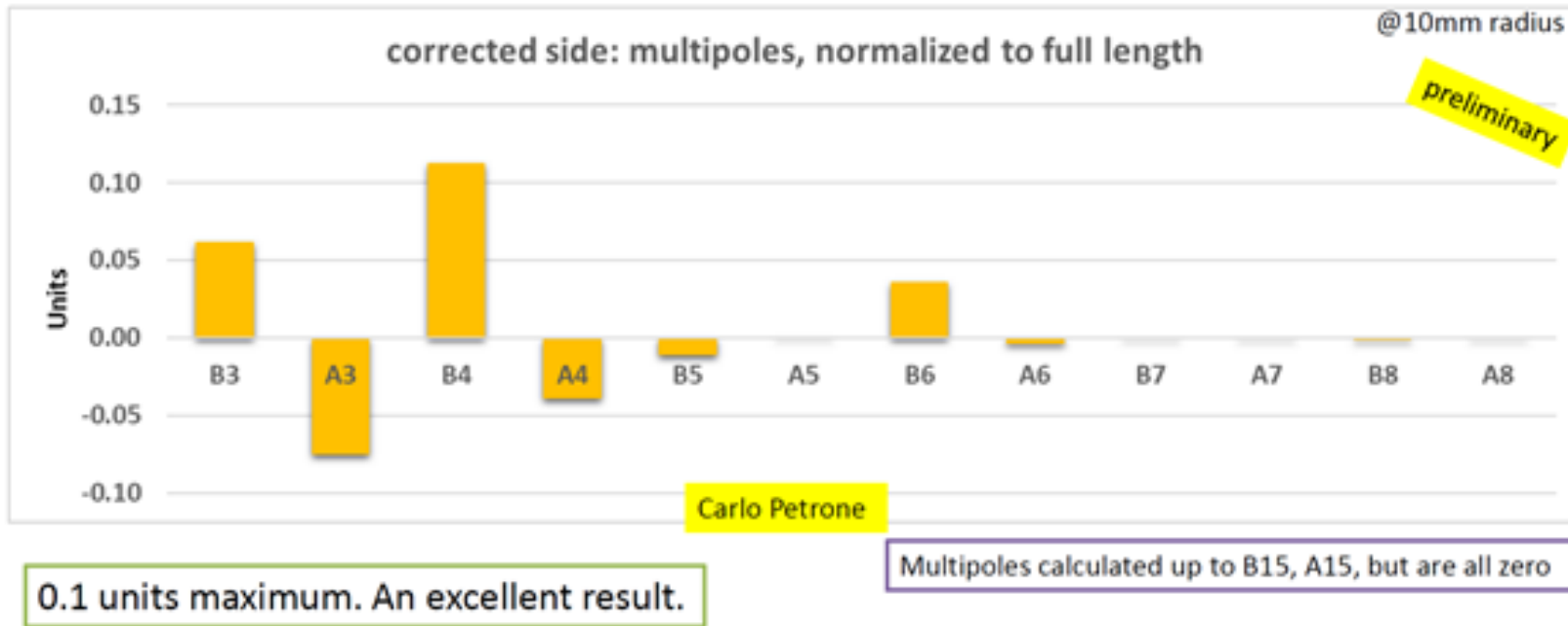


Winding tool ideas



CCT FCC quad

Field quality at the edge, with correction



The coil had magnetic material near the aperture so it may be even better still working on it

SuShi septum status report: Testing the NbTi/Nb/Cu multilayer shield & update on the concept

D. Barna, M. Novák, K. Brunner

Miro Atanasov, Carlo Petrone, Max Pascal, Jerome Feuvrier, Franco Mangiarotti, Frederic Rougemot, Yannick Thuau & the rest of the SM18 team



CERN 0.5 m CCT to test Sushi

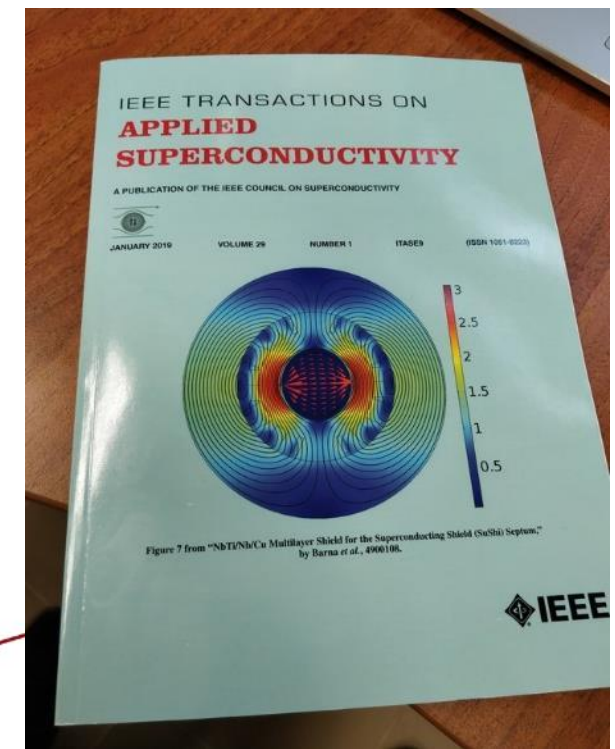
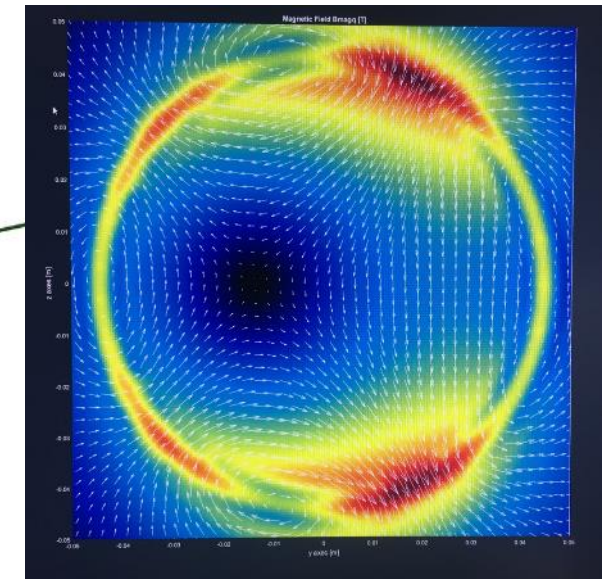
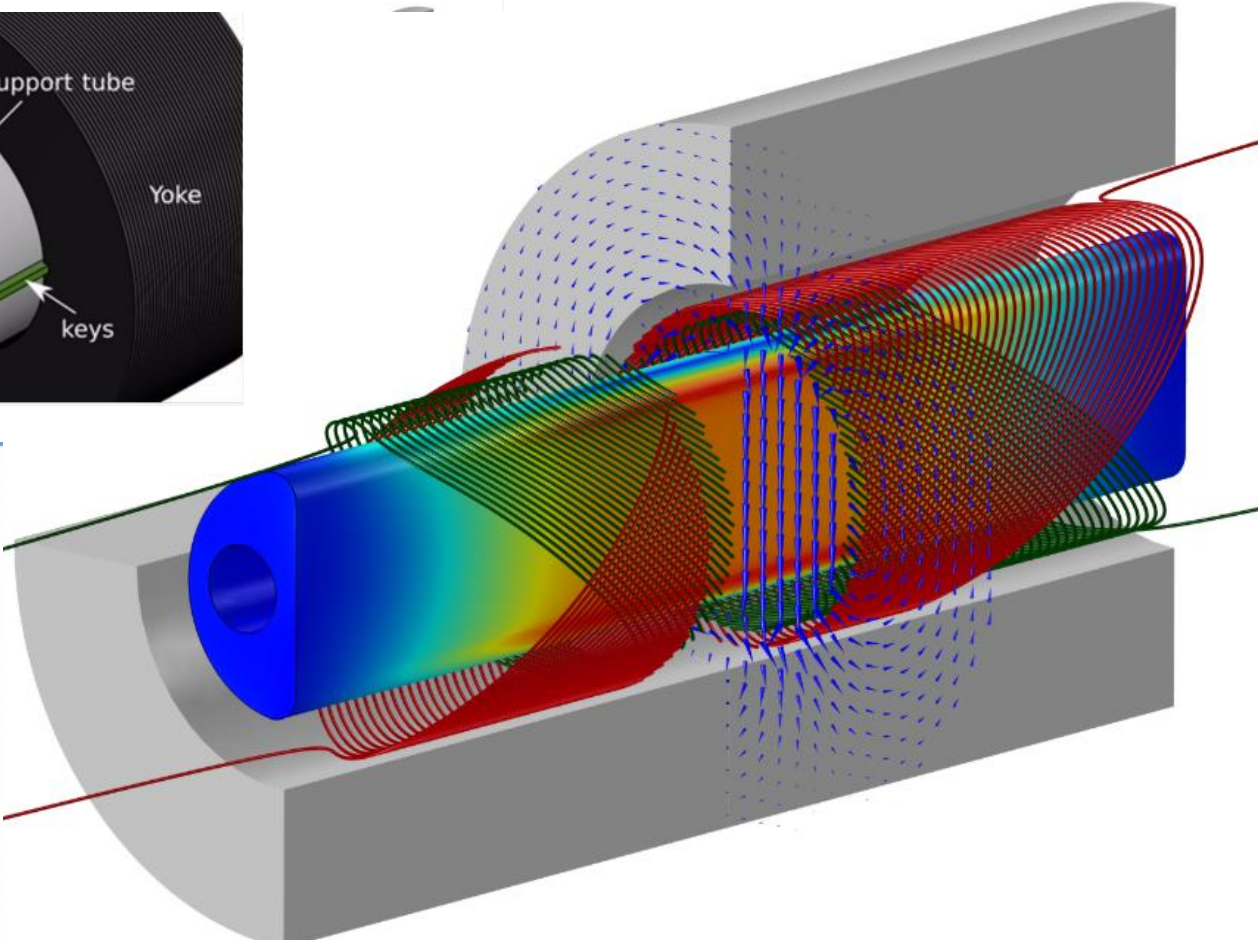
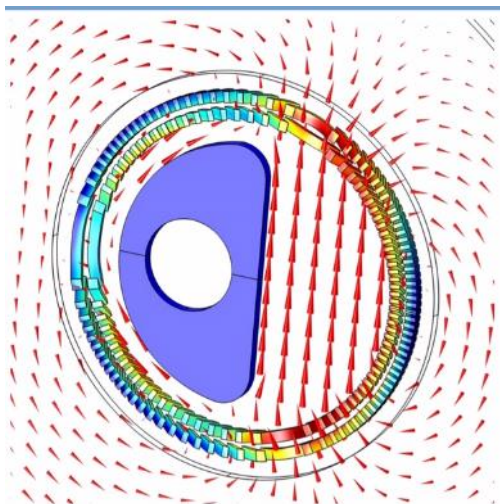
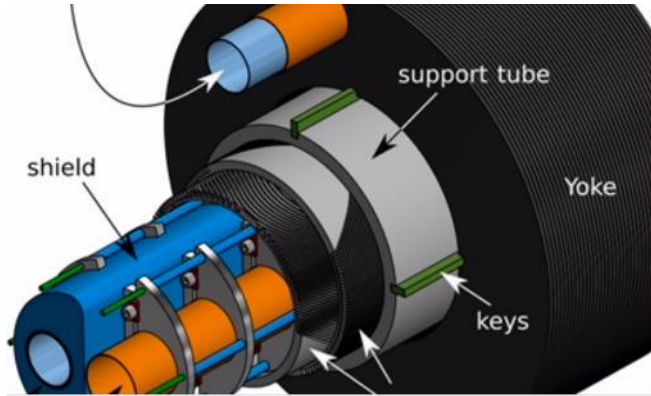
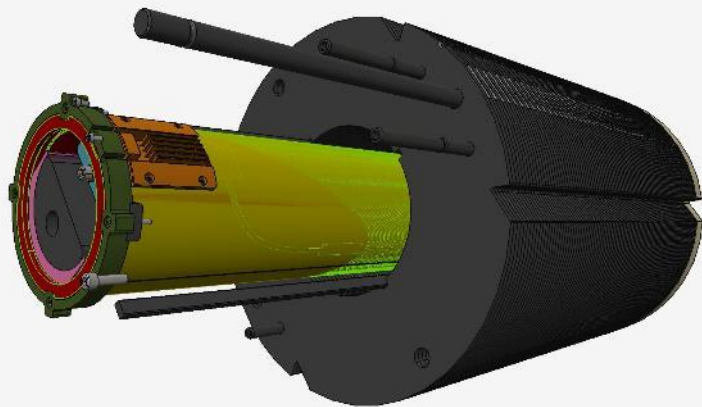
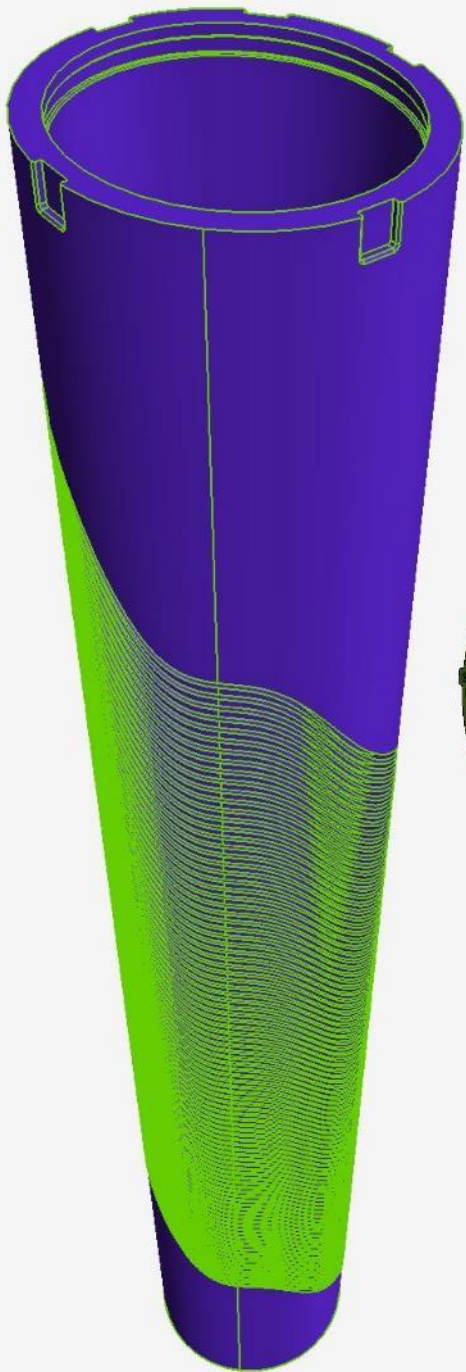


Figure 7 from "NbTi/Nb/Cu Multilayer Shield for the Superconducting Shield (SuShi) Septum," by Barna et al., 4966106.

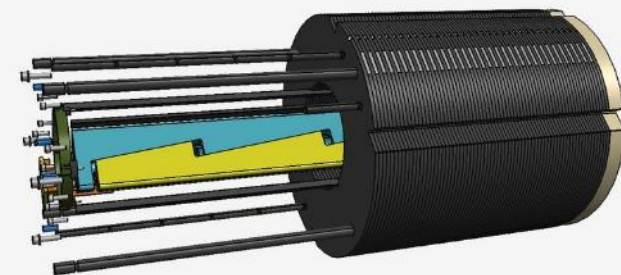




imgPlay



Sushi combined function
First test wind





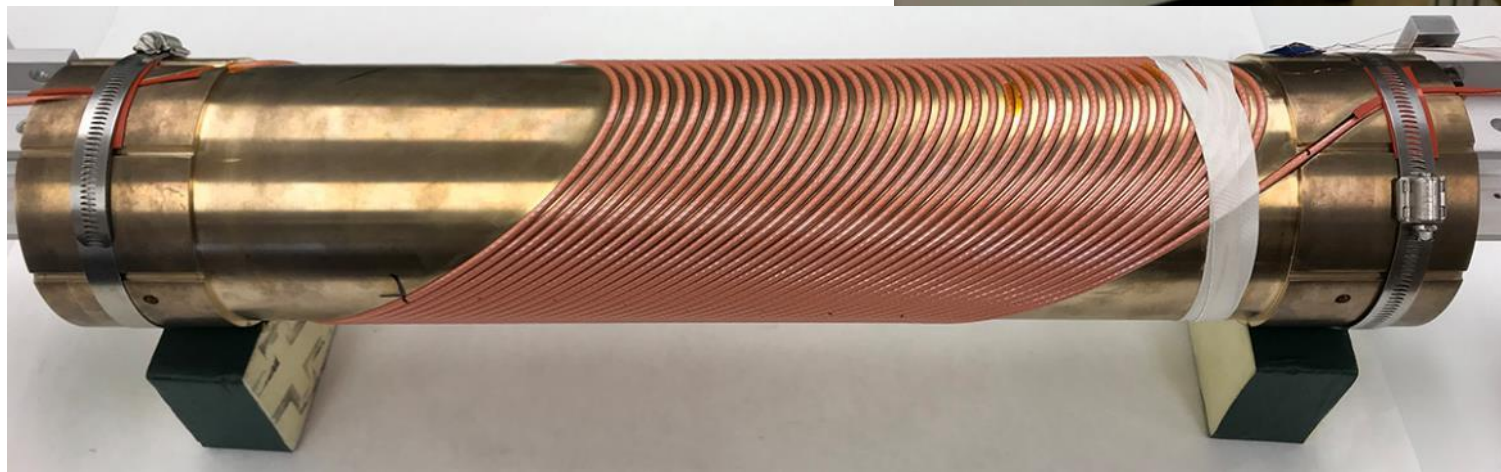
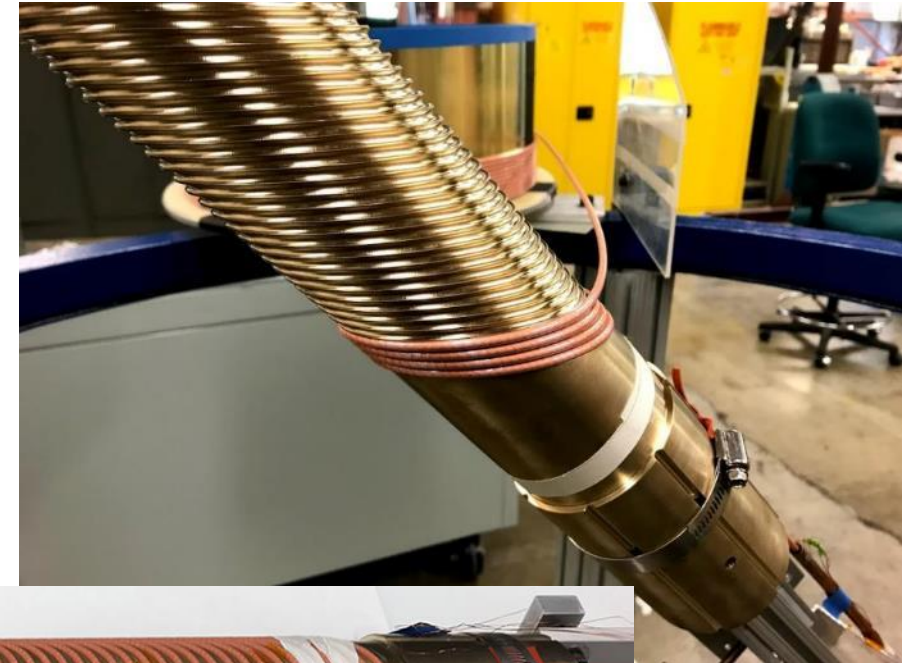
HTS quench energy equal to dropping a cannon ball 2 m !



LTS quench energy equal to dropping a pin 10 mm!

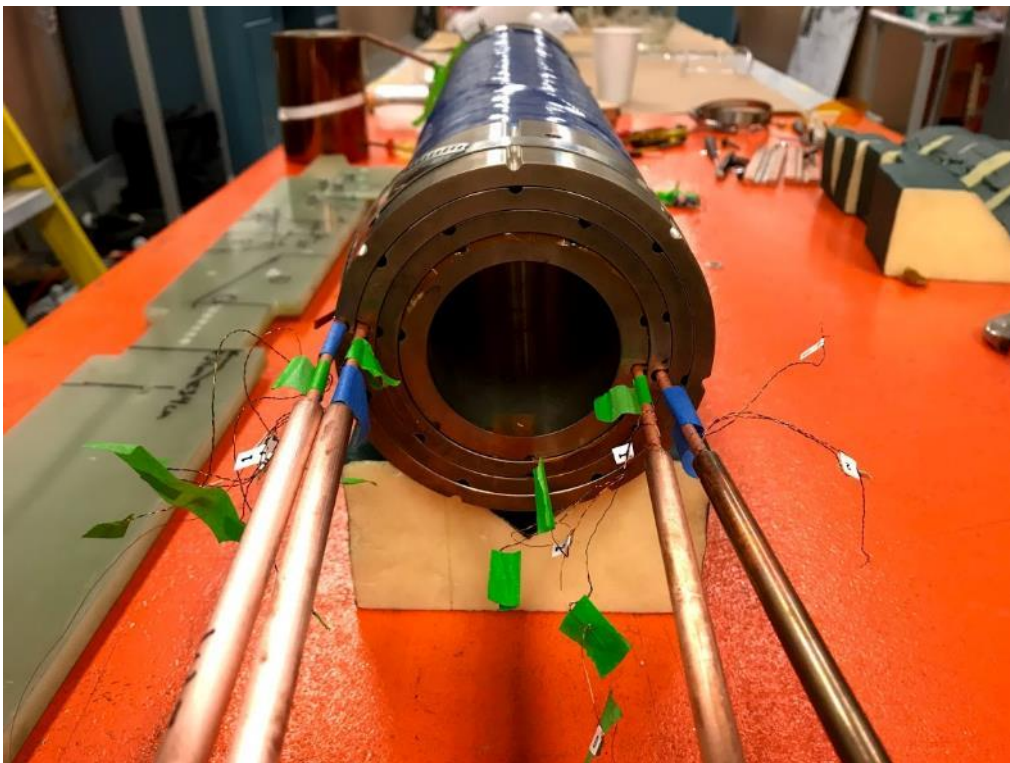
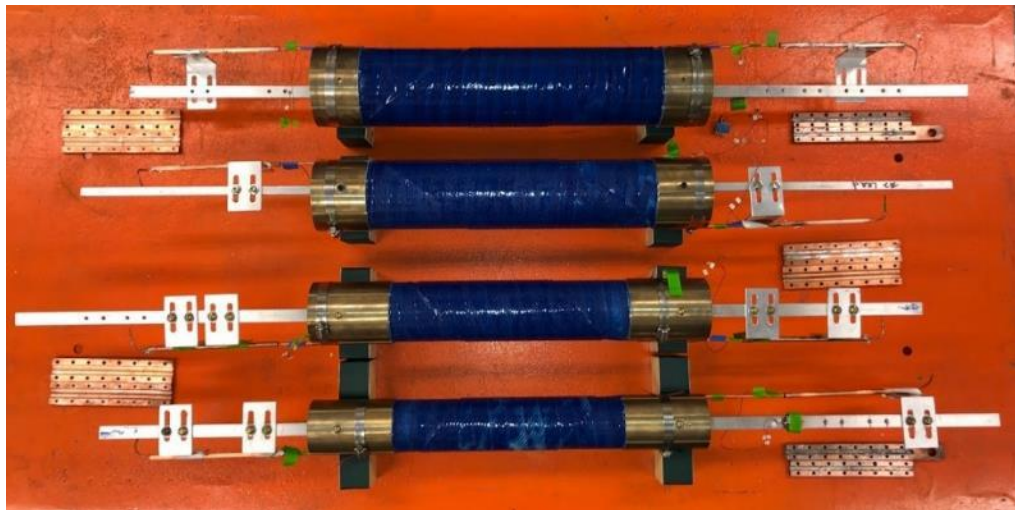
CCT-C2 layout

- 3 T at 4.2 K
- 4 Layers, 40 turns per layer
- 80 m of CORC® wire ordered by LBNL
- Aperture 85 mm
- Minimum bending diameter 60 mm

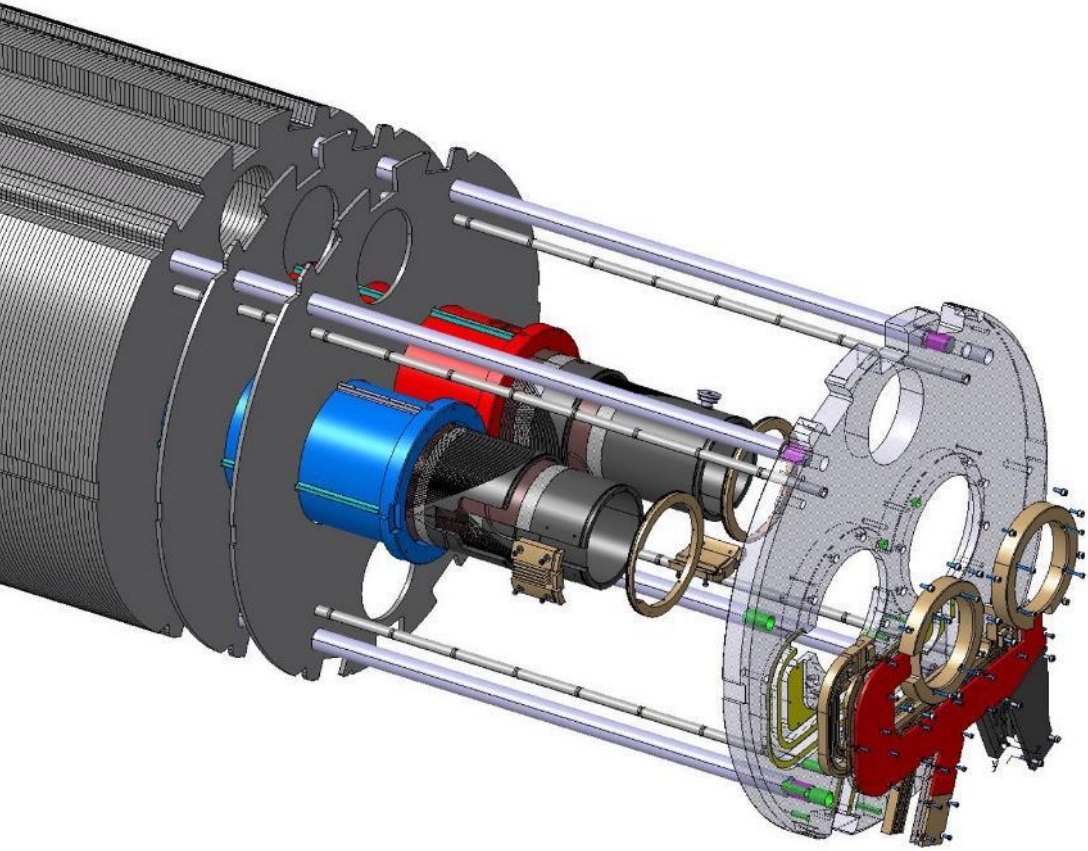


Thanks to Danko van der Laan and his team
See the full talk on my RG project log, or
<https://indico.cern.ch/event/882979/>

CCT-C2 Assembly



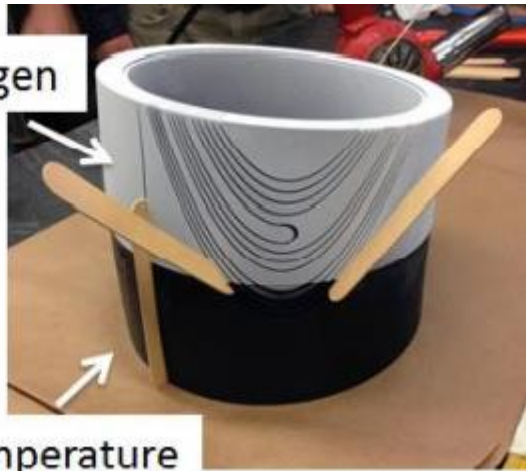
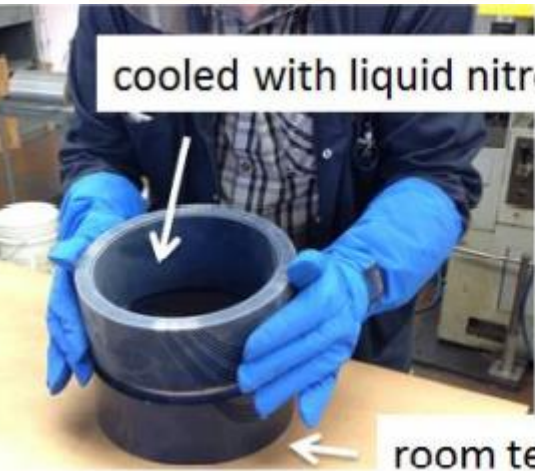
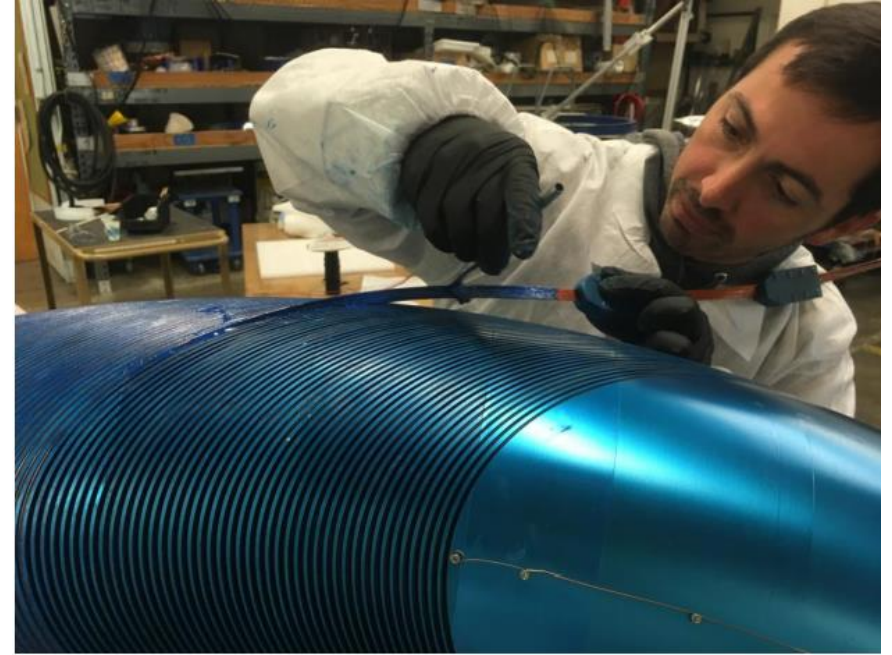
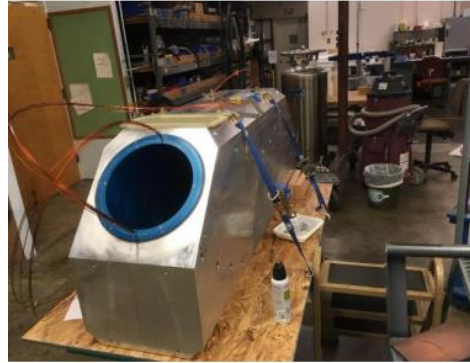
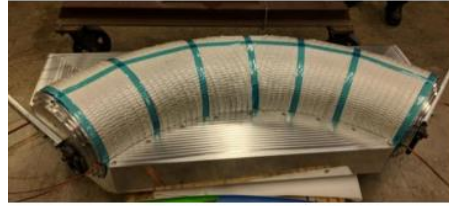
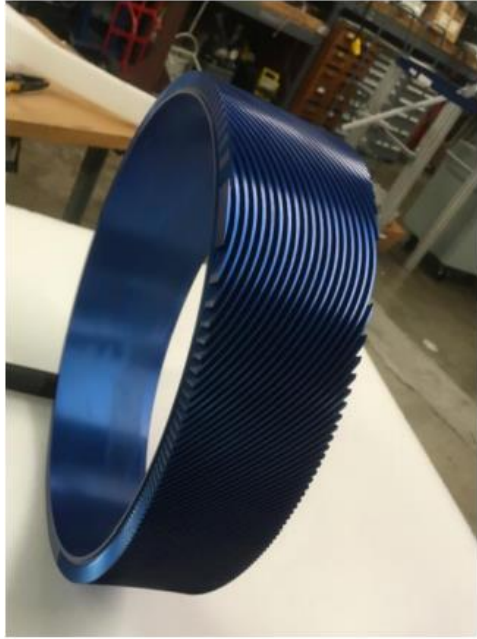
MCBRD LHC high-Lumi CCT



This week at CERN 16 May 2022

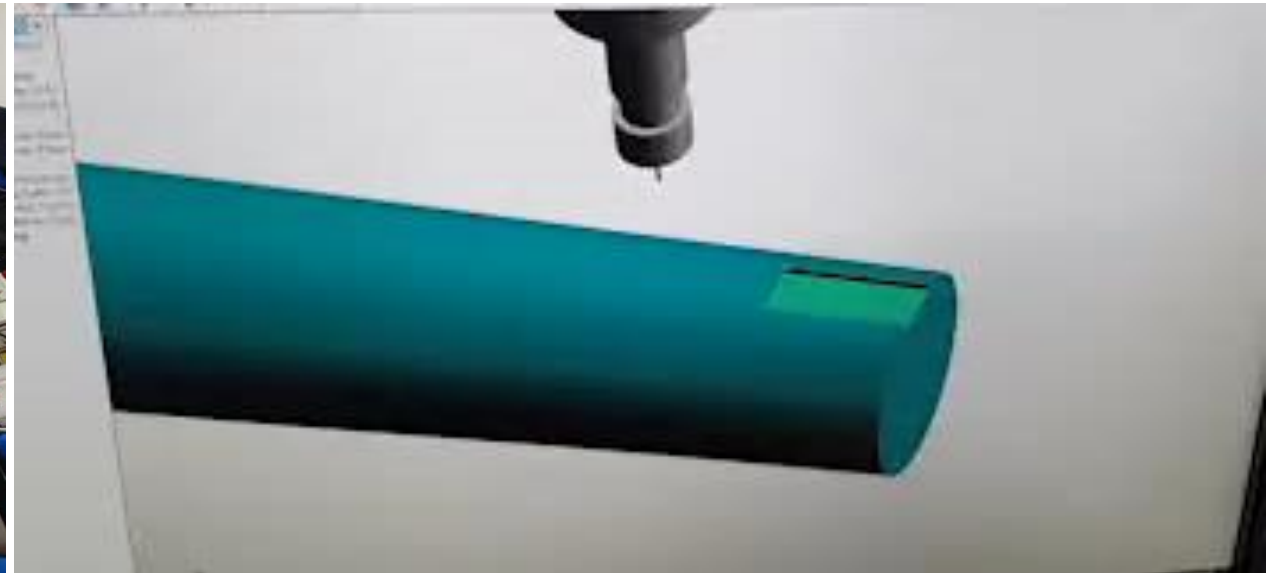
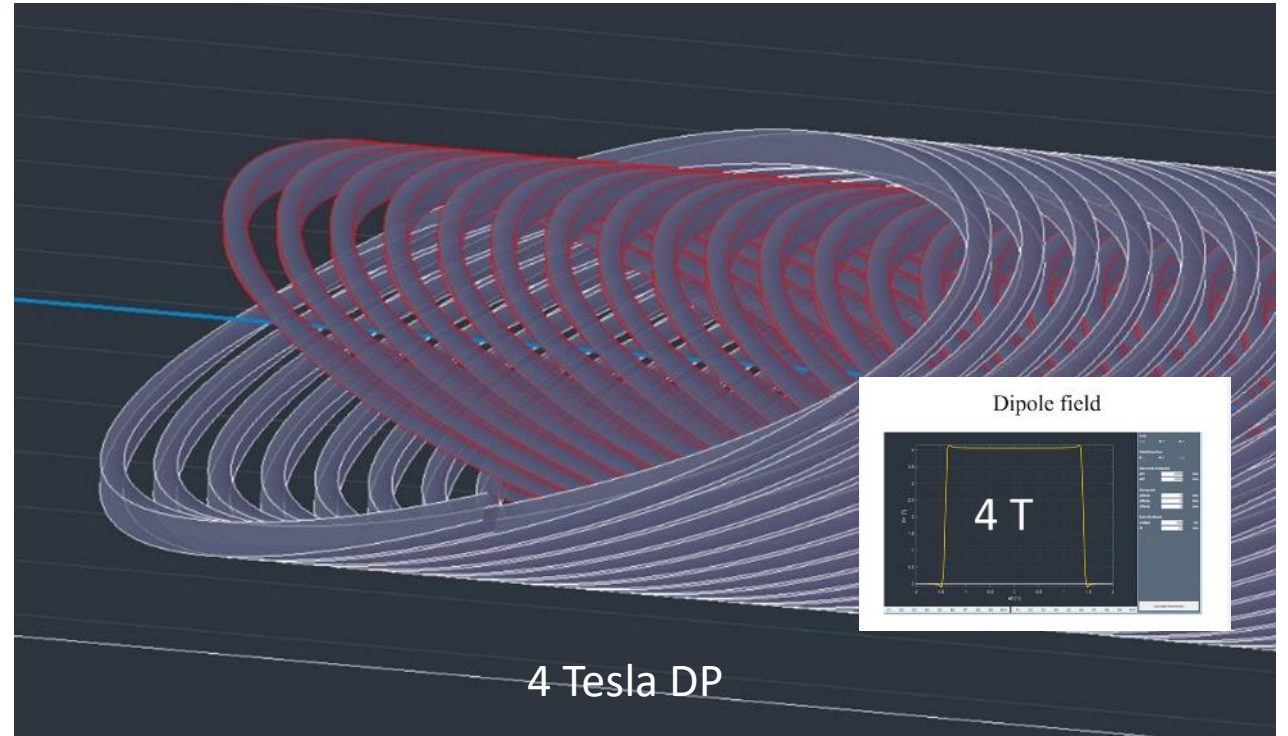
15 + apertures manufactured so far in the LHC Hi-LUMI project 9 at CERN 11 in China

LBNL curved dipole

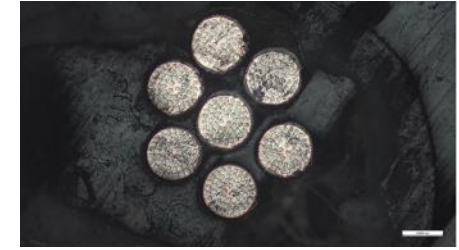


MCBY update

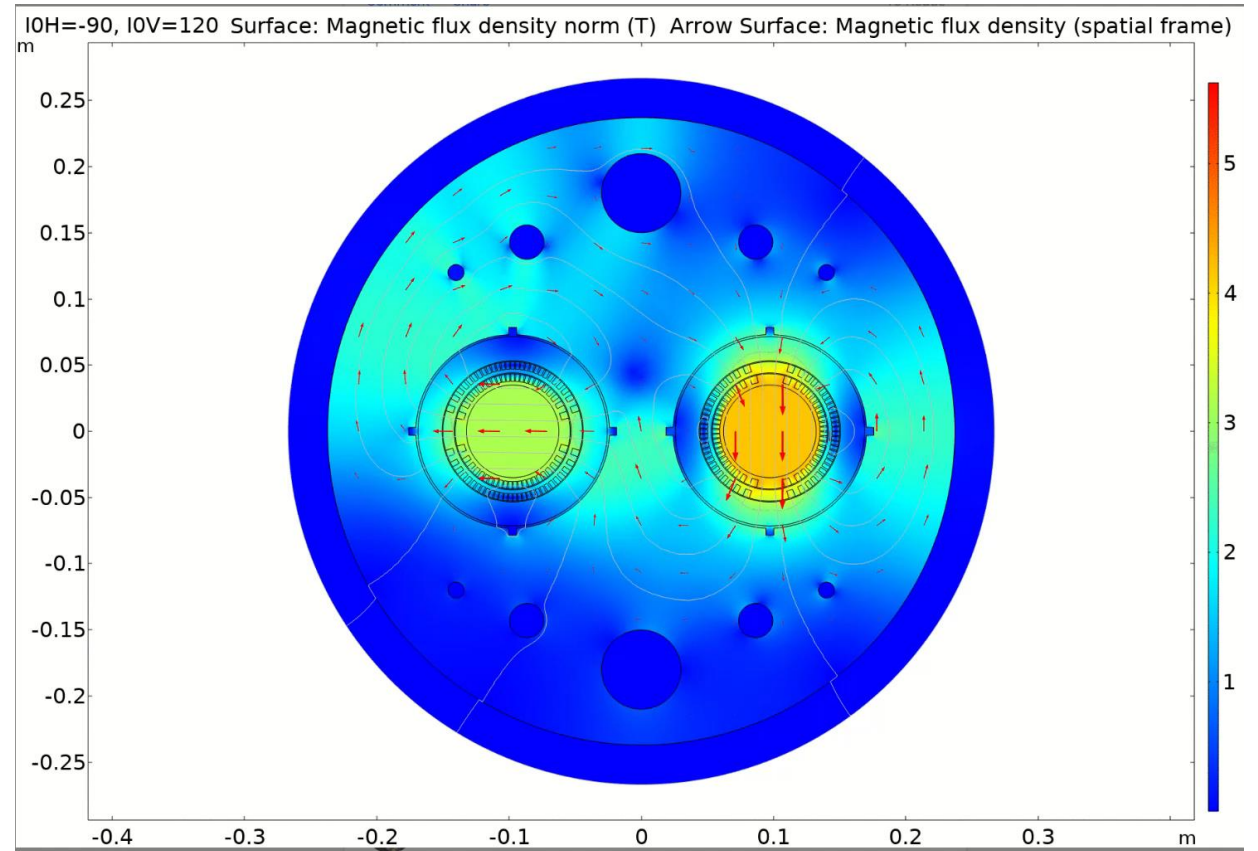
LHC need 20+ MCBC or MCBY magnet. To replace old magnets that are starting to fail due to radiation damage ! This was the first 600 A design from 2016 now the team in Sweden are building a 100 A rad hard design.



Swedish low current high radiation CCT



Uppsala University in Sweden leading the MCBY development.

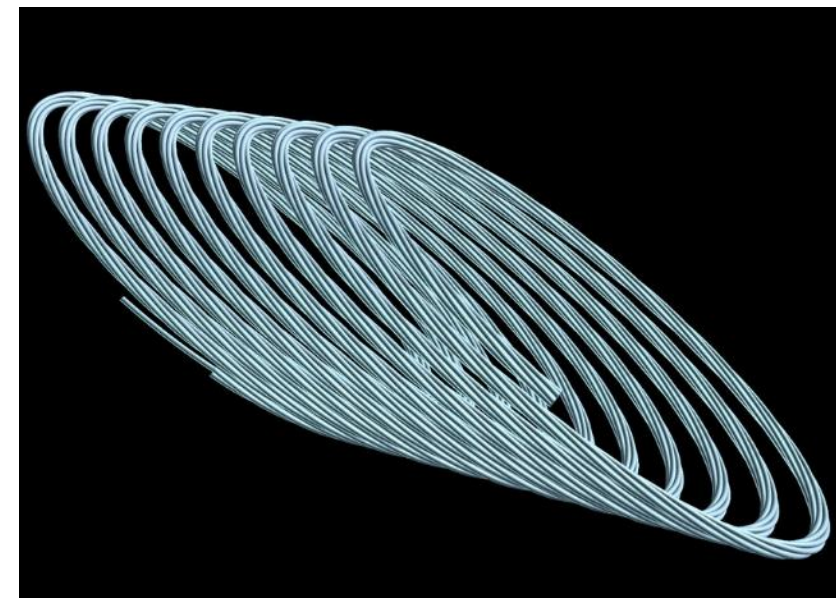
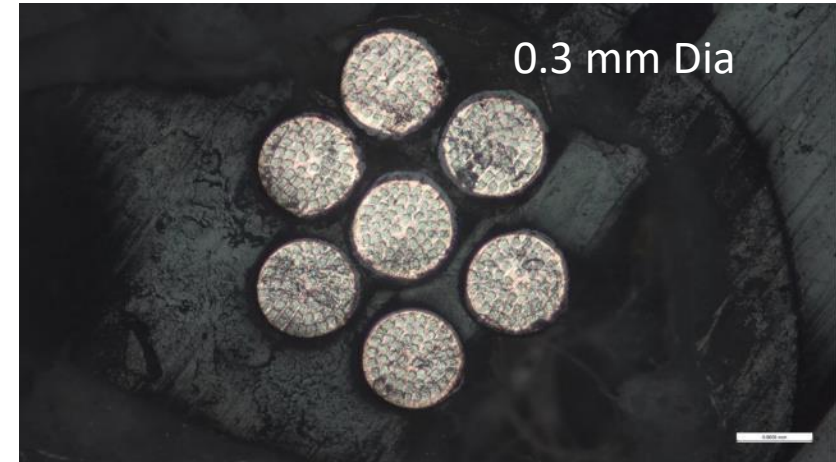
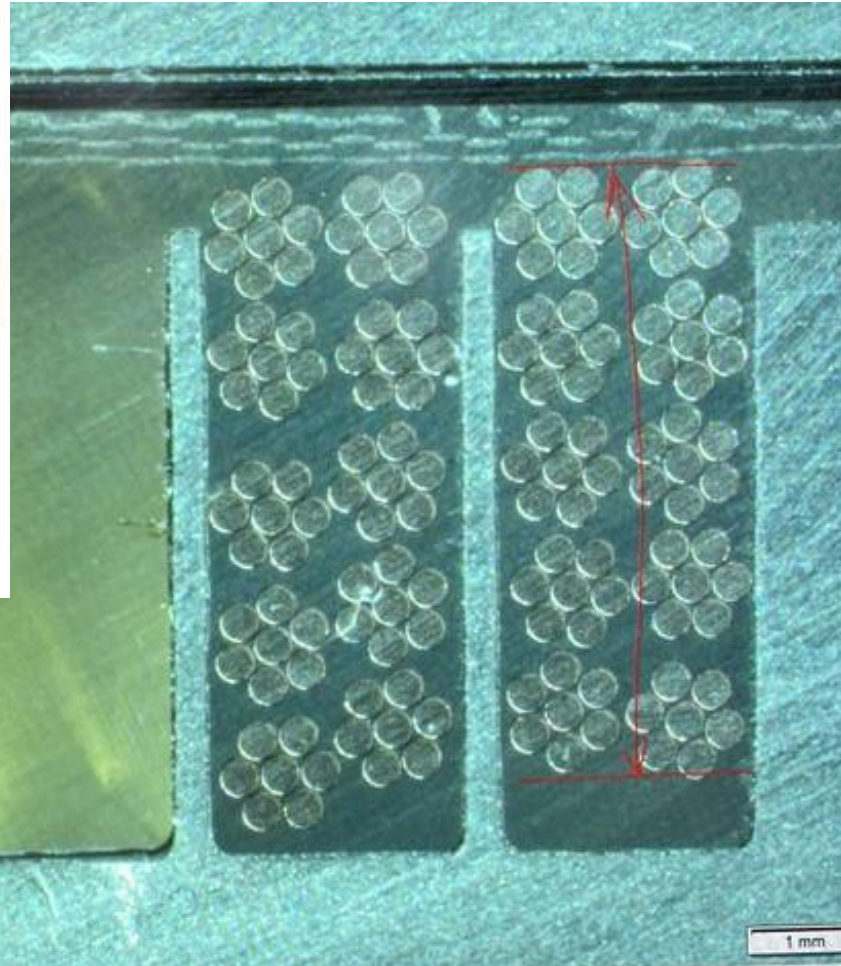


Thanks to Kevin for the MCBY CCT magnetic field model

Low current means: small wires and many turns so we selected a rope design

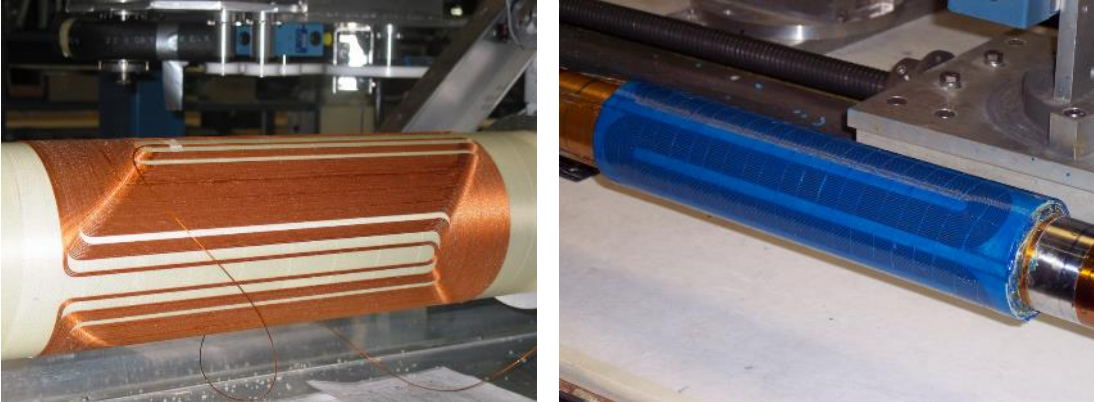


MCBY rope conductor using 7-0.3 mm strand



BNL Direct CCT winding

Stray field active shield idea

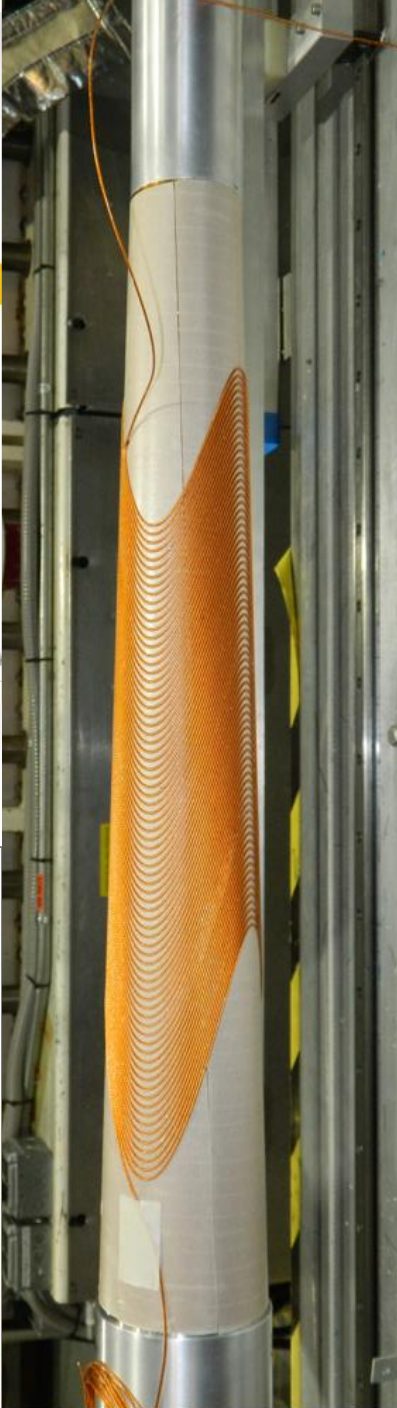


Winding machine process derived axis

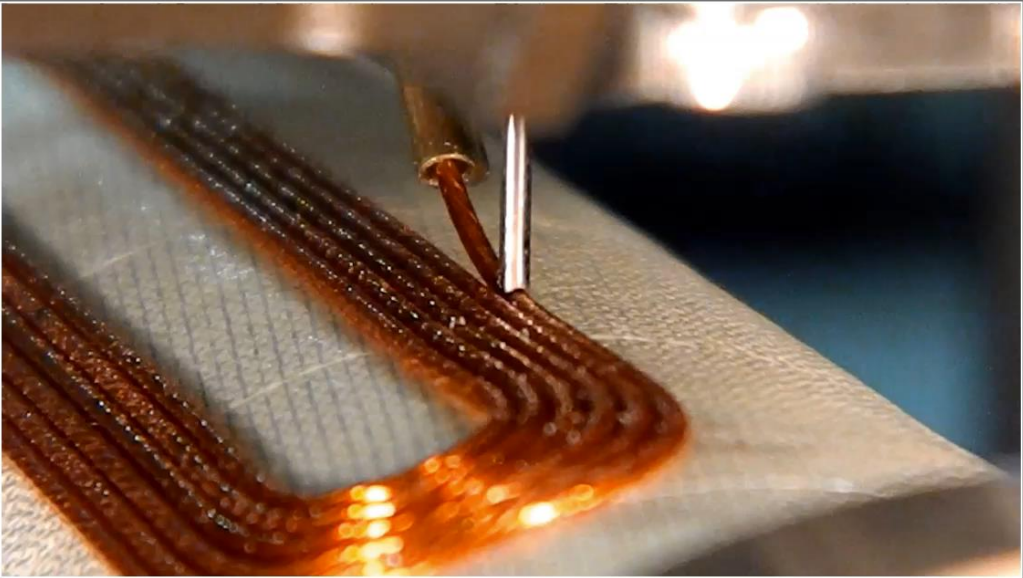
Wire feed capstan
Gate rollers
Gate actuator
Wire feedtube
Ultrasonic stylus
Stylus vertical force
Stylus tip

U.S. DEPARTMENT OF ENERGY Office of Science BROOKHAVEN NATIONAL LABORATORY

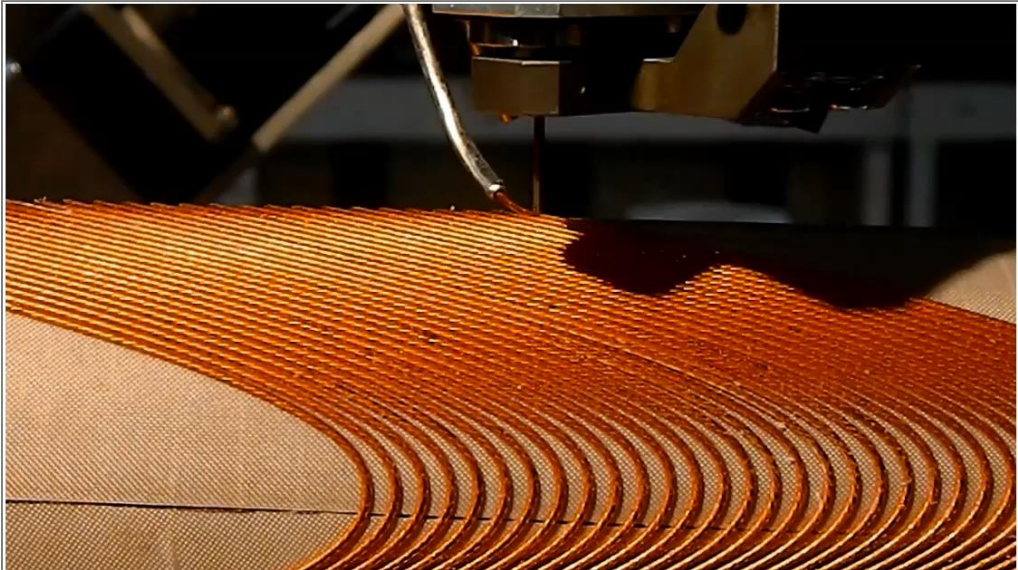
21 National Science Foundation



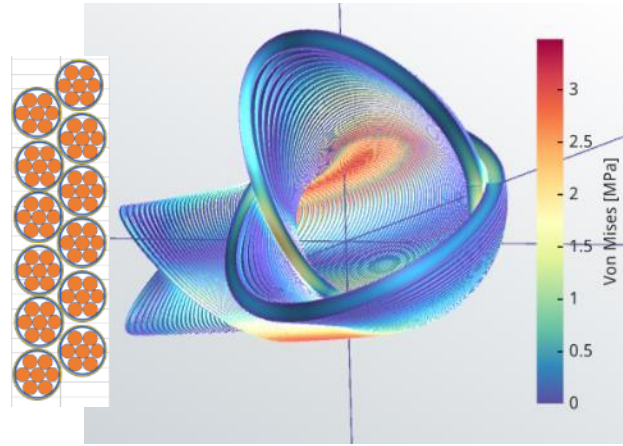
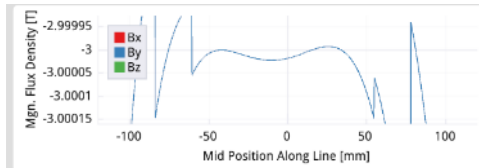
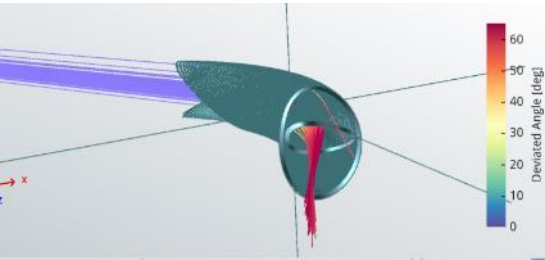
Alpha octupole winding



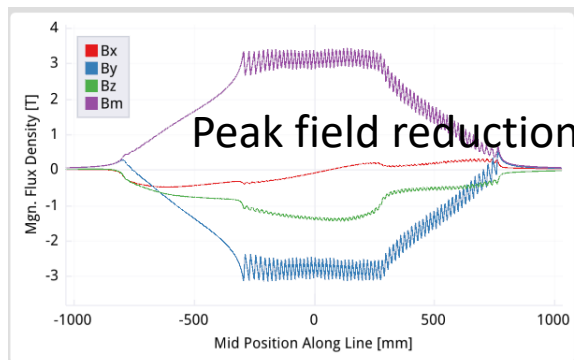
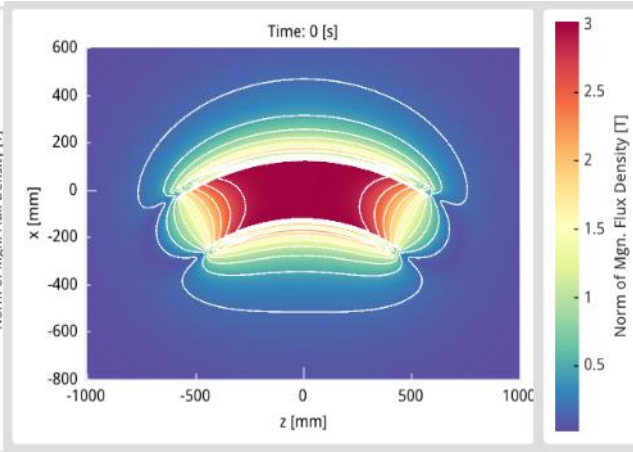
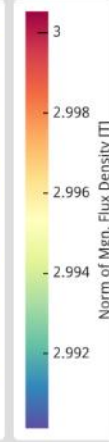
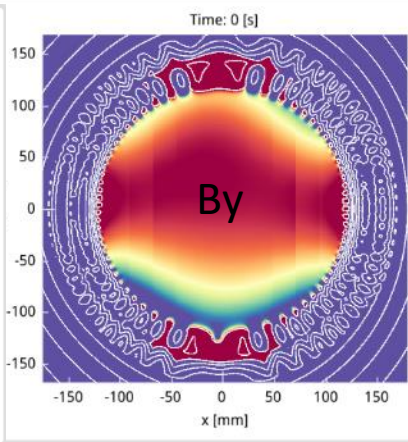
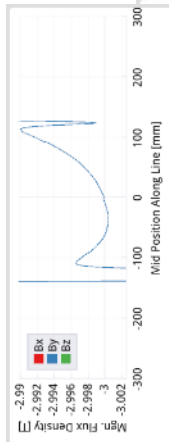
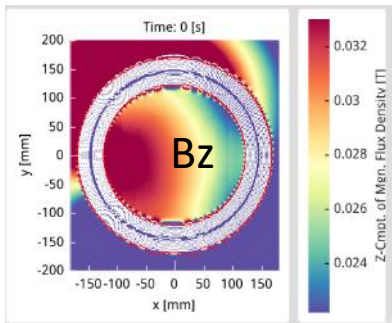
Canted cosine quadrupole direct winding



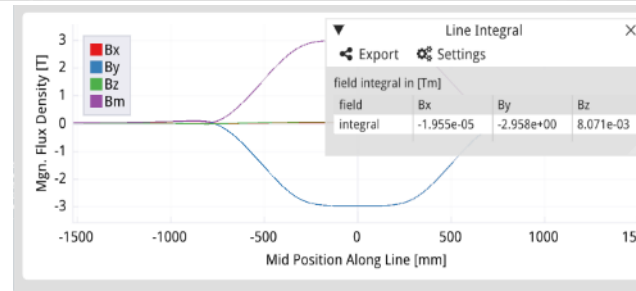
Fusillo curved CCT CERN project 2022 - 2024



Nom current 244.457A
 3.000 T, inner 3.500 T, outer 3.397 T
 Ss% inner 70.18 % & outer 69.018 %
 2.958 Tm integral
 15.57 km strand
 2.224 km rope
 84 strands in channel
 Nom rope dia 3.1 mm
 Channel size 5.884 x 20.15 mm
 log-stacking lay out.
 Pitch 6.384 mm
 Min wall 0.5 mm
 Gap between coil layers 5 mm
 T margin 1.504 K to 3.807 K
 Stress nom 3.493 MPa
 Central inner coil rad 123 mm
 DP 212.64 mm, Q 3.05 mm,
 Skew Q 0.195 mm, Sextupole 0.1 mm,
 Skew S 0.04 mm
 Radius of curvature cold 1000 mm.
 Inductance 12.359 H
 Stored energy 369.141 kJ



interp bcr	omega
4	0.02
7	0.01
-0.6	0.006384
-0.5	0.006384
-0.3	0.006384
0	0.01
0.3	0.01
0.5	0.02
0.6	0.02



Channel step file

<https://cernbox.cern.ch/index.php/s/JudKfM6sLcBMtDS>

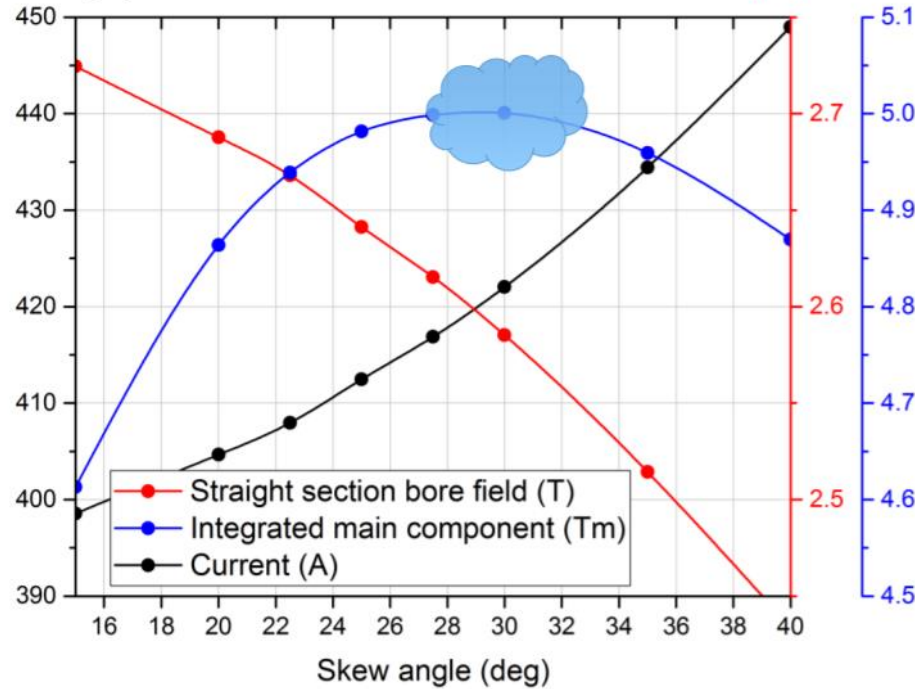
CCT Design features

- As we look at the designs, we find more and more features that can improve the magnet performance



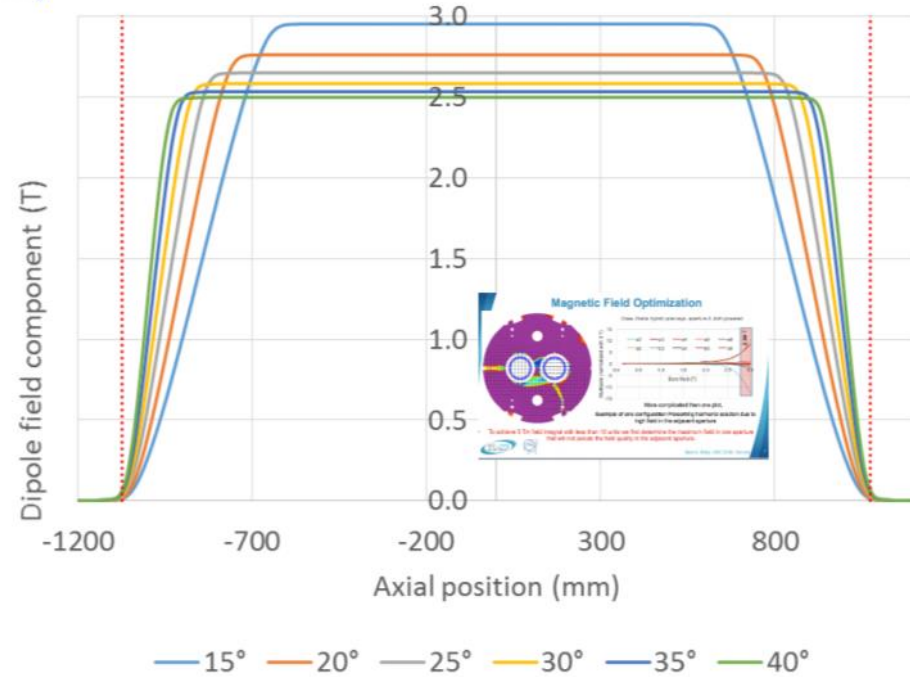
Magnet Current

(A) Skew angle optimization, $I/I_{ss} = 55.4\%$



Field (T) Field Integral (Tm)

Skew angle optimization (int $B_2=5$ Tm)

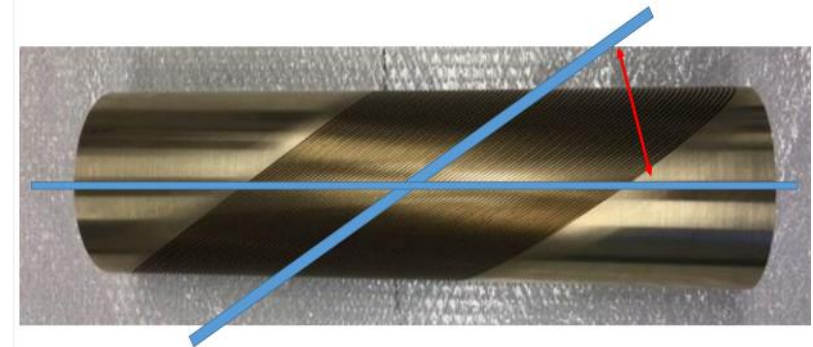


CCT skew angle optimisation

Due to the cross talk the max aperture field is set to ~ 2.7 T

For a fixed 5 Tm integral & magnet length ~ 2 m the optimum skew angle is 30 deg.

Lower skew angles give more field less conductor but have longer ends!



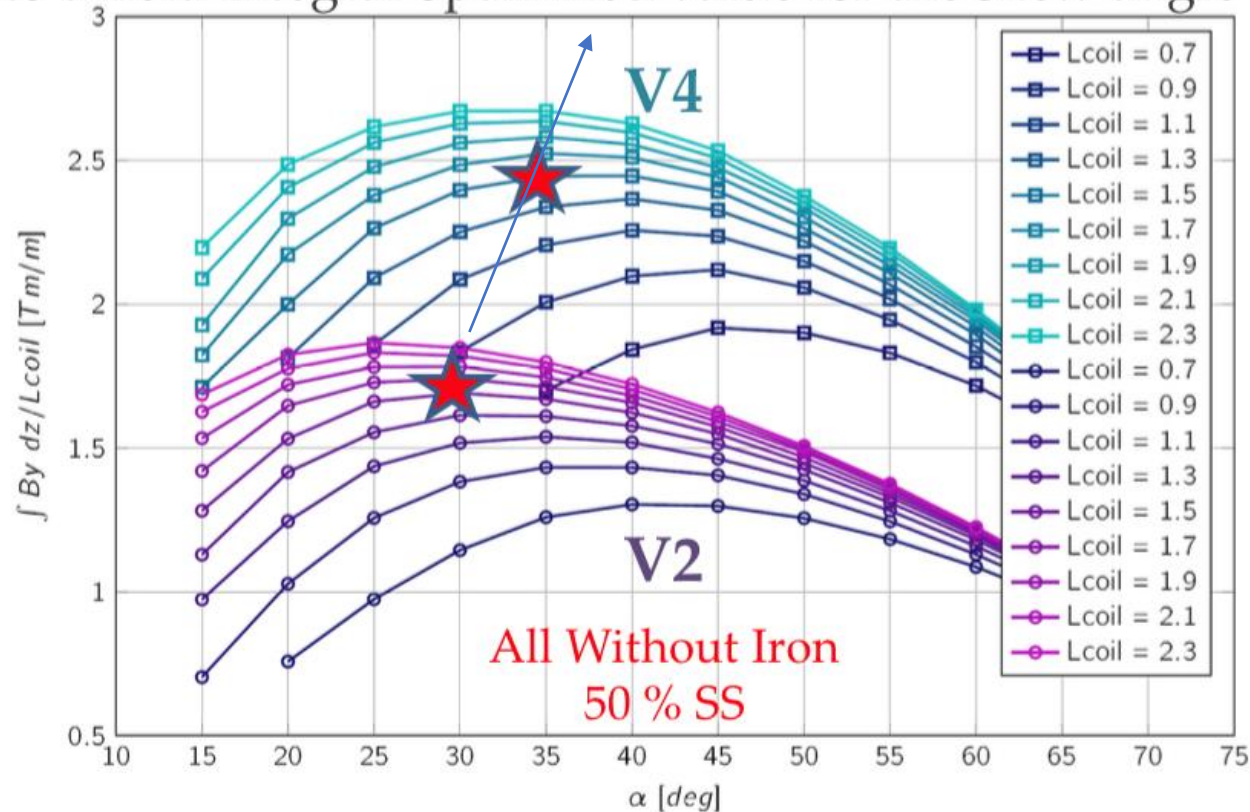
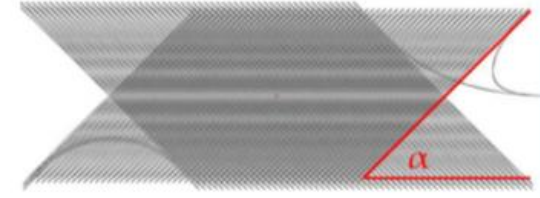
Glyn A. Kirby

Field Integral / Skew angle

8

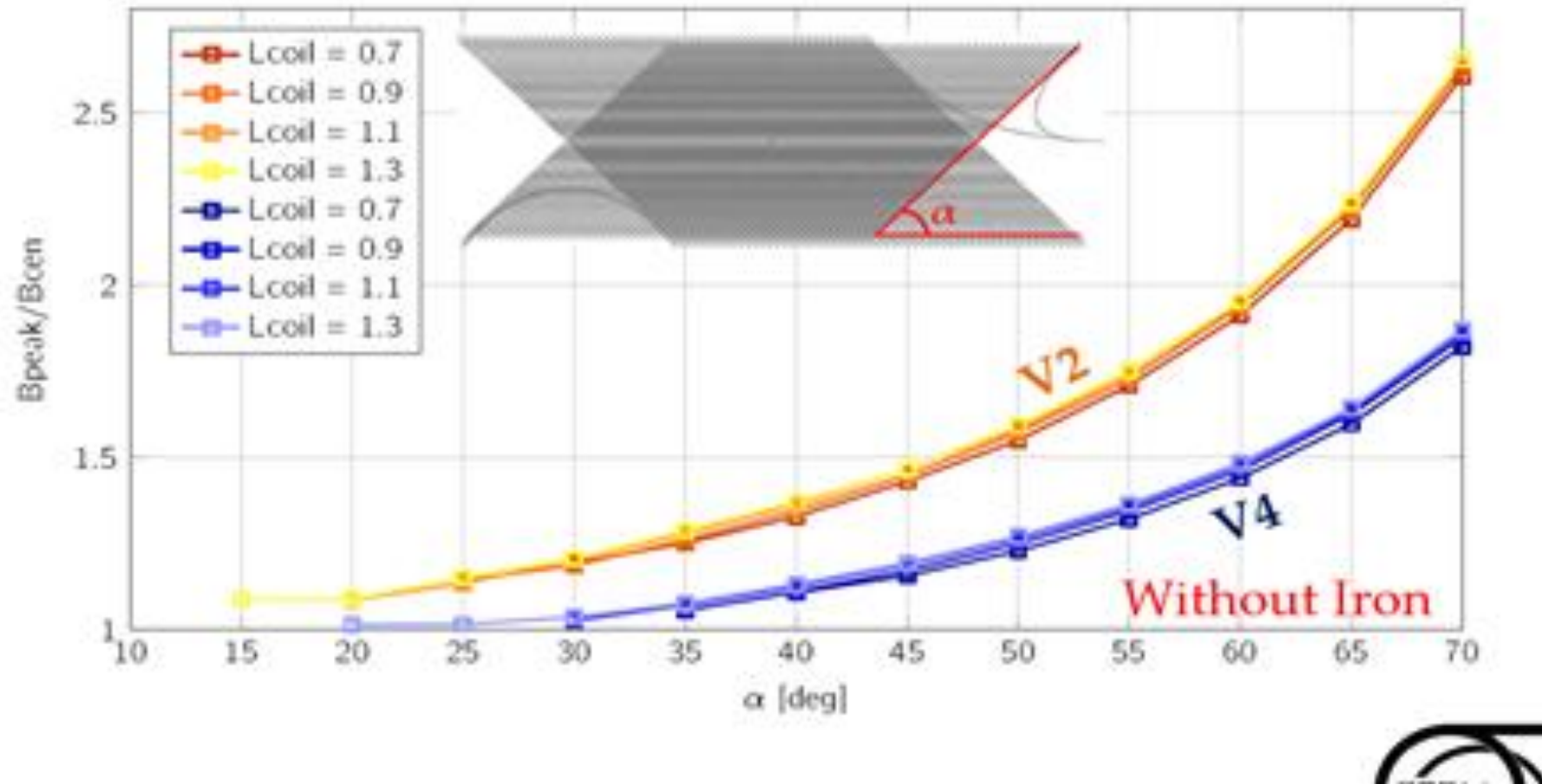
Optimization

- Two counteracting processes
 - Higher skew angle increases B_{peak}/B_{cen}
 - Lower skew angle increases length of coil ends
- Leads to a field integral optimized value for the skew angle



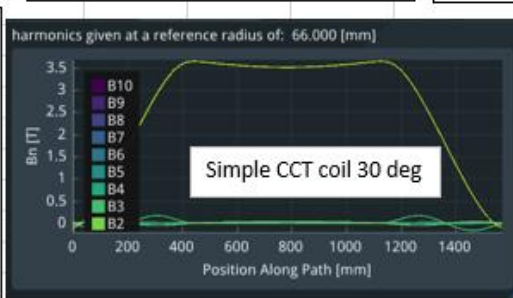
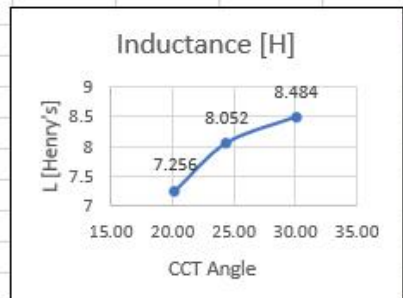
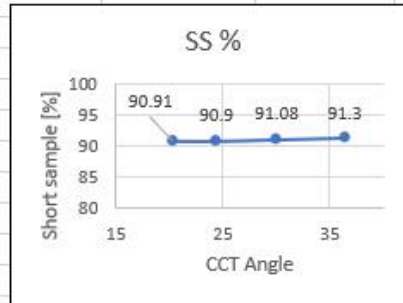
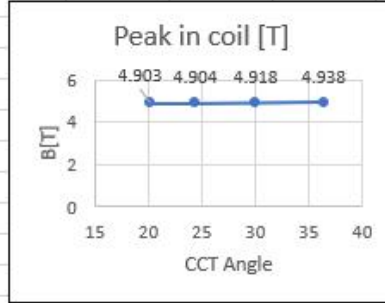
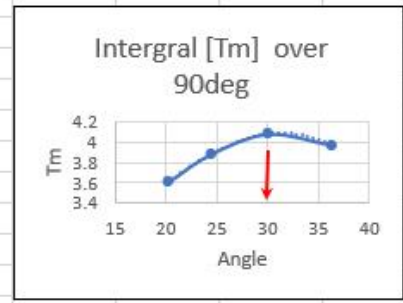
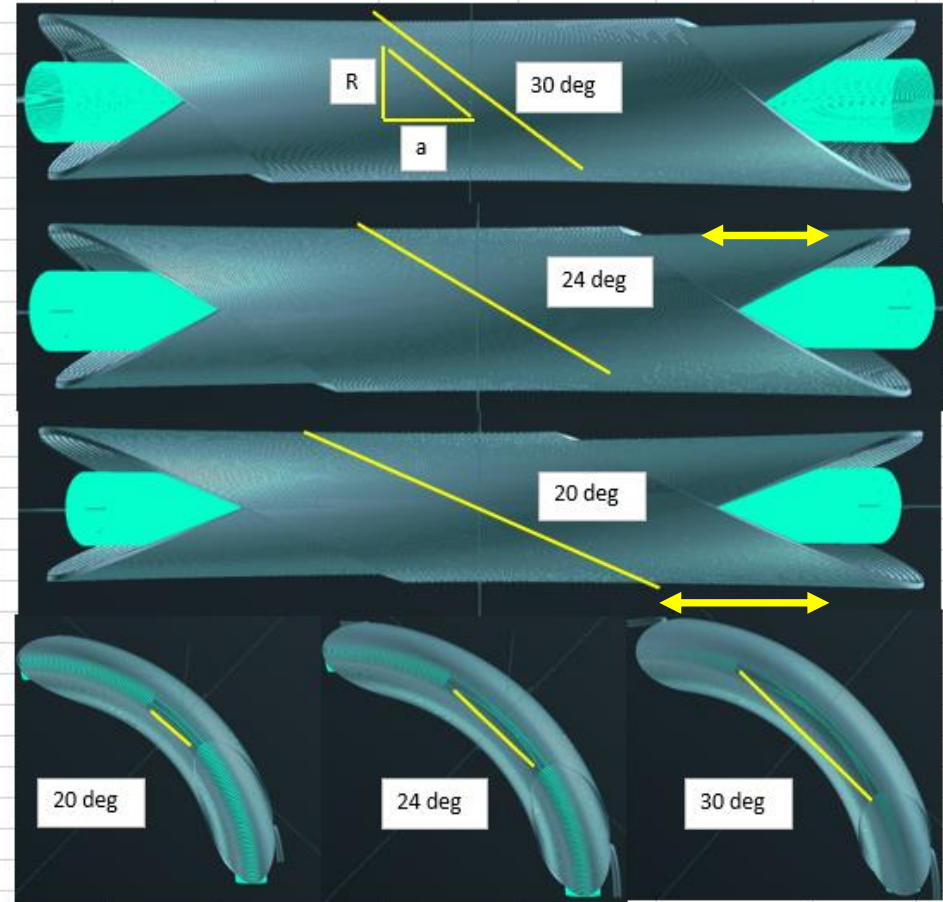
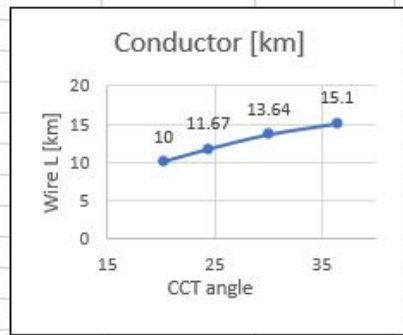
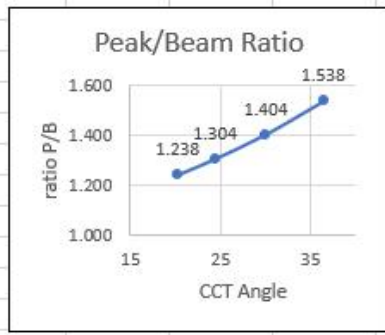
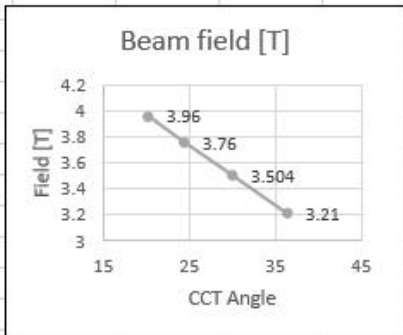
Skew Angle Influence

- Ratio B_{peak}/B_{cen} depends on skew angle and # of layers

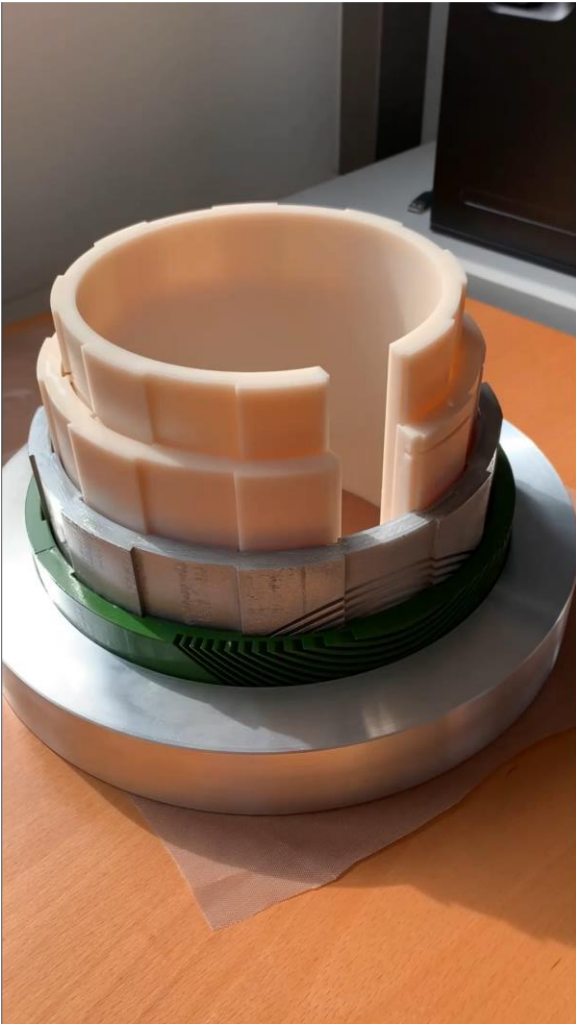


The basics of selecting the CCT angle

R	a	r/a	Bend angle	CCT Angle	SS %	I [A]	Min wall thk	Peak in coil [T]	Beam field [T]	Peak/Beam Ratio	turns	Conductor [km]	Channel turns	[Tm] over 90deg	Inductance [H]
118	160	0.7375	90	36.41	91.3	360	0.3	4.938	3.21	1.538	40	15.1	176	3.97	8.078
118	204	0.57843	90	30.05	91.08	360	0.3	4.918	3.504	1.404	40	13.64	142	4.083	8.484
118	260	0.45385	90	24.41	90.9	360	0.3	4.904	3.76	1.304	40	11.67	106	3.884	8.052
118	320	0.36875	90	20.24	90.91	360	0.3	4.903	3.96	1.238	40	10	80	3.607	7.256

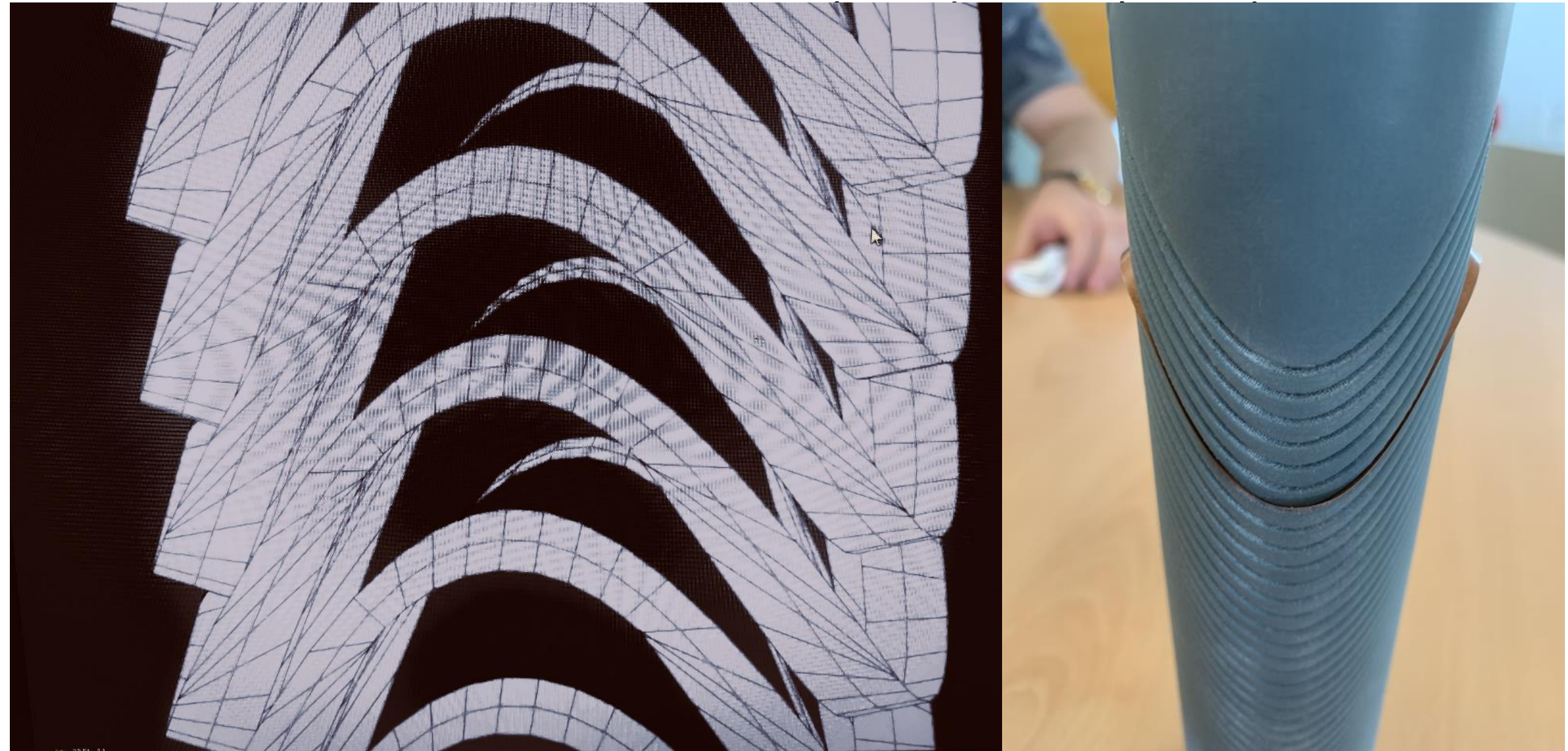


Nested castellated support between coil formers to support the very high torque

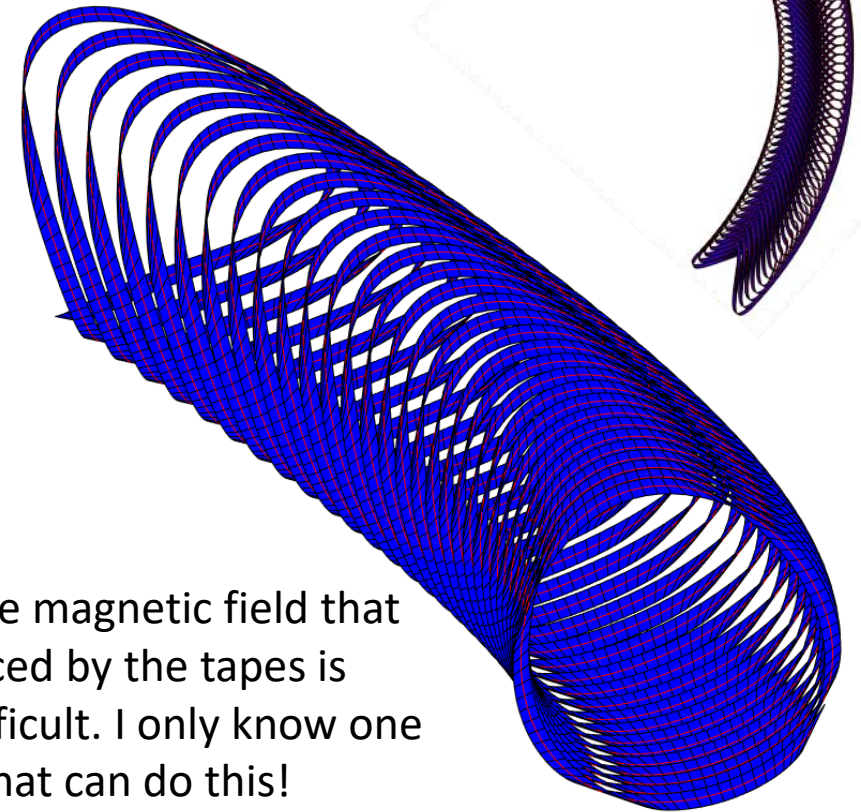
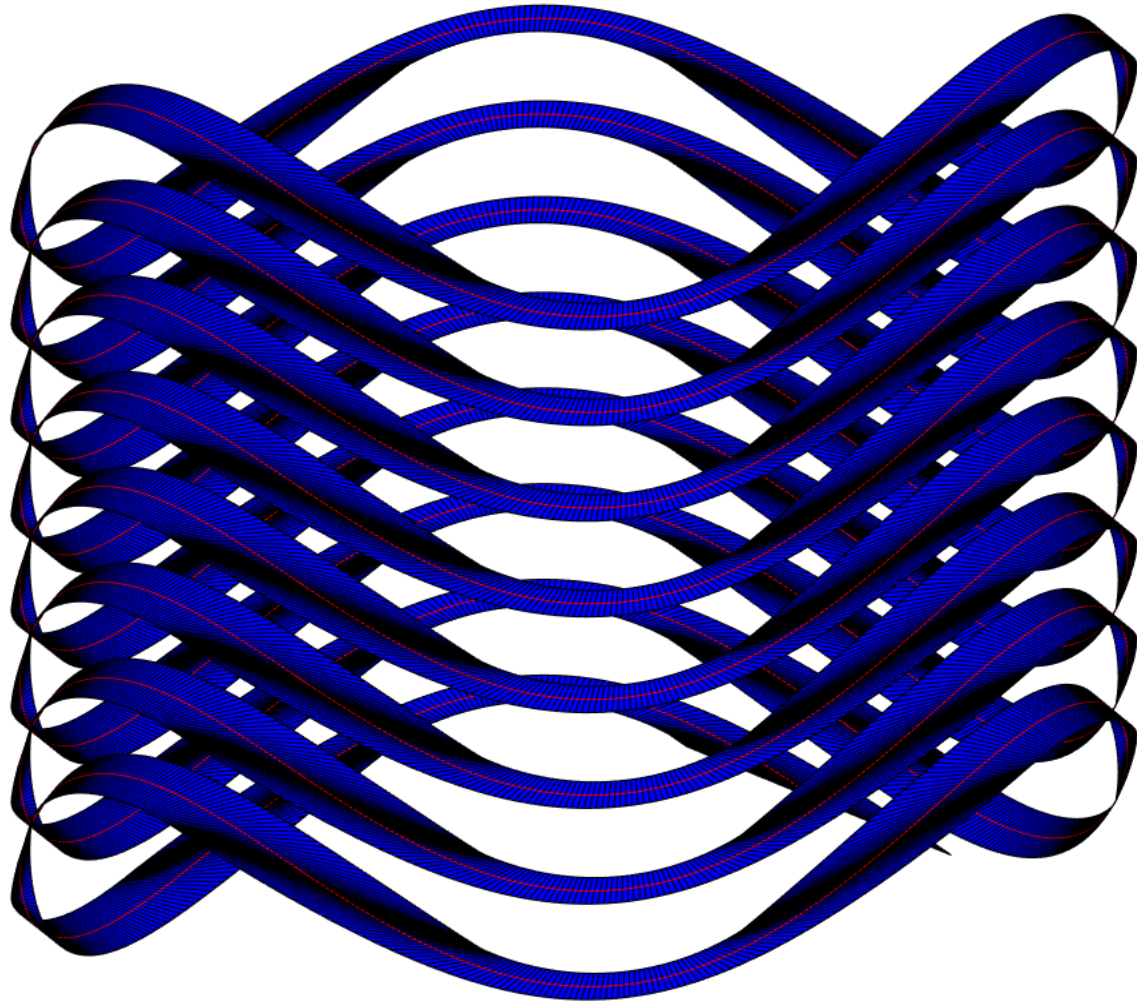


This magnet has the torque of 140 *F1* race cars in 1 m length

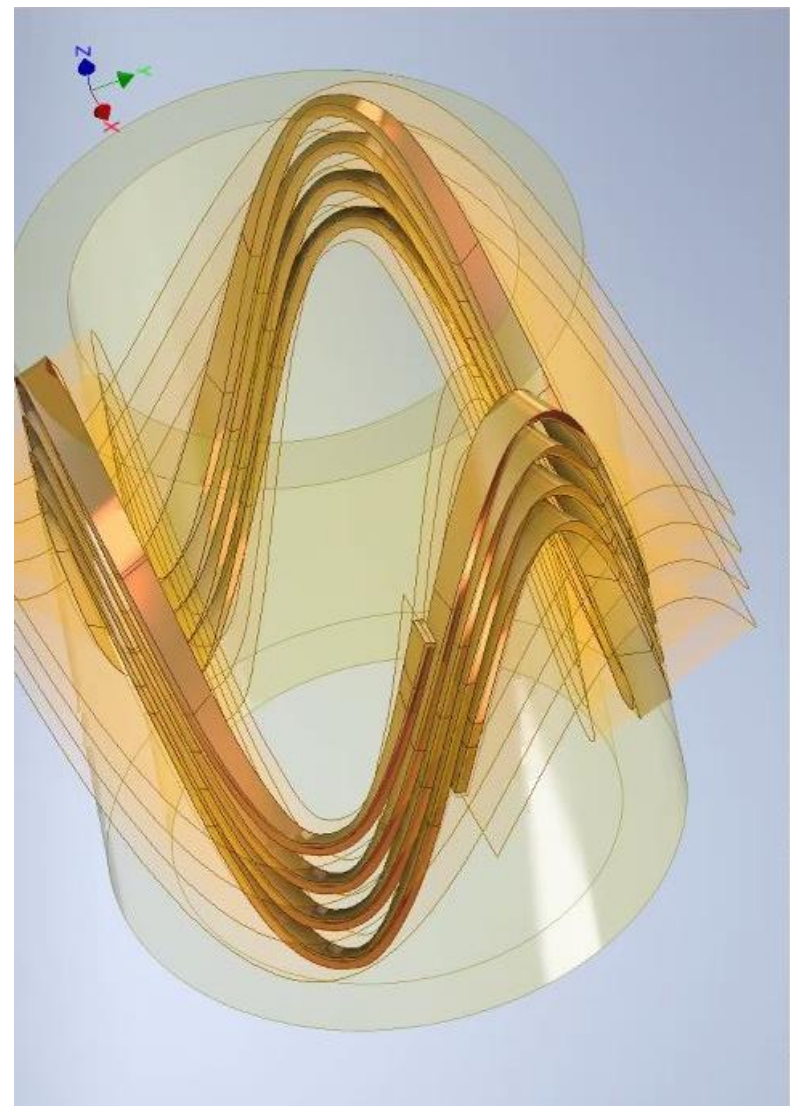
Thanks to Thomas Nes who has taken his zero-bend calculation for HTS tapes and added CCT



Zero hard way bend in the tapes that are following the CCT guiding line



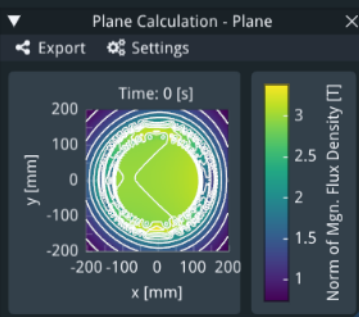
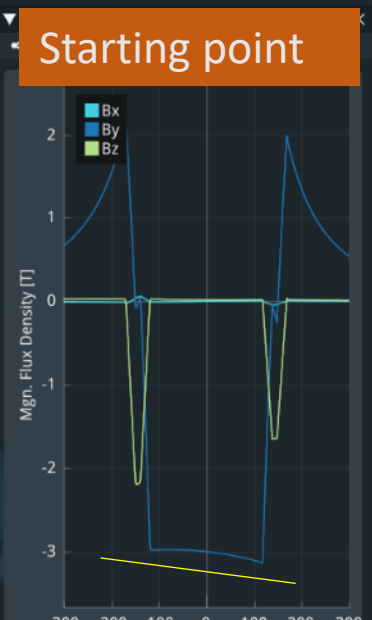
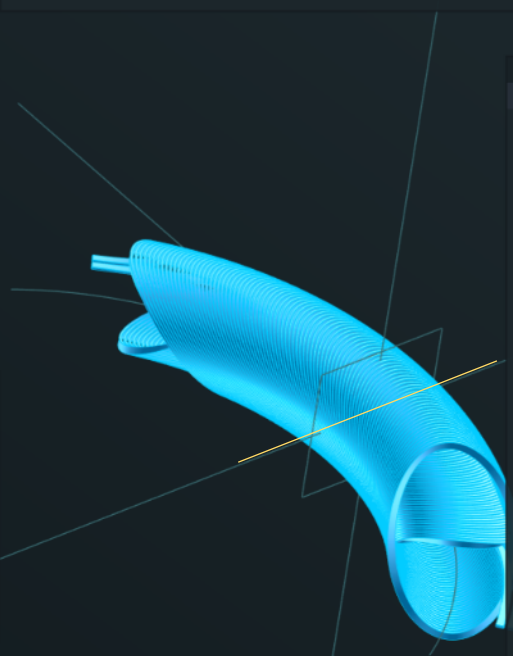
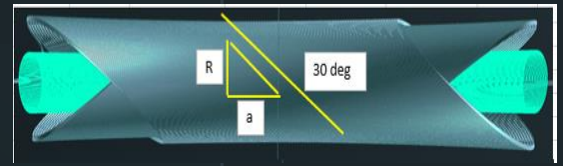
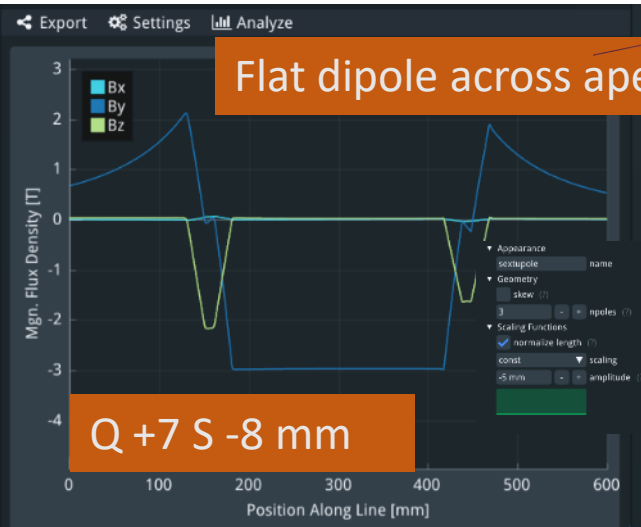
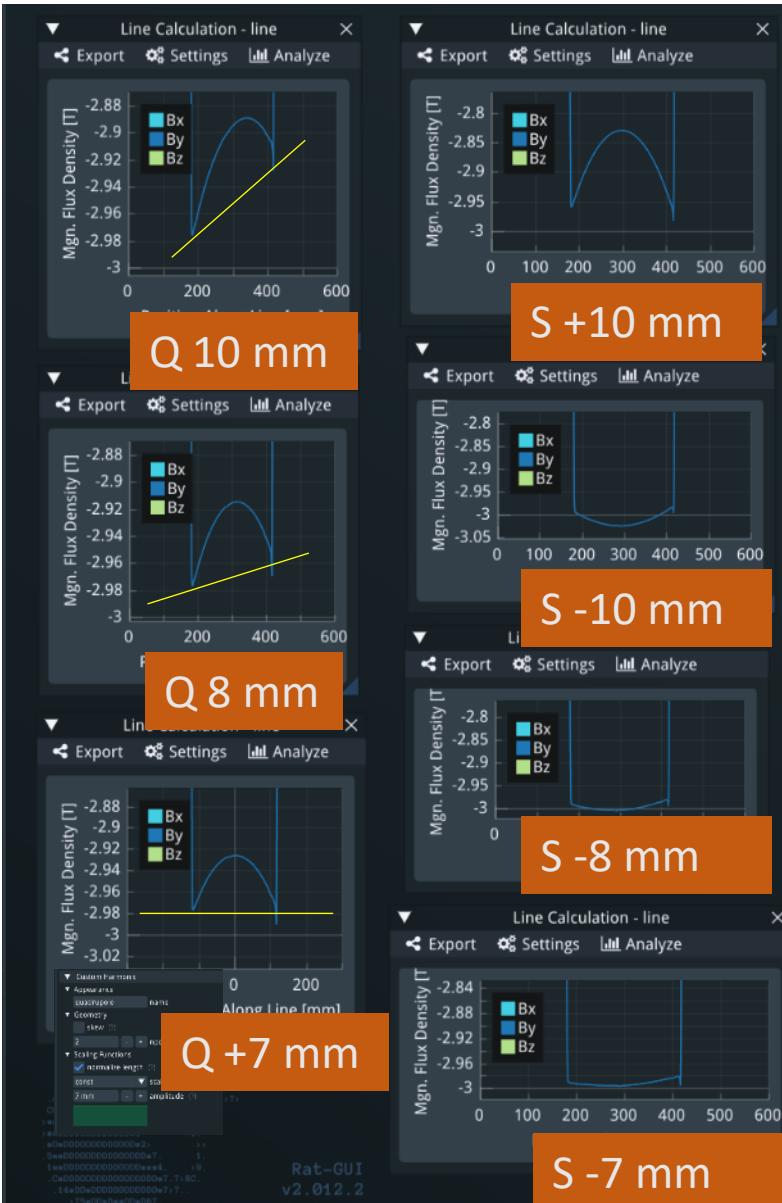
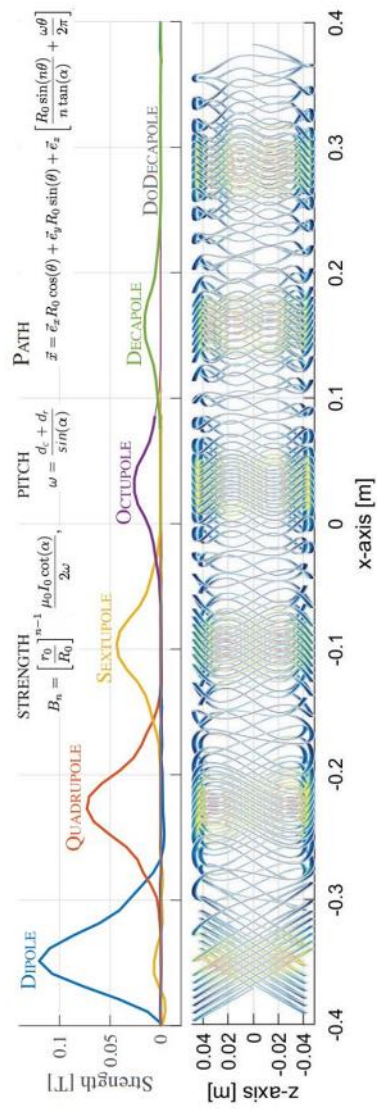
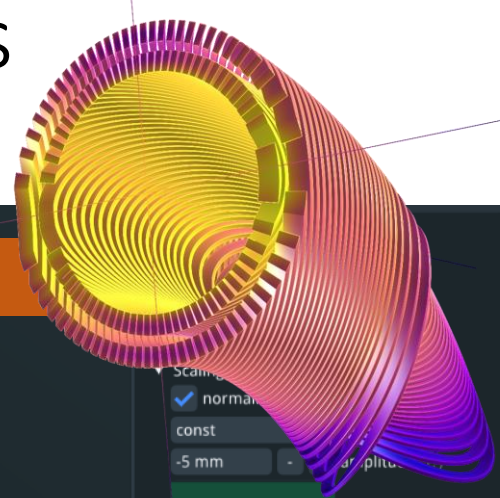
To get the magnetic field that is produced by the tapes is more difficult. I only know one person that can do this!



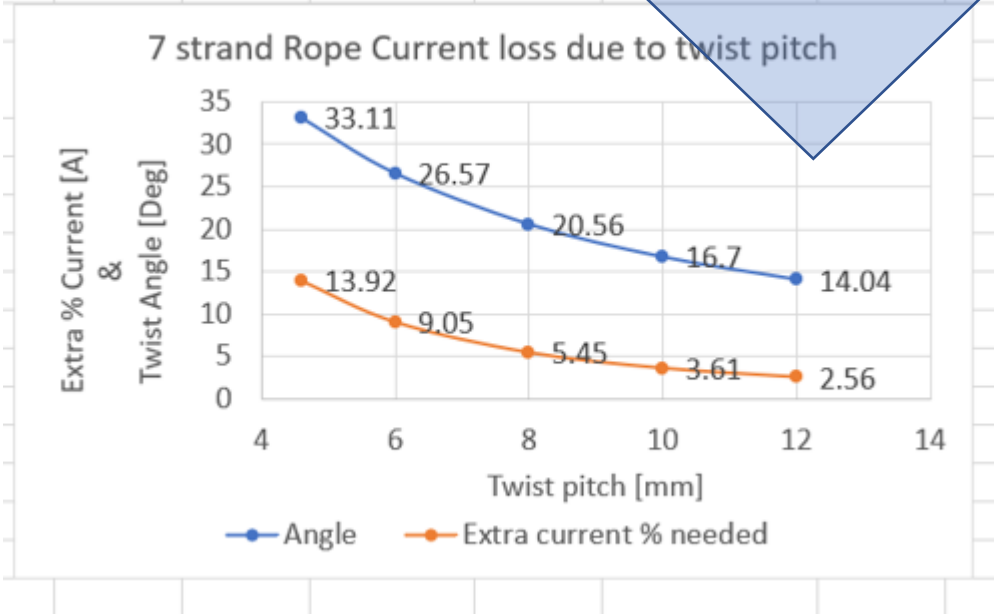
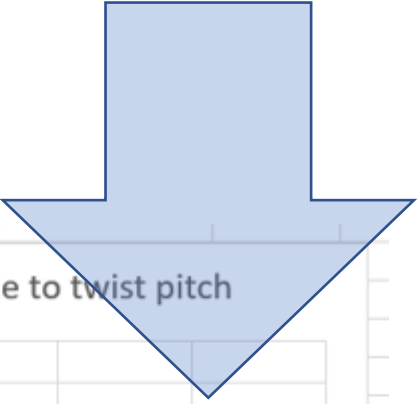
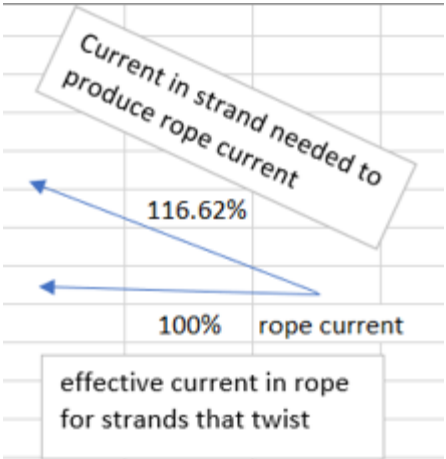
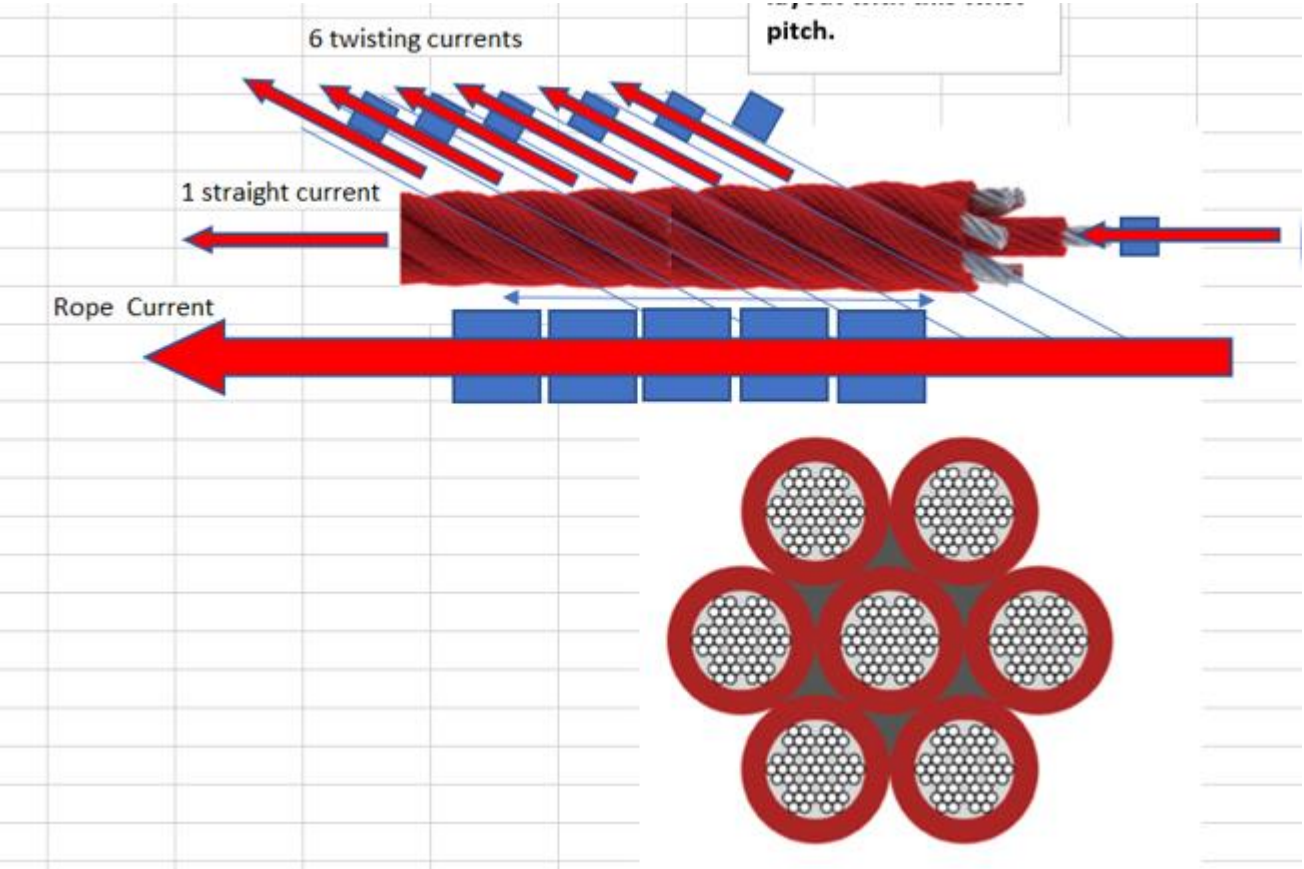
REBCO CCT IDEARS Quad & Sextuple paten pending!

Dipole gradient adjustment with combined functions Quadrupole and Sextupole

(first pass to correct not fully optimized)

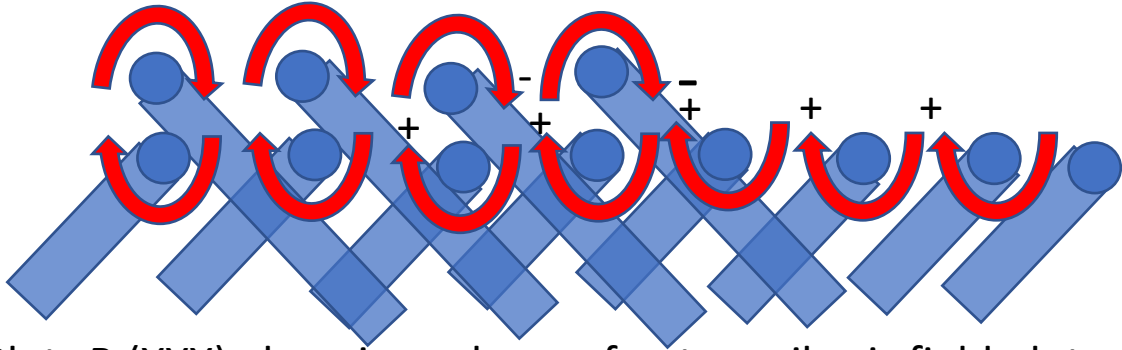


Rope twist pitch angle losses in effective current.

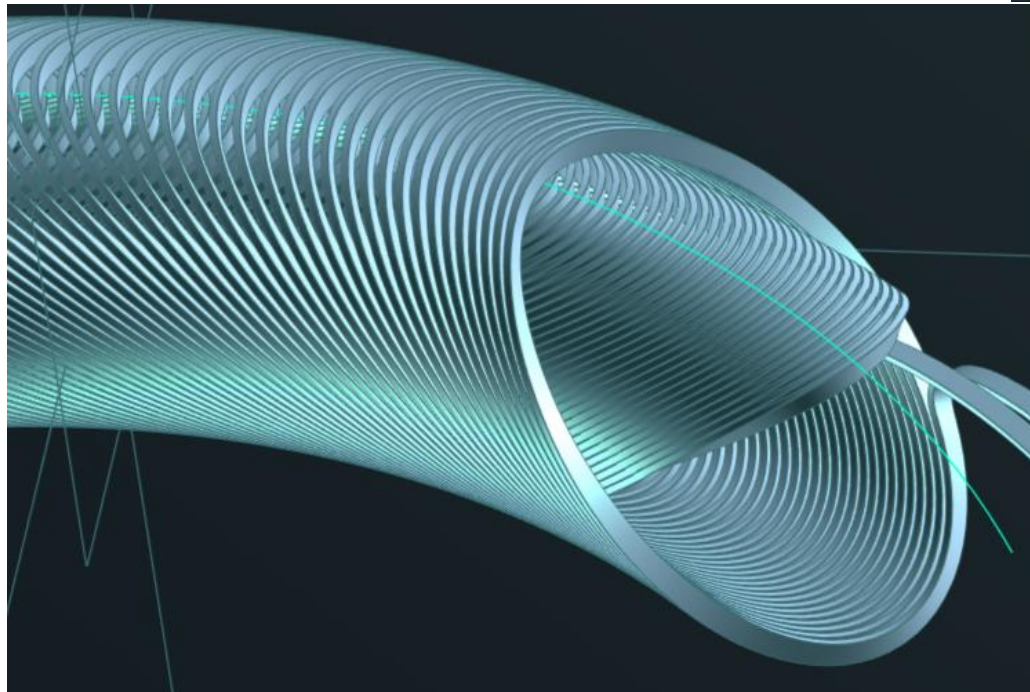
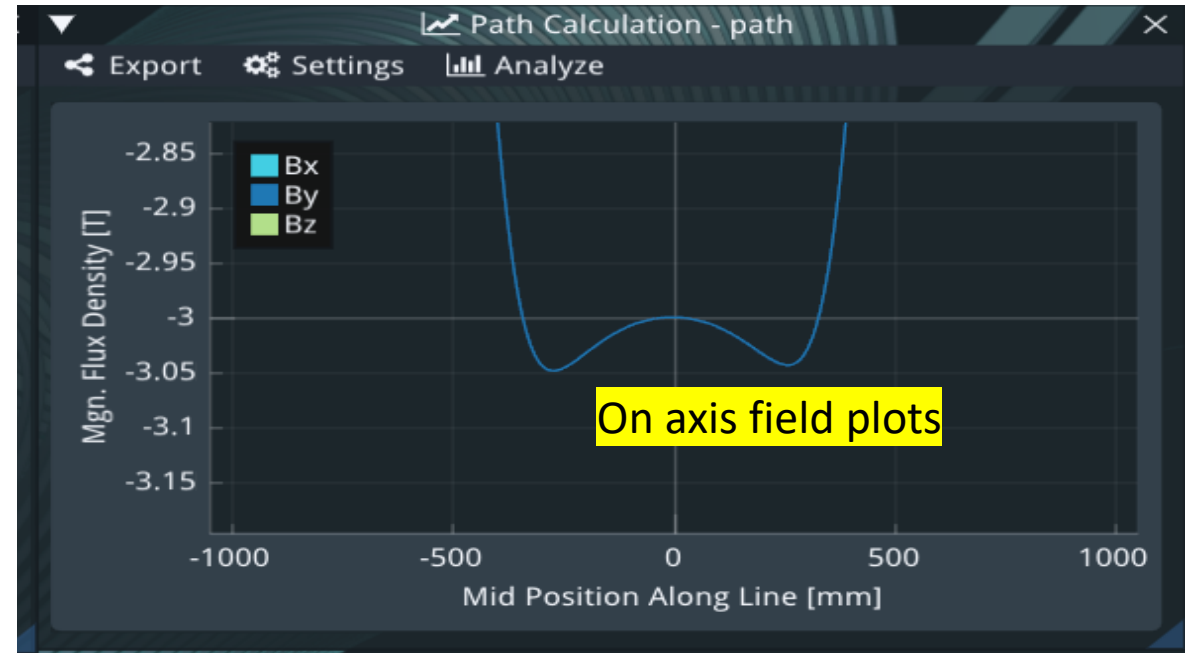


Peak field in ends

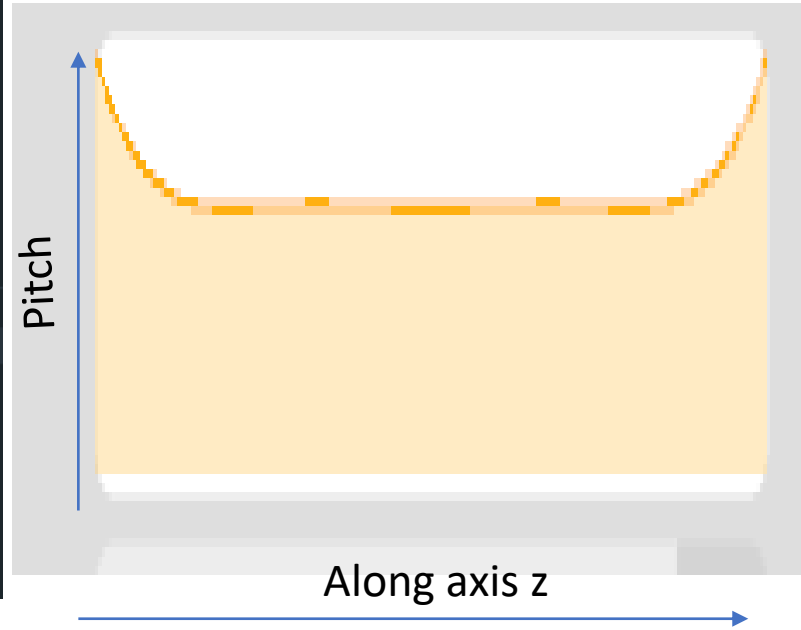
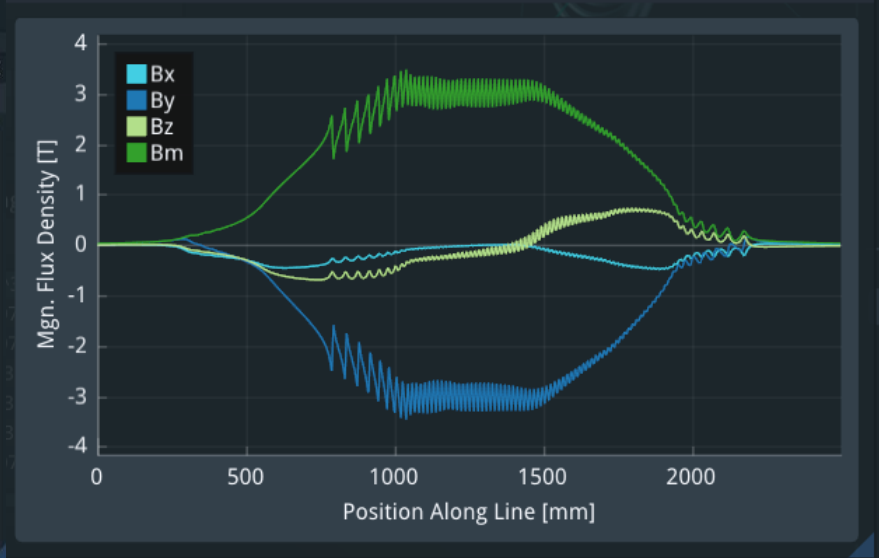
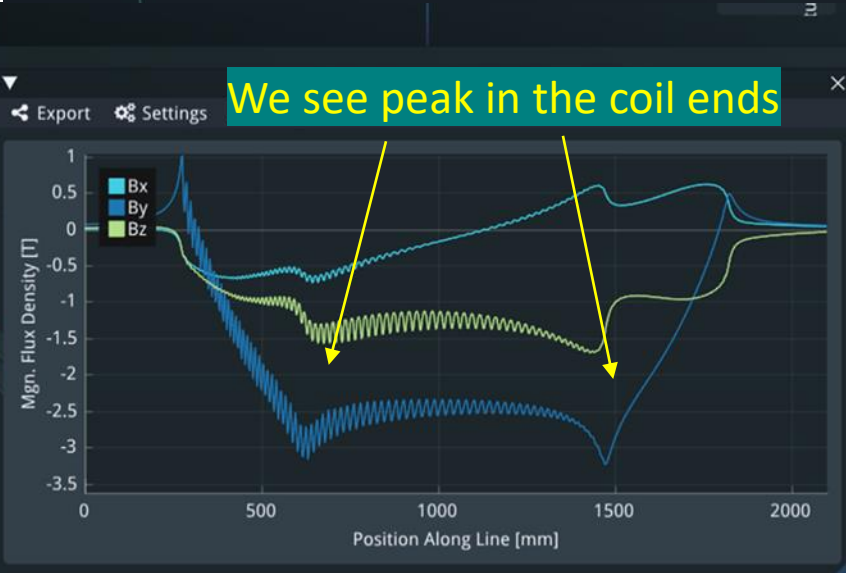
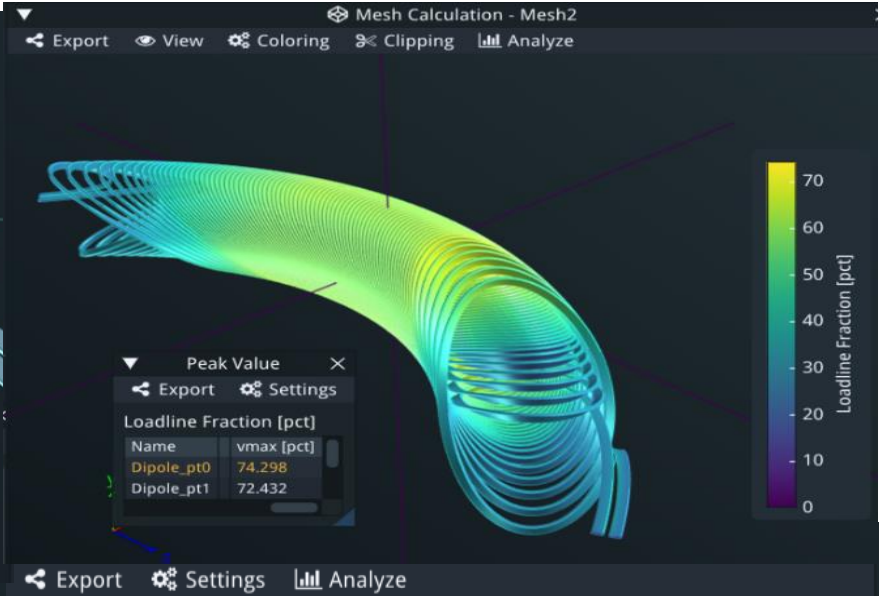
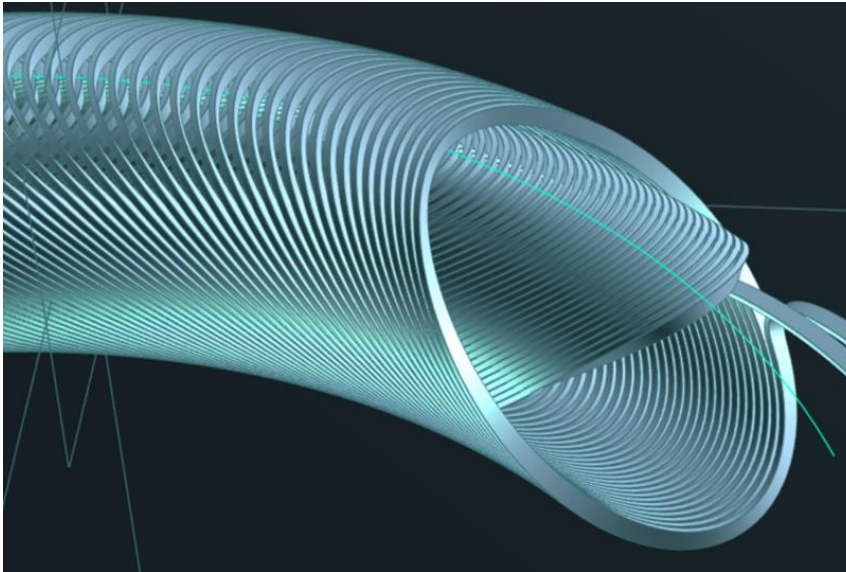
The peak field is at in the coil ends and occurs due to the not having an infinitely long coil,



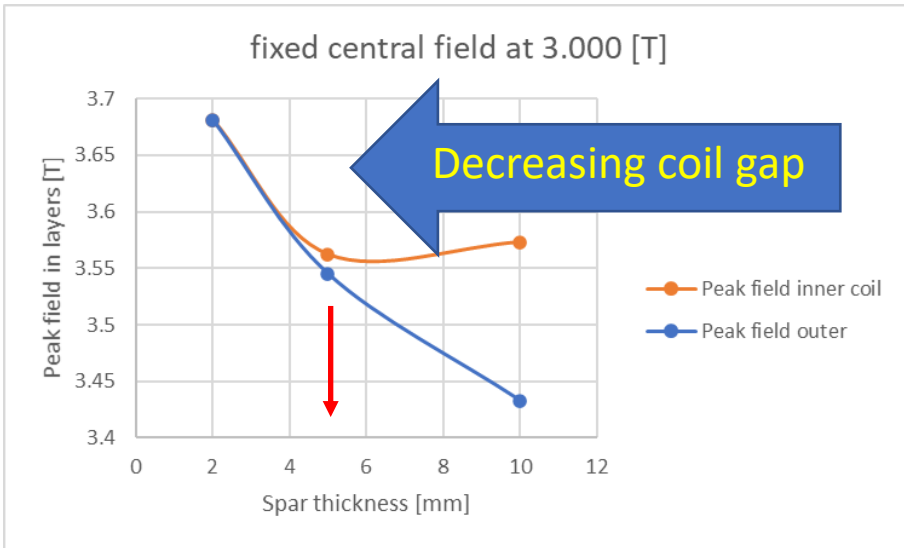
Plots B (XYX) along inner layer of outer coil axis field plots



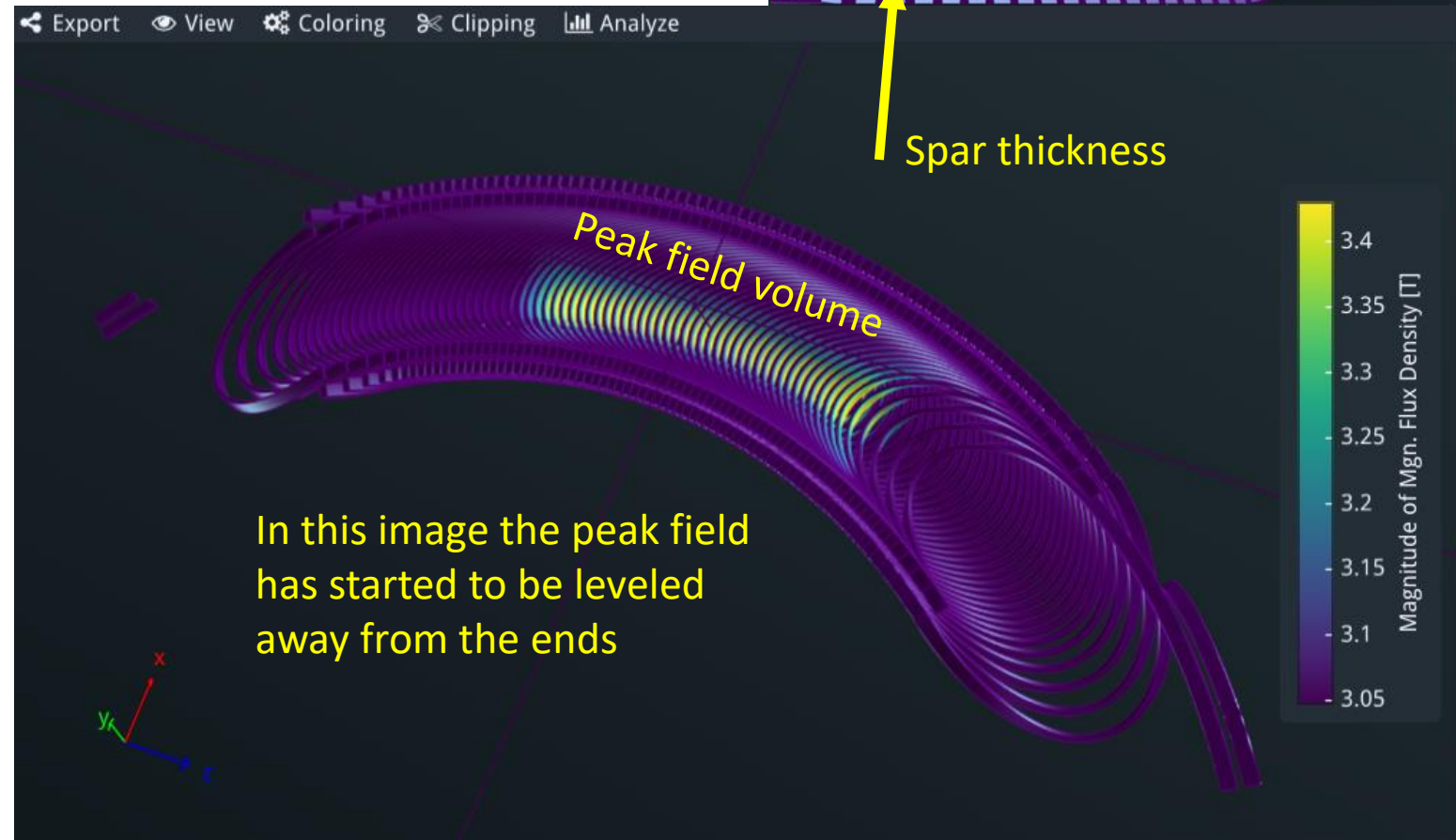
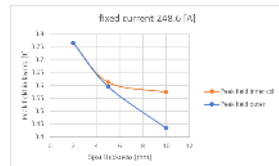
Peak field Smoothing



Peak field due to spar thickness or more precisely the gap between coils



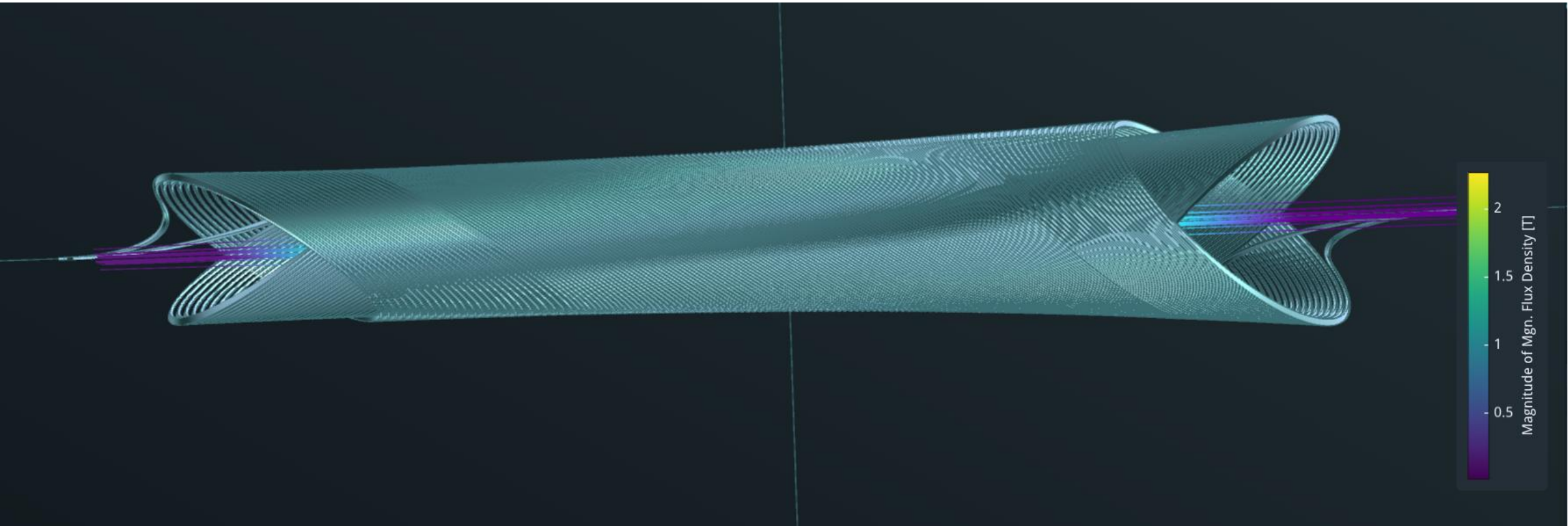
As the SPAR reduces in thickness the layers get closer and at 5 mm (for this coil) both inner and outer coil peak field are equal further reduction in the gap increases peak field



In this image the peak field has started to be leveled away from the ends

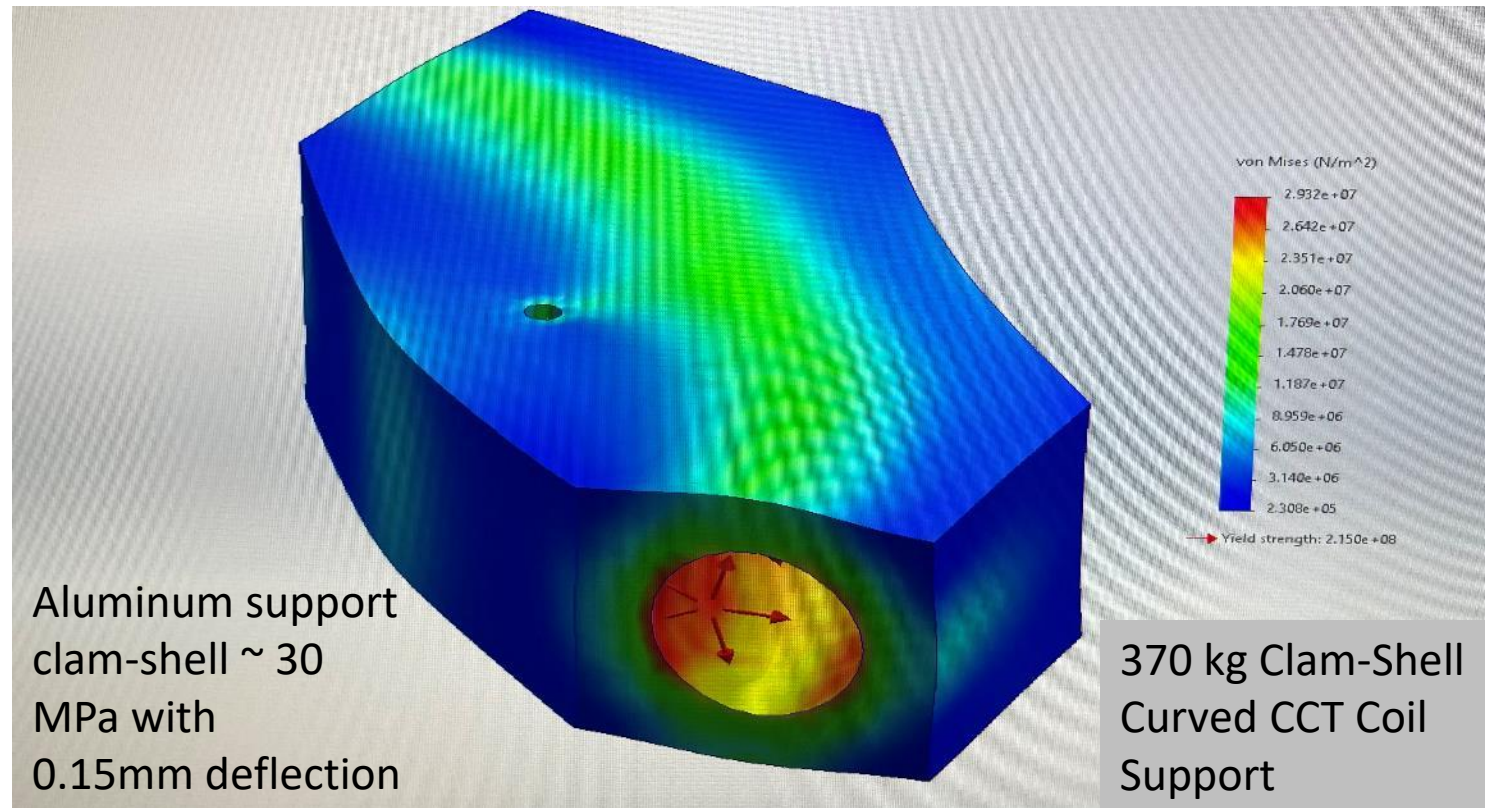
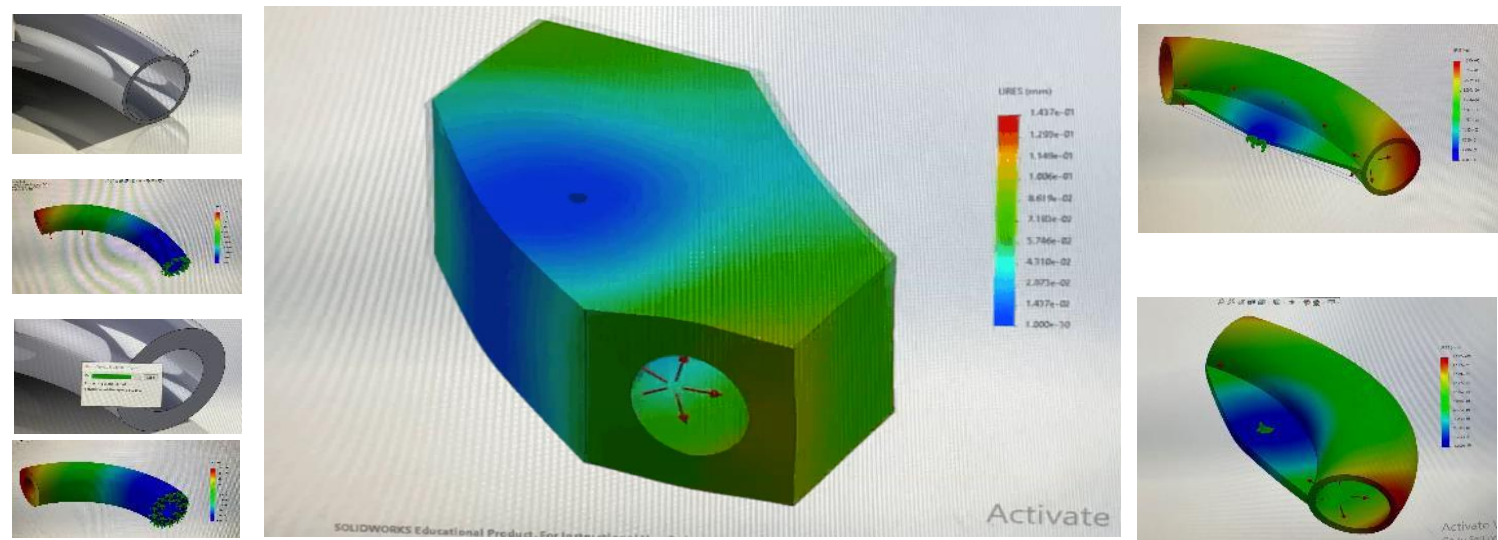
Tapered Coil aperture 230 mm to 235 mm

this helps with *assembly* and *radial pressure*,
but the taper produces a skew quadrupole that is then corrected out!



Coil Support Conceptual Design deflection stress

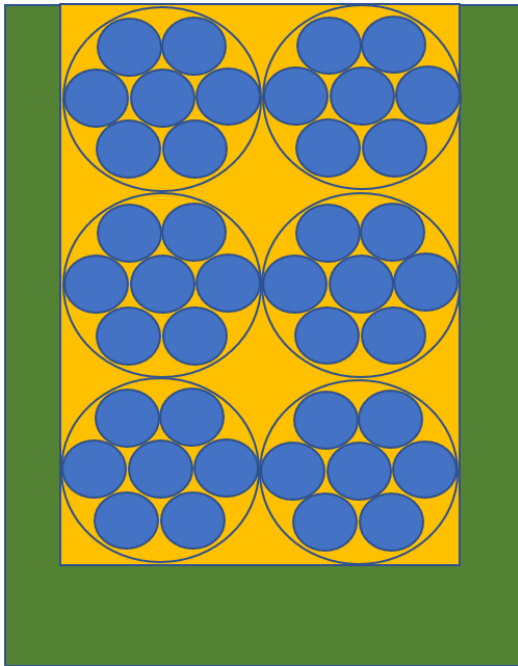
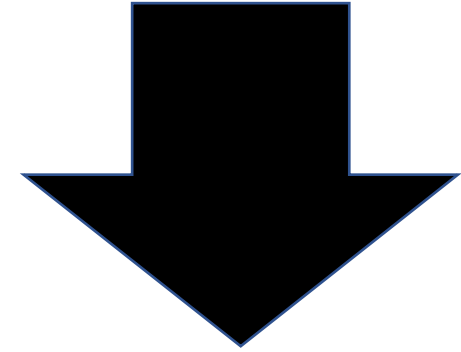
The initial support was just a thin 15 mm thick curved tube as in MCBRD! however, the deflection with a curved coil ~ 80 mm. Increasing the thickness to 100 mm reduced the deflection to about 4 mm. reducing the tube to 20 mm thick and adding a 10 mm thick wed reduced the support's mass, but the deflection was still 4 mm. increasing the wed to 20 mm took the deflection to 1 mm. The pragmatic massive aluminum block clam-shell design reduced the deflection to ~ 0.15 mm with Von Mises max stress at ~ 30 MPa the support block mass is ~ 370 Kg. This is just an initial look at the deflection and using internal pressure derived from the magnetic forces in the magnet at 3 tesla. Targets are 2.2 T, < 0.3 mm deflection , & stress < 200 MPa.



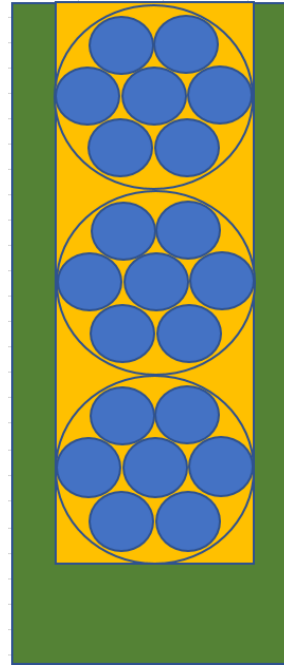
Thanks to Oliver Kirby for the modelling

Channel layouts *some ideas*

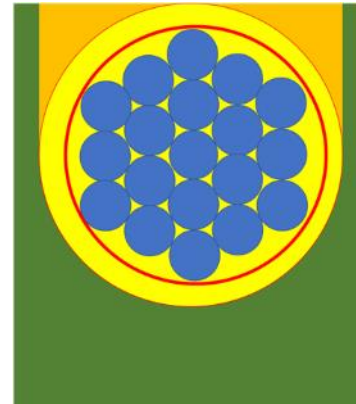
Some channels with different packing lay out



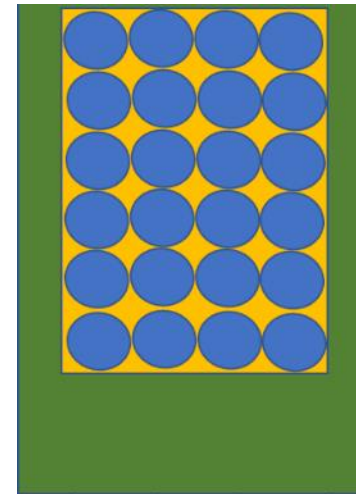
6 x 7 strand
ropes 42 wires
~5 kA
Je 61.09 %



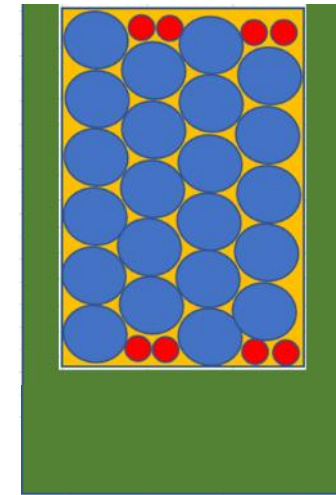
3 x 7 strand ropes
21 wires ~ 5 kA
Je 61.09 %



19 strand rope
13.5 kA
Je < 59.6 %



24 wires
710 A
Je 78.54%



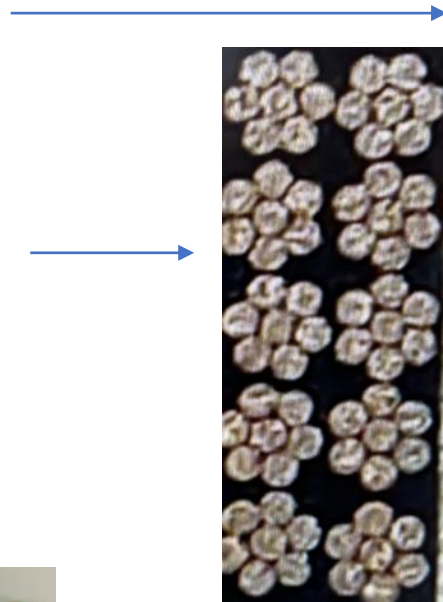
22 wires
710 A
Je 83.8%

Log Stacking

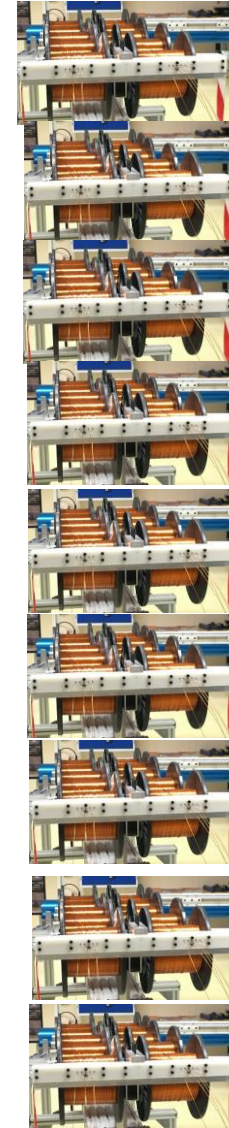
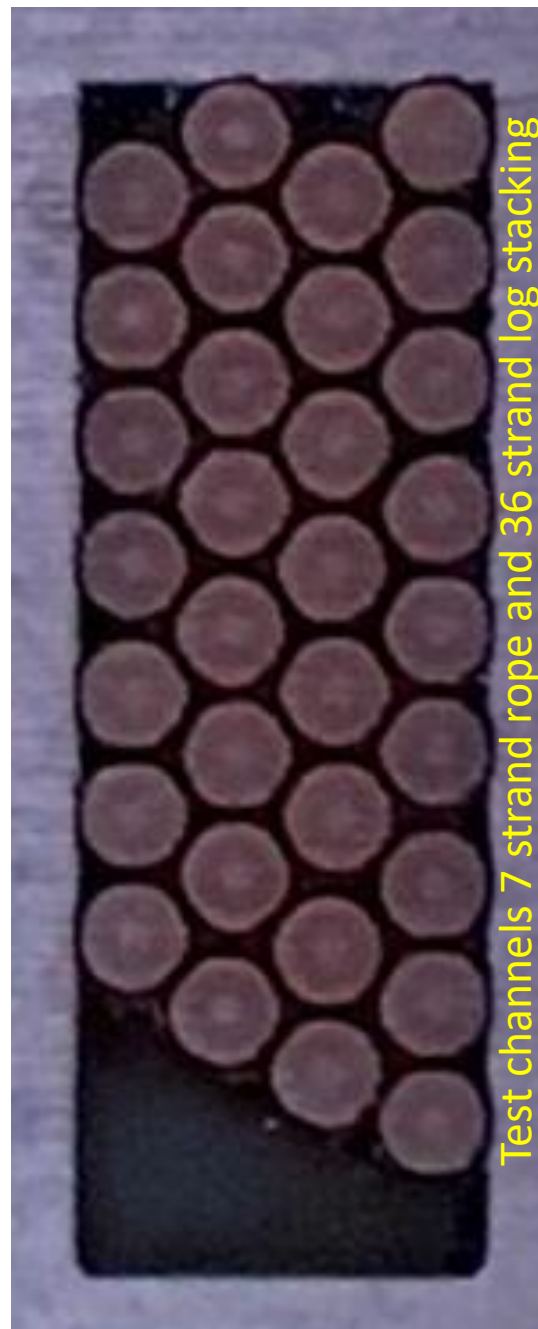
Layout in channel	Je %
Log stacking	83.8
Rectangular stacking	78.45
7 strand rope	61.09
19 strand rope	59.6



10 spools

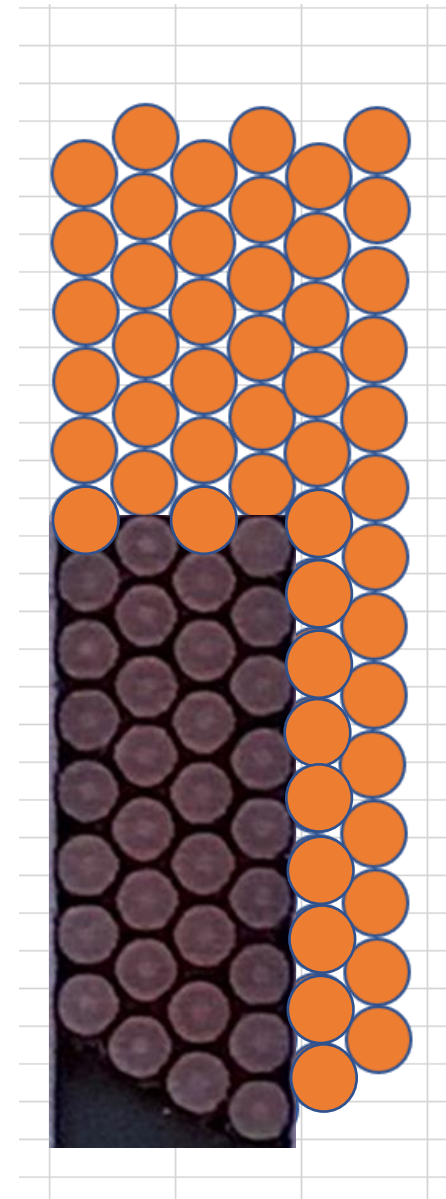


MCBY coil pack
in Sweden
7 strand rope
0.3mm strands



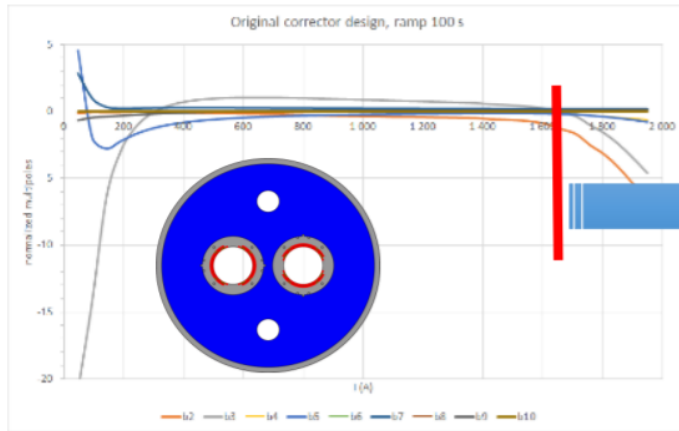
90 spools

?
Fusillo 84 strand log stacking with
chisel base to add stacking



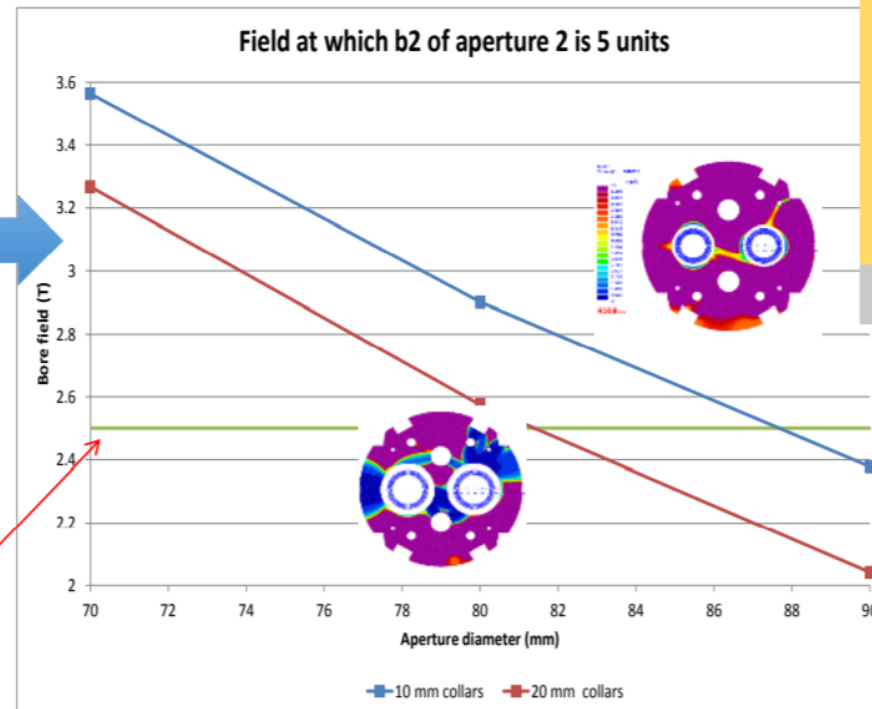
Yoke steel between apertures?

- Low current option – cross talk
- MQY yoke diam. (475 mm) & 10/20 mm collars.



Ref magnet Harmonics
f(current) at 100 sec ramp

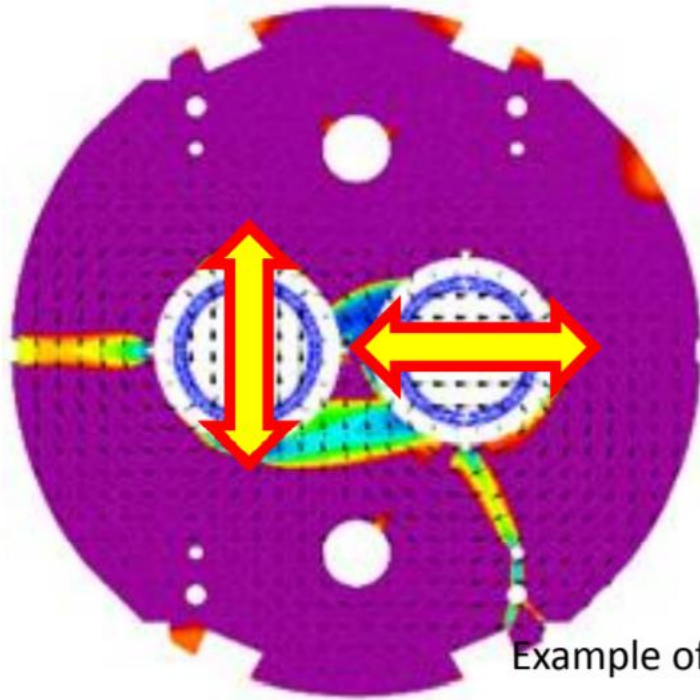
Limit of **4.5 Tm** & ~1.8 m magnetic length



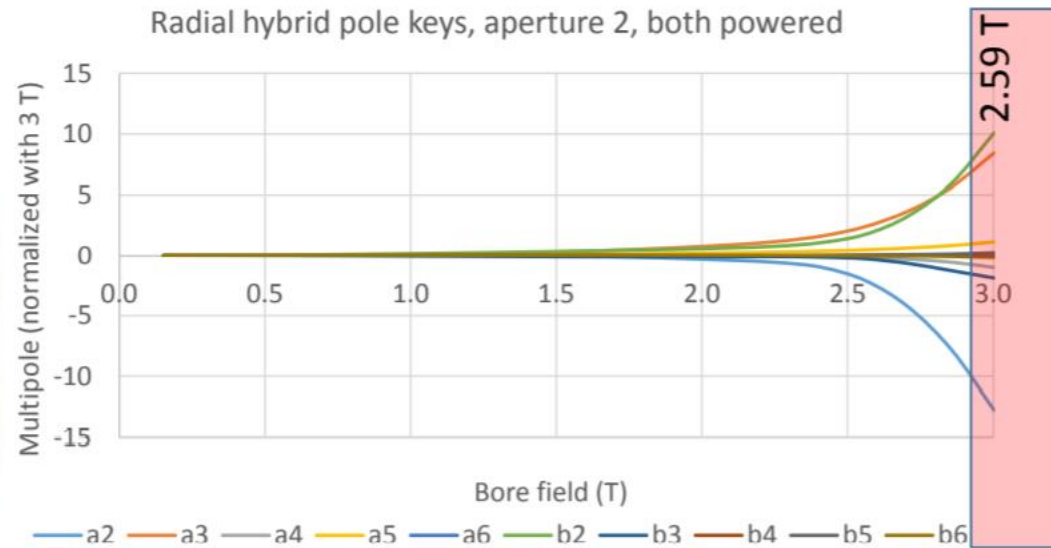
Bore field	Magnetic length
2	2.25
2.1	2.14
2.2	2.05
2.3	1.96
2.4	1.88
2.5	1.80
2.6	1.73
2.7	1.67
2.8	1.61
2.9	1.55
3	1.50
3.1	1.45
3.2	1.41
3.3	1.36
3.4	1.32
3.5	1.29
3.6	1.25
3.7	1.22
3.8	1.18

Magnetic Field Optimization, Independently powered apertures

- To achieve 5 Tm field integral with less than 10 units we first determine the **maximum field in one aperture** that will not pollute the field quality in the adjacent aperture.

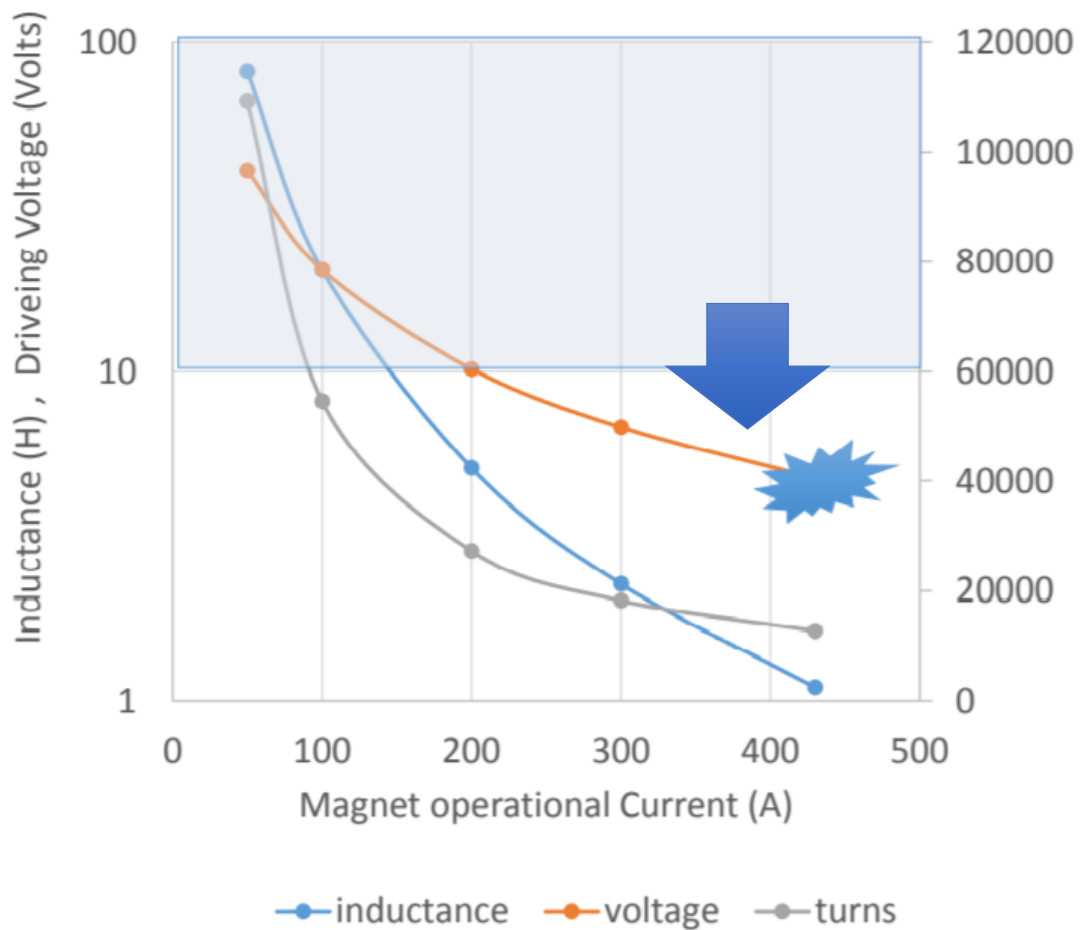


Example of one configuration Presenting harmonic solution due to high field in the adjacent aperture



More complicated than one plot, Details to follow!

100 sec driving voltage



+&- 600A, 4 quadrant, 10 V, with 0.7 to 1.0 ohm Dump.

Approximate Power supply Costs

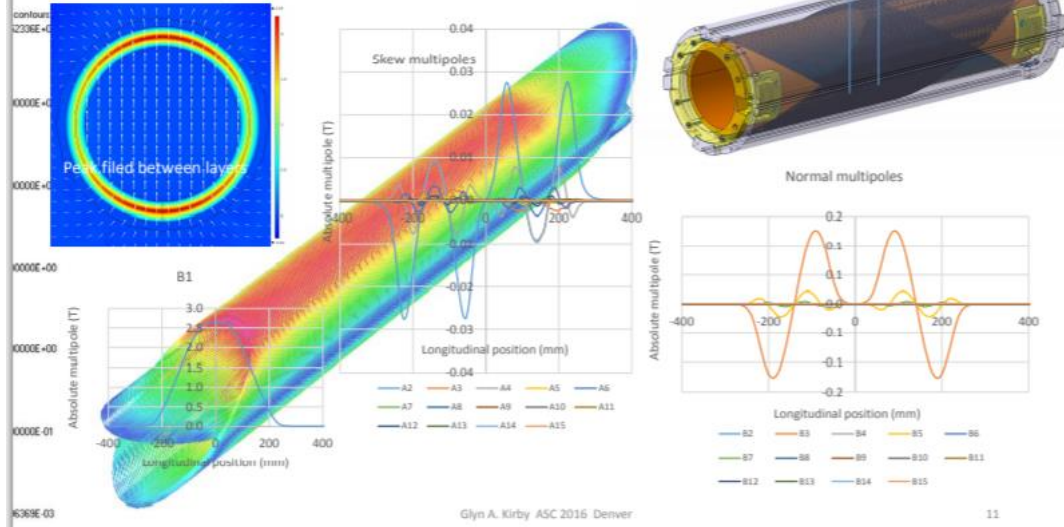
Power converter	Current	Voltage	Quadrant	Unit price KCHF
Type 1	16.5kA	20V	1	500
Type 2	13kA	18V	1	350
Type 3	6kA	8V	1	200
Type 4	±2kA	±10V	4	150
Type 5	±600A	±10V or ±40V	4	50
Type 6	±200A	±10V	4	10
Type 7	±120A	±10V	4	10

<http://te-epc-lpc.web.cern.ch/te-epc-lpc/general.stm>

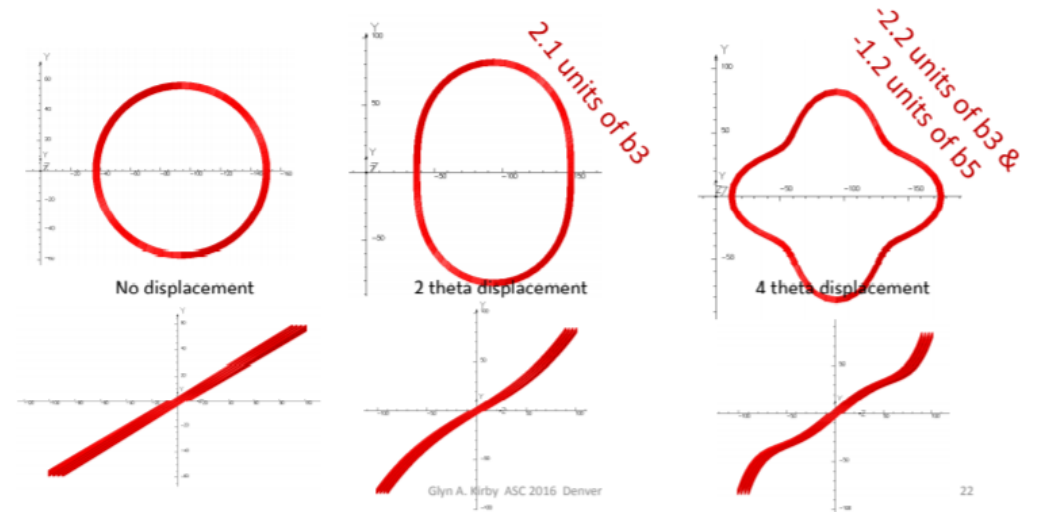
Power In 3 ~ 230V/16A
 Power Out +/- 600A +/-10V (or +/-40V)
 Converter Type 4 Quadrant
 Control type FGC2 / WorldFip
 Current Accuracy 10 ppm@ 30 mn
 50 ppm@ 24 h
 200 ppm@ 1 year
 (1 ppm=0.6mA)



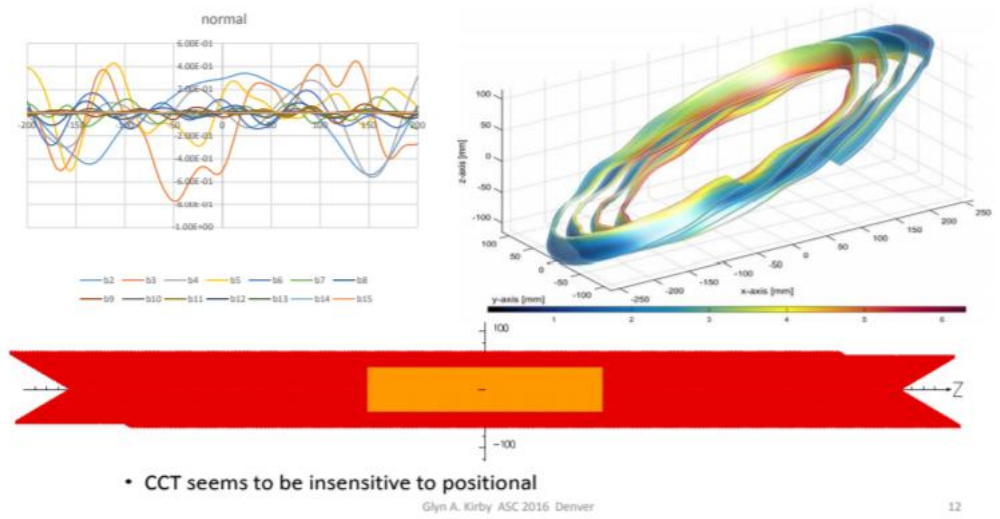
CCT Field profiles



50 microns systematic radial errors

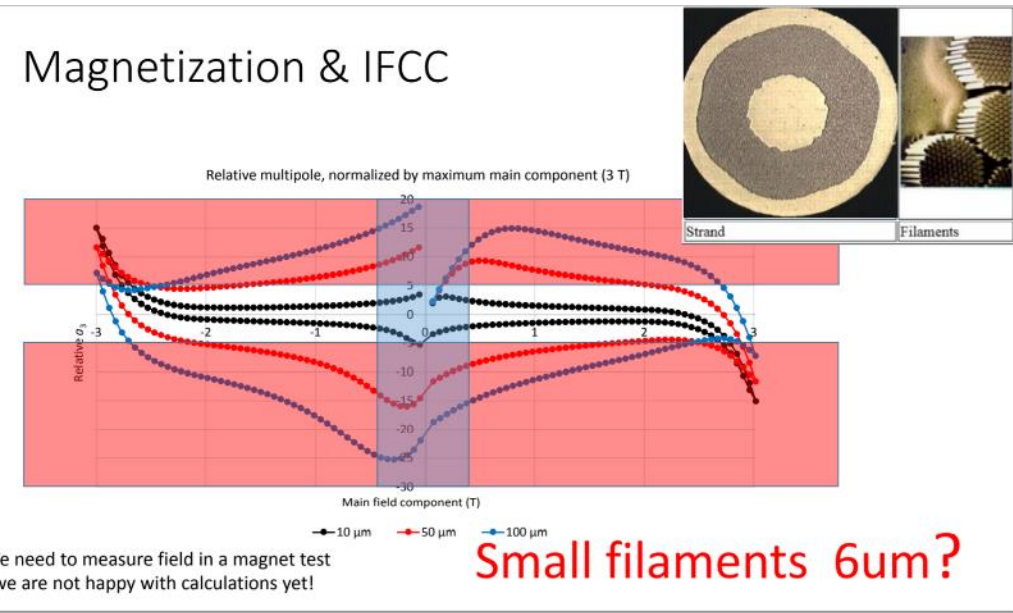


CCT Random multipoles with 50 μm displacements



• CCT seems to be insensitive to positional
Glyn A. Kirby ASC 2016 Denver

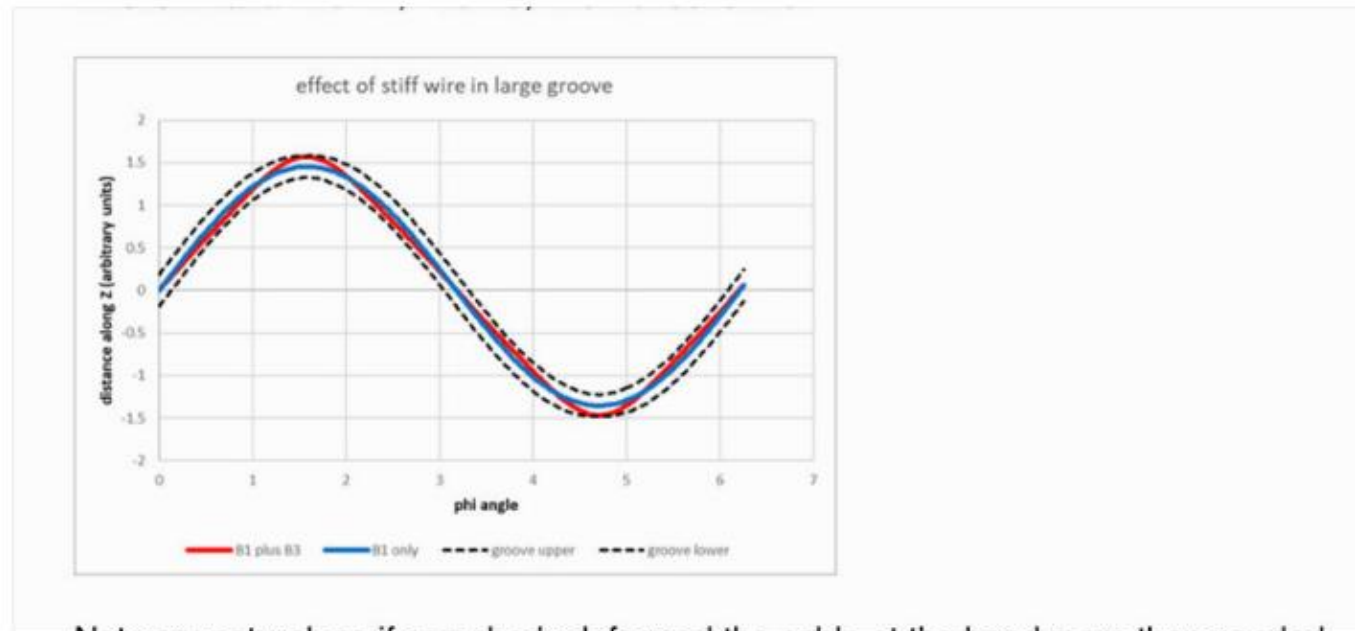
Magnetization & IFCC



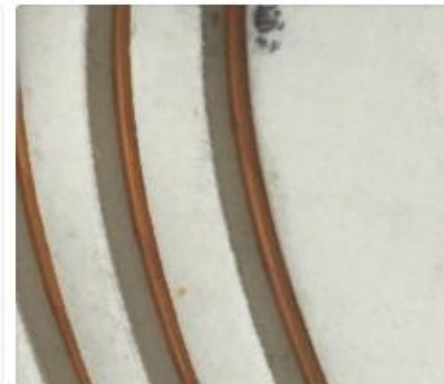
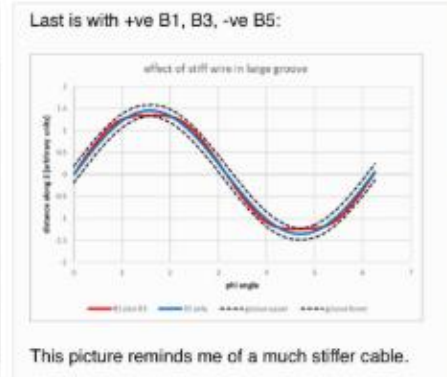
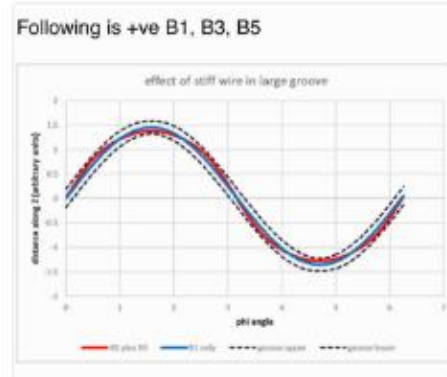
? We need to measure field in a magnet test
As we are not happy with calculations yet!

Small filaments 6μm?

Effect of wire placement in channel

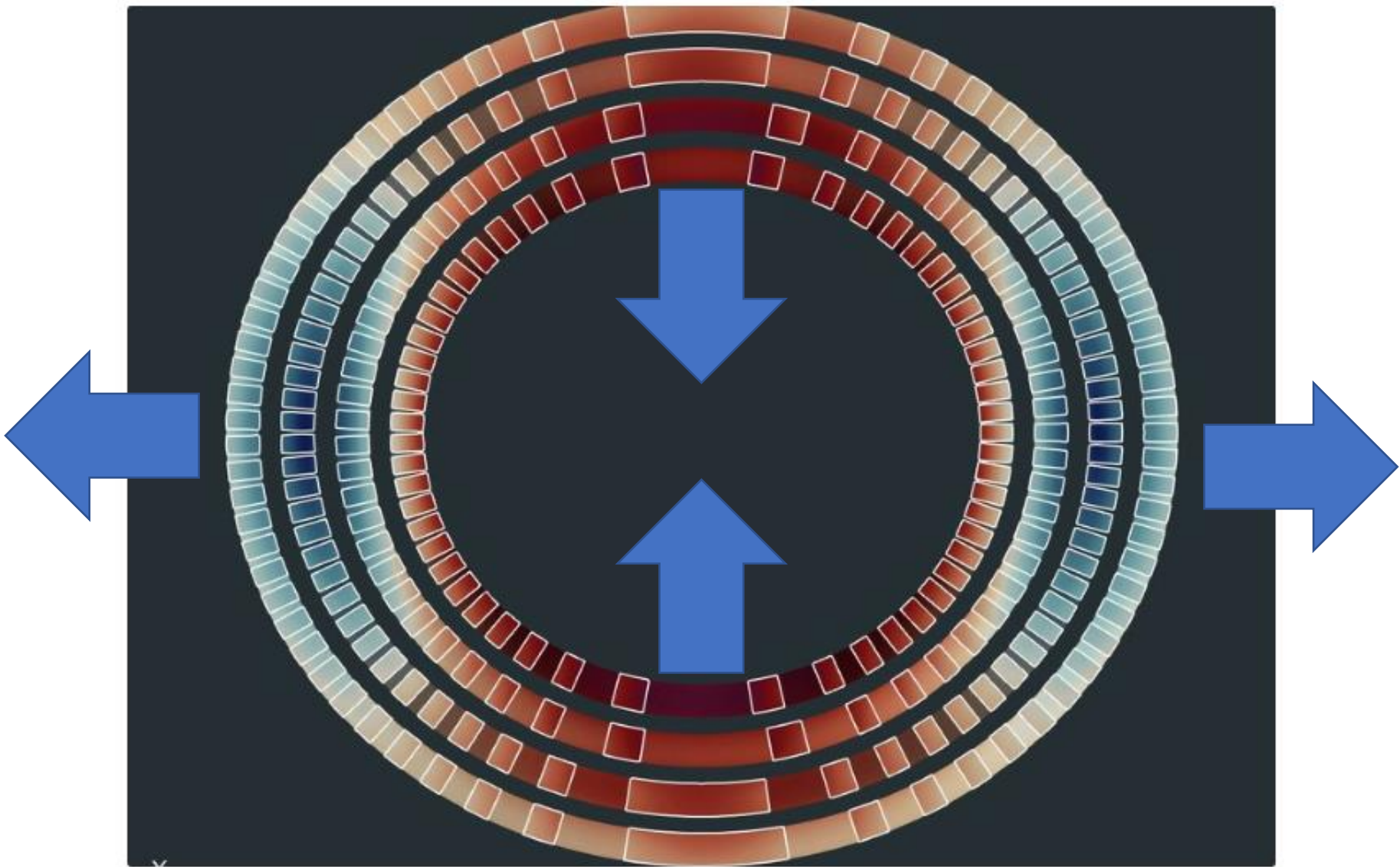


Not very natural as if some body deformed the cable at the bend more than needed



This picture reminds me of a much stiffer cable.

Some Calculations to look at field errors due to wire misplaced in the channel



Field errors due to coil deformation.

We calculated the effect on the field quality of a squeezed/oval CCT. If the aperture is stretched by 1% i.e. on 105 mm that is 1.05 mm extra. It only get 2 units of B3 field error. To get to 10 units it would need to stretch by 5%. So 5 mm.

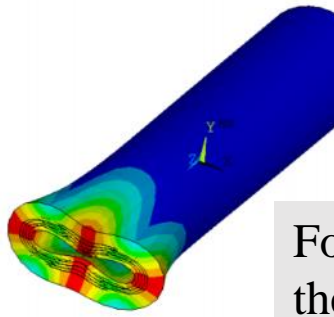
Large apertures need internal support due to reduced resistance to buckling

Buckling multipliers

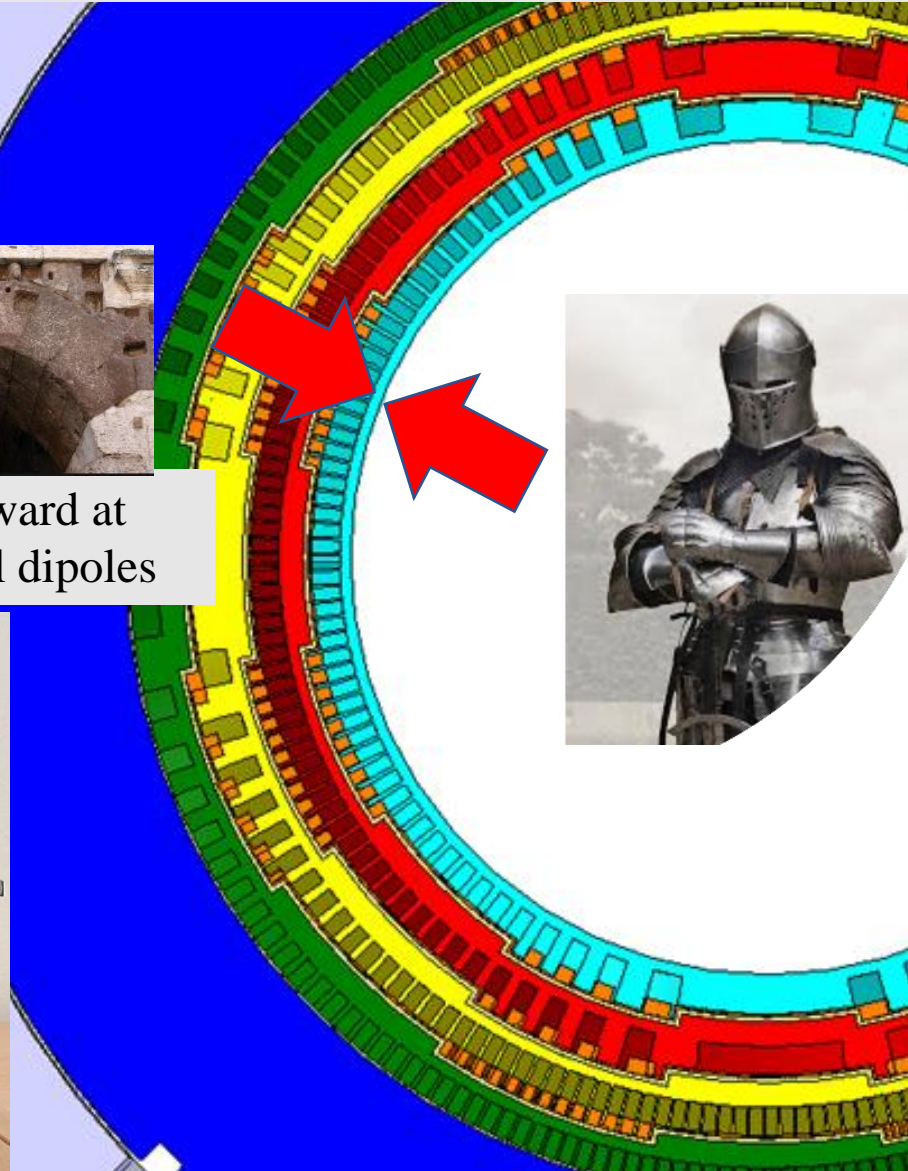
SET1	TIME/FREQ	LOAD STEP	SUBSTEP	CUMULATIVE
1	1.5556	1	1	1
2	1.7894	1	2	2
3	1.9806	1	3	3

1st buckling multiplier 1.55, so the structure is safe

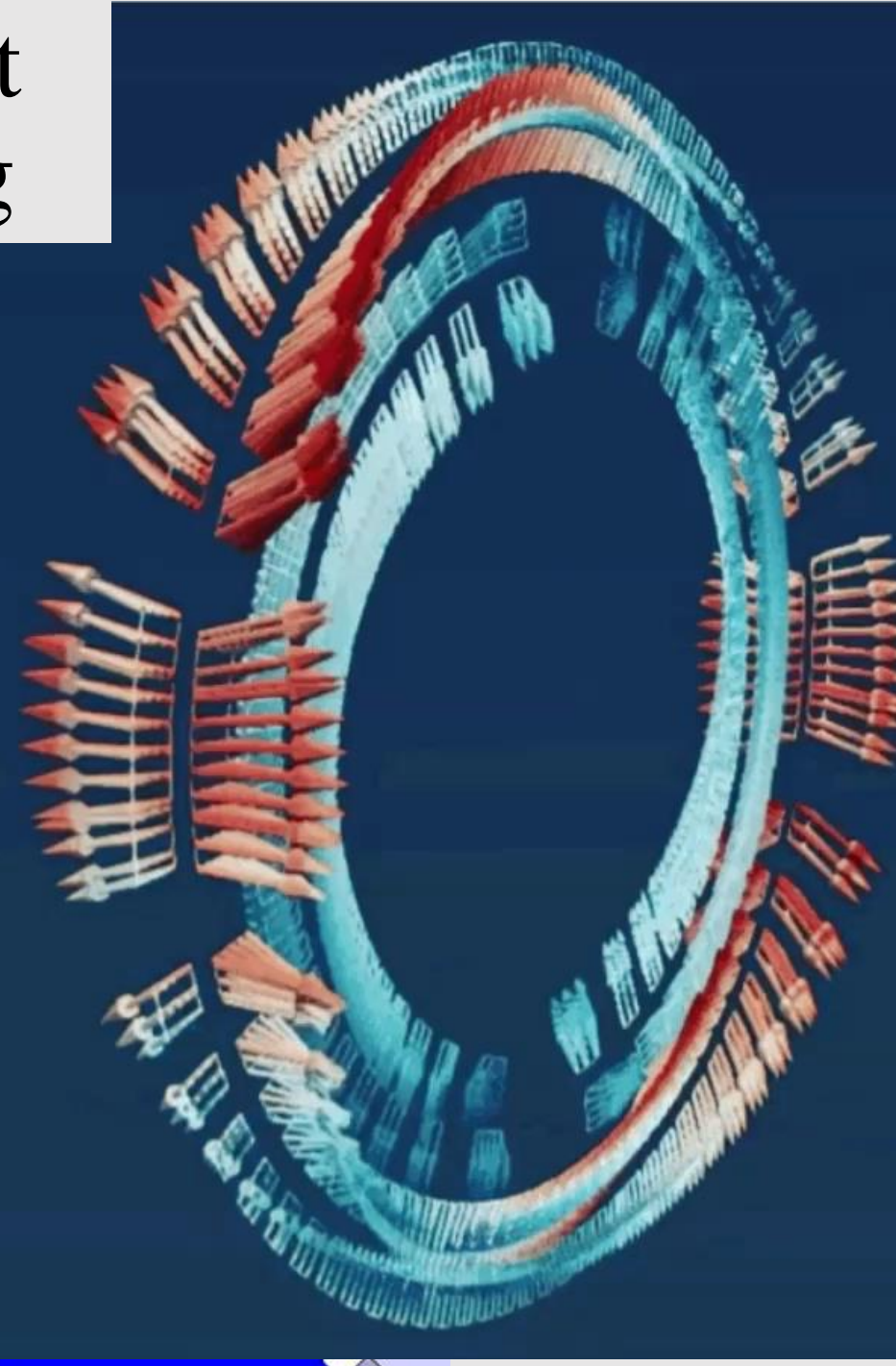
1st buckling mode shape



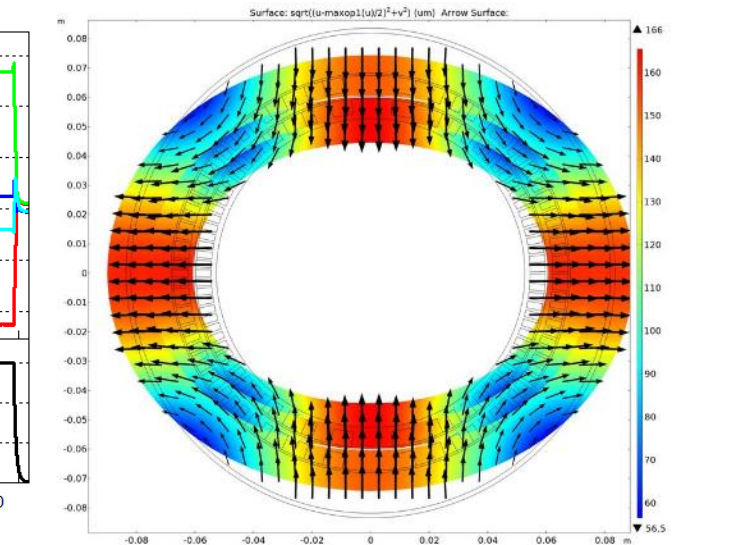
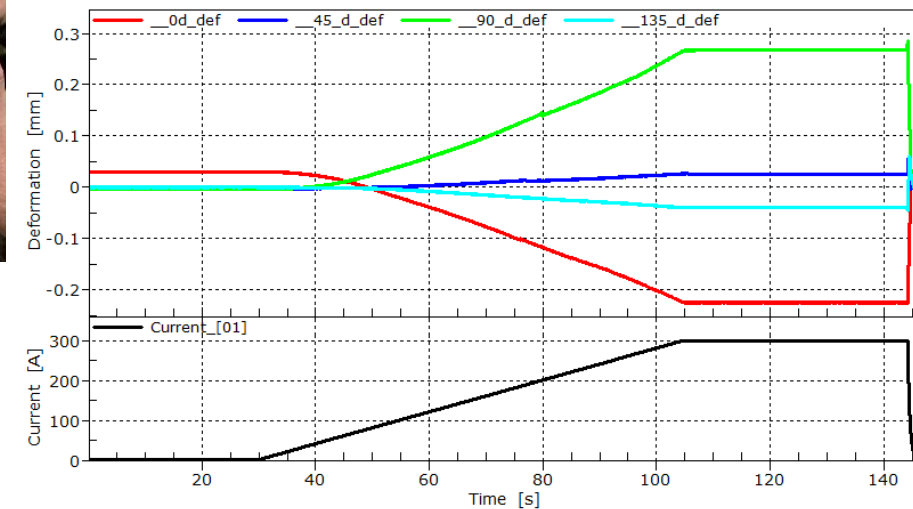
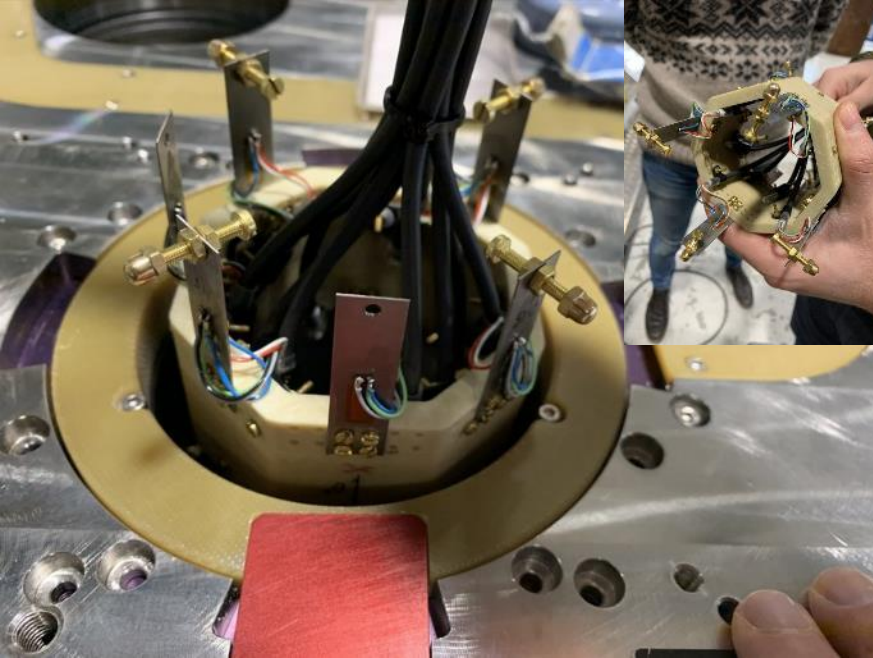
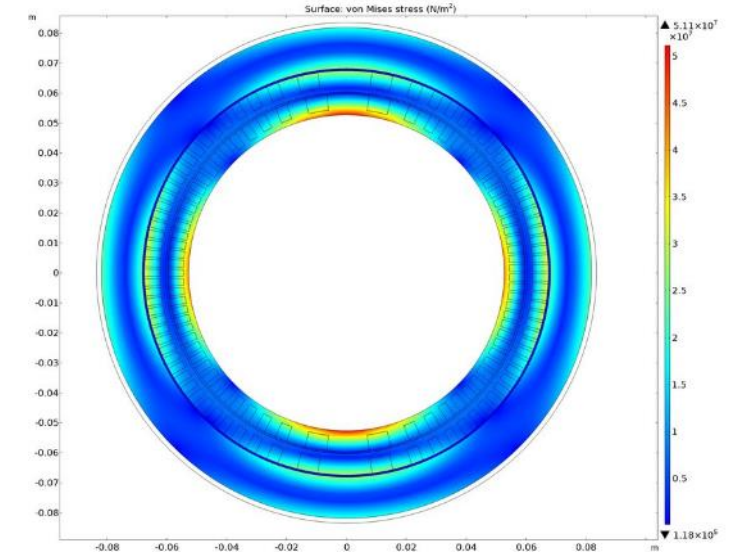
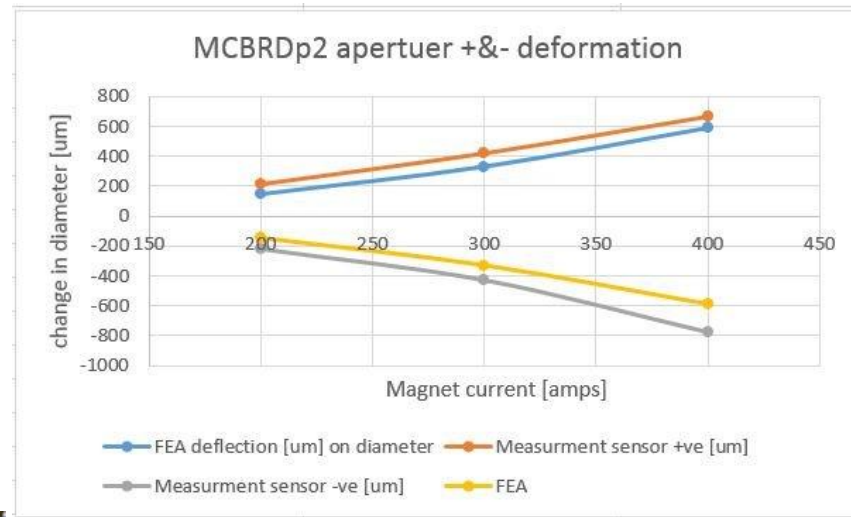
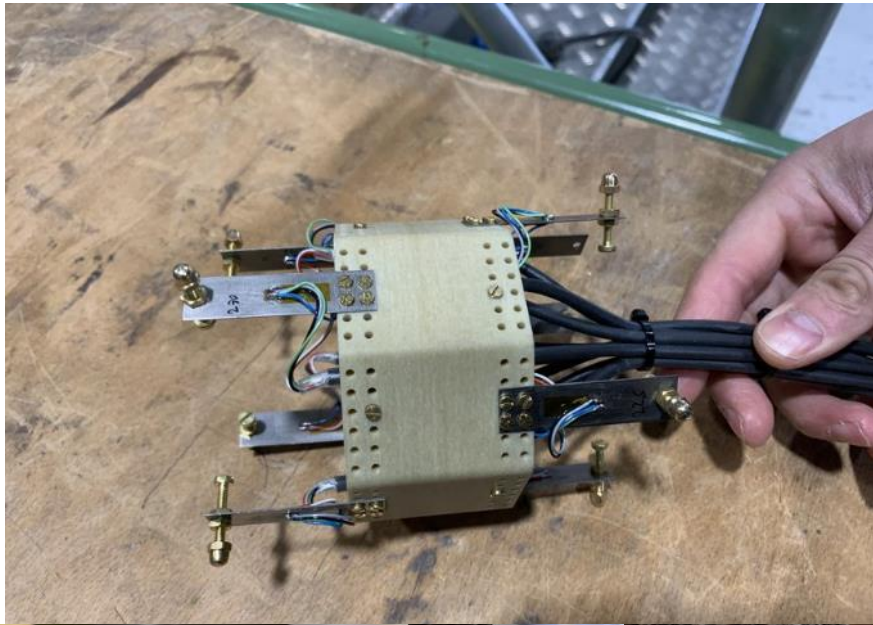
Forces are inward at the ends of all dipoles



LHC small apertures with wide coils are more stable



Aperture deflection cold measurement



Former material selection

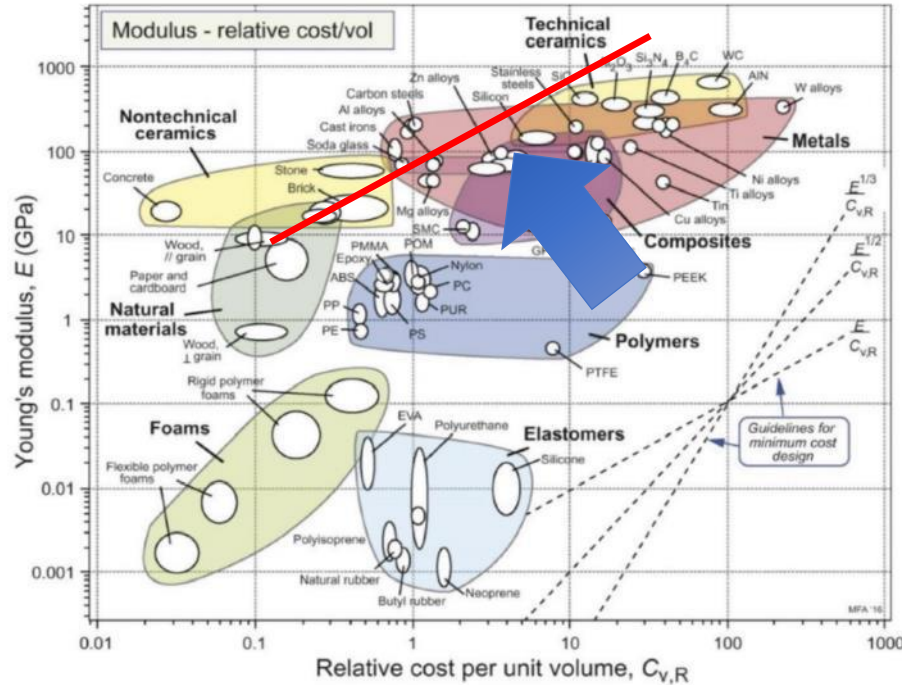
Ashby.... plots and toughness

- Machinability
- Material availability
- Insulating coating compatibility
- Strength
- Fracture Toughness
- Notch sensitivity
- Crack sensitivity
- Electrical resistivity
- Cost

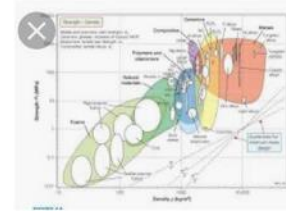
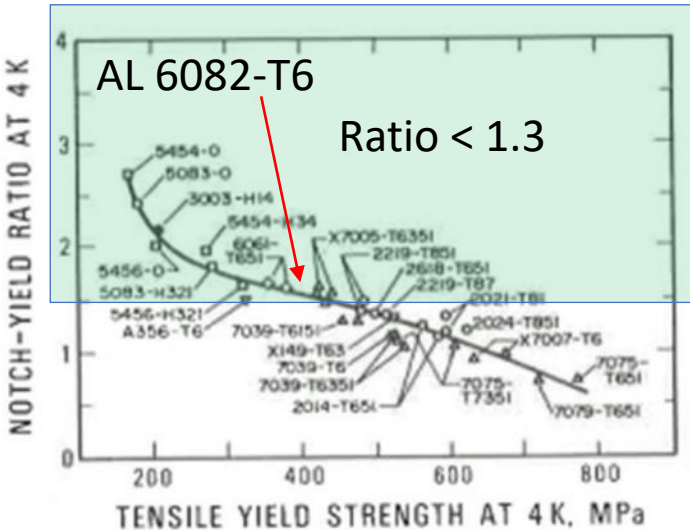
Columns support compressive loads: the legs of a table; the pillars of the Parthenon. Derive the index for selecting materials for the cheapest cylindrical column of specified height t , H , that will safely support a load F without buckling elastically. You will find the equation for the load F_{crit} at which a slender column buckles. It is

$$F_{crit} = \frac{n^2 \pi^2 E I}{H^2}$$

Where n is a constant that depends on the end constraints and $I = \pi r^3 t$ is the second moment of area of the column (see Appendix B for both). Assume that the thickness 't' is constant. Plot the index you derive onto the Modulus-relative cost chart of figure 3.26 to find the cheapest candidates.



Al 6082-T6 with a hard anodized surface



Calculate The Upper Limit For The Sha...
chegg.com

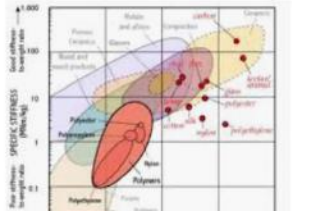


Figure 9-14 Structural materials stiffness and strength

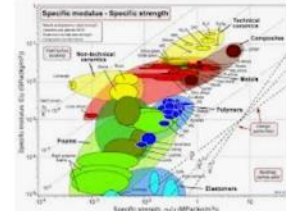
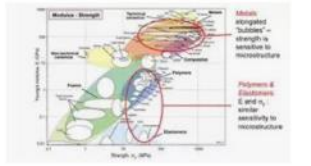
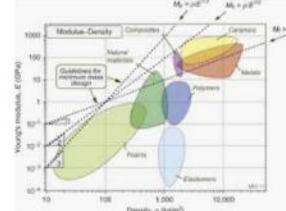


Figure 2 - Ashby materials selection ch...
co.pinterest.com

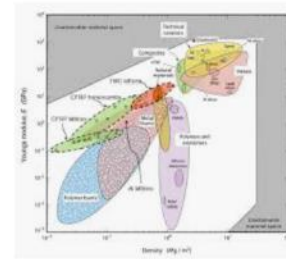
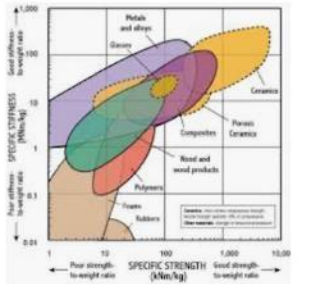
Specific Strength - Tenacity
tensegritywiki.com



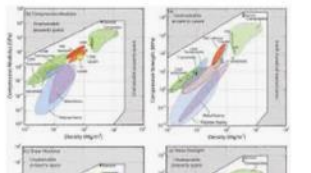
Is there any relation between elasticity ...
quora.com

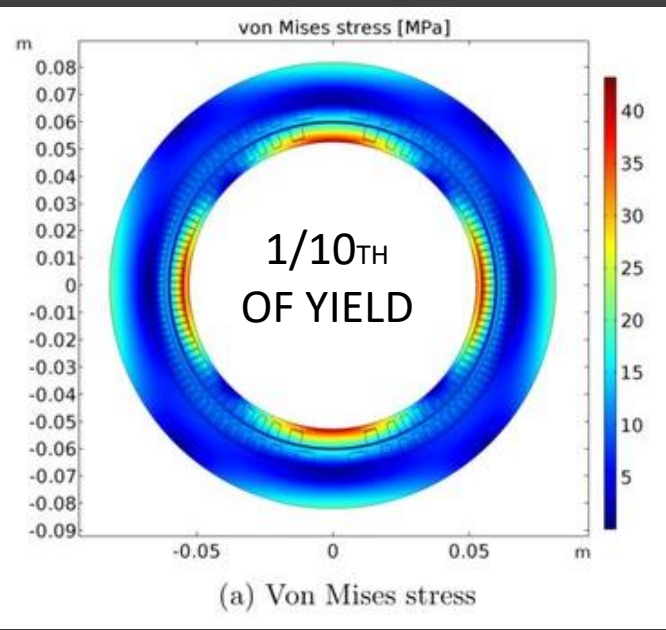


Material Property Chart - an overview | ...
sciencedirect.com



Specific stiffness - Specific strength
www-materials.eng.cam.ac.uk





2.1 Tensile tes at 4K

Tensile tests at 4K were performed with the UTS tensile machine on four specimens, mean values and standard deviation are given in table 1, tensile curves were presented in chart 1 and sample before and after the test could be seen on figure 1 and 2.

Sample N° 2 was not take in account since artefact happen during the mechanical test, values were calculated using samples 1, 3 and 4.

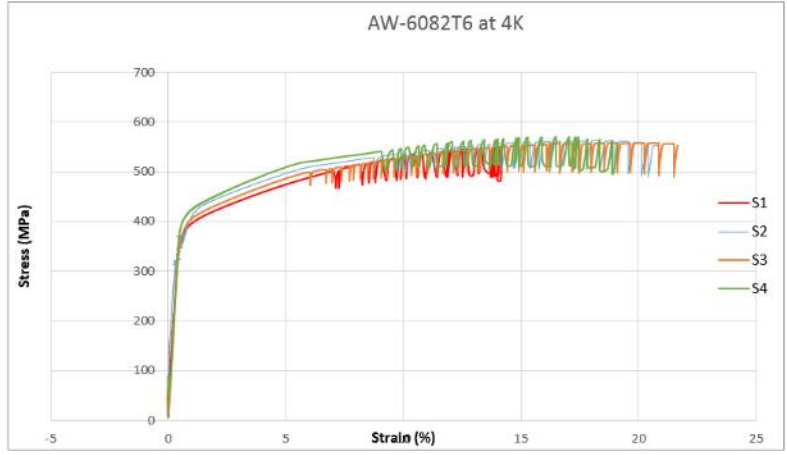


Figure 2 – Samples after the test

YS (MPa)	UTS (MPa)	E (GPa)	A (%)
389 ± 14	560 ± 7	79 ± 3	17.6 ± 4.3

Table 1 – Mechanical properties (Avergae ± St. Dev.)

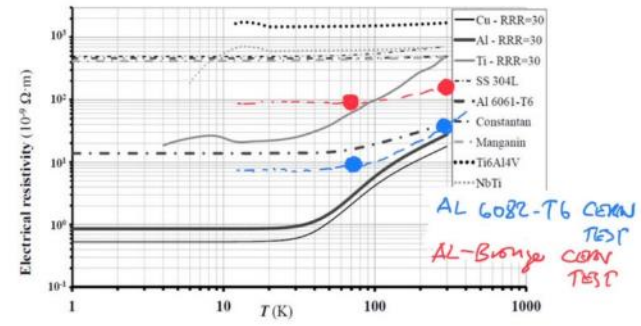
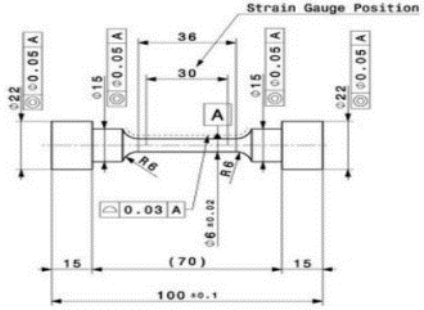
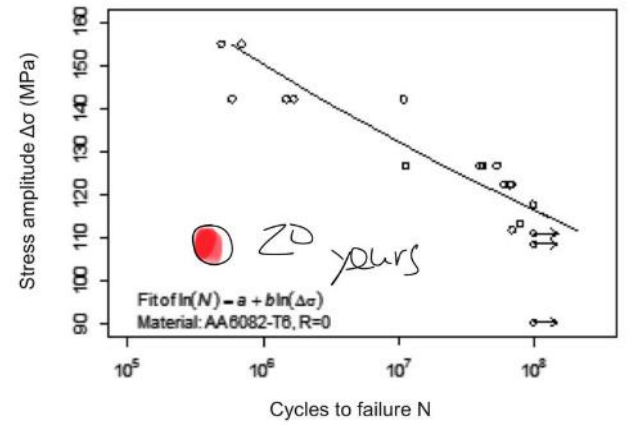


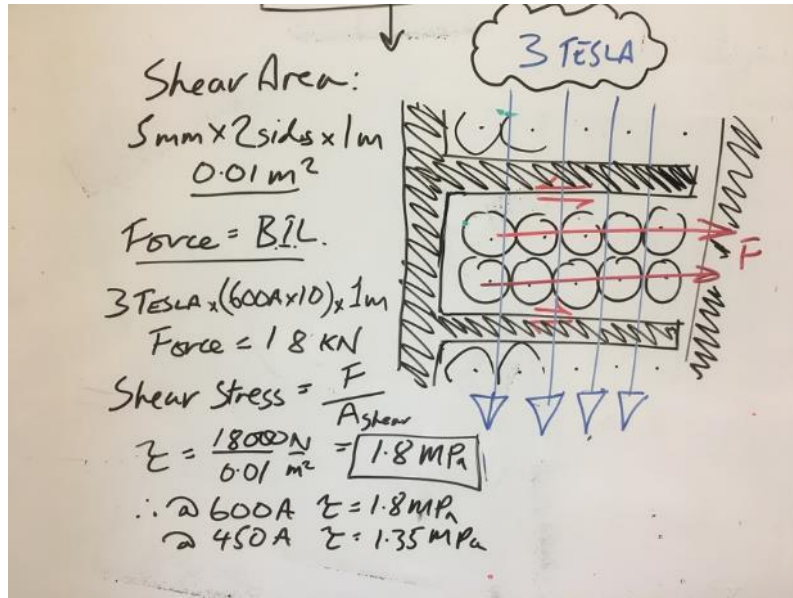
Fig. 10: Electrical resistivity ρ ($\Omega \cdot m$) of various materials versus temperature T . Metals are plotted with solid lines, metallic alloys with dot-dashed lines, and two superconducting alloys with dotted lines.



Yield < 400 MPa (40 MPa in former)
RRR Al >> Al-Bronze
Fatigue lim >> operation point

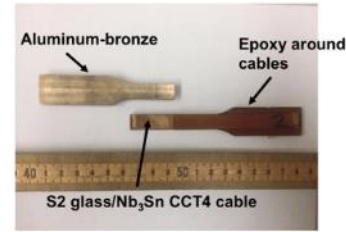
Former
material
AL6082T6

Bond shear strength is very low

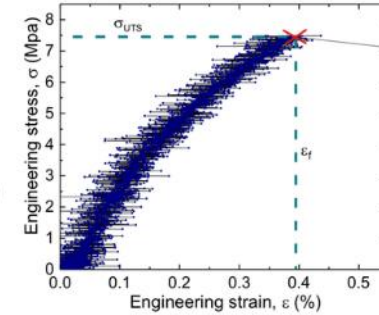


CERN CCT Shear at 3 T ~ 2 MPa but that's not the problem, it's the resin

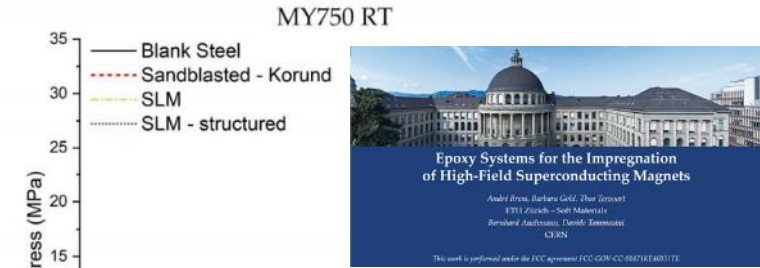
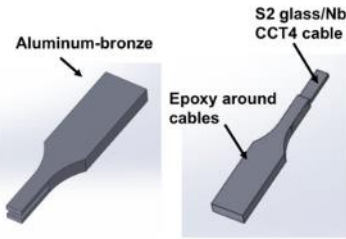
Preliminary results – fracture shear stress is low – double-lap shear test



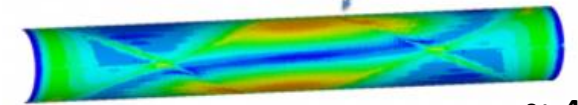
Fracture shear stress test of CTD101K/954/Nb₃Sn Rutherford cable at RT



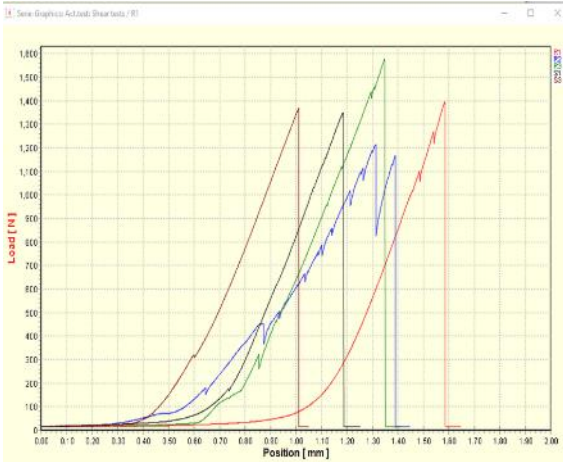
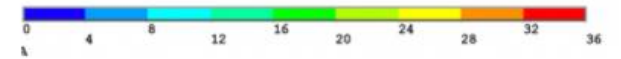
How does fracture shear stress of epoxy change with surface treatment such as sand-blasting?



large shear between layers at pole of bonded model



~ 40 MPa



LBNL test Al-Bronze 7 Mpa
 CERN shear tests Al anodized surface ~ 7 to 5 Mpa

Many papers report low values in the same range

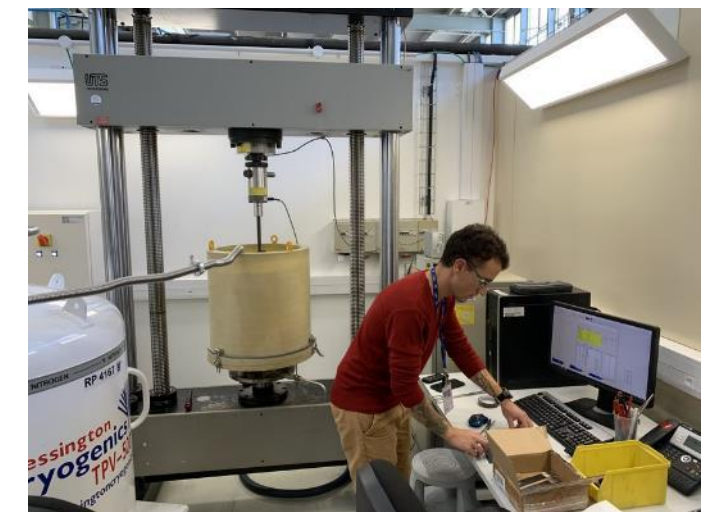
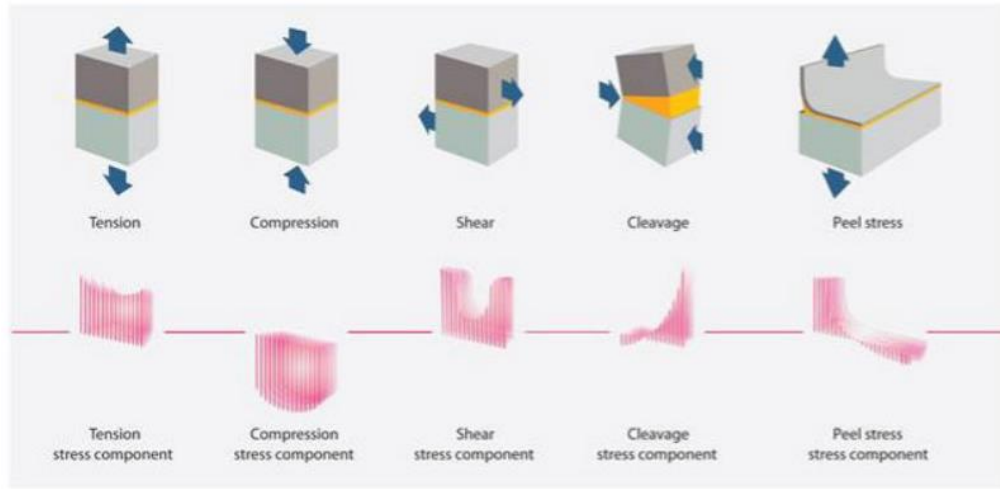
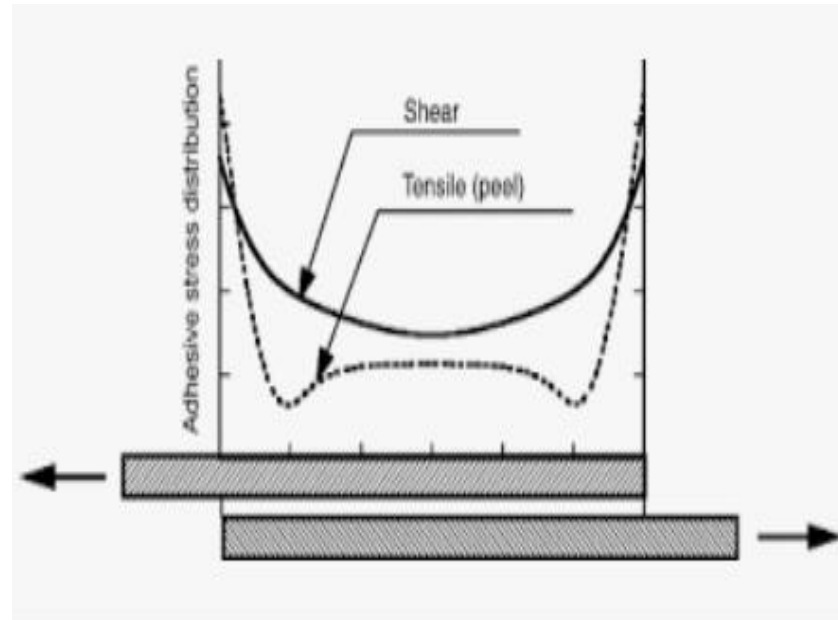


Fig.3 Loading conditions

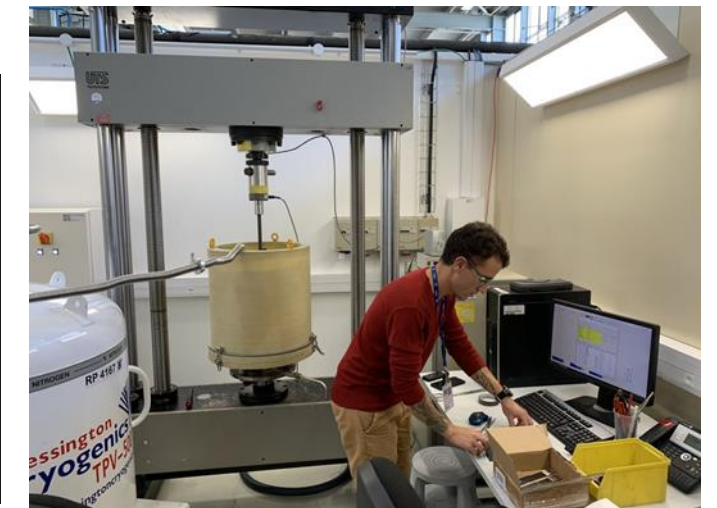
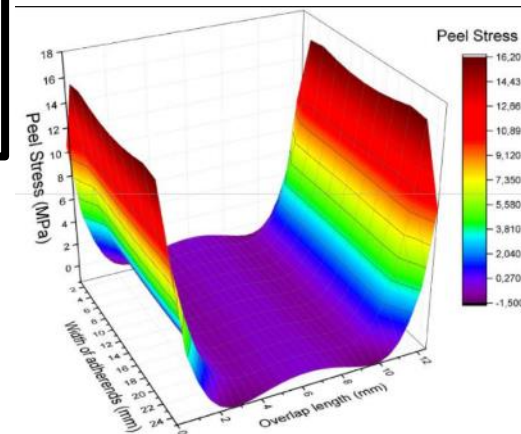
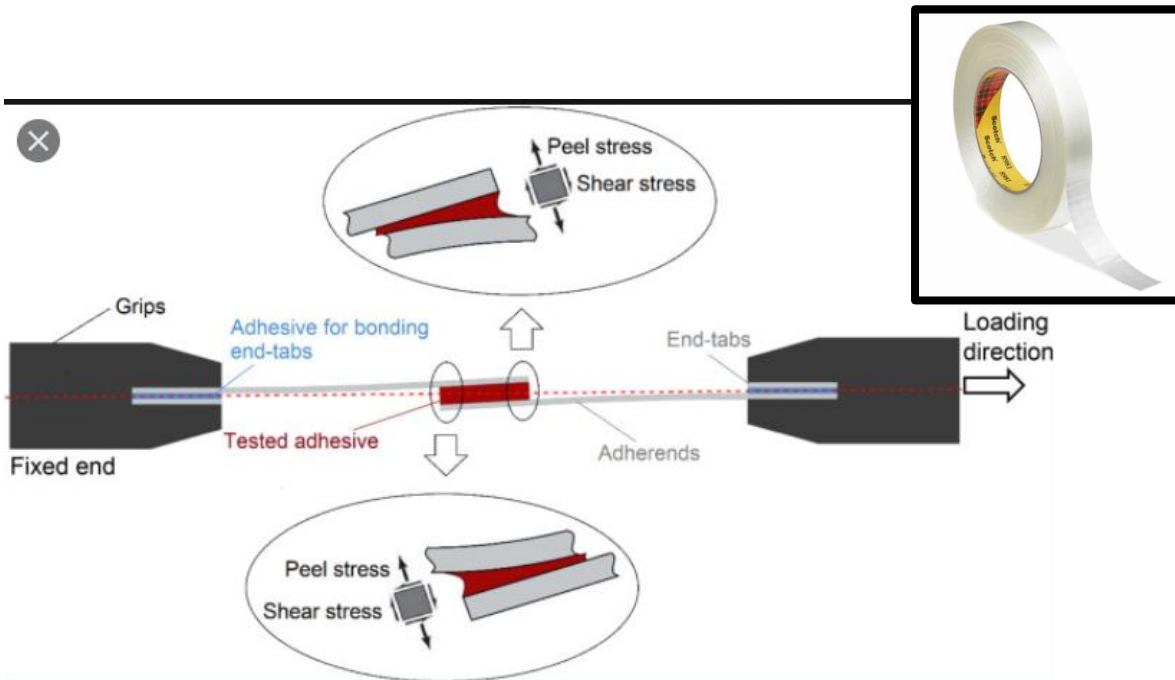


A bonded joint can be loaded in five basic ways (as shown in the diagrams above). Cleavage and peel loading are the most severe as they concentrate the applied force into a single line of high stress. In practice, a bonded structure has to sustain a combination of forces. For optimum strength, the bonded assembly should be designed in such a way as to avoid cleavage and peel stresses.

<https://www.composites.media/huntsman-to-provide-advice-for-adhesive-bonding-applications/>



<https://inpressco.com/wp-content/uploads/2017/05/Paper1564-70.pdf>



Bond -STRENGTH

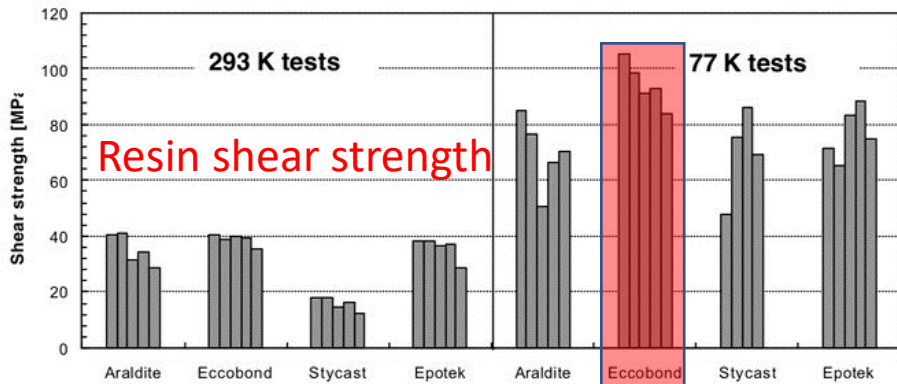


FIGURE 4. Results of the compression/shear tests at 293 K and 77K

strength which is about 15 MPa for these adhesives. Only the Stycast adhesive appears to have a significantly lower strength of 15.3 MPa. Concerning the spread of the measured values, the Eccobond specimens show a significantly smaller relative deviation of 5%, while the other adhesives have all relative deviations between 12 % and 16 %.

At 77 K the average shear strength increases considerably with all values ranging between 70 MPa and 95 MPa. While all adhesives show improved strength at 77 K, the Eccobond adhesive, with an average shear strength of 95 MPa produces joints with significantly higher strength than the other adhesives. The relative standard deviation of the measured shear strength at 77 K is the same as the ones obtained at room temperature. The value of 8 % obtained with the Eccobond adhesive is also significantly lower than the value measured with the other adhesives.

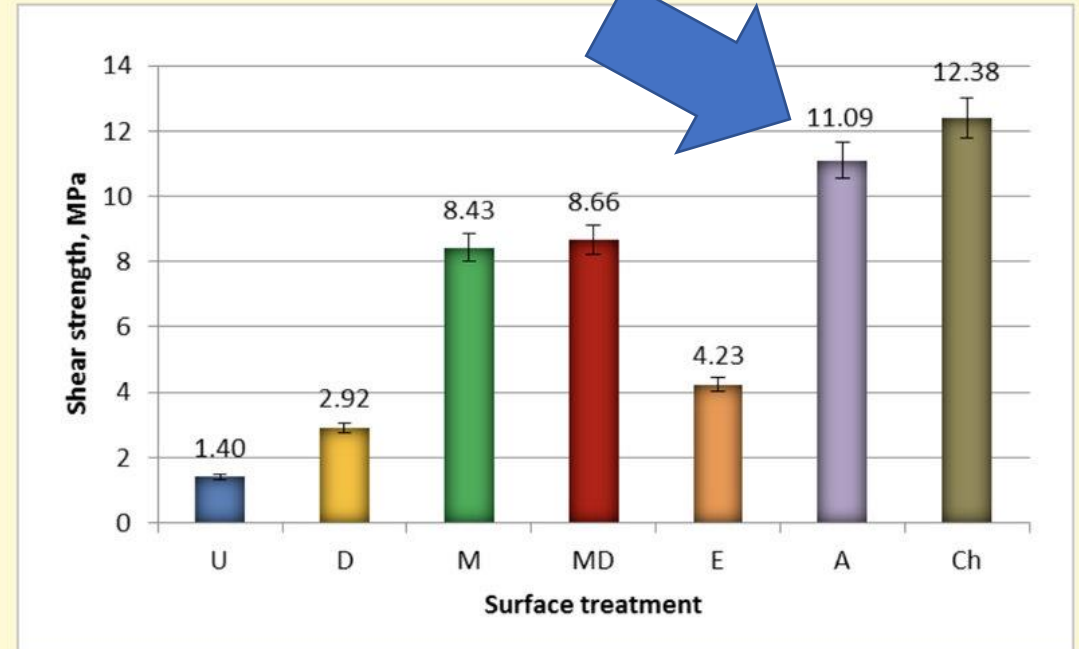


Figure 2.

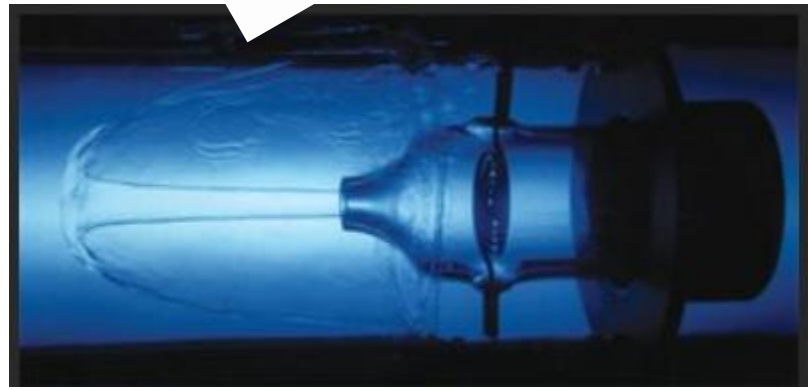
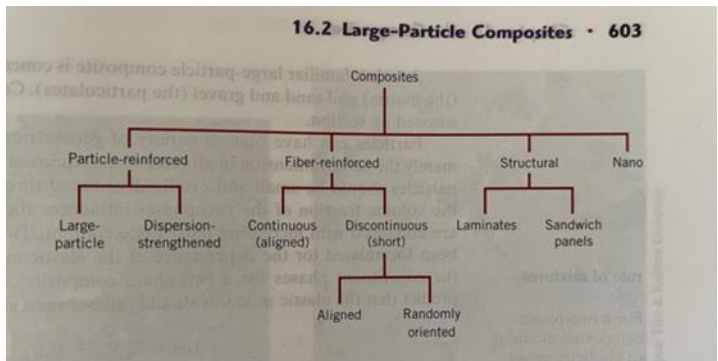
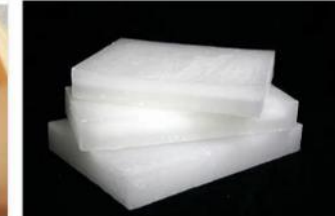
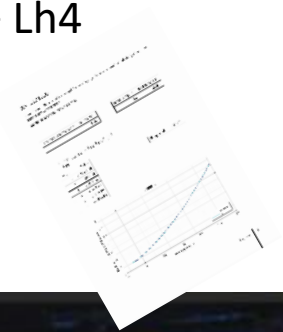
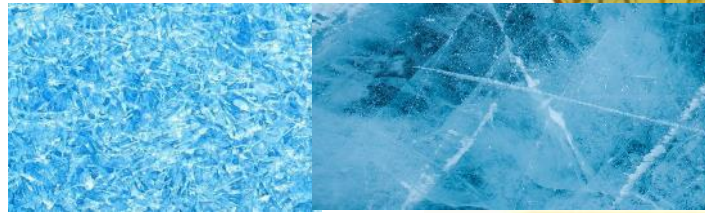
Shear strength tests of EN AW-2024PLT₃ aluminium alloy sheet adhesive joints after different surface treatment methods: U - untreated, D - degreasing (chemical cleaning), M - mechanical treatment, MD - mechanical treatment and degreasing, E - etching A - anodizing, Ch - chromate treatment

Impregnation ? What should we use?

We use CTD101K because we follow the USA development its qualified for radiation.

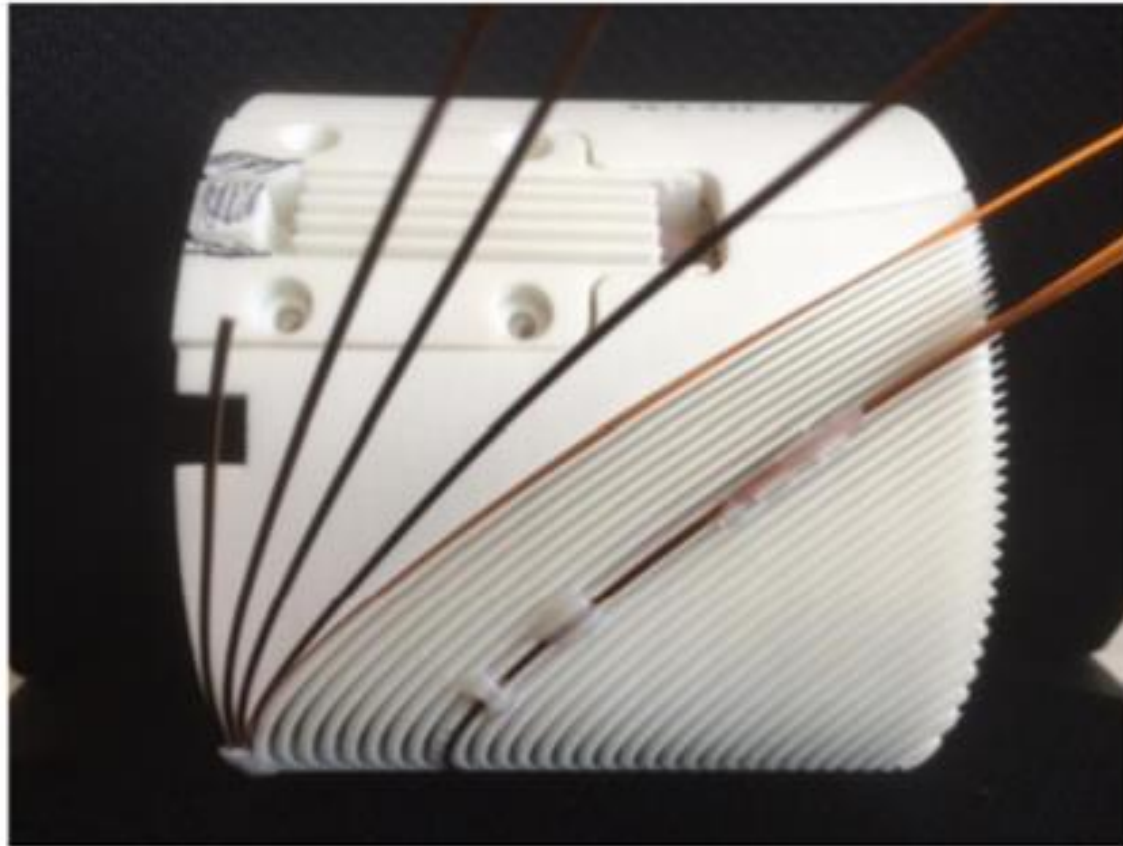
BUT I have other ideas we could try:

- 1) MY750 a much tougher resin. 12 mm/m
- 2) Amorphous-Water expands
- 3) Bee's wax
- 4) Paraffin wax
- 5) Teflon coated former, no impregnation-> Lh4
- 6) CTD101G thermal contraction 5 mm/m
- 7) Nano partials in resin need studying ?
- 8) Invar spacers to prestress?
- 9) Kevlar -ve thermal expansion.....?



1st winding test with the rectangular wire

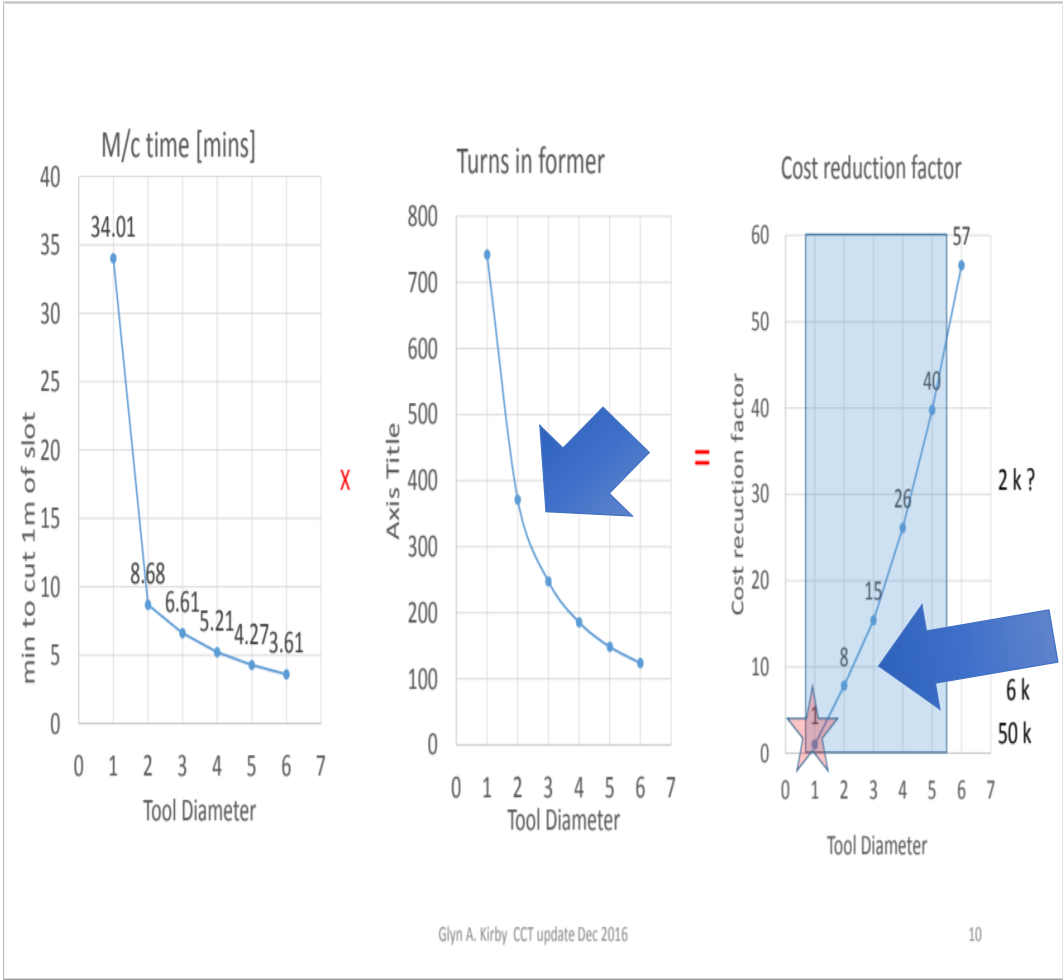
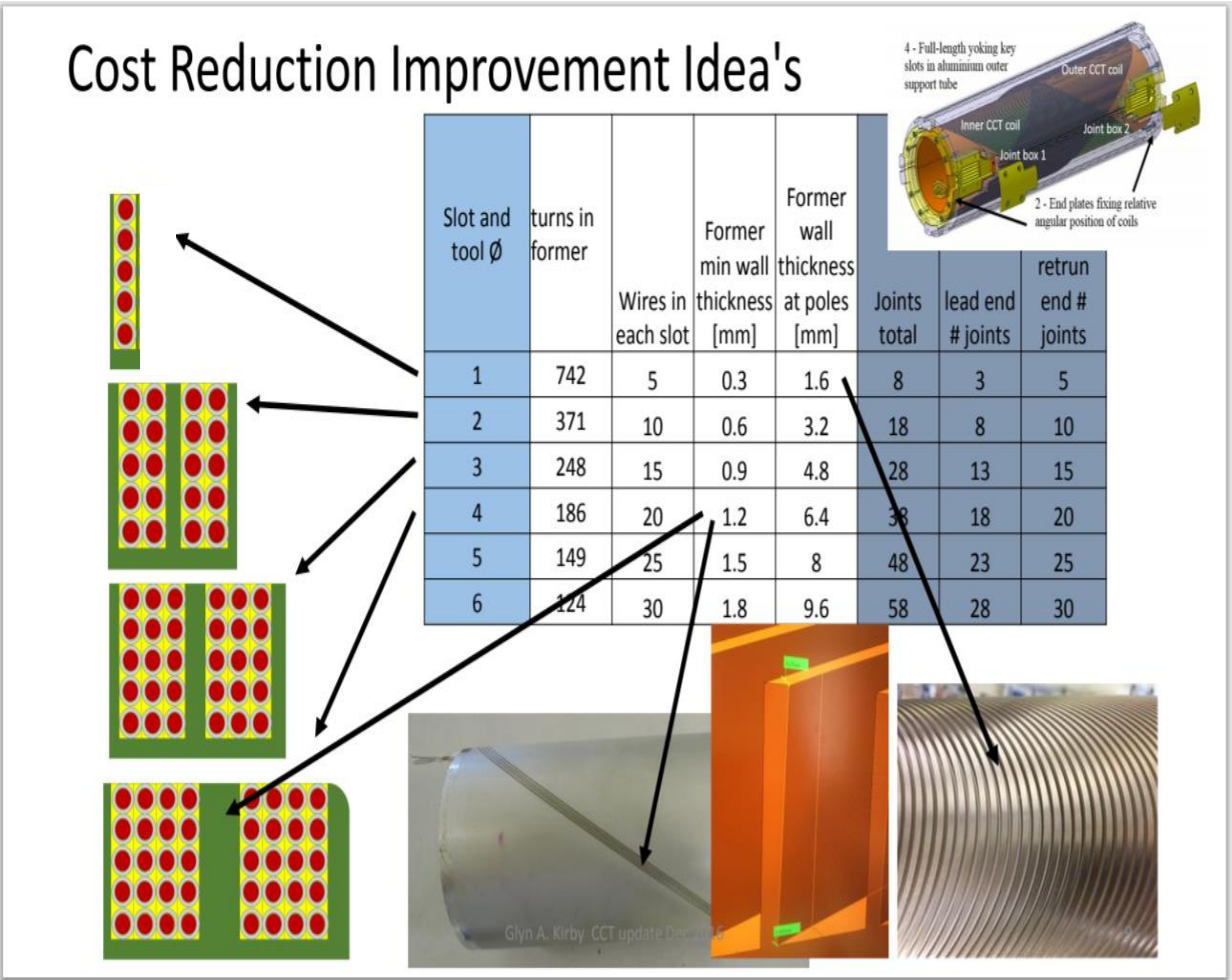
!!!!failed!!!!



The enamel rectangular wire rotated as we tried to wind and finally was impossible to wind into the slot!



Machining 5 to 1 ratio limit



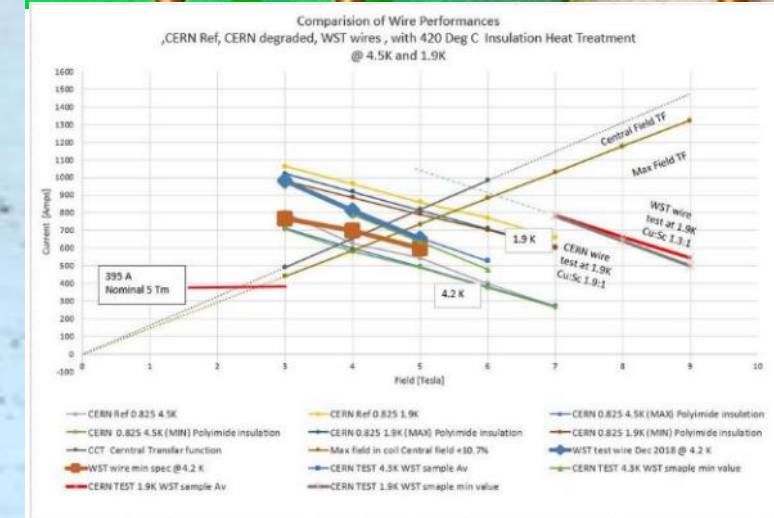
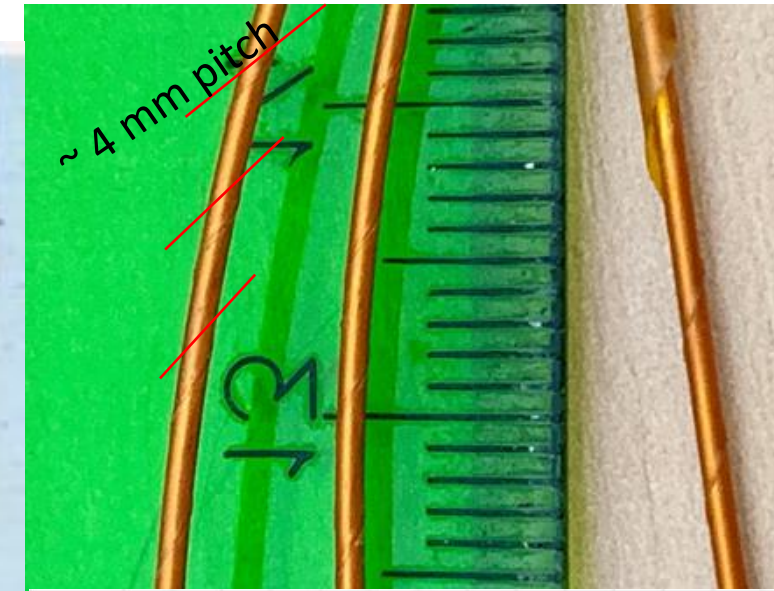
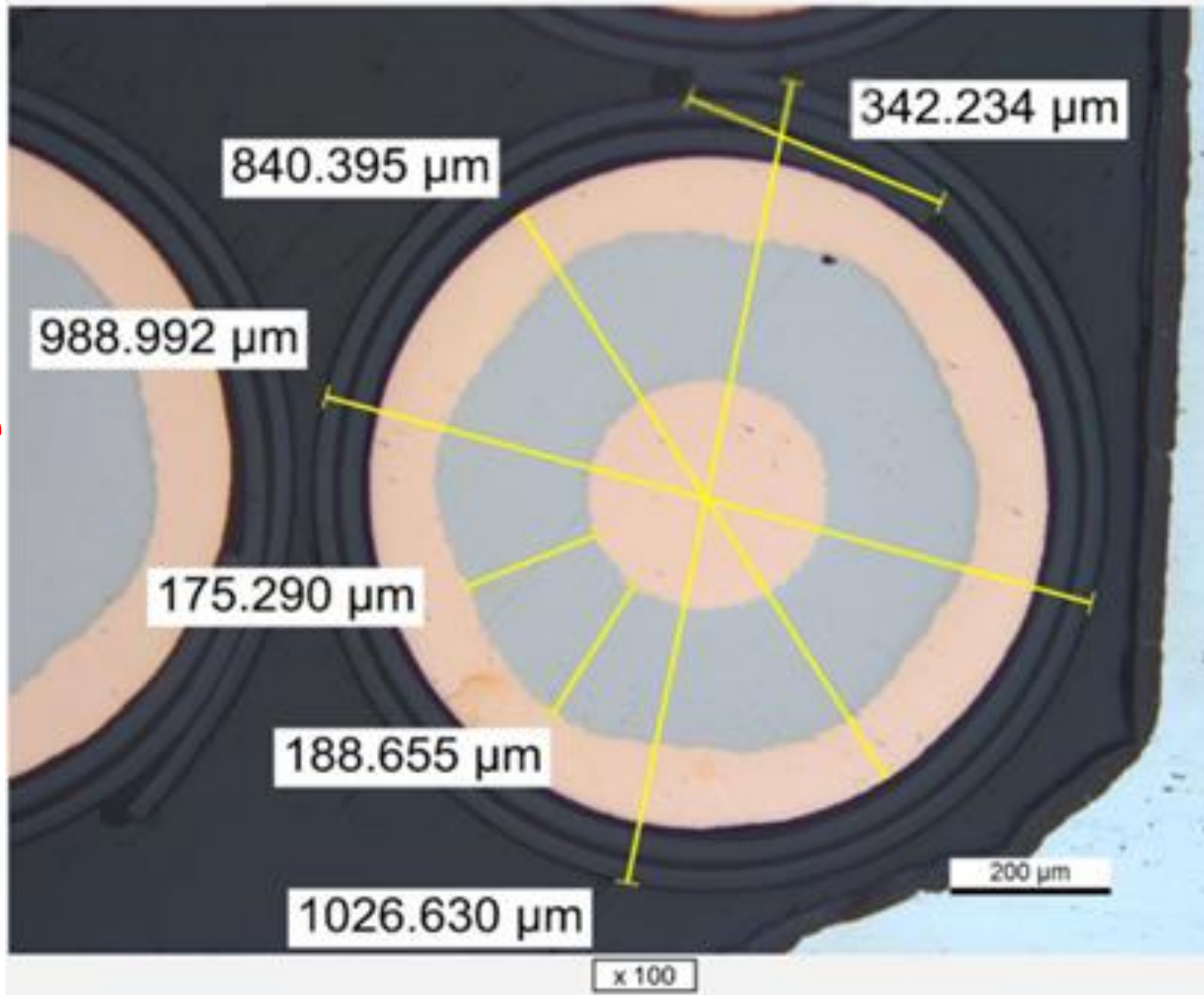
Costing is out of date! Much less now!

Wire insulation is key!

Wire insulation & Performance

CERN 1.9:1
 filaments 6 μm
 Prototype stock
 CERN wire
 Magnet SS 55%

55% overlap 2 layers + 3 layer spiraling
 spacer rib !



11kV wire
 insulation

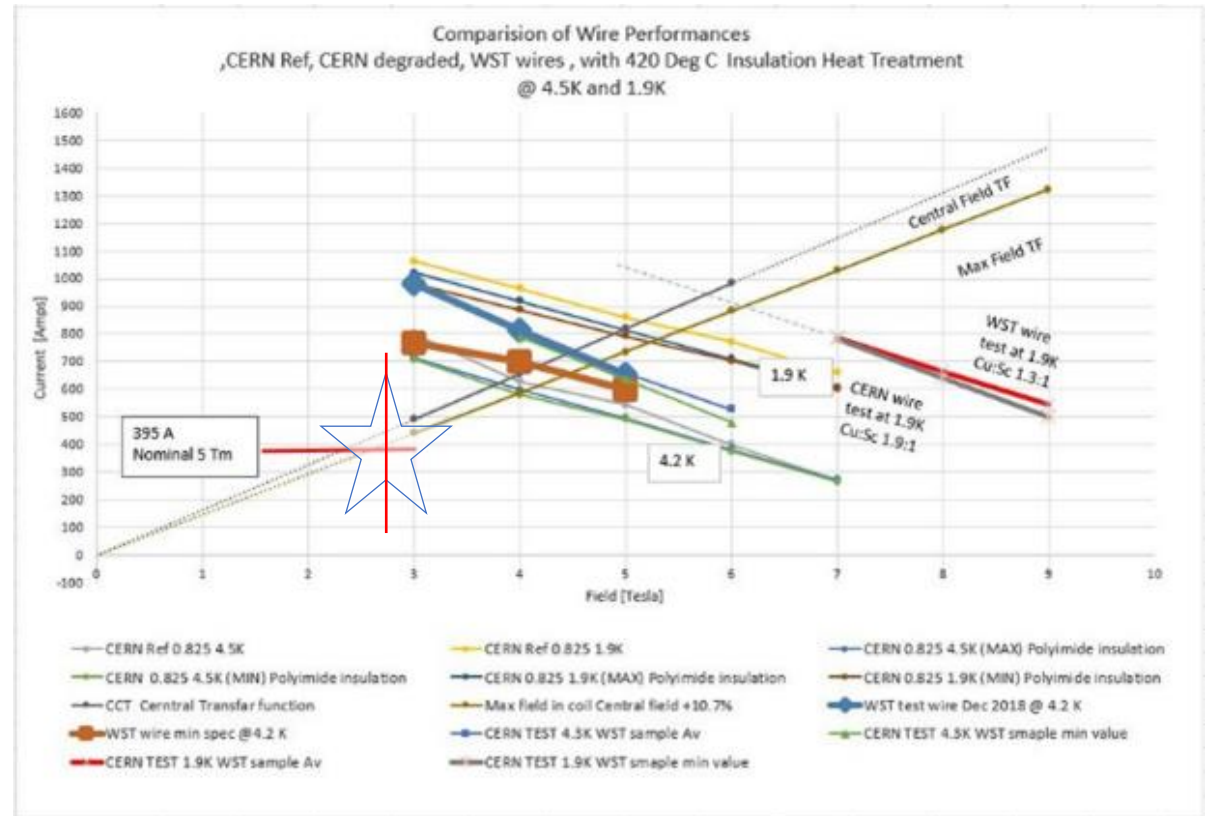
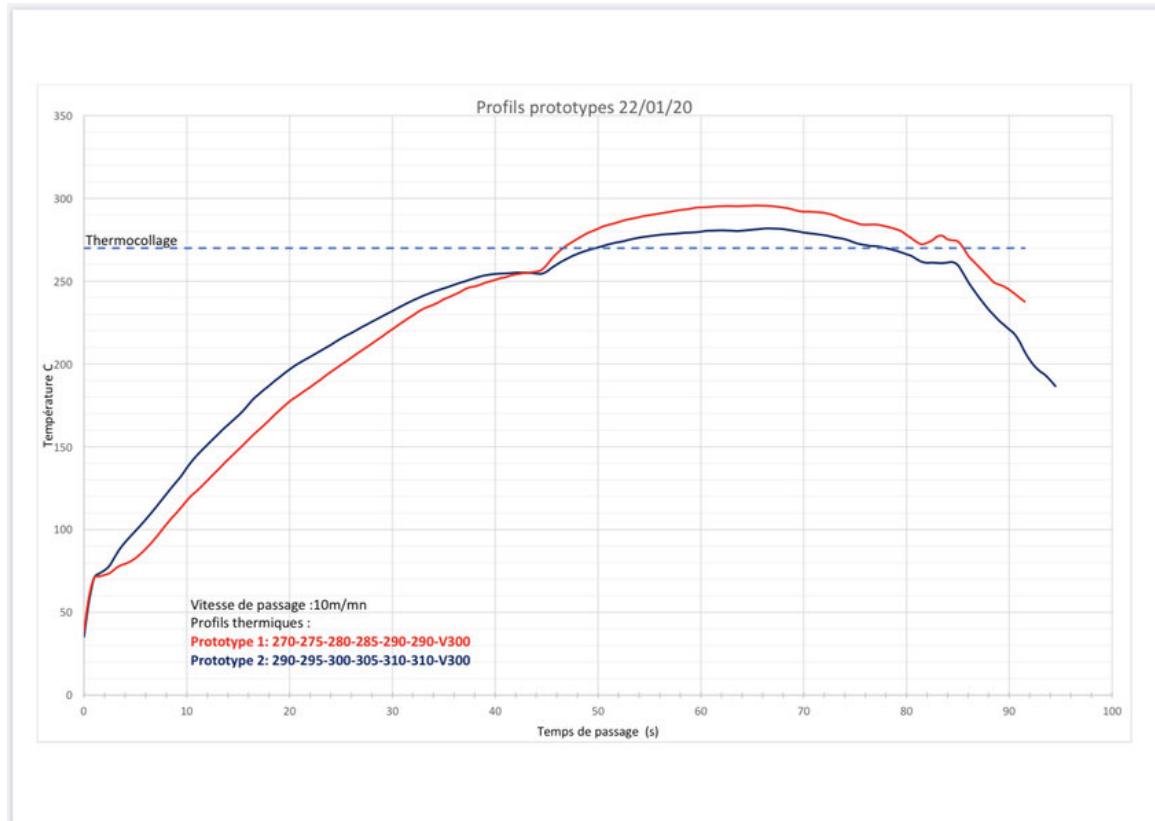
Strong bond to
 wire!

Bonding Polyimide into wire

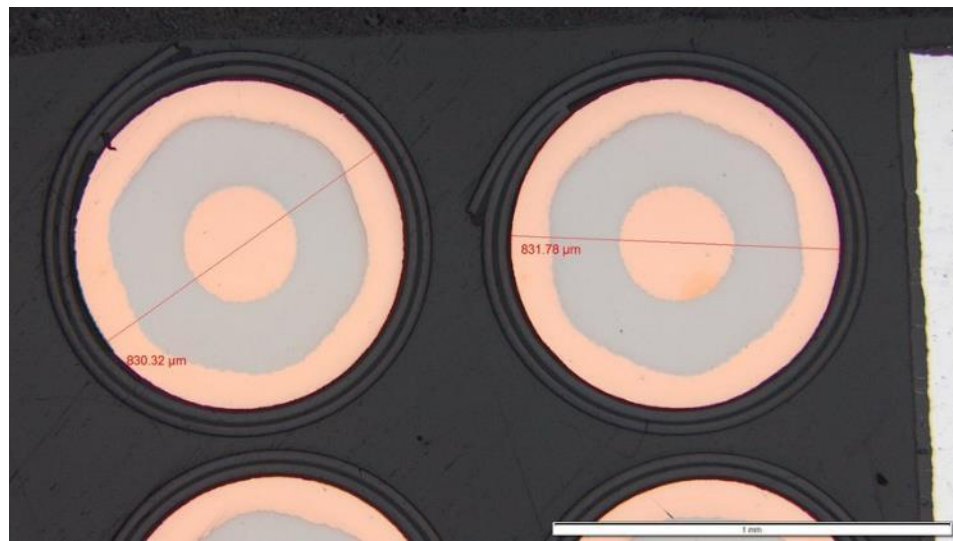
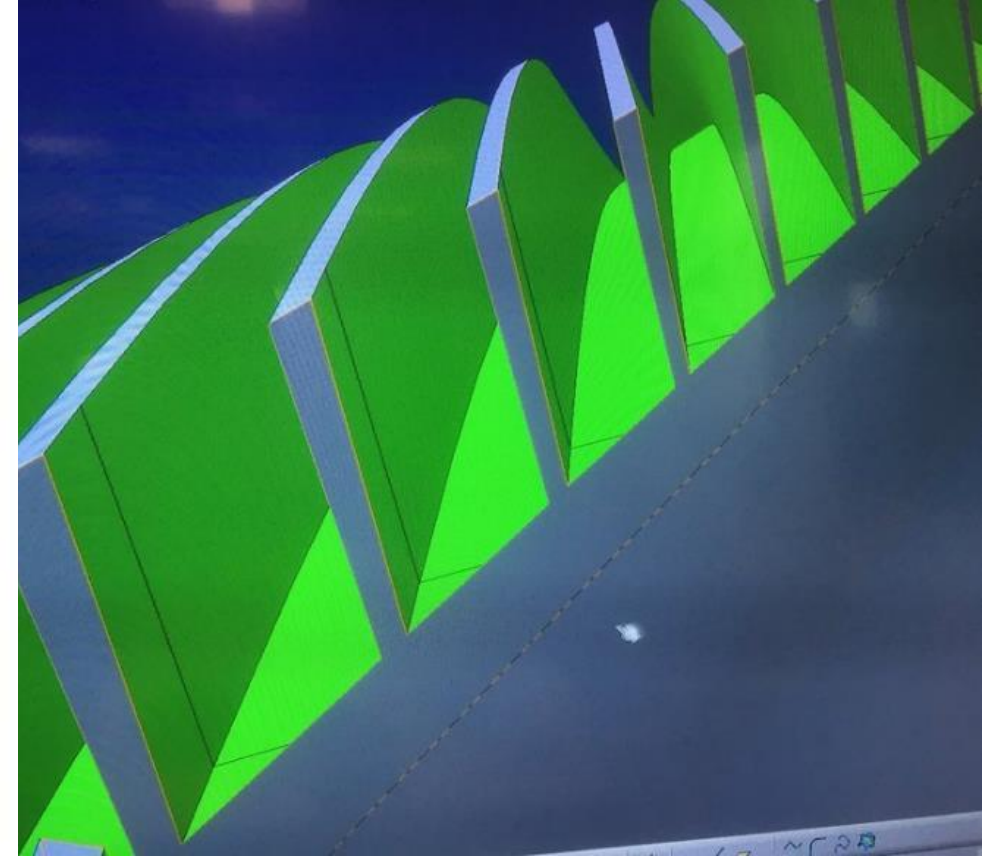
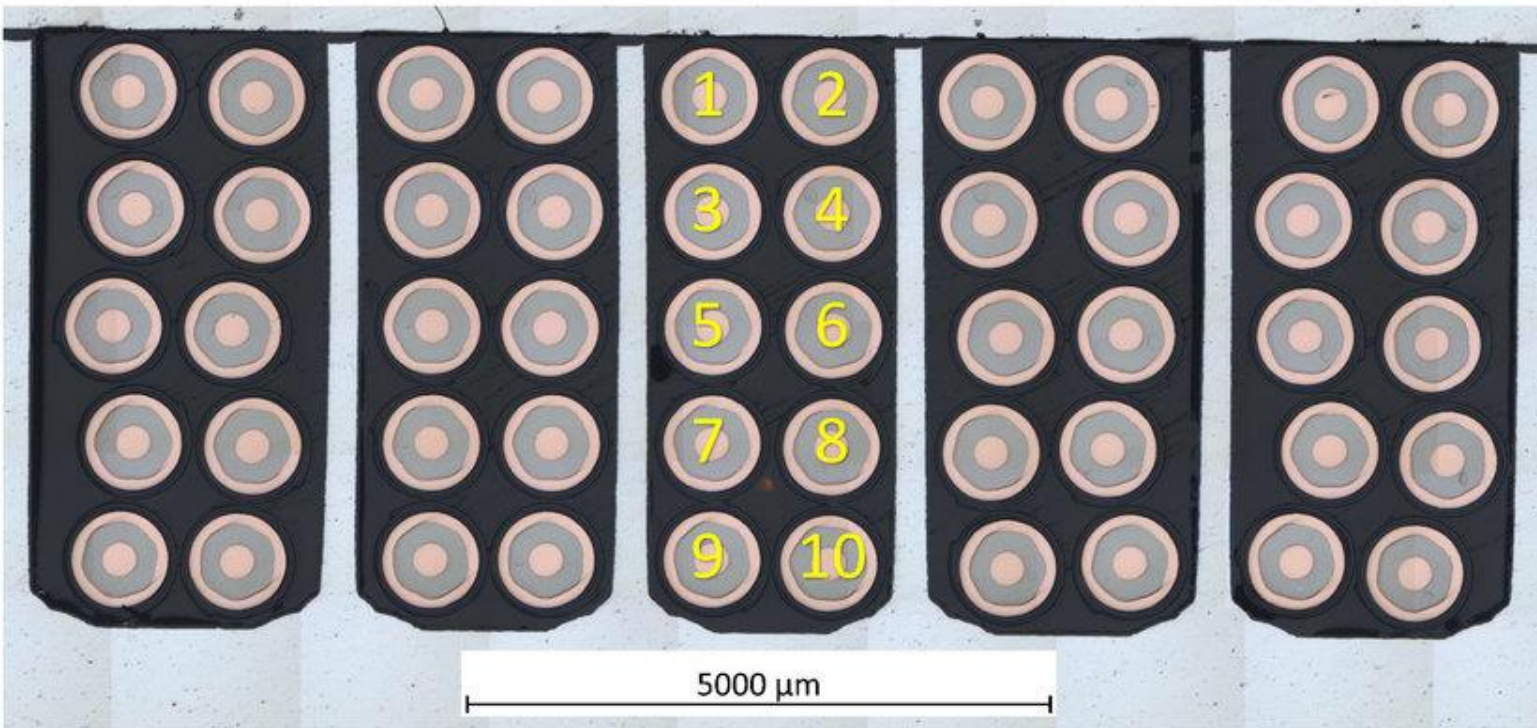
First tests bonded at 420C with 7% degradation but strong bond !

Later we reduce to 250 C no degradation but weak bond and insulation!

Final bonding 300C no degradation and strong bond!



Channel 1 Channel 2 Channel 3 Channel 4 Channel 5



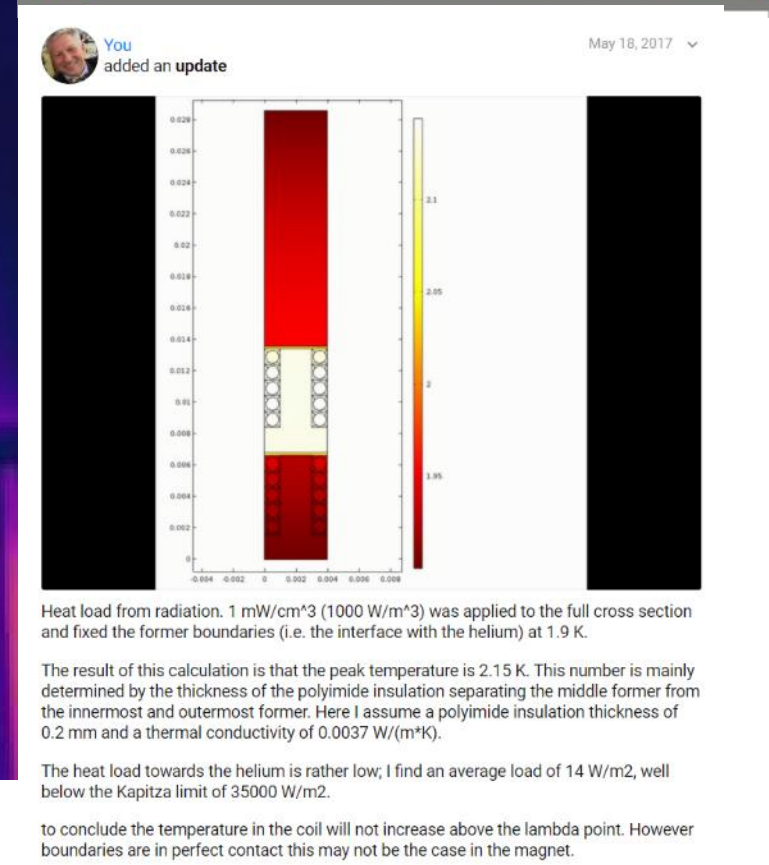
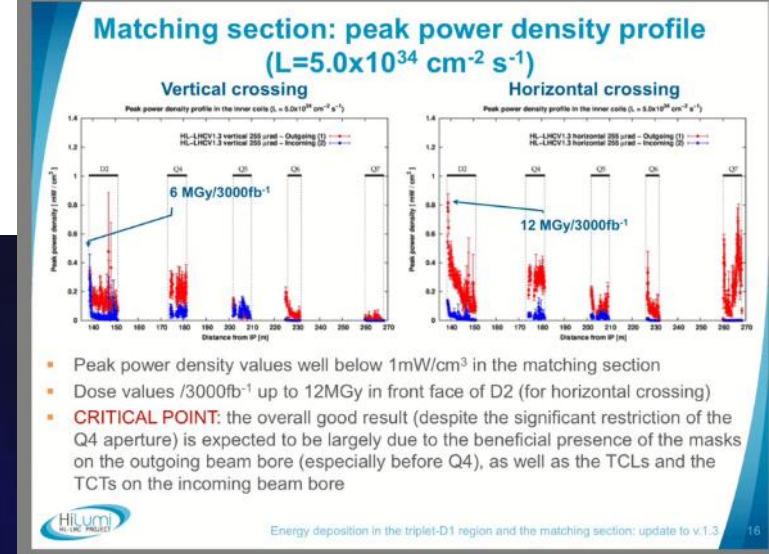
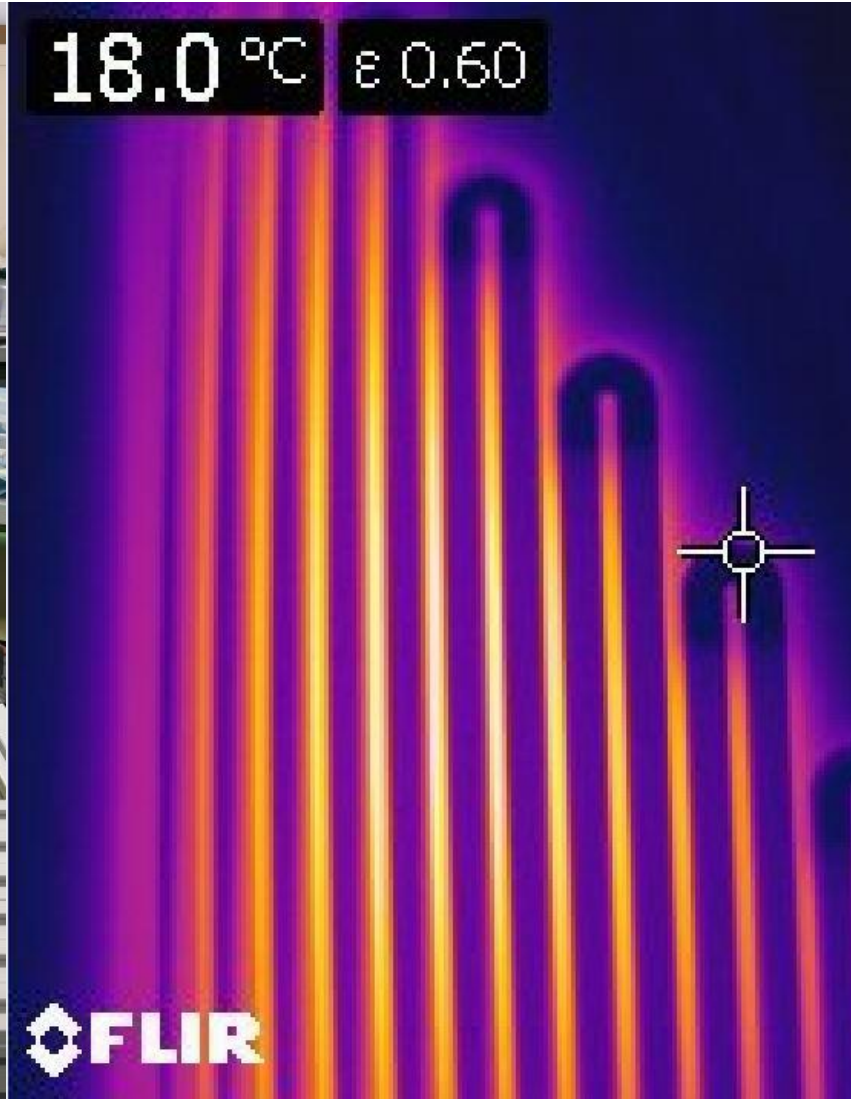
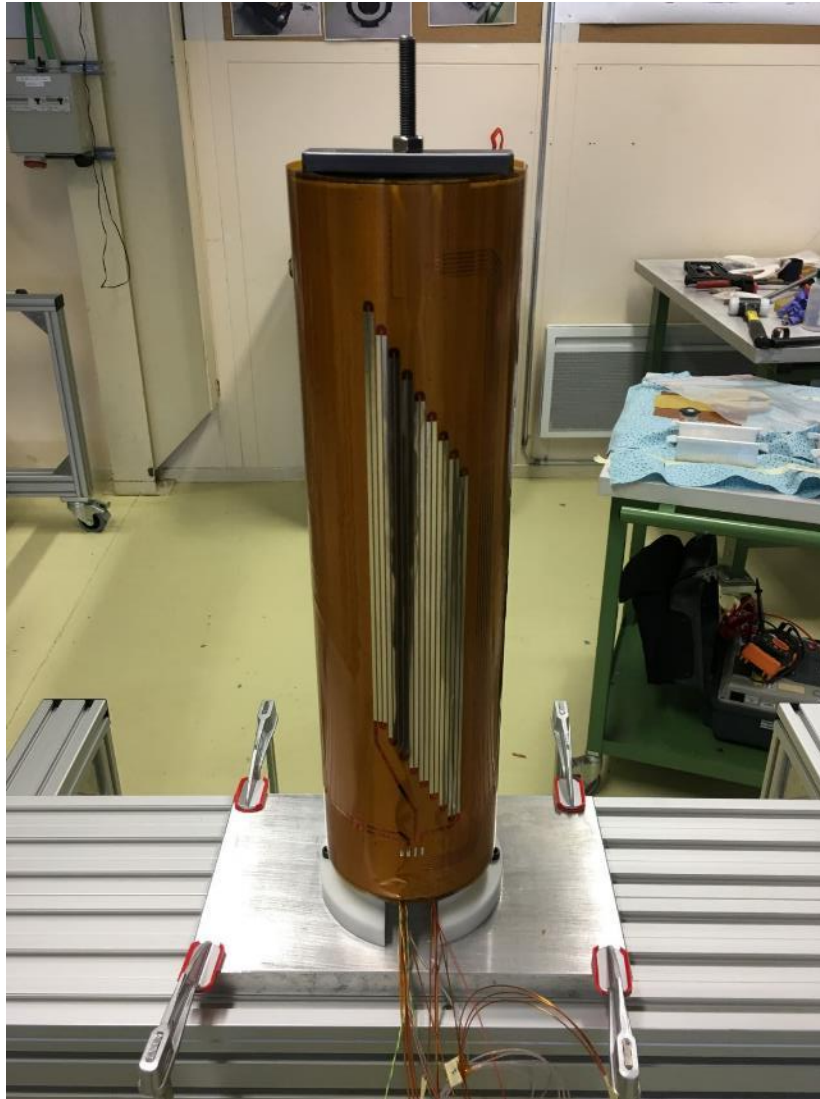
Set of test channels to find the best width.

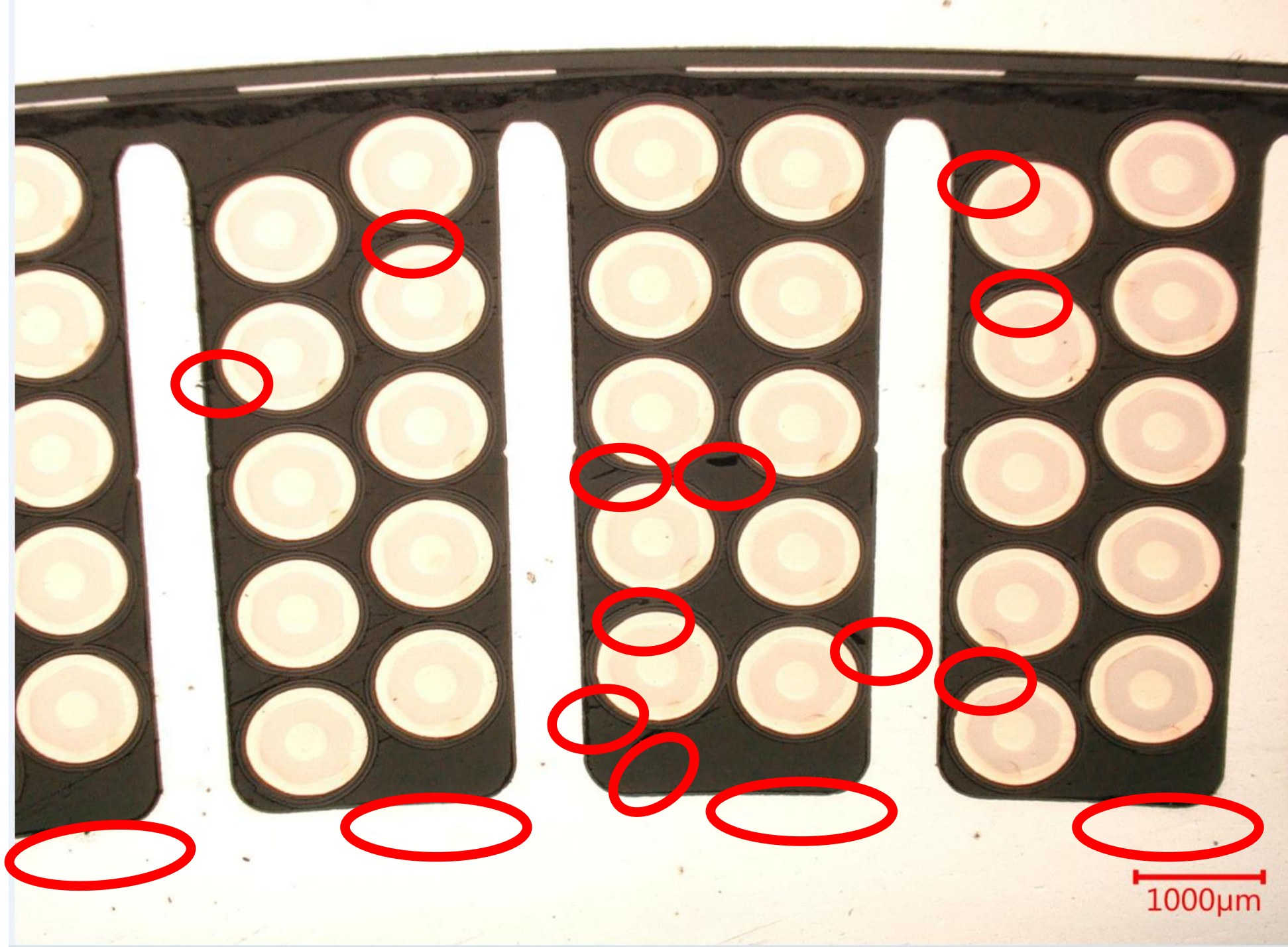
we tested the min wall thickness, achieves 0.1mm but selected 0.3 mm

The depth of the channel 5:1 ration with width limit for M/c tools !

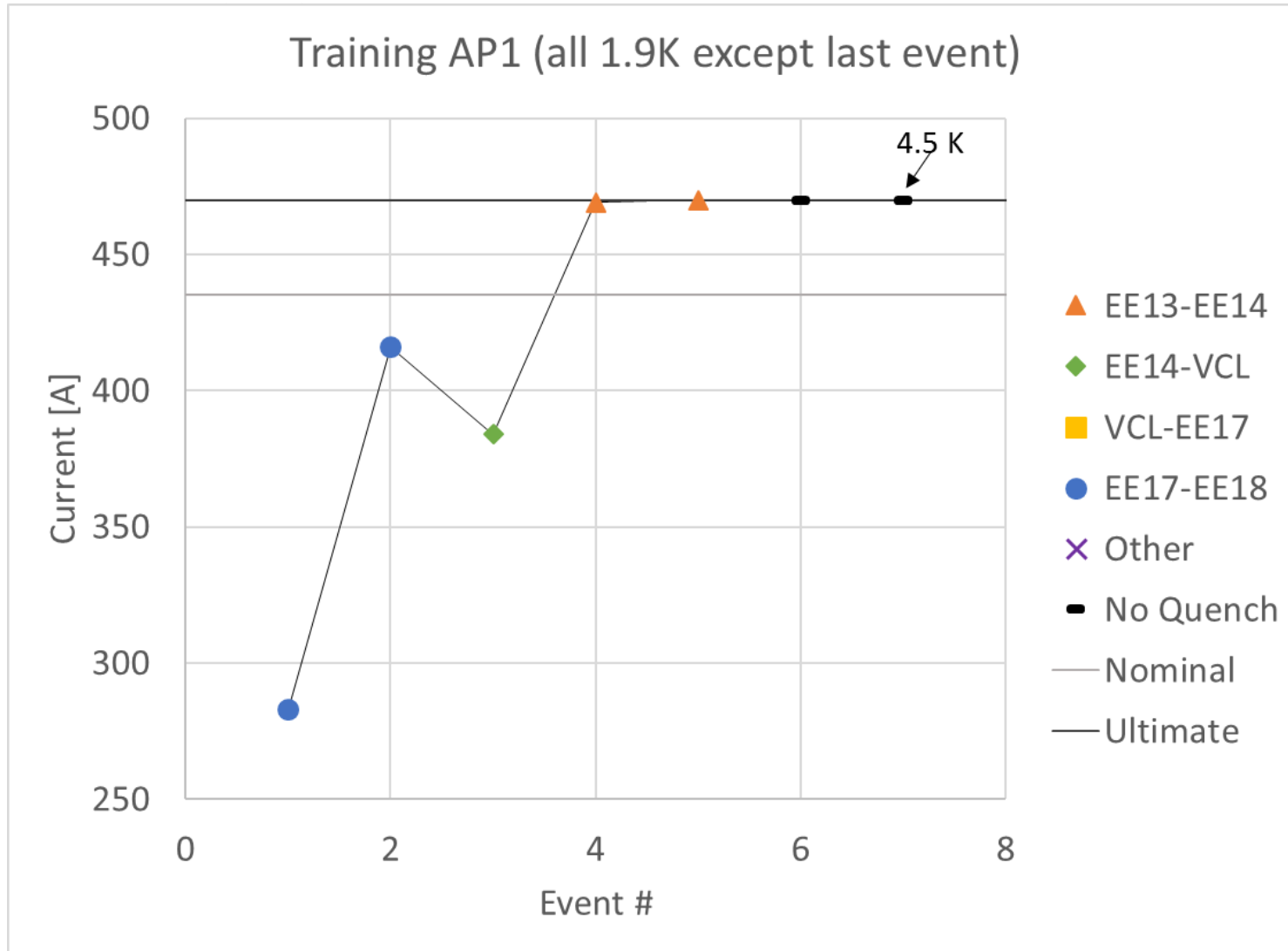
Beam simulation & heating test

Beam heating calc predicted increase the outer former above lambda 2.15K
 Cold heating injected 3 x the expected heat before quench! ;-)





1st cold test quench performance

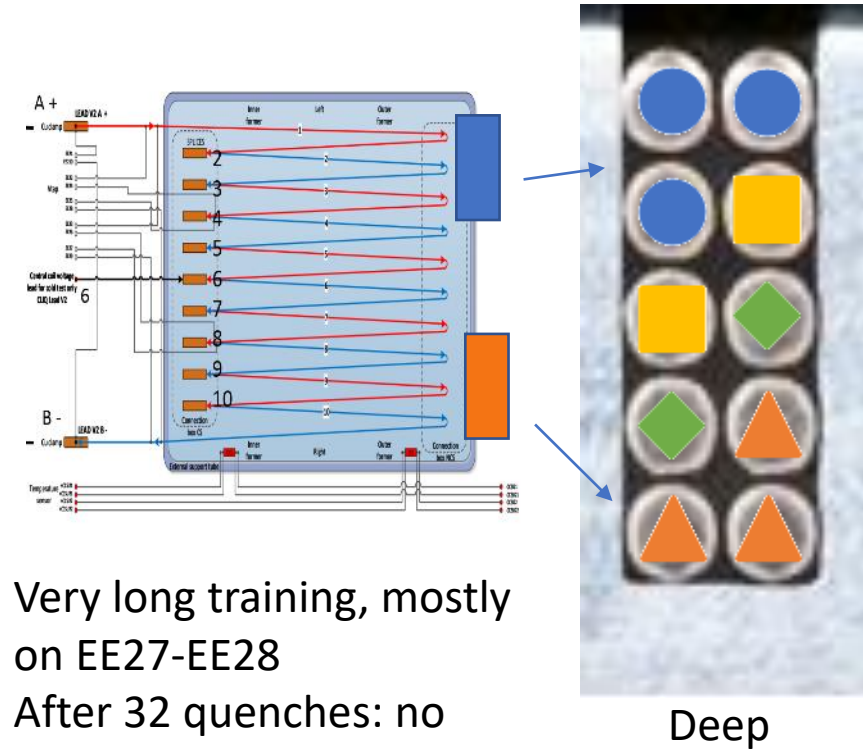
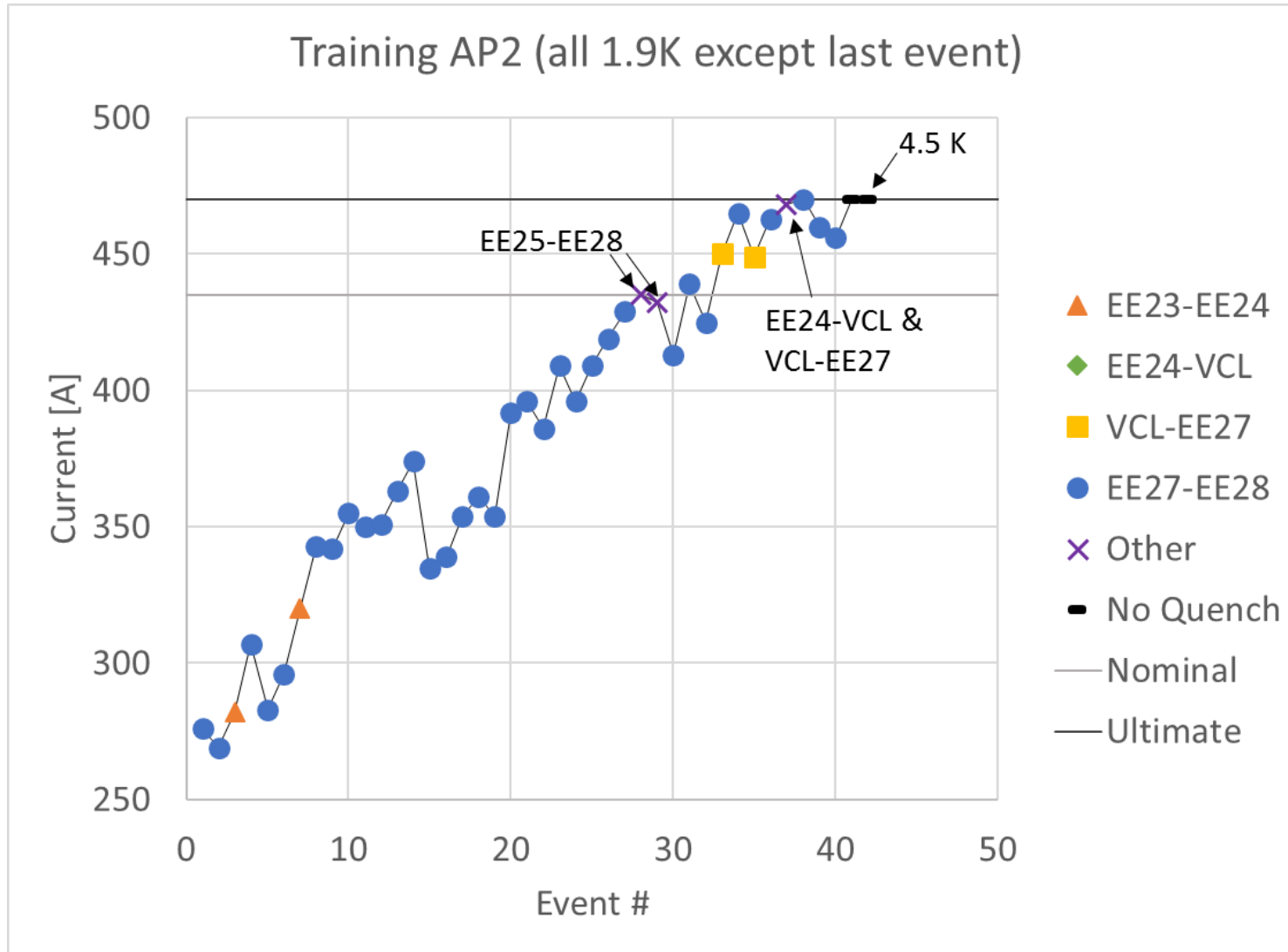


- Three quenches to nominal current
- Two last quenches within 1 A of ultimate current (in the decelerating ramp)
- No precursor in any quench
- Afterwards: held 2 h at ultimate current
- Protection: first two quenches above maximum allowed QI (hotspot temperature ~350 K)
 - More on this later



CERN Training AP2 Blue

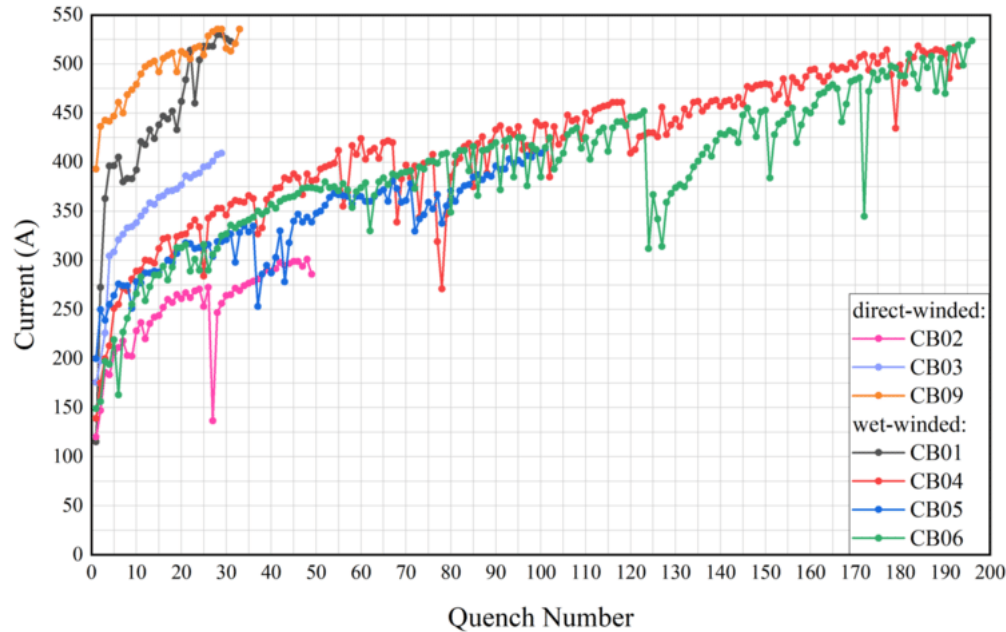
We can't separate the position inner and outer former quenches



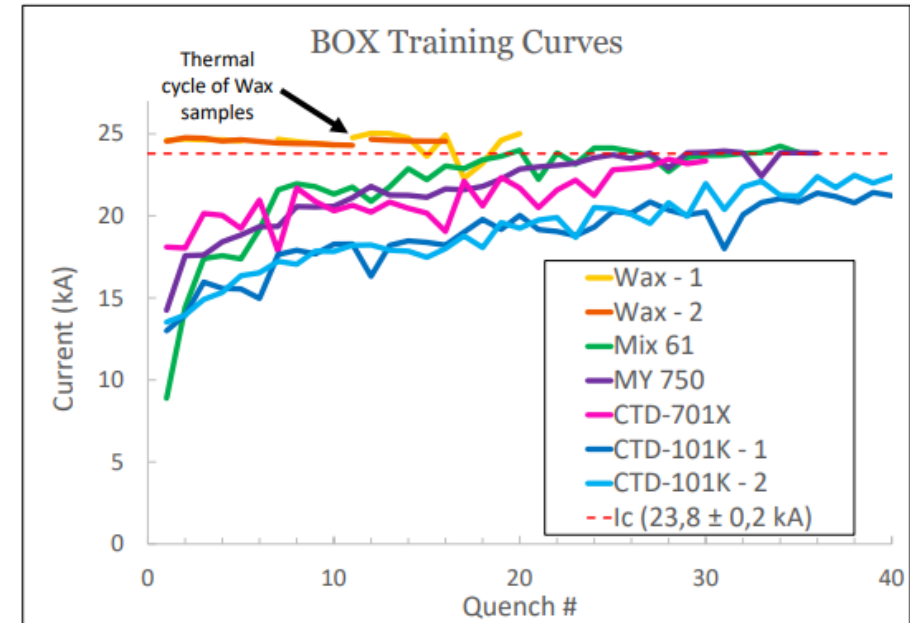
- Very long training, mostly on EE27-EE28
- After 32 quenches: no quench below nominal
- After 40 quenches training finished to ultimate current
- Held 2h at ultimate
- Quench #37 is symmetric

Quench training ! Superconducting magnets

Training History of the HL-LHC CCT Coils



LTS quench with very low energy input



With low temperature superconductors, the magnet can QUENCH with the energy that is in a pin doped 10 mm any
So small crack can trigger a quench!

What we need is an elastic support or very low friction! Tests with cold WAX have been very promising. My first every magent was potted in wax, and all ultra high field NMR 20 T + magnets use wax!

Stress in the channel is it + or - ? principal stress?

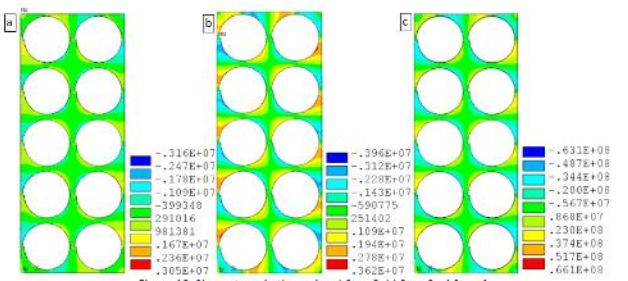
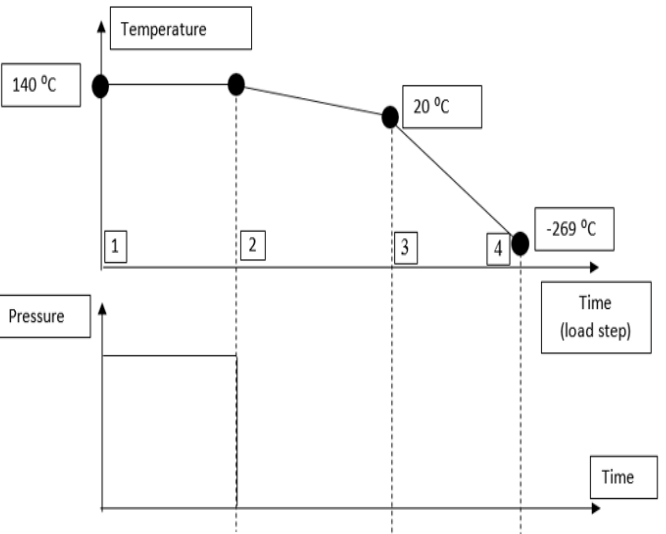


Figure 10. Shear stress in the resin: a) Step 2, b) Step 3, c) Step 4

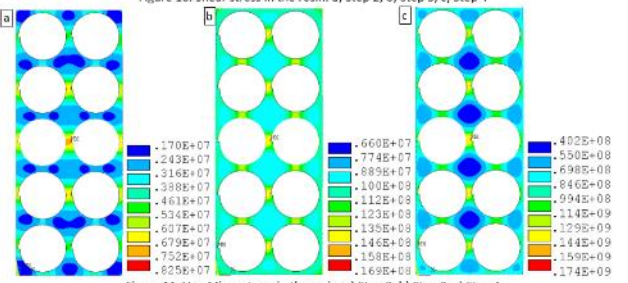
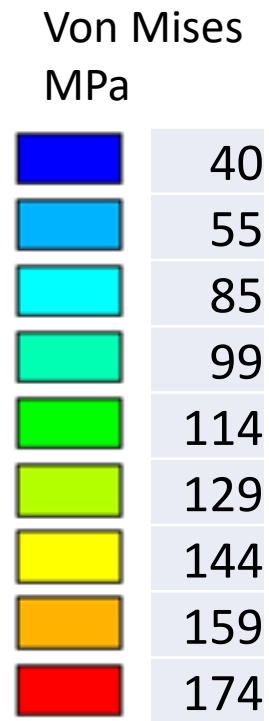
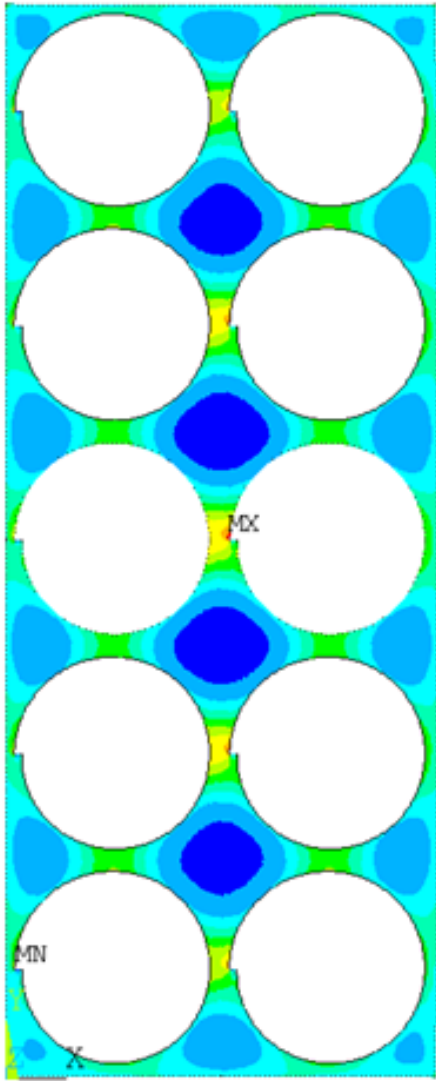
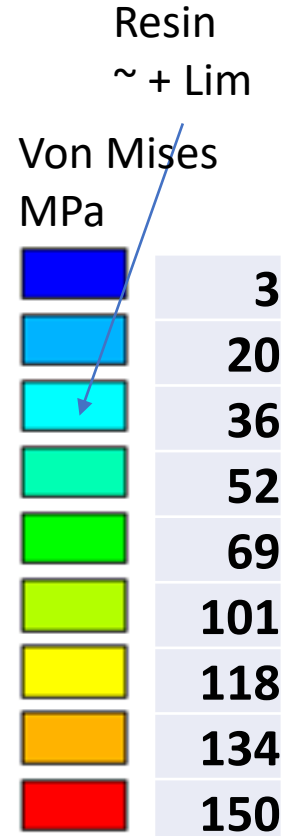
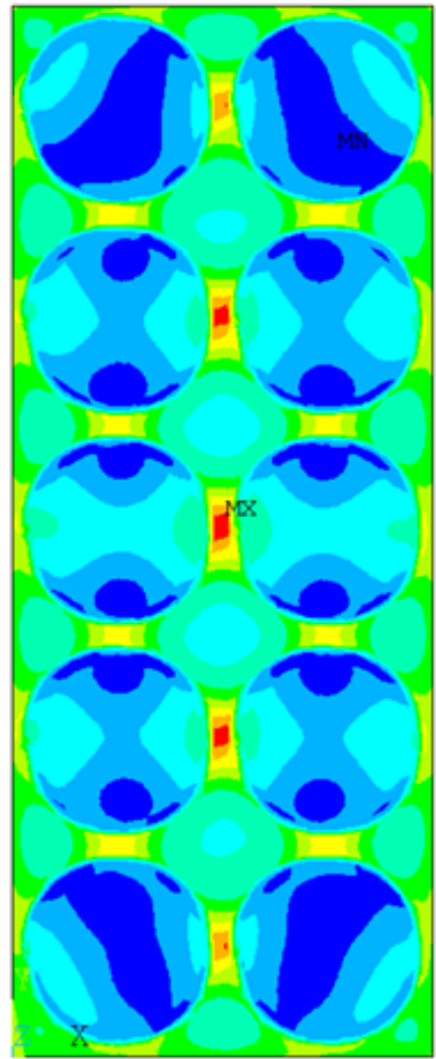


Figure 11. Von Mises stress in the resin: a) Step 2, b) Step 3, c) Step 4



Von Mises stress in the resin Mpa



Von Mises stress in cross section

Free at the Wall

The bonds will brake at the surfaces of the insulated wire and at the walls with ~ 5 MPa in shear or 10 MPa tension.

At 4 K one side will has released. When the magnet is powered the other side brakes free, (quench?)

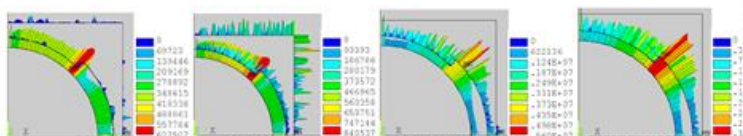


Figure 16. Contact pressure [Pa] for the 2nd case with frictional contacts ($\mu=0.3$): a) Step 1, b) Step 2, c) Step 3, d) Step 4

The shear stress in the resin reached 7 MPa at the interface with Kapton at RT and up to 40 MPa at 4 K (Figure 17).

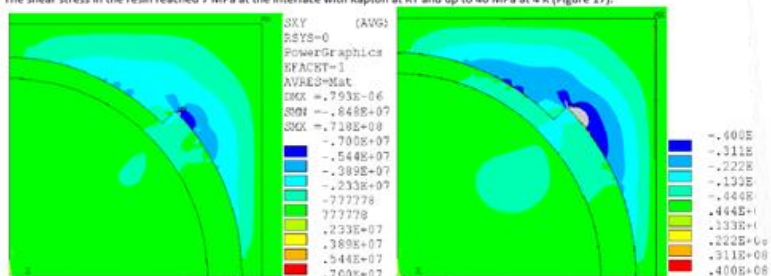
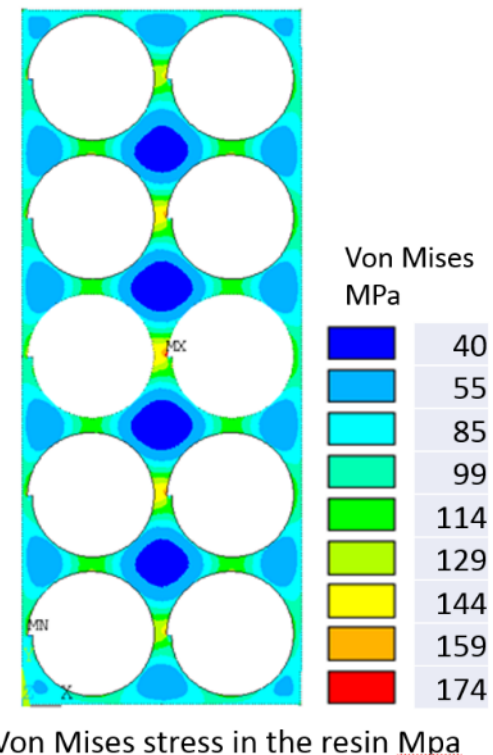
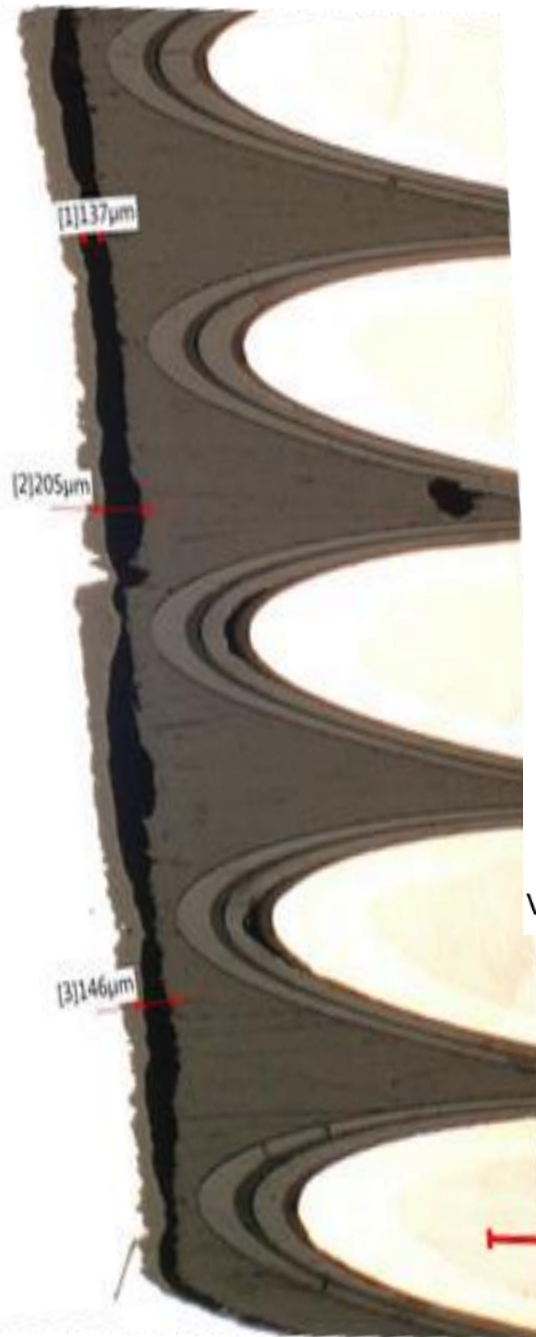


Figure 17. Shear stress (τ_{xy}) in Pa for the 2nd case with frictional contacts ($\mu=0.3$): a) after cool-down to RT (step 3), shear stress limited to 27 MPa, b) after cool-down to 4 K (step 4), shear stress limited to 140 MPa



Coil stress on channel after cooling down

CTD101K 12 mm/m
CTD101K at 4K **150 Mpa to 4 MPa**

After one-time thermal cycle



CTD101

After one-time thermal cycle



CTD101G 5 mm/m
CTD101G at 4K **47.5 Mpa to 6 MPa**

After

CTD101K
With Powders

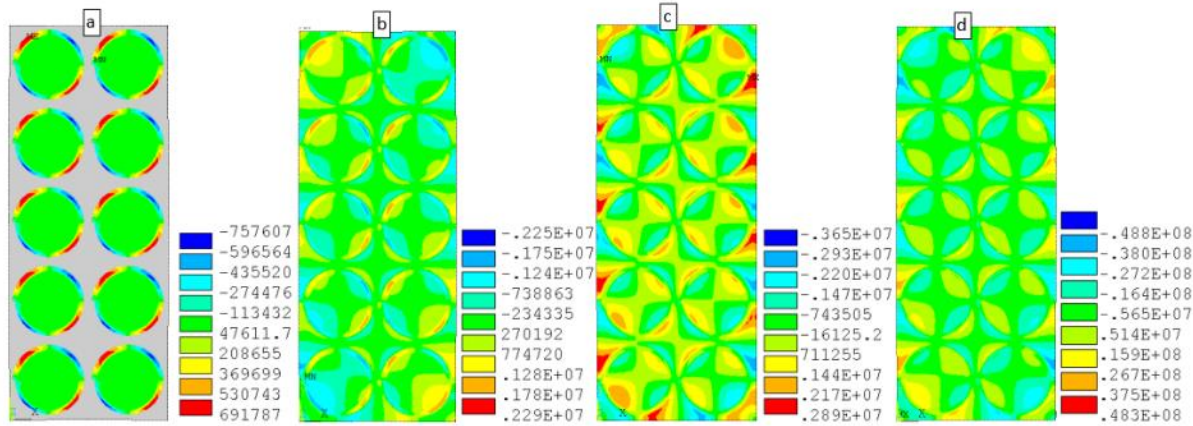
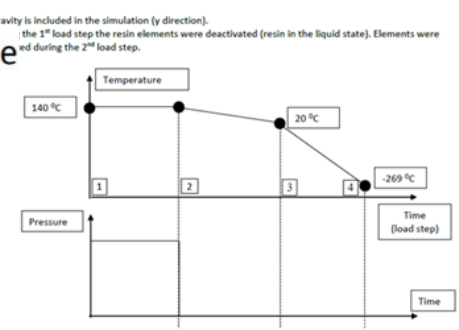


Figure 12. Shear stress in the strand, resin and Kapton: a) Step 1, b) Step 2, c) Step 3, d) Step 4

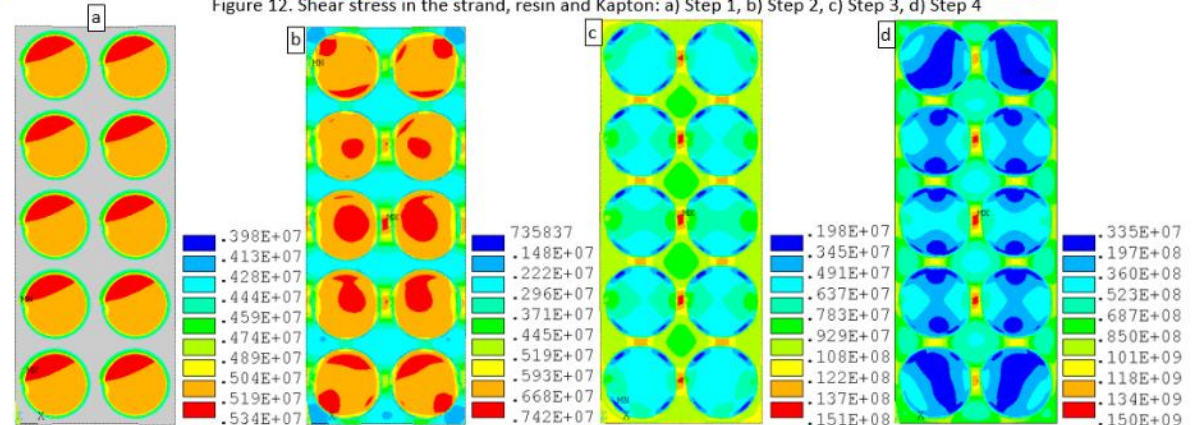


Figure 13. Von Mises stress in the strand, resin and Kapton: a) Step 1, b) Step 2, c) Step 3, d) Step 4

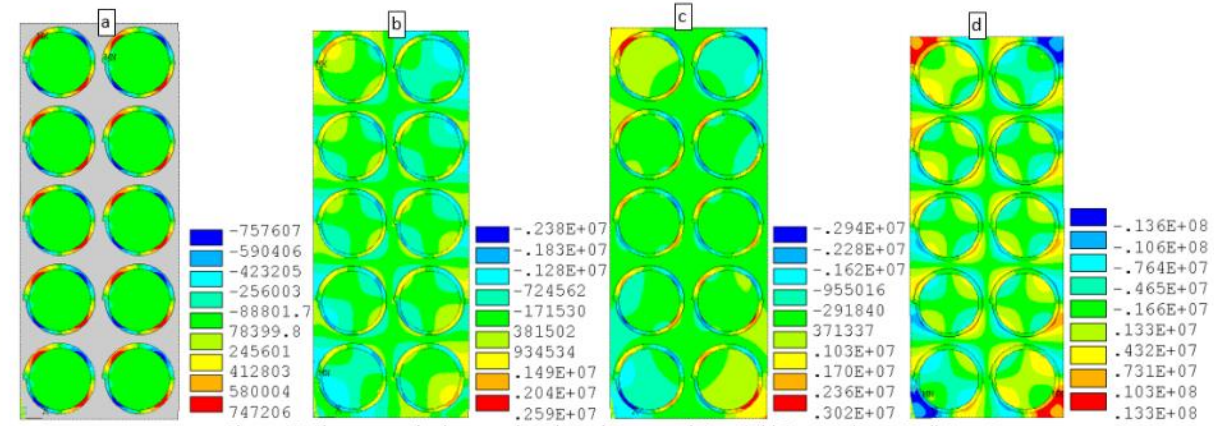


Figure 12. Shear stress in the strand, resin and Kapton: a) Step 1, b) Step 2, c) Step 3, d) Step 4

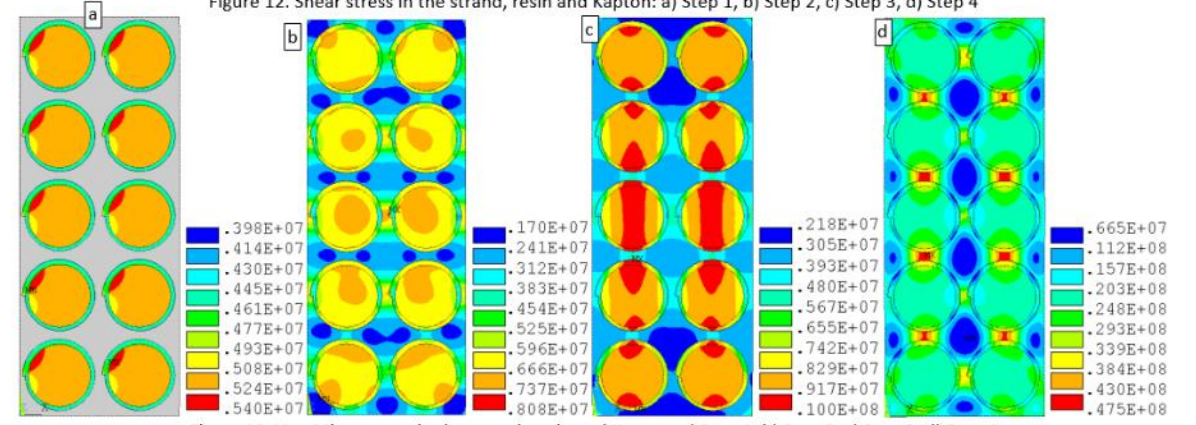


Figure 13. Von Mises stress in the strand, resin and Kapton: a) Step 1, b) Step 2, c) Step 3, d) Step 4

Internal forces

- Adding magnetic forces, give a small increase in stress, but its not uniformly distributed in the channel

3 TESLA

Shear Area:
 $5\text{mm} \times 2\text{sides} \times 1\text{m}$
 0.01m^2

Force = BIL .

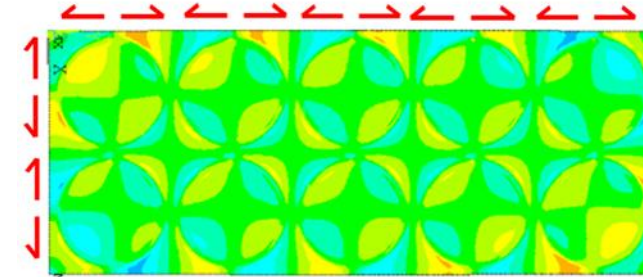
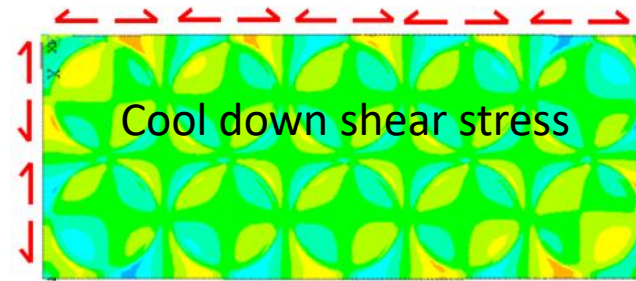
$3\text{TESLA} \times (600 \times 10) \times 1\text{m}$
 Force = 1.8 kN

Shear Stress = $\frac{F}{A_{\text{shear}}}$

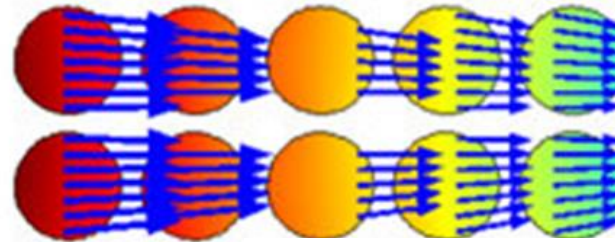
$\tau = \frac{1800\text{N}}{0.01\text{m}^2} = 1.8\text{MPa}$

\therefore @ 600A $\tau = 1.8\text{MPa}$
 @ 450A $\tau = 1.35\text{MPa}$

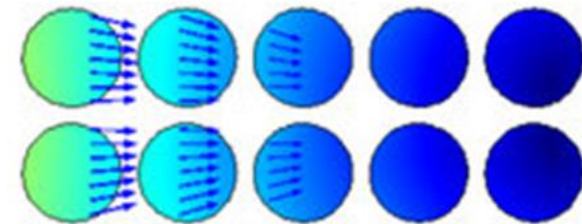
- “log stacking” strand positioning may help reduce resin volumes and transfer forces



Inner former



Outer former

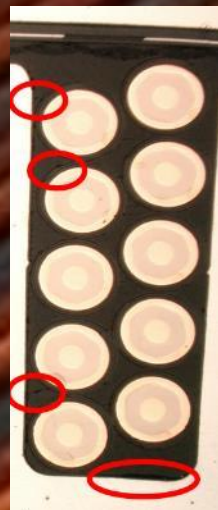


$t=0$ (i.e. regular operation),
 max Lorentz force per strand: 1070 N/m

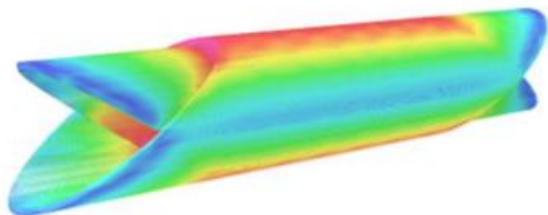
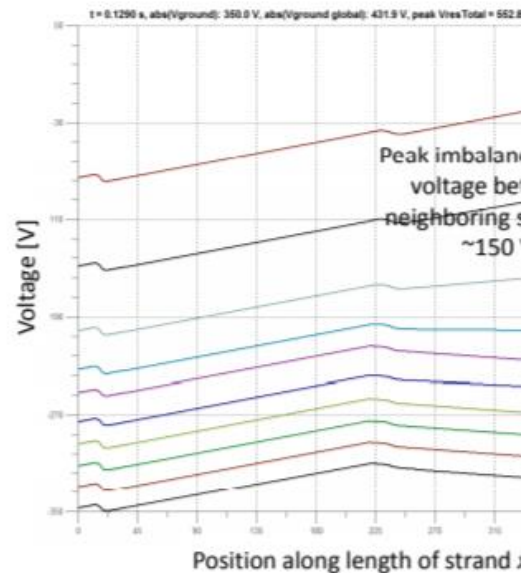
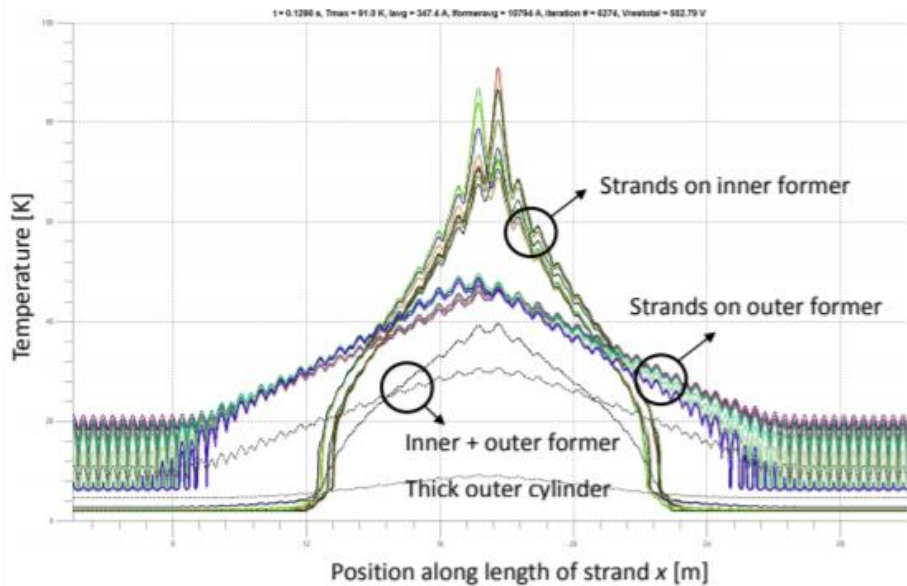
Stable Stacking



We can see at the winding stage that the wires are miss placed



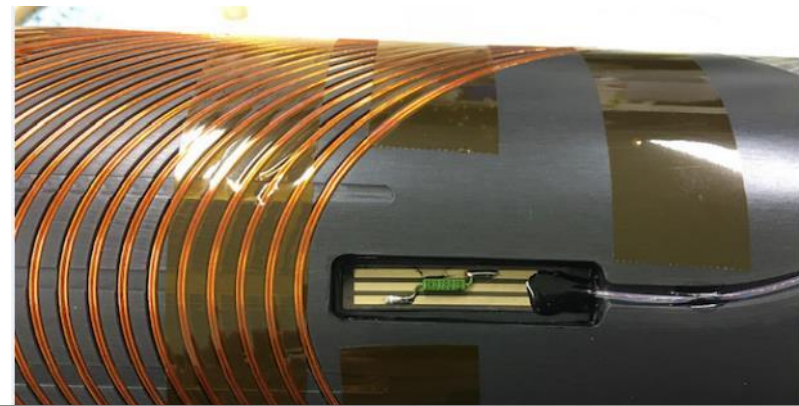
2020/10/27 13:13



Inhomogeneous quench-back: Inner-most strands quench before outer-most strand, strands on outer former quench before those on inner former

Quench patterns in CCT's thanks to:
Dr. Matthias Mentink.

Temp of formers quench-back



Temperature sensors in formers.

- Monitor and control cool down
- Measure eddy current temp rise quench dT 20 K
- Measure beam heating in LHC

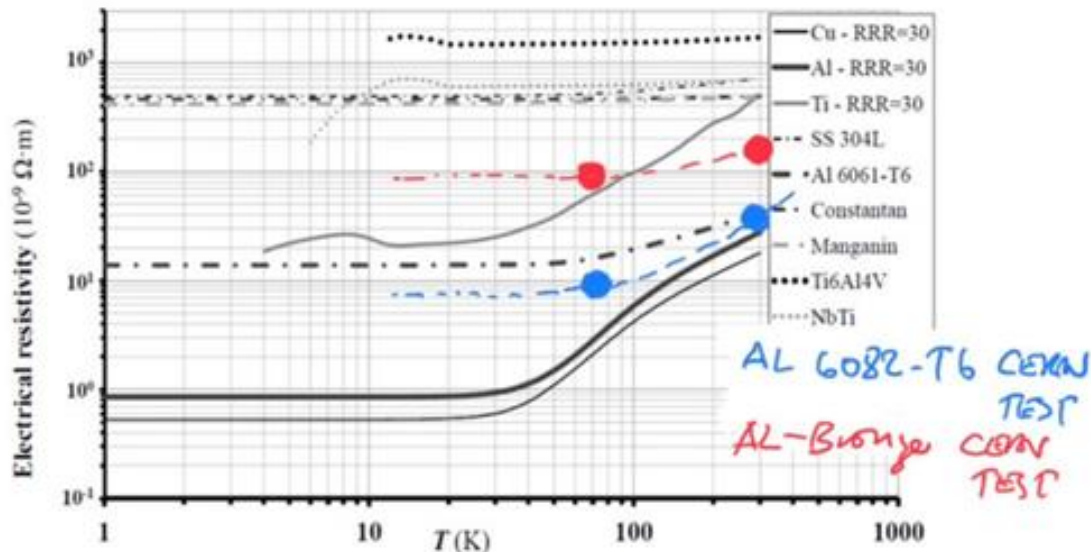
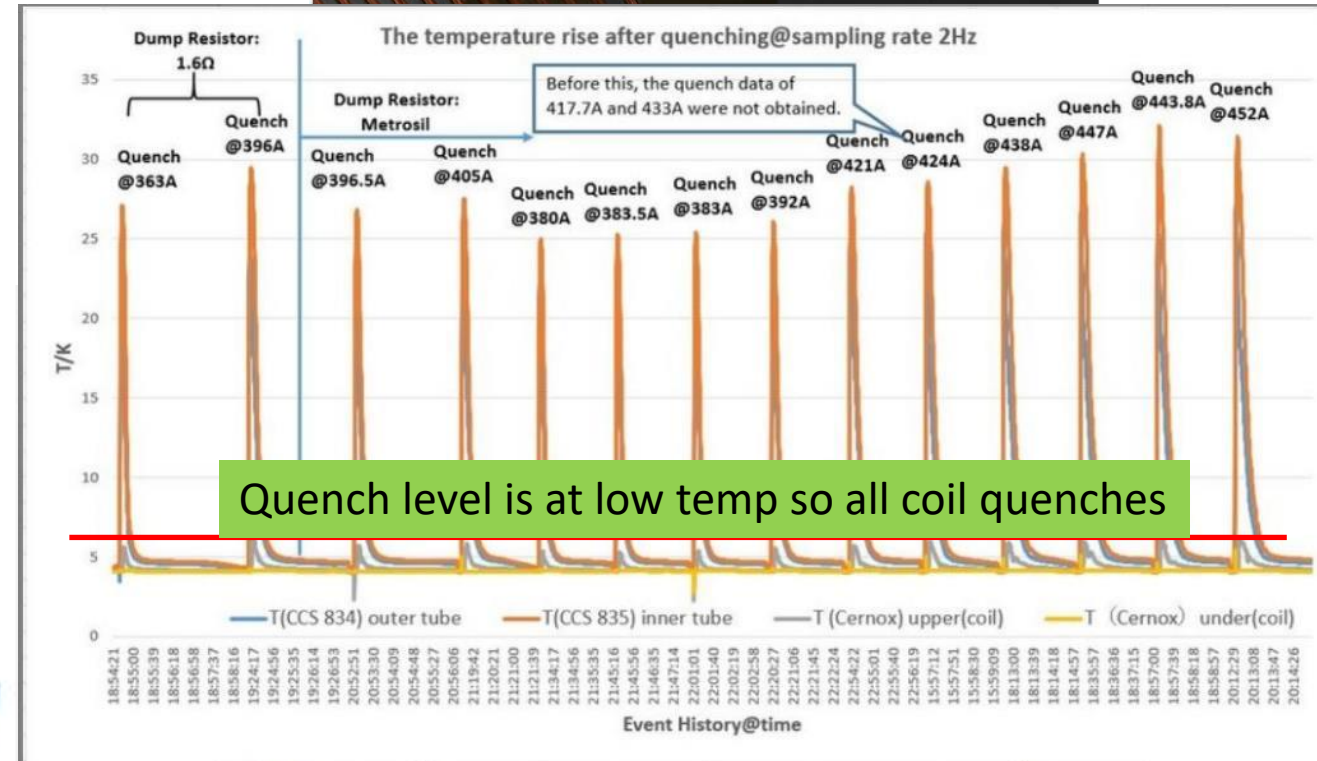


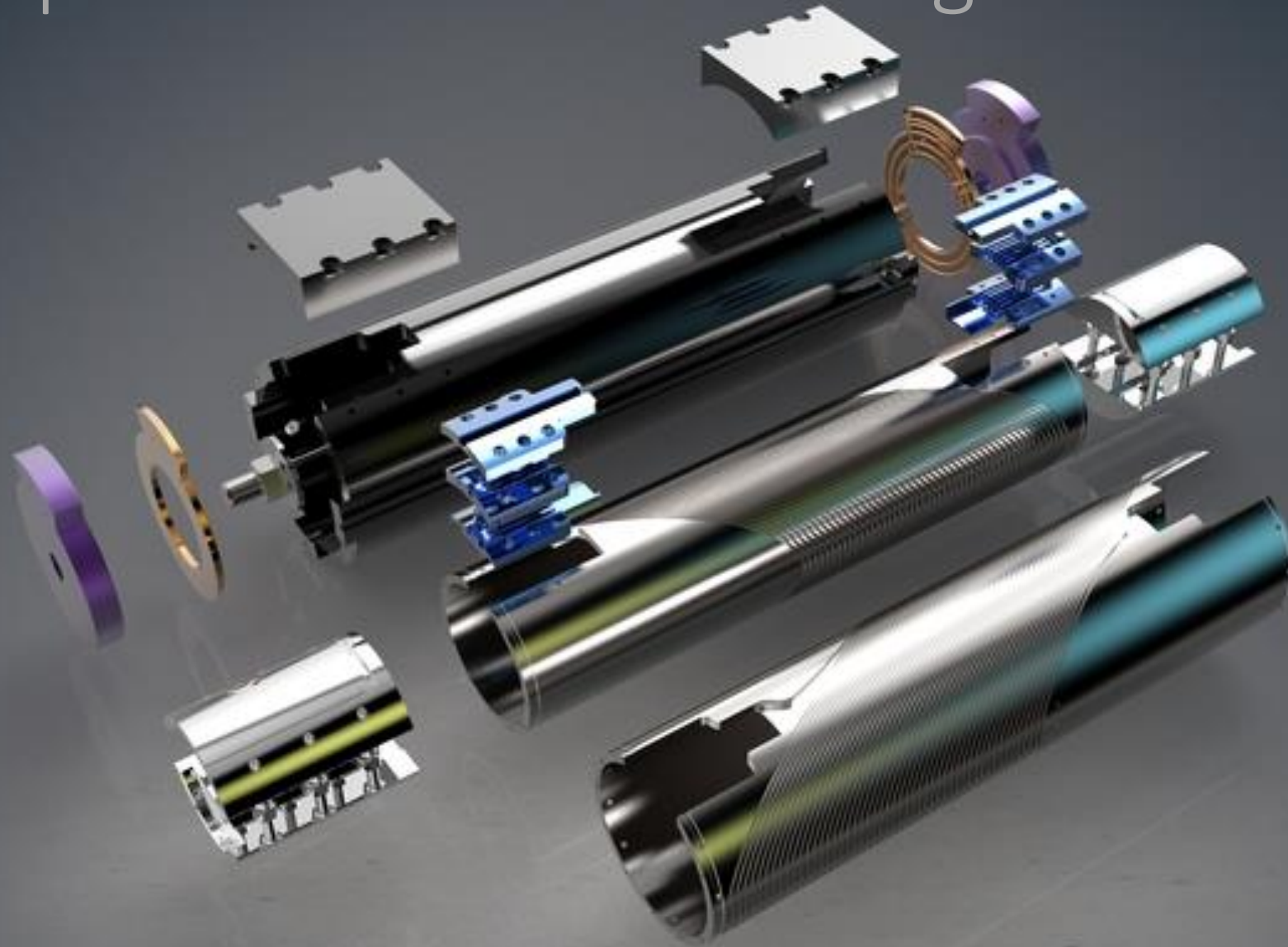
Fig. 10: Electrical resistivity ρ ($\Omega\cdot m$) of various materials versus temperature T . Metals are plotted with solid lines, metallic alloys with dot-dashed lines, and two superconducting alloys with dotted lines.



IMP test of Bama 1 aperture, former temperature during quench events

The CCS temperature sensors that are embedded in the former's inner and outer ! gave some consistent data points. On the plot we also see the CERNOX that are mounted on the yoke in the liquid as expected much less sensitive. the CCS will be an interesting sensor to see beam heating inside LHC

All the parts for the model magnet and tooling

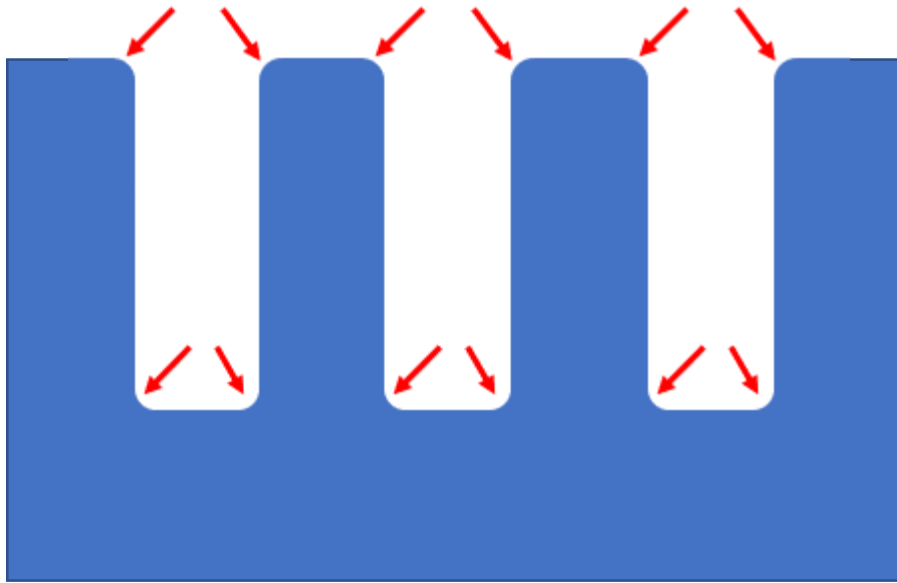




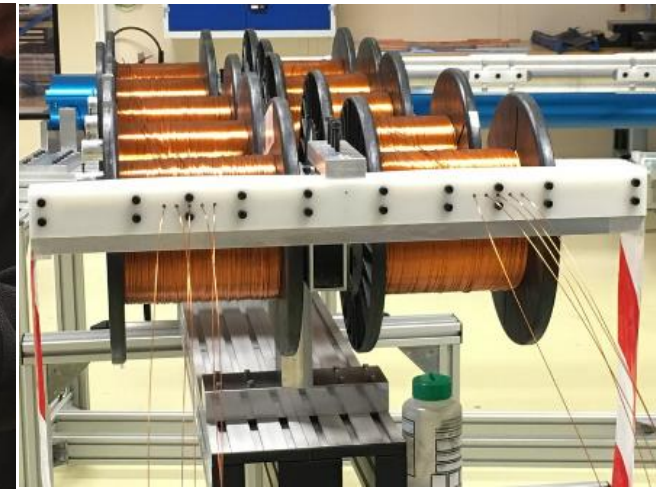
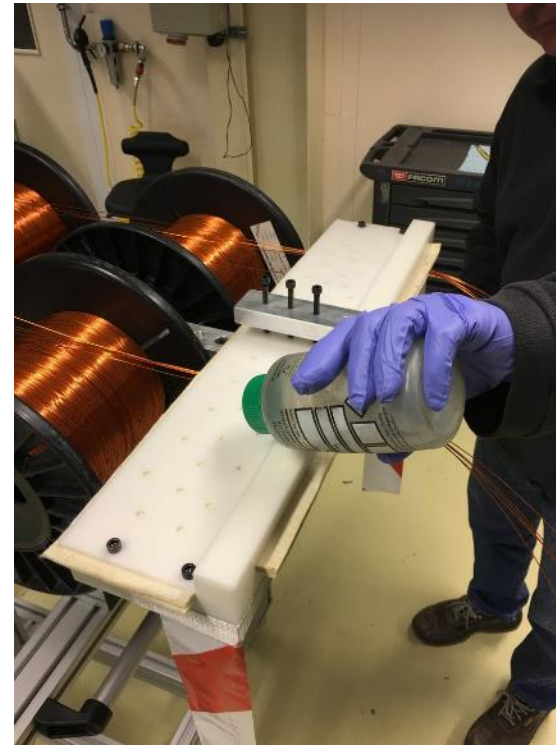
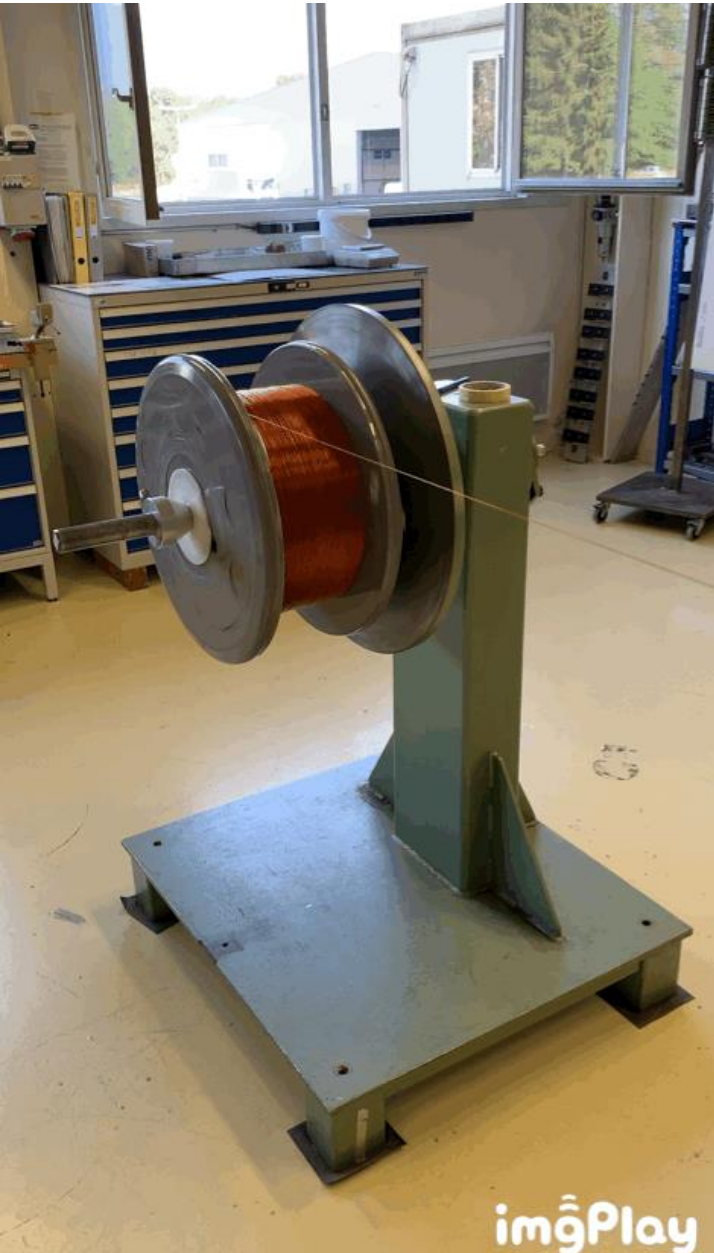
Remove sharp edges before anodization



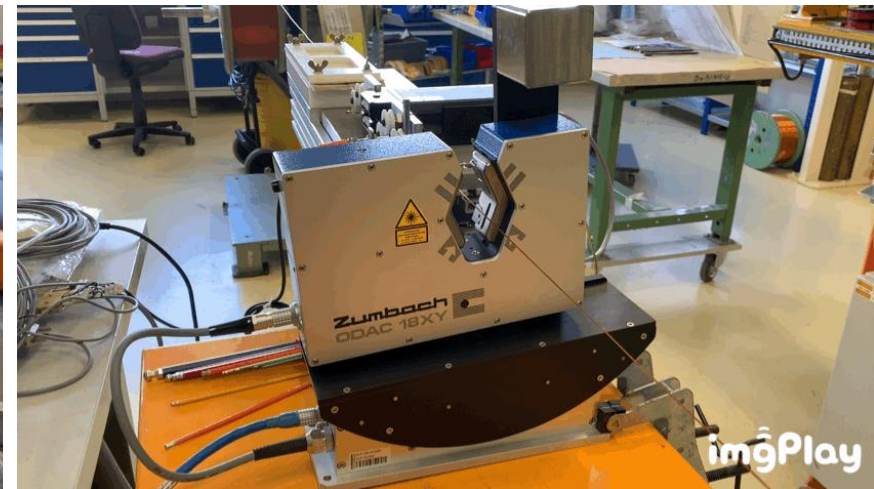
Radii are *very* important



Cleaning the Insulated Wire

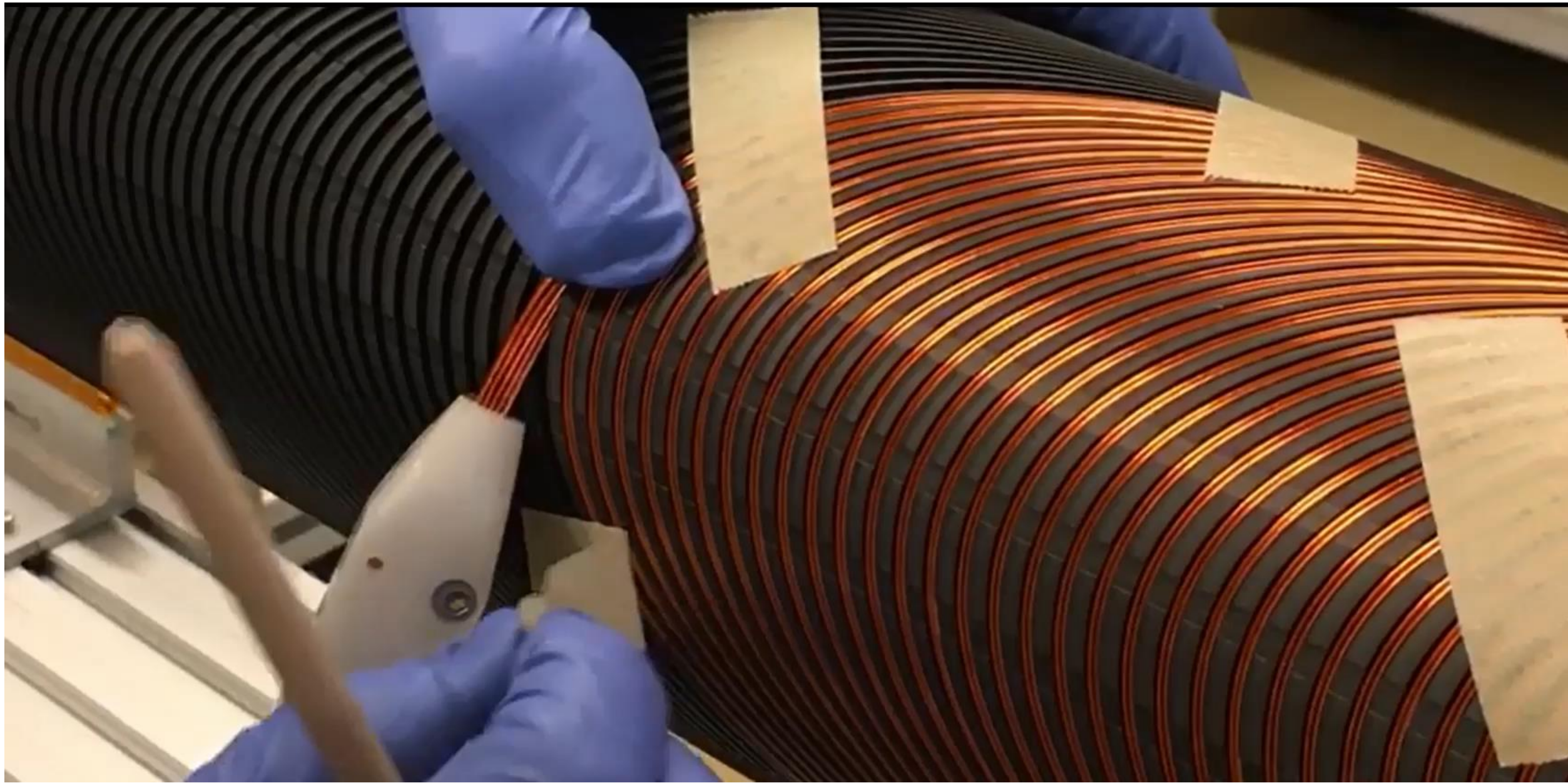


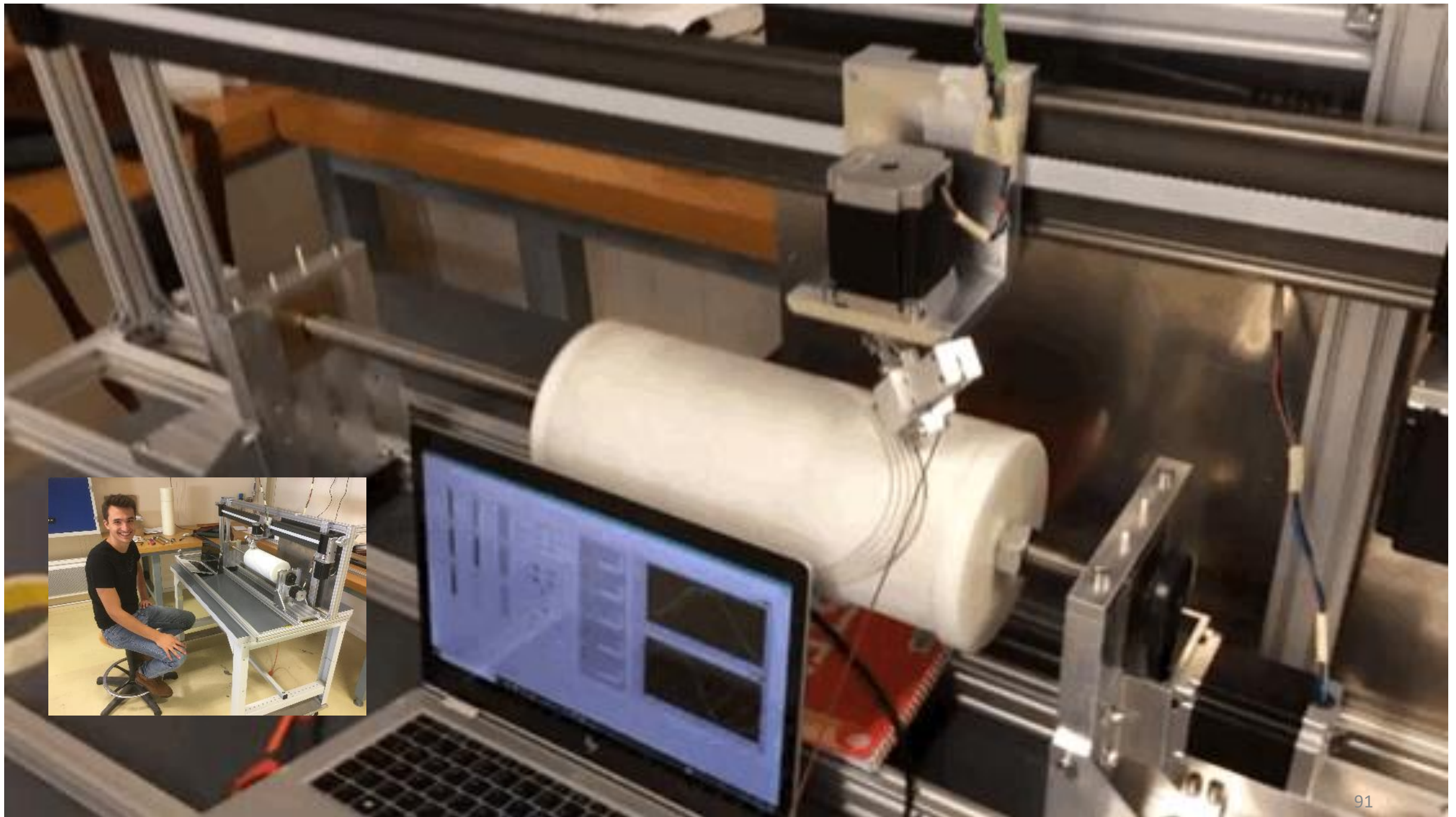
Wire Cleaning ,
Voltage test ,
Size measures.





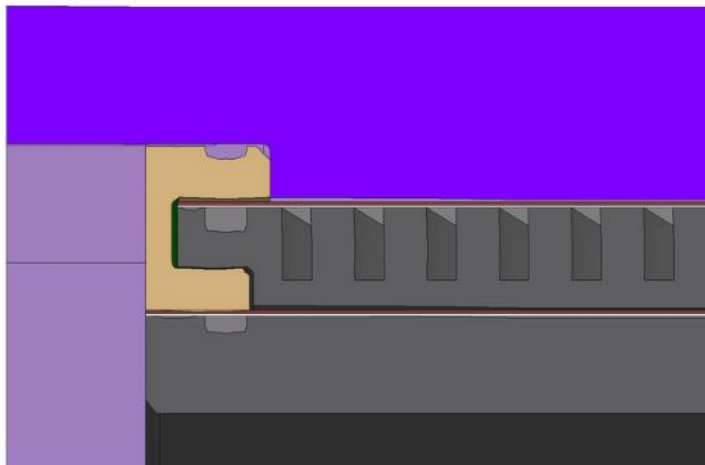
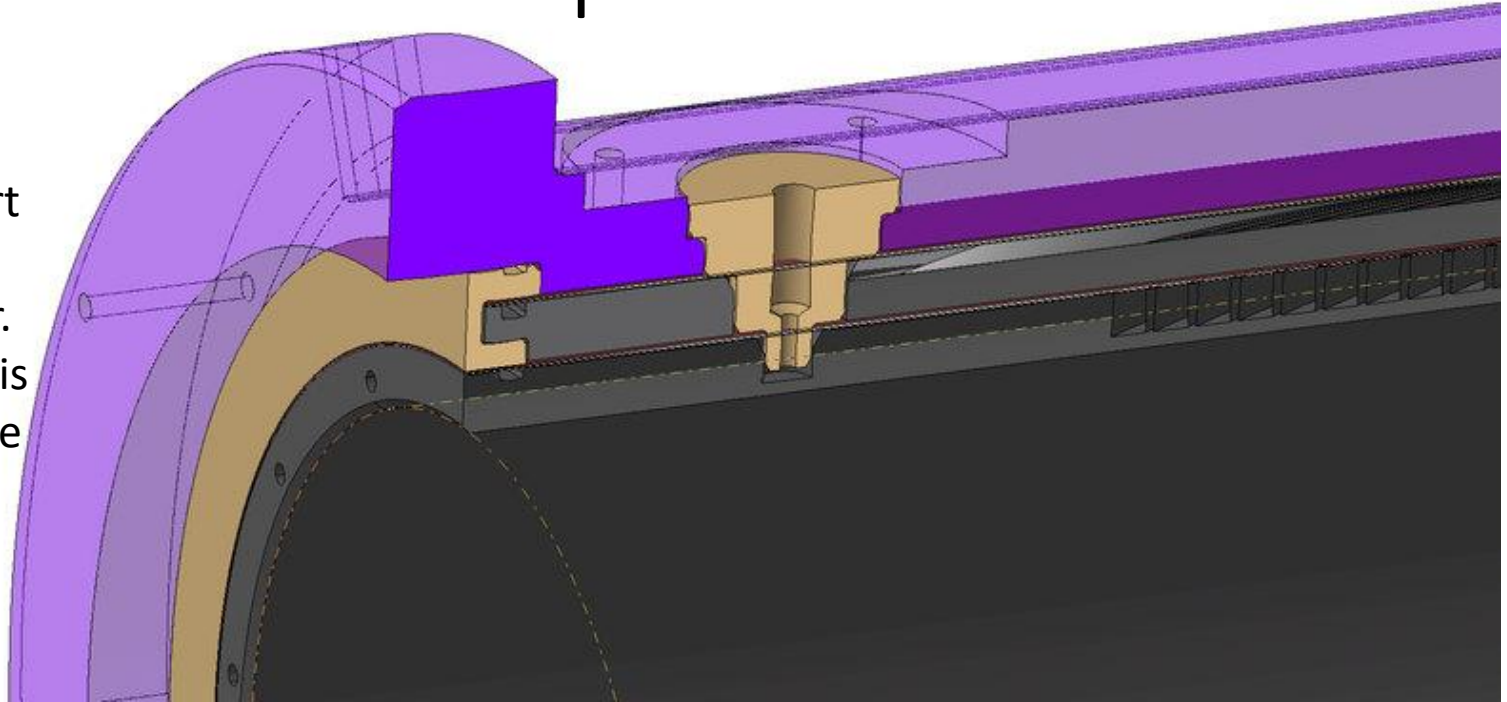
10 spools with insulated wire, Wire cleaning, Hard anodized aluminium 6082-T6 CCT former





Ground insulation & location pins

The voltage path between the two formers and between the outer former and the outer support ring is at least 4 to 5 mm. The two layers of Kapton sheet provide a general electrical barrier. At the ends we need the 4 to 5 mm distance. This also applies at the alignment pin, the pin is made of a glass resin, the ends are also protected by a labyrinth insulating ring.

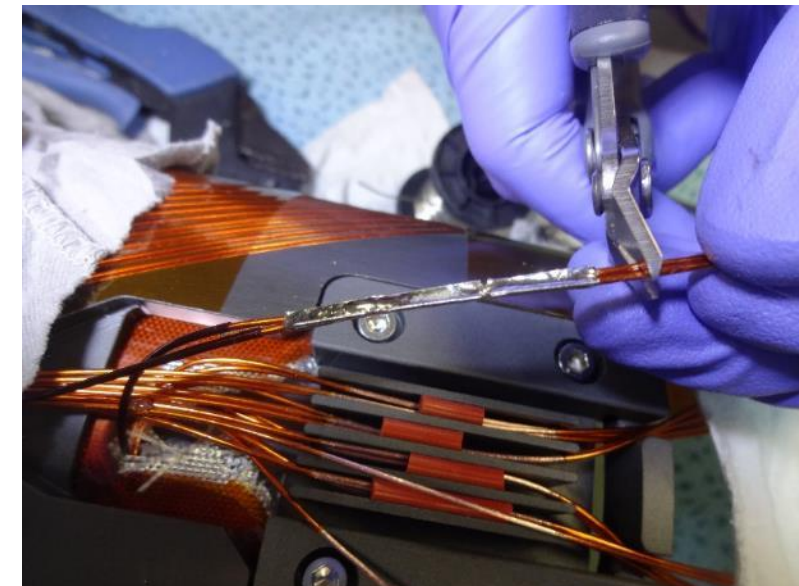
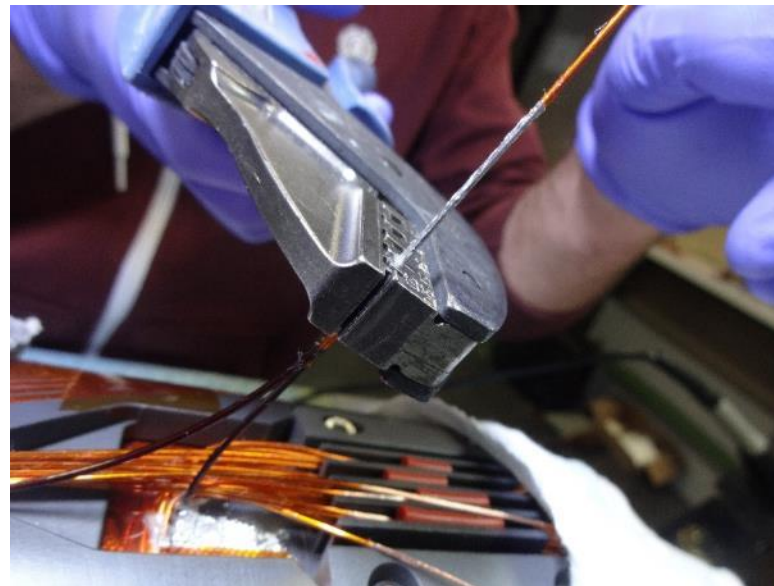
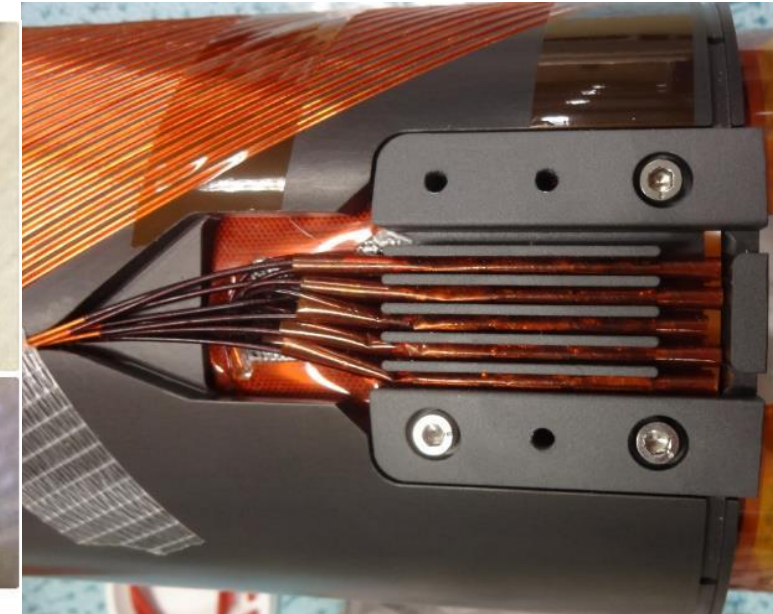


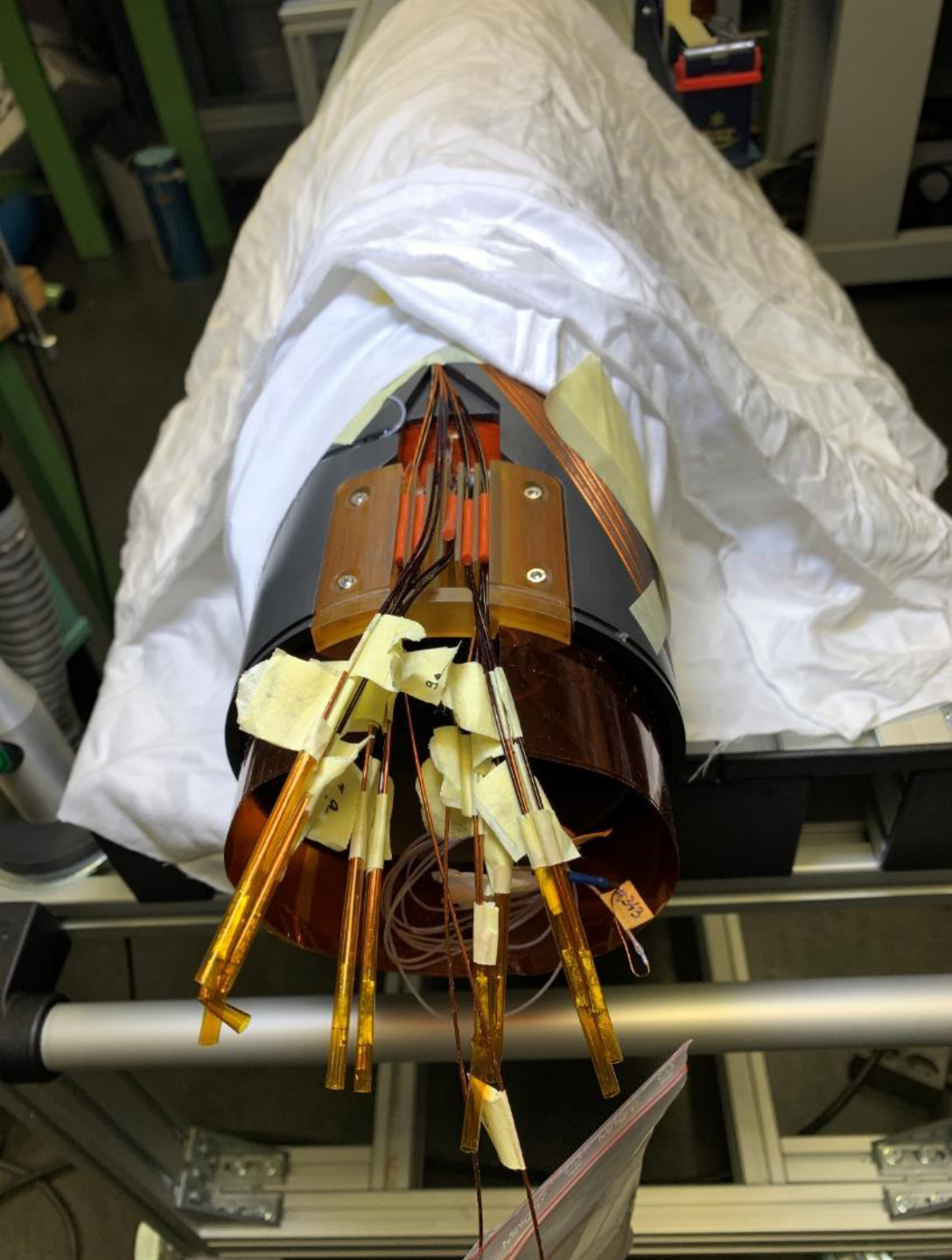
III. Splicing / Jointing

- Short MCBRDS : 21 splices per aperture
- Prototype MCBRDP : 9 splices
- 45 mm long
- Crimping with “non insulated end-sleeve” (= tube)
- Sn96Ag4 welding alloy
- Flux MOB39
- Poly-imide sleeve for protection
- Connexion box



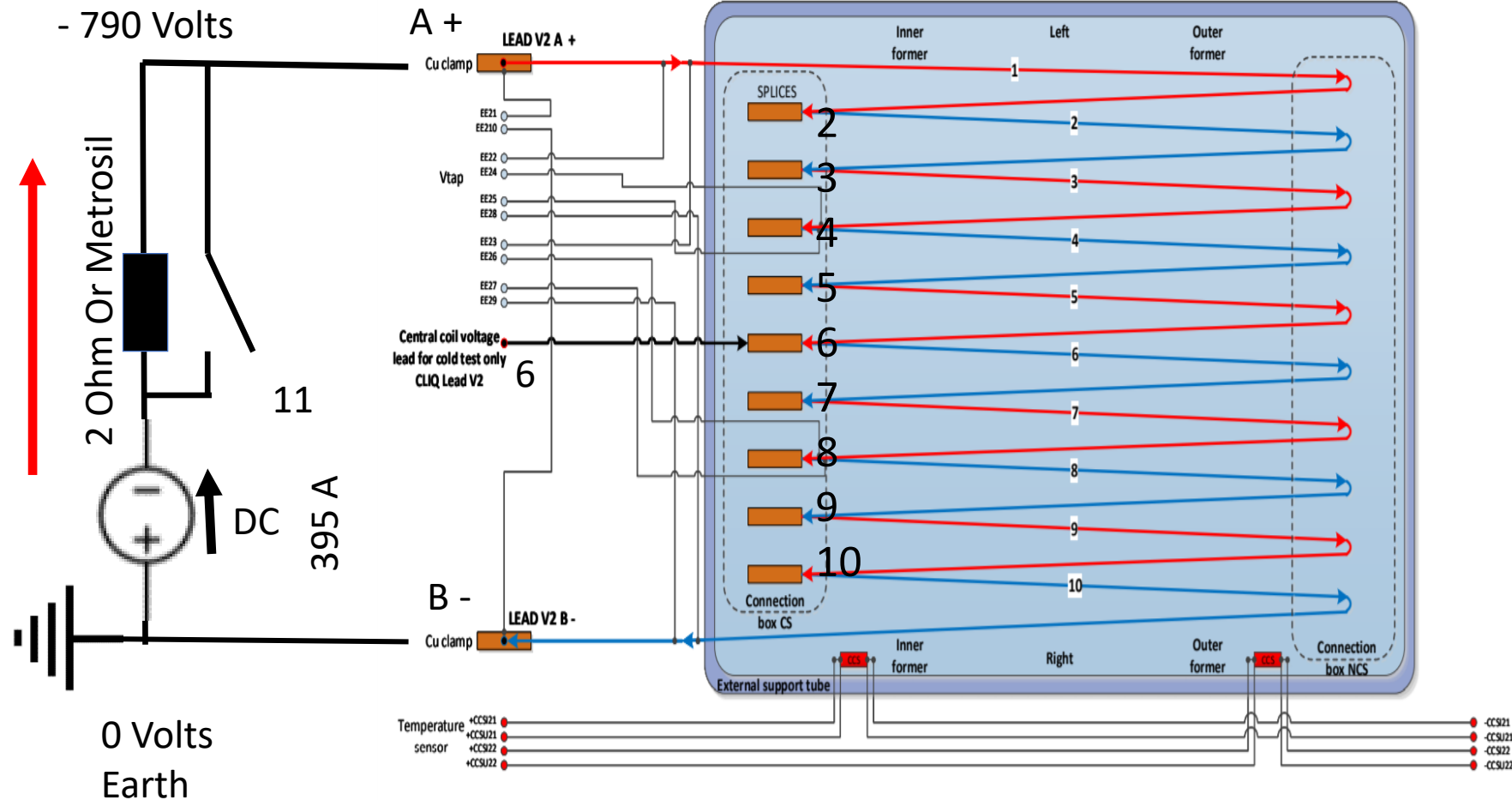
600A joint Copper tube tined with solder, crimped, and soldered,



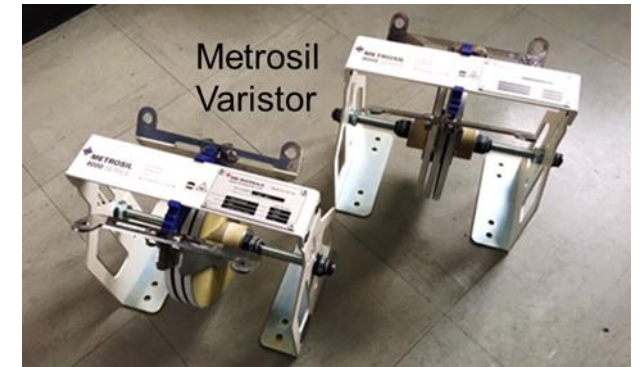
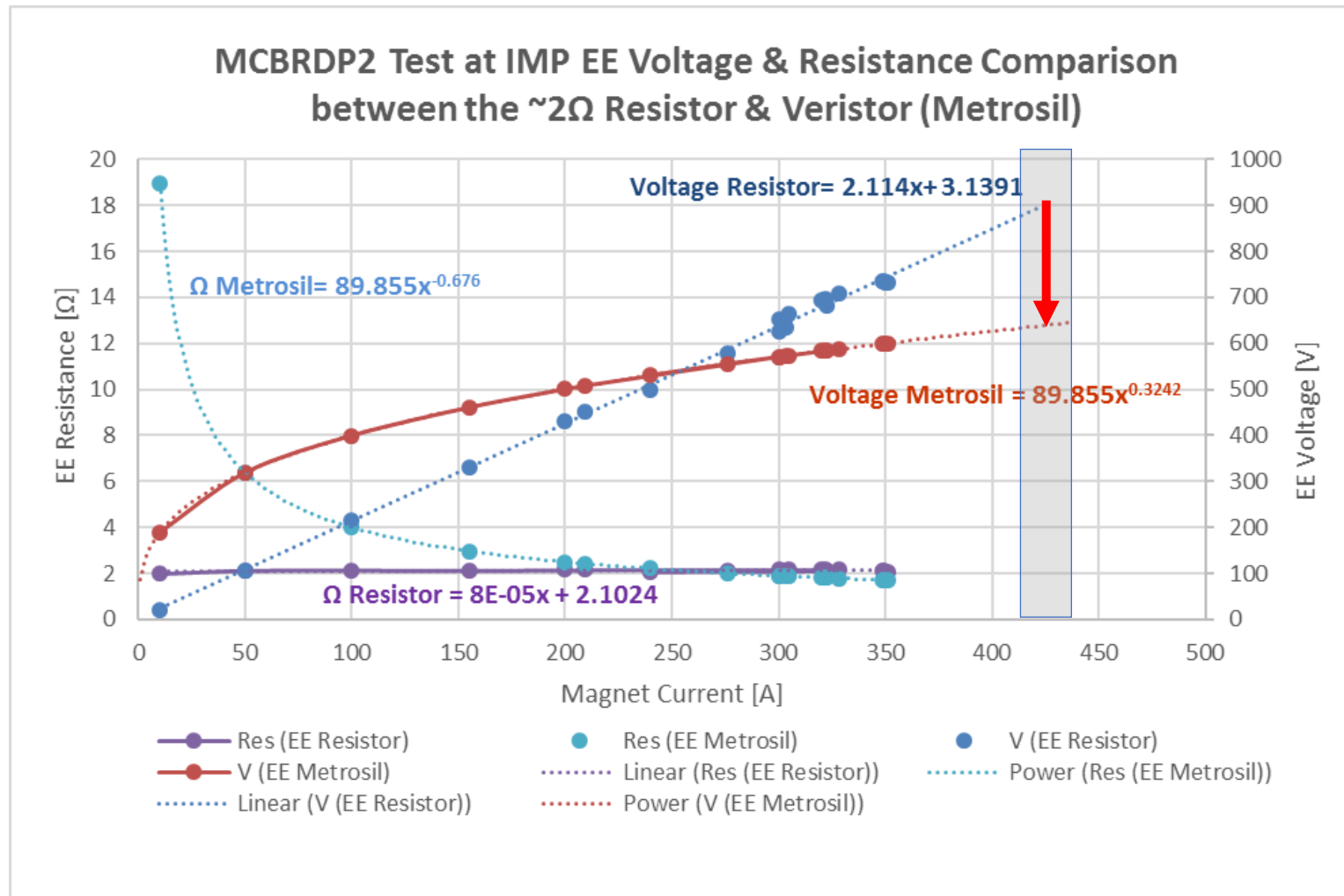


Voltage in the circuit with 2 ohm EE at 395 A

dV =	79	71.1
Voltage position	2 ohm Dump Res.	Metrosil 2 ohm equivalent
#	[V]	[V]
1	-790	-711
2	-711	-639.9
3	-632	-568.8
4	-553	-497.7
5	-474	-426.6
6	-395	-355.5
7	-316	-284.4
8	-237	-213.3
9	-158	-142.2
10	-79	-71.1
11	0	0

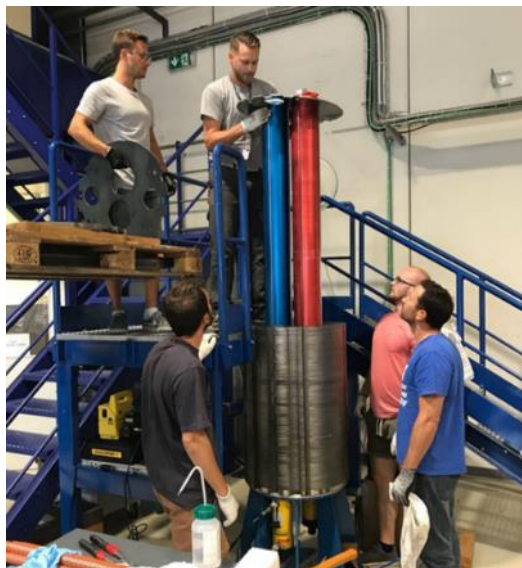
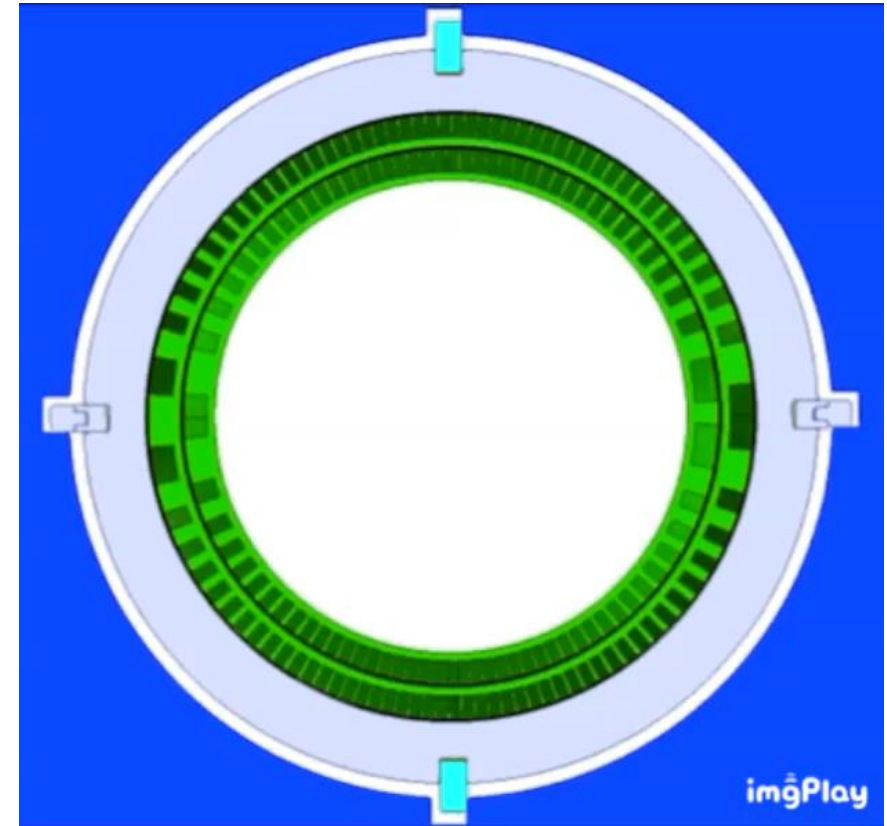


Energy Extraction optimization for low hot-spot & low Vmax



The first Varistor was used at CERN in 1980's if we replace the std Dump resistor with a varistor we can reduce both quench hot spots, and importantly voltages. In this test at IMP for a fixed hot spot of $\sim 150K$ the voltage drops by $\sim 30\%$

Magnet yoke assembly



Vertical yoke assembly

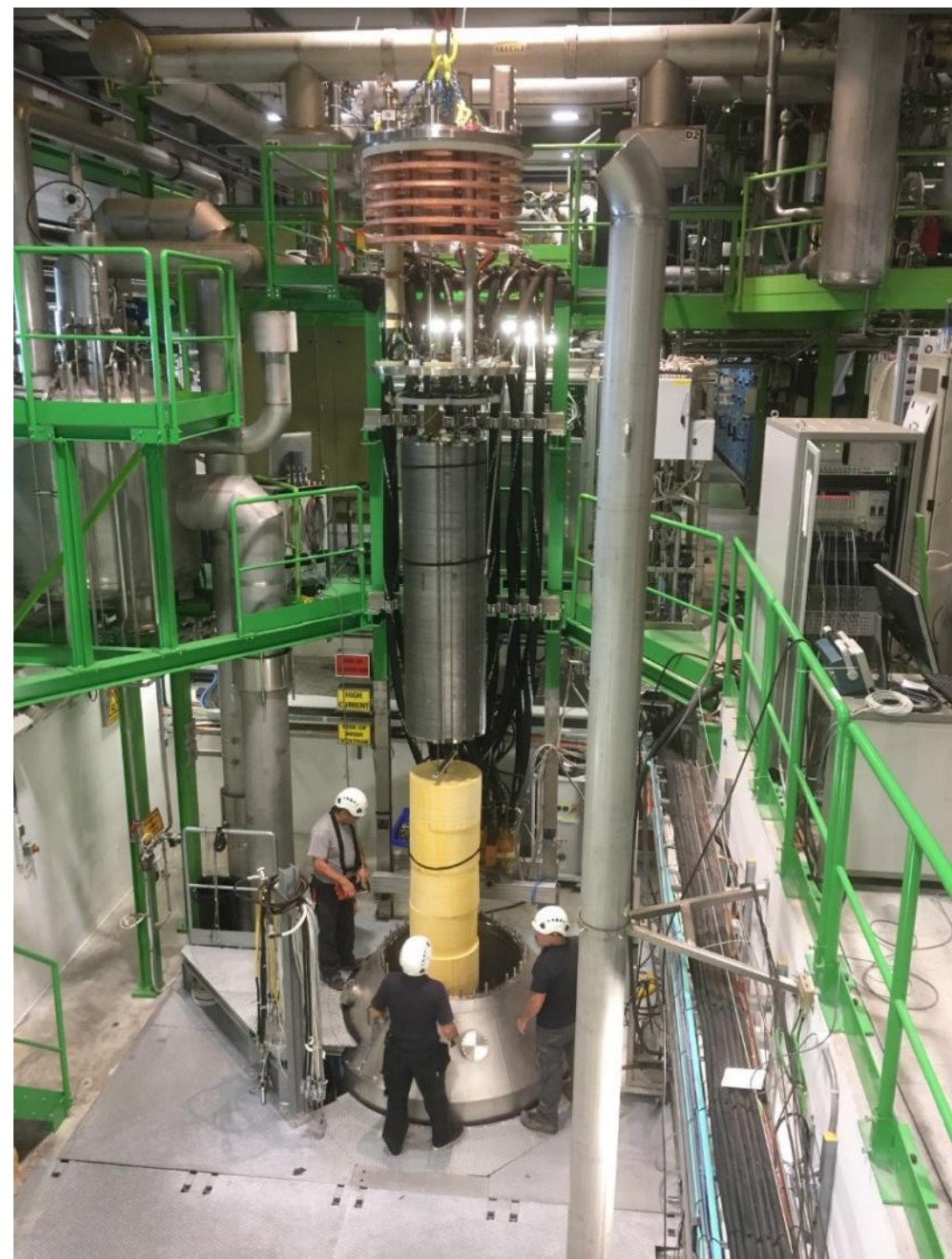
364 yoke laminations, 5.8mm nominal thickness gave the design length

Axial Yoke packing factor 98.64%

Compressed with hydraulic jacks and held with tie rods.

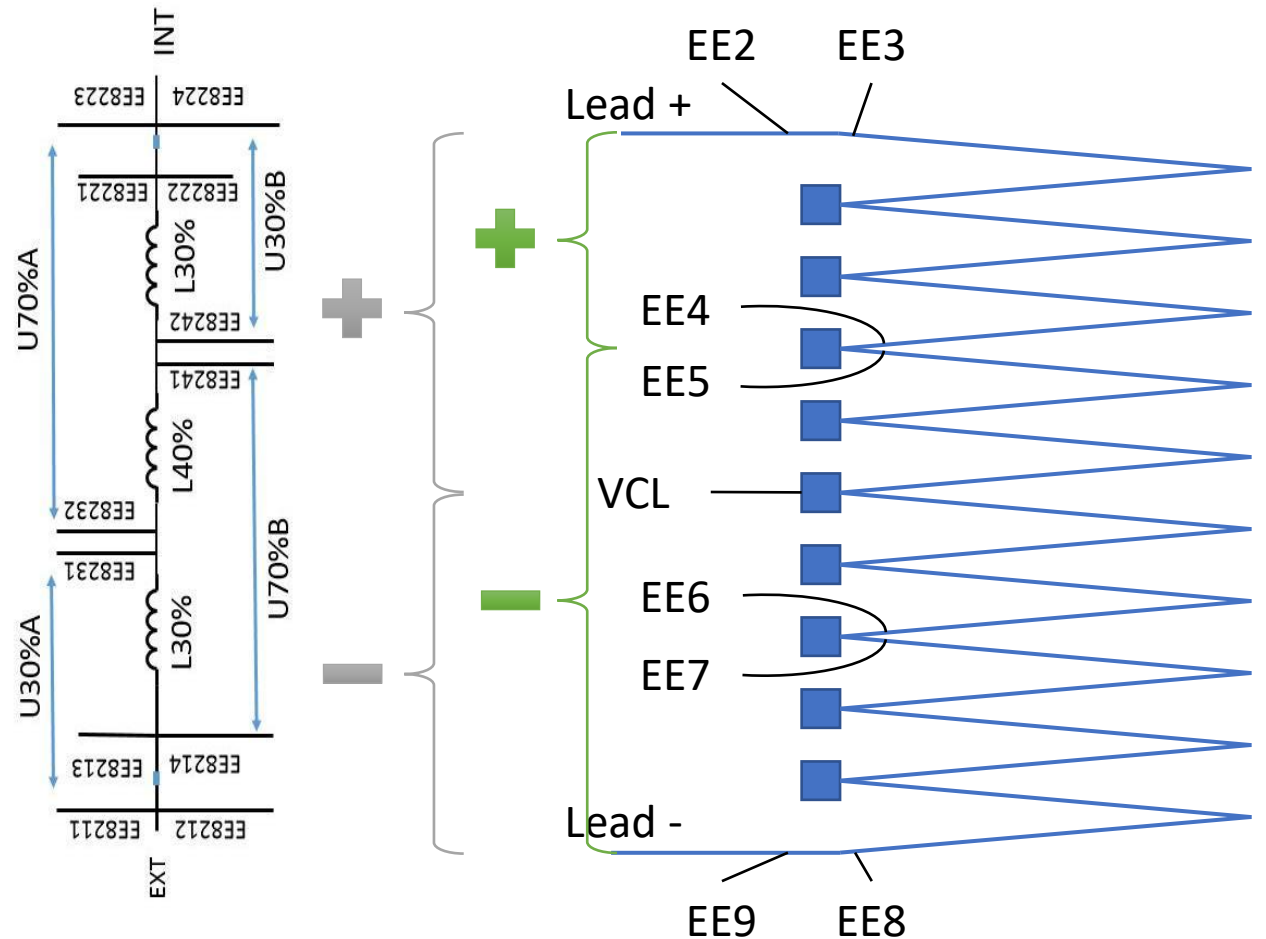
The first cold test of a full size CCT for LHC hi-Lumi

- MCBRDP1 with two individually powered apertures, 1.9K
- One standard LHC 2 x 600 A power converters
- One standard LHC 600 A energy extraction rack with two switches and two energy extraction dumps (Resistor or Metrosil)



Symmetric Quench detection card

- QDS setup (baseline):
 - $2.3(EE3-EE5) - (EE5-EE8)$
 - Trigger after 4 ms @ 100 mV
- Potaim setup:
 - $(EE3-VCL) - (VCL-EE8)$
 - Trigger after 10 ms @ 50 mV



New protection card against symmetric quenches!

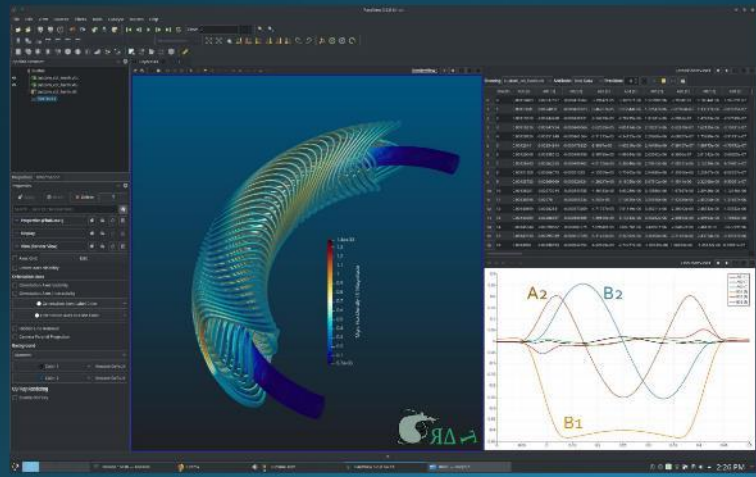
mid- MARCH ready to place orders
Main work shop project.

Item	Item Number	Description	Quantity	Unit	Material	Last Modification	ECOM	Cap Ref
ITEM	ST026275	2m DC CONNECTION ASSEMBLY	1			03.02.2017 16:49		
ITEM	ST026276	2m MAGNET COIL ASSEMBLY	2					
ITEM	ST026278	DC FREE EXTREMITY PLATE	1		EN 1.4308 (St. Steel 304L)			
ITEM	ST026279	DC FREE EXTREMITY PLATE	1		EN 1.4308 (St. Steel 304L)			
ITEM	ST026280	DC CONNECTION YOKE v6	206		ARMCO P/4 (St. Steel)			
ITEM	ST026281	2m BEP	4		EN 1.4308 (St. Steel 304L)			
ITEM	ST026282	DC INSULATING WIRE LINE 1	1		Applty OF EP GC 200 (E-1)			
ITEM	ST026283	DC INSULATING WIRE LINE 2	1		Applty OF EP GC 200 (E-1)			
ITEM	ST026284	DC INSULATING WIRE COVER	1		Applty OF EP GC 200 (E-1)			
ITEM	ST026285	2m HYBRID HOVING KEY ASSEMBLY	12					
ITEM	ST026286	2m HYBRID HOVING KEY ASSEMBLY	12		Alu EN 5056 (216)			
ITEM	ST026287	2m OUTER COIL	2		Alu EN 5056 (216)			
ITEM	ST026288	2m INTERNAL PIPE	2		Alu EN 5056 (216)			
ITEM	ST026289	INSULATING RIVET PLATE	4		Applty OF EP GC 200 (E-1)			
ITEM	ST026290	WIRE CRY BOX	2		Applty OF EP GC 200 (E-1)			
ITEM	ST026291	EXTERNAL BOX WIRE CAGE	42		Coil (1.4308)			
ITEM	ST026292	CONNECTION BOX COVER	4		Alu EN 5056 (216)			
ITEM	ST026293	CONNECTION BOX INNER PLATE	4		Alu EN 5056 (216)			
ITEM	ST026294	CONNECTION BOX MIDDLE PLATE	4		Alu EN 5056 (216)			
ITEM	ST026295	2m HYBRID HOVING KEY INNER PART	12		EN 1.4308 (St. Steel 304L)			
ITEM	ST026296	2m HYBRID HOVING KEY OUTER PART	12		ARMCO P/4 (St. Steel)			
ITEM	ST026297	HYBRID KEY JIG	4		EN 1.4308 (St. Steel 304L)			
ITEM	HD 4762_M04-A4	HEX KEY HD CAP SCREW_M04	17		St. Steel A4		47.62.17.100.0	
ITEM	HD 4762_M06-A4	HEX KEY HD CAP SCREW_M06	16		St. Steel A4		47.62.16.100.0	
ITEM	HD 4762_M08-A4	HEX KEY HD CAP SCREW_M08	16		St. Steel A4		47.62.16.100.0	
ITEM	HD 4762_M10-A4	HEX KEY HD CAP SCREW_M10	16		St. Steel A4		47.62.16.100.0	
ITEM	HD 4762_M12-A4	HEX KEY HD CAP SCREW_M12	16		St. Steel A4		47.62.16.100.0	
ITEM	HD 4762_M16-A4	HEX KEY HD CAP SCREW_M16	16		St. Steel A4		47.62.16.100.0	
ITEM	HD 4762_M20-A4	HEX KEY HD CAP SCREW_M20	16		St. Steel A4		47.62.16.100.0	
ITEM	HD 4762_M24-A4	HEX KEY HD CAP SCREW_M24	16		St. Steel A4		47.62.16.100.0	
ITEM	HD 4762_M30-A4	HEX KEY HD CAP SCREW_M30	16		St. Steel A4		47.62.16.100.0	
ITEM	HD 4762_M36-A4	HEX KEY HD CAP SCREW_M36	16		St. Steel A4		47.62.16.100.0	
ITEM	HD 4762_M42-A4	HEX KEY HD CAP SCREW_M42	16		St. Steel A4		47.62.16.100.0	
ITEM	HD 4762_M48-A4	HEX KEY HD CAP SCREW_M48	16		St. Steel A4		47.62.16.100.0	
ITEM	HD 4762_M54-A4	HEX KEY HD CAP SCREW_M54	16		St. Steel A4		47.62.16.100.0	
ITEM	HD 4762_M60-A4	HEX KEY HD CAP SCREW_M60	16		St. Steel A4		47.62.16.100.0	
ITEM	HD 4762_M66-A4	HEX KEY HD CAP SCREW_M66	16		St. Steel A4		47.62.16.100.0	
ITEM	HD 4762_M72-A4	HEX KEY HD CAP SCREW_M72	16		St. Steel A4		47.62.16.100.0	
ITEM	HD 4762_M78-A4	HEX KEY HD CAP SCREW_M78	16		St. Steel A4		47.62.16.100.0	
ITEM	HD 4762_M84-A4	HEX KEY HD CAP SCREW_M84	16		St. Steel A4		47.62.16.100.0	
ITEM	HD 4762_M90-A4	HEX KEY HD CAP SCREW_M90	16		St. Steel A4		47.62.16.100.0	
ITEM	HD 4762_M96-A4	HEX KEY HD CAP SCREW_M96	16		St. Steel A4		47.62.16.100.0	
ITEM	HD 4762_M102-A4	HEX KEY HD CAP SCREW_M102	16		St. Steel A4		47.62.16.100.0	
ITEM	HD 4762_M108-A4	HEX KEY HD CAP SCREW_M108	16		St. Steel A4		47.62.16.100.0	
ITEM	HD 4762_M114-A4	HEX KEY HD CAP SCREW_M114	16		St. Steel A4		47.62.16.100.0	
ITEM	HD 4762_M120-A4	HEX KEY HD CAP SCREW_M120	16		St. Steel A4		47.62.16.100.0	
ITEM	HD 4762_M126-A4	HEX KEY HD CAP SCREW_M126	16		St. Steel A4		47.62.16.100.0	
ITEM	HD 4762_M132-A4	HEX KEY HD CAP SCREW_M132	16		St. Steel A4		47.62.16.100.0	
ITEM	HD 4762_M138-A4	HEX KEY HD CAP SCREW_M138	16		St. Steel A4		47.62.16.100.0	
ITEM	HD 4762_M144-A4	HEX KEY HD CAP SCREW_M144	16		St. Steel A4		47.62.16.100.0	
ITEM	HD 4762_M150-A4	HEX KEY HD CAP SCREW_M150	16		St. Steel A4		47.62.16.100.0	
ITEM	HD 4762_M156-A4	HEX KEY HD CAP SCREW_M156	16		St. Steel A4		47.62.16.100.0	
ITEM	HD 4762_M162-A4	HEX KEY HD CAP SCREW_M162	16		St. Steel A4		47.62.16.100.0	
ITEM	HD 4762_M168-A4	HEX KEY HD CAP SCREW_M168	16		St. Steel A4		47.62.16.100.0	
ITEM	HD 4762_M174-A4	HEX KEY HD CAP SCREW_M174	16		St. Steel A4		47.62.16.100.0	
ITEM	HD 4762_M180-A4	HEX KEY HD CAP SCREW_M180	16		St. Steel A4		47.62.16.100.0	
ITEM	HD 4762_M186-A4	HEX KEY HD CAP SCREW_M186	16		St. Steel A4		47.62.16.100.0	
ITEM	HD 4762_M192-A4	HEX KEY HD CAP SCREW_M192	16		St. Steel A4		47.62.16.100.0	
ITEM	HD 4762_M198-A4	HEX KEY HD CAP SCREW_M198	16		St. Steel A4		47.62.16.100.0	
ITEM	HD 4762_M204-A4	HEX KEY HD CAP SCREW_M204	16		St. Steel A4		47.62.16.100.0	
ITEM	HD 4762_M210-A4	HEX KEY HD CAP SCREW_M210	16		St. Steel A4		47.62.16.100.0	
ITEM	HD 4762_M216-A4	HEX KEY HD CAP SCREW_M216	16		St. Steel A4		47.62.16.100.0	
ITEM	HD 4762_M222-A4	HEX KEY HD CAP SCREW_M222	16		St. Steel A4		47.62.16.100.0	
ITEM	HD 4762_M228-A4	HEX KEY HD CAP SCREW_M228	16		St. Steel A4		47.62.16.100.0	
ITEM	HD 4762_M234-A4	HEX KEY HD CAP SCREW_M234	16		St. Steel A4		47.62.16.100.0	
ITEM	HD 4762_M240-A4	HEX KEY HD CAP SCREW_M240	16		St. Steel A4		47.62.16.100.0	
ITEM	HD 4762_M246-A4	HEX KEY HD CAP SCREW_M246	16		St. Steel A4		47.62.16.100.0	
ITEM	HD 4762_M252-A4	HEX KEY HD CAP SCREW_M252	16		St. Steel A4		47.62.16.100.0	
ITEM	HD 4762_M258-A4	HEX KEY HD CAP SCREW_M258	16		St. Steel A4		47.62.16.100.0	
ITEM	HD 4762_M264-A4	HEX KEY HD CAP SCREW_M264	16		St. Steel A4		47.62.16.100.0	
ITEM	HD 4762_M270-A4	HEX KEY HD CAP SCREW_M270	16		St. Steel A4		47.62.16.100.0	
ITEM	HD 4762_M276-A4	HEX KEY HD CAP SCREW_M276	16		St. Steel A4		47.62.16.100.0	
ITEM	HD 4762_M282-A4	HEX KEY HD CAP SCREW_M282	16		St. Steel A4		47.62.16.100.0	
ITEM	HD 4762_M288-A4	HEX KEY HD CAP SCREW_M288	16		St. Steel A4		47.62.16.100.0	
ITEM	HD 4762_M294-A4	HEX KEY HD CAP SCREW_M294	16		St. Steel A4		47.62.16.100.0	
ITEM	HD 4762_M300-A4	HEX KEY HD CAP SCREW_M300	16		St. Steel A4		47.62.16.100.0	
ITEM	HD 4762_M306-A4	HEX KEY HD CAP SCREW_M306	16		St. Steel A4		47.62.16.100.0	
ITEM	HD 4762_M312-A4	HEX KEY HD CAP SCREW_M312	16		St. Steel A4		47.62.16.100.0	
ITEM	HD 4762_M318-A4	HEX KEY HD CAP SCREW_M318	16		St. Steel A4		47.62.16.100.0	
ITEM	HD 4762_M324-A4	HEX KEY HD CAP SCREW_M324	16		St. Steel A4		47.62.16.100.0	
ITEM	HD 4762_M330-A4	HEX KEY HD CAP SCREW_M330	16		St. Steel A4		47.62.16.100.0	
ITEM	HD 4762_M336-A4	HEX KEY HD CAP SCREW_M336	16		St. Steel A4		47.62.16.100.0	
ITEM	HD 4762_M342-A4	HEX KEY HD CAP SCREW_M342	16		St. Steel A4		47.62.16.100.0	
ITEM	HD 4762_M348-A4	HEX KEY HD CAP SCREW_M348	16		St. Steel A4		47.62.16.100.0	
ITEM	HD 4762_M354-A4	HEX KEY HD CAP SCREW_M354	16		St. Steel A4		47.62.16.100.0	
ITEM	HD 4762_M360-A4	HEX KEY HD CAP SCREW_M360	16		St. Steel A4		47.62.16.100.0	
ITEM	HD 4762_M366-A4	HEX KEY HD CAP SCREW_M366	16		St. Steel A4		47.62.16.100.0	
ITEM	HD 4762_M372-A4	HEX KEY HD CAP SCREW_M372	16		St. Steel A4		47.62.16.100.0	
ITEM	HD 4762_M378-A4	HEX KEY HD CAP SCREW_M378	16		St. Steel A4		47.62.16.100.0	
ITEM	HD 4762_M384-A4	HEX KEY HD CAP SCREW_M384	16		St. Steel A4		47.62.16.100.0	
ITEM	HD 4762_M390-A4	HEX KEY HD CAP SCREW_M390	16		St. Steel A4		47.62.16.100.0	
ITEM	HD 4762_M396-A4	HEX KEY HD CAP SCREW_M396	16		St. Steel A4		47.62.16.100.0	
ITEM	HD 4762_M402-A4	HEX KEY HD CAP SCREW_M402	16		St. Steel A4		47.62.16.100.0	
ITEM	HD 4762_M408-A4	HEX KEY HD CAP SCREW_M408	16		St. Steel A4		47.62.16.100.0	
ITEM	HD 4762_M414-A4	HEX KEY HD CAP SCREW_M414	16		St. Steel A4		47.62.16.100.0	
ITEM	HD 4762_M420-A4	HEX KEY HD CAP SCREW_M420	16		St. Steel A4		47.62.16.100.0	
ITEM	HD 4762_M426-A4	HEX KEY HD CAP SCREW_M426	16		St. Steel A4		47.62.16.100.0	
ITEM	HD 4762_M432-A4	HEX KEY HD CAP SCREW_M432	16		St. Steel A4		47.62.16.100.0	
ITEM	HD 4762_M438-A4	HEX KEY HD CAP SCREW_M438	16		St. Steel A4		47.62.16.100.0	
ITEM	HD 4762_M444-A4	HEX KEY HD CAP SCREW_M444	16		St. Steel A4		47.62.16.100.0	
ITEM	HD 4762_M450-A4	HEX KEY HD CAP SCREW_M450	16		St. Steel A4		47.62.16.100.0	
ITEM	HD 4762_M456-A4	HEX KEY HD CAP SCREW_M456	16		St. Steel A4		47.62.16.100.0	
ITEM	HD 4762_M462-A4	HEX KEY HD CAP SCREW_M462	16		St. Steel A4		47.62.16.100.0	
ITEM	HD 4762_M468-A4	HEX KEY HD CAP SCREW_M468	16		St. Steel A4		47.62.16.100.0	
ITEM	HD 4762_M474-A4	HEX KEY HD CAP SCREW_M474	16		St. Steel A4		47.62.16.100.0	
ITEM	HD 4762_M480-A4	HEX KEY HD CAP SCREW_M480	16		St. Steel A4		47.62.16.100.0	
ITEM	HD 4762_M486-A4	HEX KEY HD CAP SCREW_M486	16		St. Steel A4		47.62.16.100.0	
ITEM	HD 4762_M492-A4	HEX KEY HD CAP SCREW_M492	16		St. Steel A4		47.62.16.100.0	
ITEM	HD 4762_M498-A4	HEX KEY HD CAP SCREW_M498	16		St. Steel A4		47.62.16.100.0	
ITEM	HD 4762_M504-A4	HEX KEY HD CAP SCREW_M504	16		St. Steel A4		47.62.16.100.0	
ITEM	HD 4762_M510-A4	HEX KEY HD CAP SCREW_M510	16		St. Steel A4		47.62.16.100.0	
ITEM	HD 4762_M516-A4	HEX KEY HD CAP SCREW_M516	16		St. Steel A4		47.62.16.100.0	
ITEM	HD 4762_M522-A4	HEX KEY HD CAP SCREW_M522	16		St. Steel A4		47.62.16.100.0	
ITEM	HD 4762_M528-A4	HEX KEY HD CAP SCREW_M528	16		St. Steel A4		47.62.16.100.0	
ITEM	HD 4762_M534-A4	HEX KEY HD CAP SCREW_M534	16		St. Steel A4		47.62.16.100.0	
ITEM	HD 4762_M540-A4	HEX KEY HD CAP SCREW_M540	16		St. Steel A4		47.62.16.100.0	
ITEM	HD 4762_M546-A4	HEX KEY HD CAP SCREW_M546	16		St. Steel A4		47.62.16.100.0	
ITEM	HD 4762_M552-A4	HEX KEY HD CAP SCREW_M552	16		St. Steel A4		47.62.16.100.0	
ITEM	HD 4762_M558-A4	HEX KEY HD CAP SCREW_M558	16		St. Steel A4		47.62.16.100.0	
ITEM	HD 4762_M564-A4	HEX KEY HD CAP SCREW_M564	16		St. Steel A4		47.62.16.100.0	
ITEM	HD 4762_M570-A4	HEX KEY HD CAP SCREW_M570	16		St. Steel A4		47.62.16.100.0	
ITEM	HD 4762_M576-A4	HEX KEY HD CAP SCREW_M576	16		St. Steel A4		47.62.16.100.0	
ITEM	HD 4762_M582-A4	HEX KEY HD CAP SCREW_M582	16		St. Steel A4			

Big Thanks to Jerone for his Field and now Rat programs Used for Designing CCT's and much more!

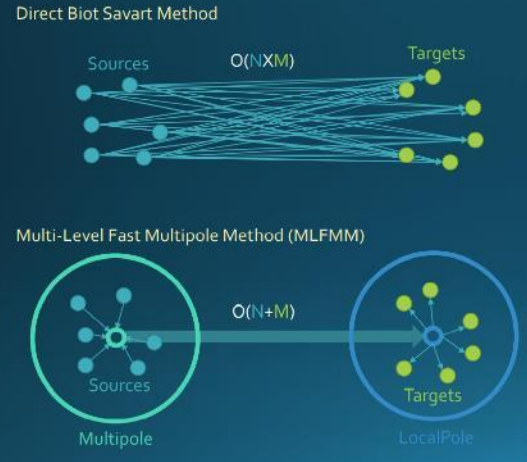


CCT Customization



- For CCT magnets quite a bit of customization is possible
- The magnets can be bend and the harmonics can be calculated along a path
- Combined function magnets can be created with varying harmonic content along their length

Reducing Complexity

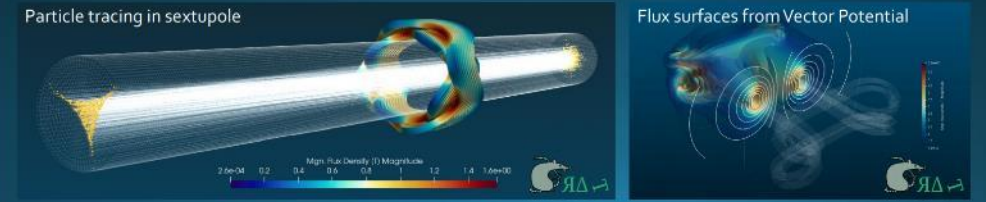


- Consider a system with **N** sources and **M** targets
- Each line represents a field evaluation
- Straight forward Biot-Savart integration leads to complexity **O(NXM)**
- By using the **Multipoles** and **Localpoles** as a middle-man the complexity is reduced to **O(N+M)**

$$L_n^m = \sum_{k=0}^{\infty} \sum_{l=-k}^k M_{nl}^m G_{nl}^m(r^*) (r^*)^{nl} \quad G_n^m(r^*) = \frac{(-1)^{n-m} (n-m)!}{r^{m+1}} e^{im\phi} P_n^m(\cos\alpha)$$

Types of Calculation

- Current calculation types are:
 - **Line** – The field A/B is calculated on a provided path
 - **Grid** – The field A/B is calculated in a volume grid of points
 - **Mesh** – The field A/B is calculated on the mesh of the coil
 - **Surface** – The field is calculated on the surface of the coil
 - **Harmonics** – The coil harmonics are calculated along a provided path
 - **Inductance** – The inductance matrix and stored energy is calculated
 - **Tracks** – The field B is calculated on a mesh after which it is used for particle tracing



What is New/Different

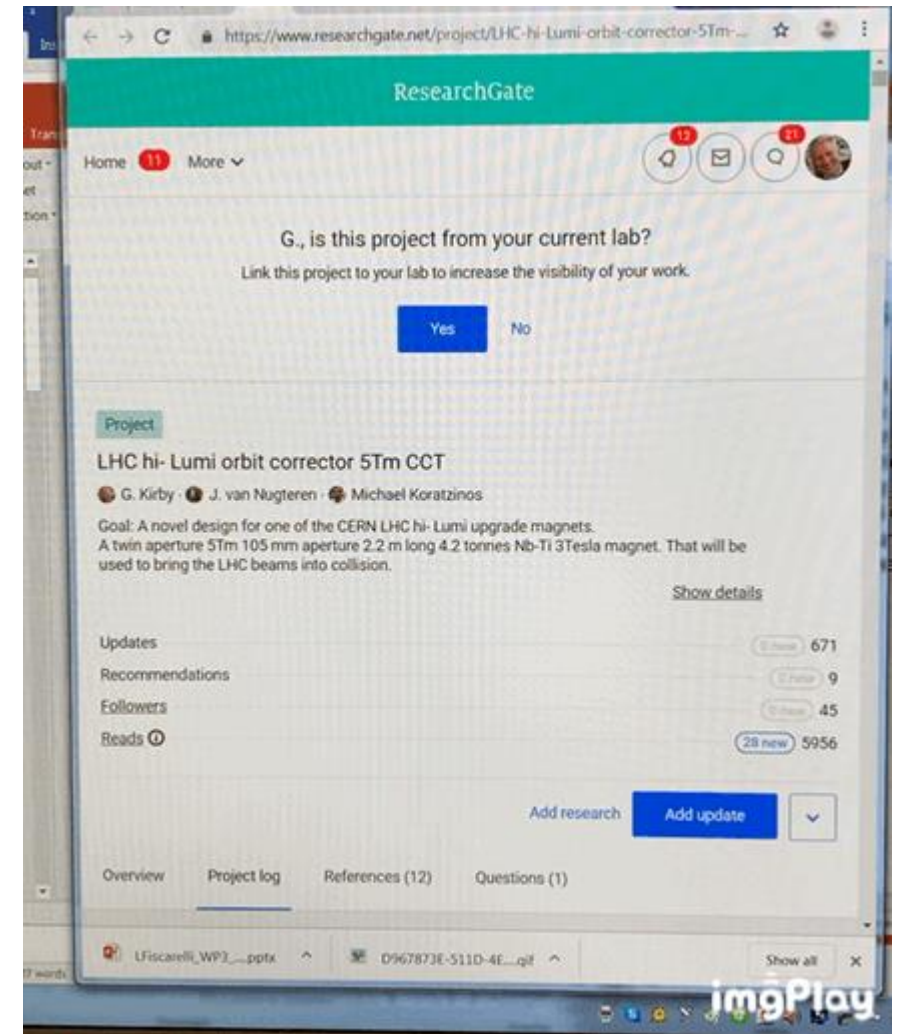
- It is written in C++ to avoid dependency on proprietary software (more work)
- This means that post processing is done in VTK and Paraview (**OpenSource**)
- In RAT all the steps of the MLFMM are **vectorised** using (mostly) dense matrix-matrix products
- As these are part of **BLAS** (CPU) and **CUBLAS** (GPU) they can be executed in a heavily optimized way
- The **Armadillo** library is used as a wrapper around BLAS as it results in code similar to MATLAB
- The sources and targets are de-coupled from the MLFMM. This allows for running almost any 1/R problem. Like stellar dynamics.
- The GPU S2T step is written using tiles making better use of shared memory.
- Rat does not have a GUI yet



Conclusions

CCT's

- *Low cost!*
- *Good field quality*
- *Simple to design, you can do it with paper and pen.*
- *lots of opportunity to invent new magnets.*



Follow day by day, and look back over 5 years the progress on my ResearchGate G Kirby project log with every idea, paper, success and failure !

<https://www.researchgate.net/project/LHC-hi-Lumi-orbit-corrector-5Tm-CCT>

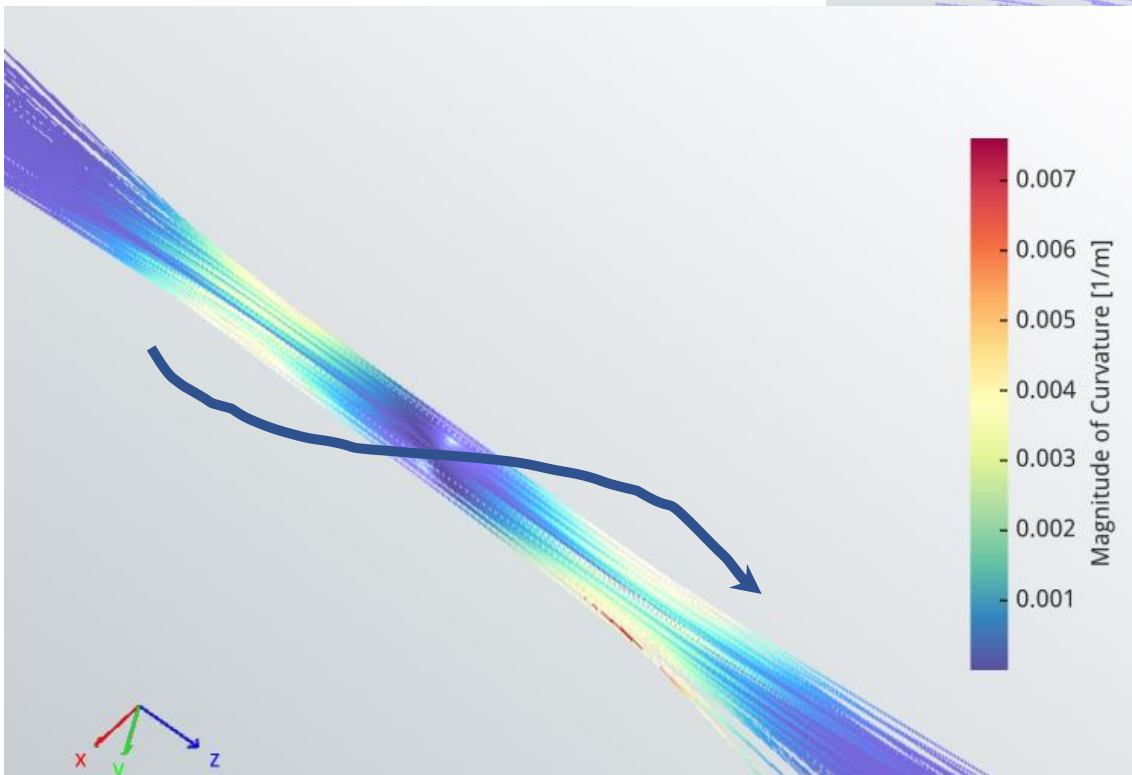
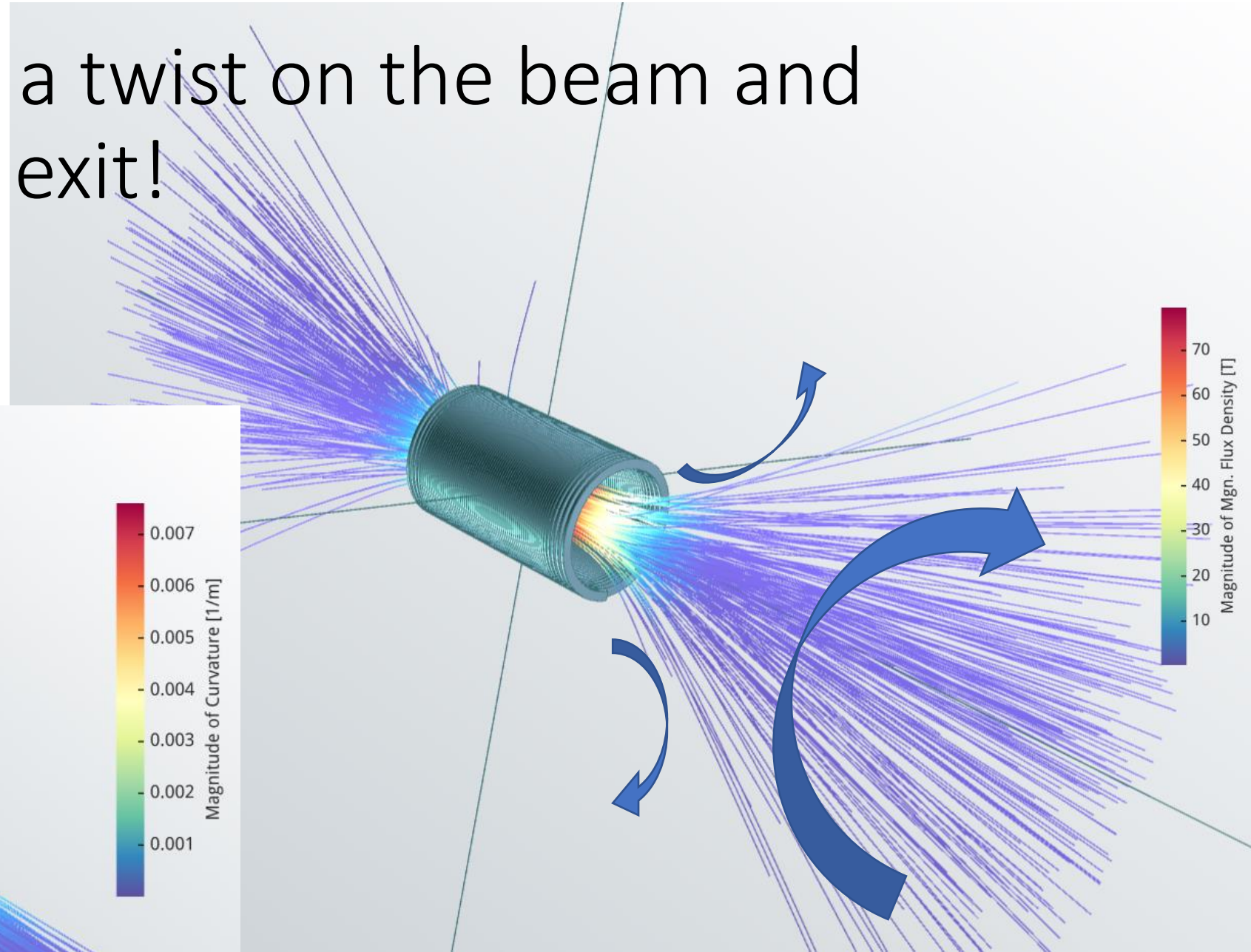
Thanks to all who have contributed to the CCT development over the last 10 years

- *Jeroen Van Nugteren,*
- *The design office team Matt and Luca.*
- *All the 927 team, Jacky, Francois-Olivier, Carols, Nicolas, Sebatian, Juan, & all the rest!*
- *Gijs, Ezio, Andrea and the many students form inside and outside of CERN .*
- *Matthias Mentink , Emmanuele Ravaioli & and the protection team, Mike.*
- *Rafal Ortwein, & Daniel and his Sushi team, Arnaud Foussat.*
- *Karol and the CERN main machine shop.*
- *all SM18 test teams.*
- *Magnetic measurement team: Lucio, Carlo, ...*
- *The materials testing team, Stefano , Mickael Denis Crouvizier, The IHEP, IMP test team all in china.*
- *Oscar Sacristan De Frutos.*
- *Shlomo, Bernhard, Mike, Stefania, Thomas, Chris.*
- *Lucio Rossi, Luca Bottura.*
- *Kevin and the team in Sweden*
- *And many more that have helped start this new era in accelerator magnet design!*



The End

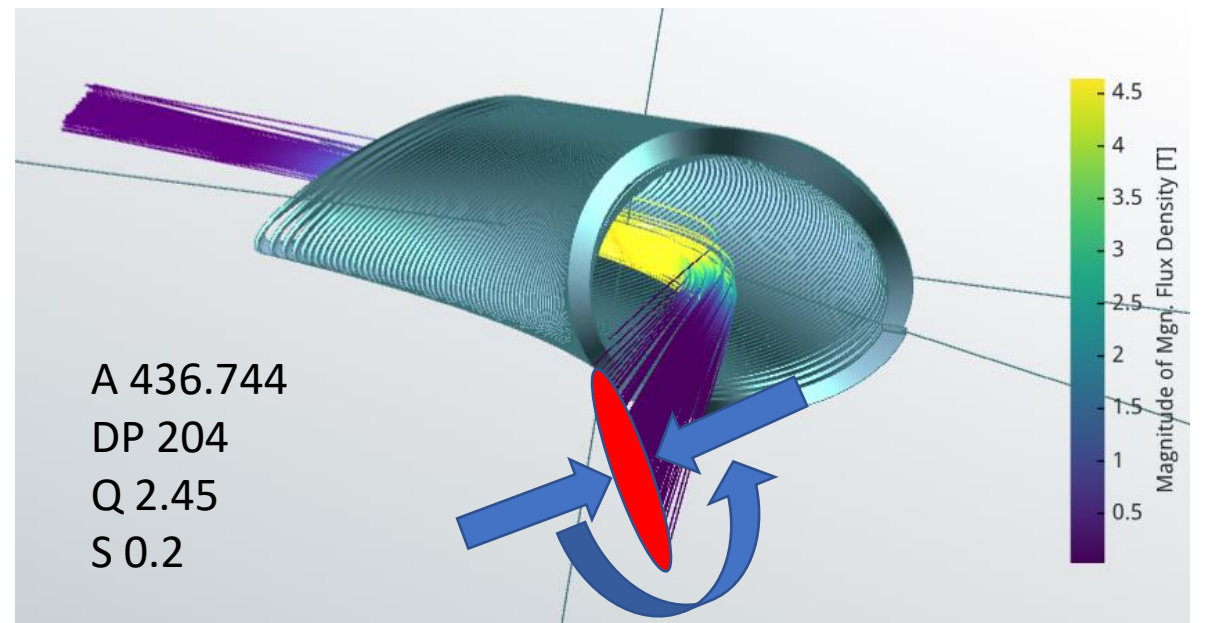
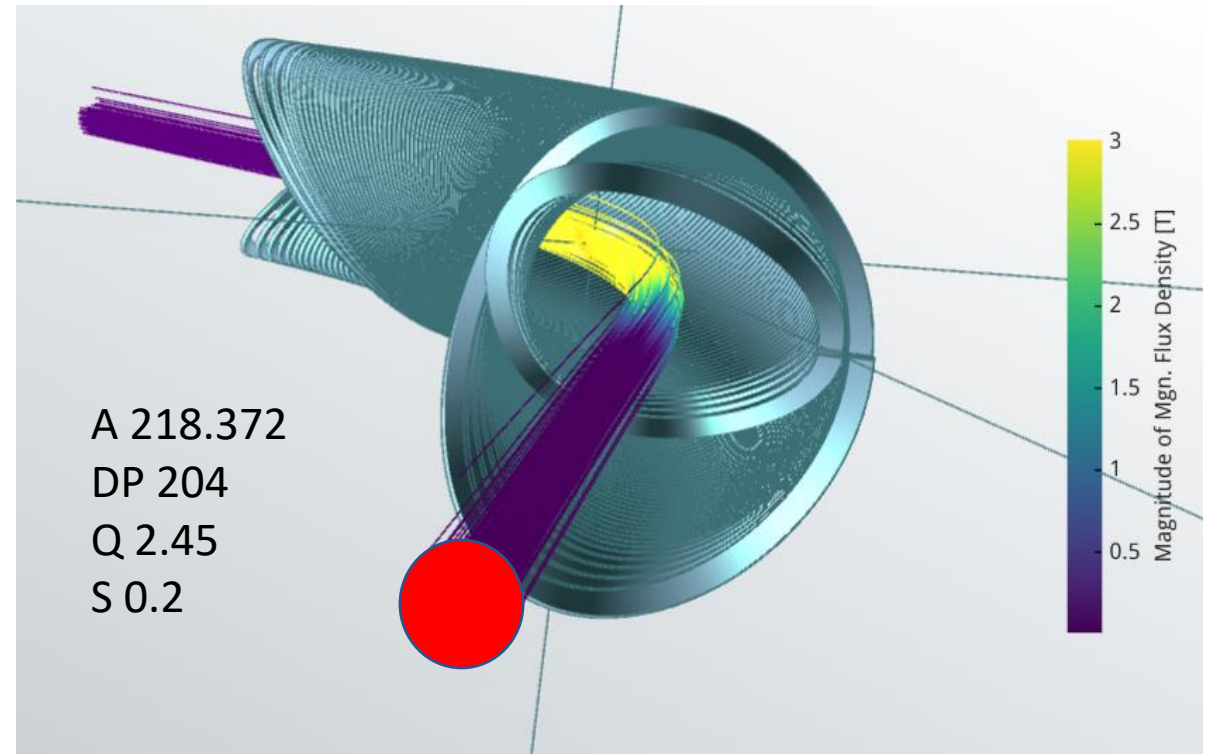
Solenoid puts a twist on the beam and divergence at exit!



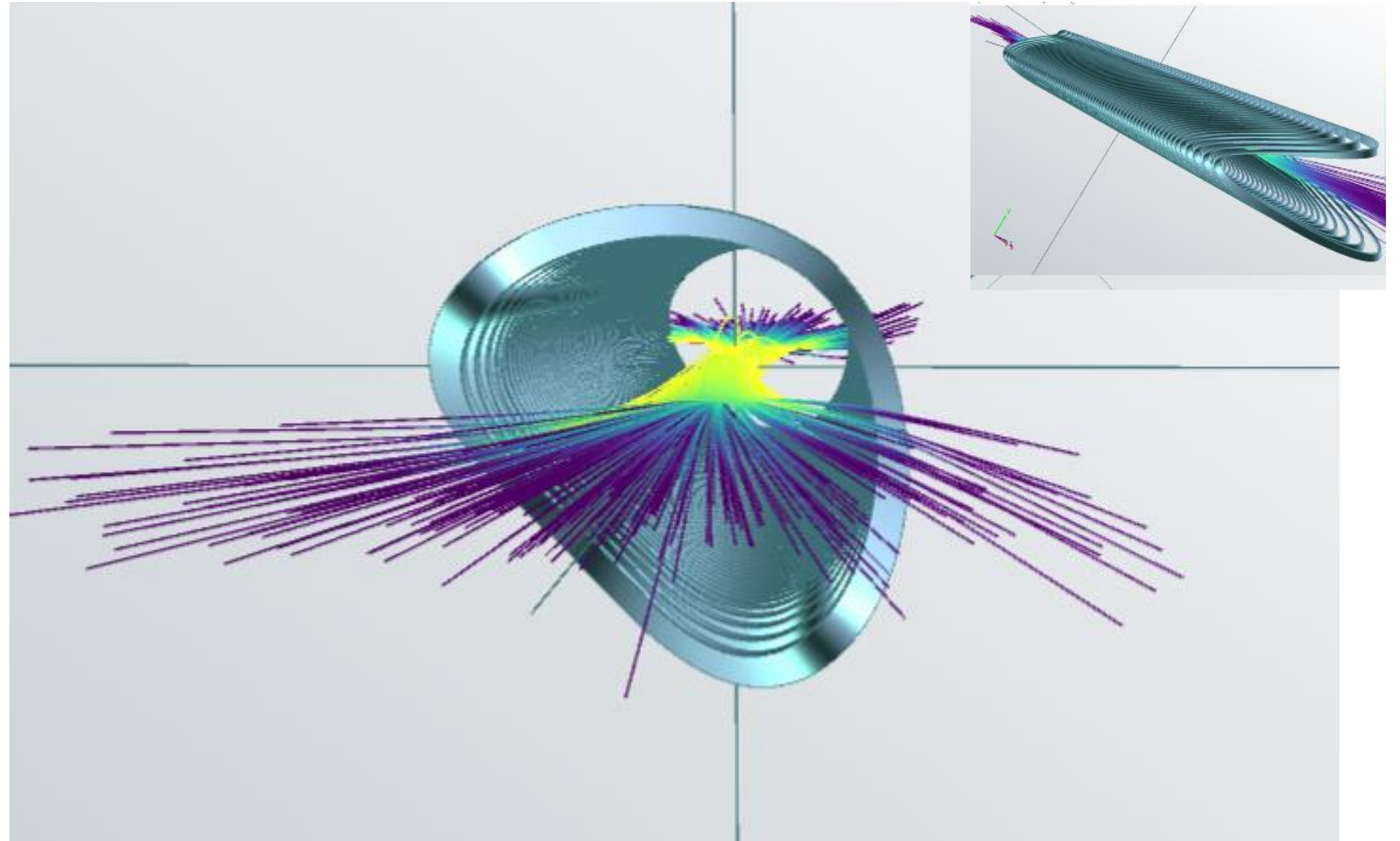
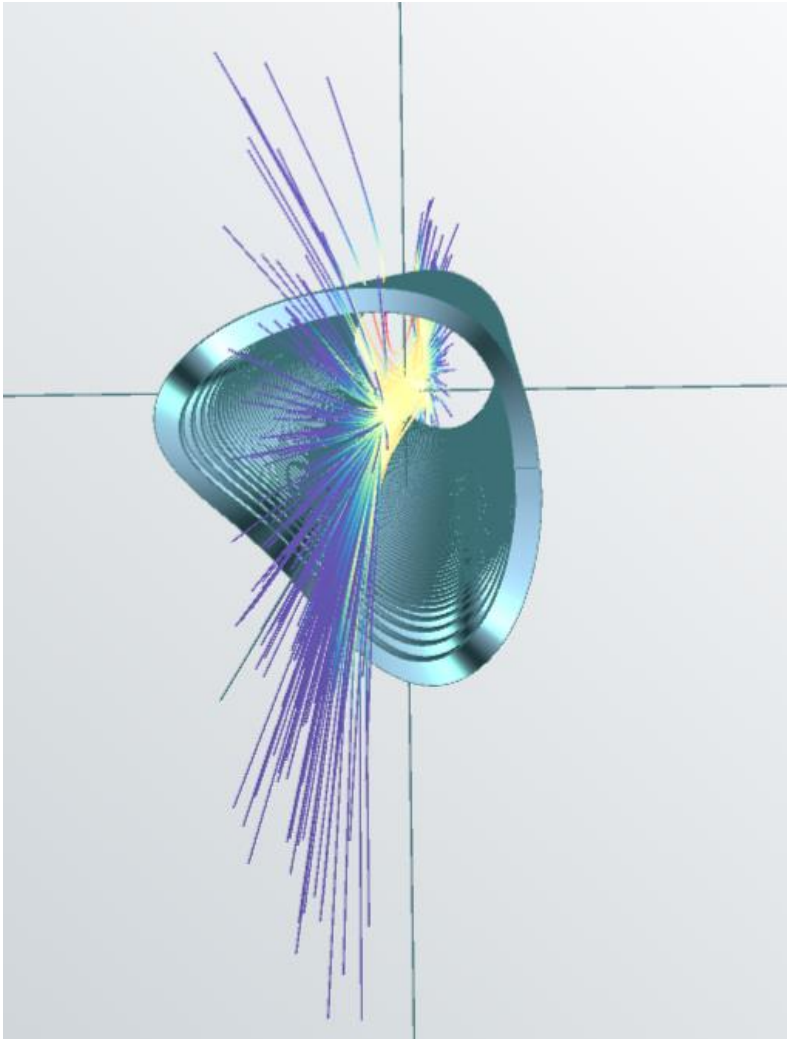
Dipole pushes beam round the corner.

Two layers cancels the solenoid field

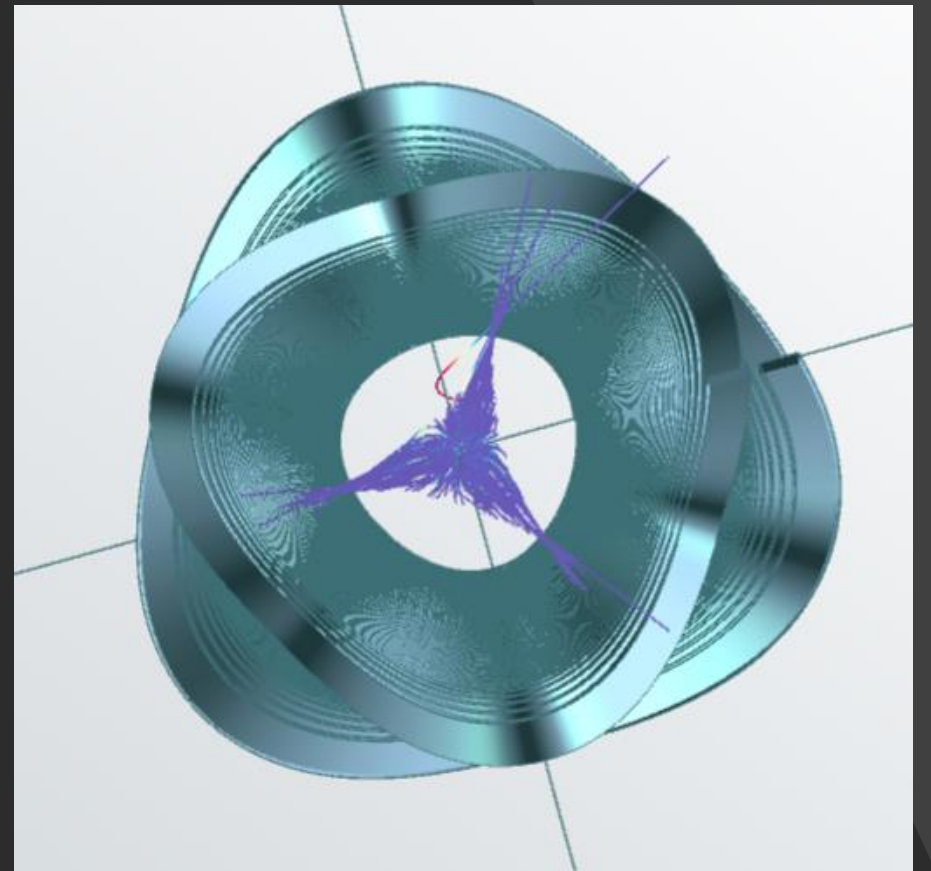
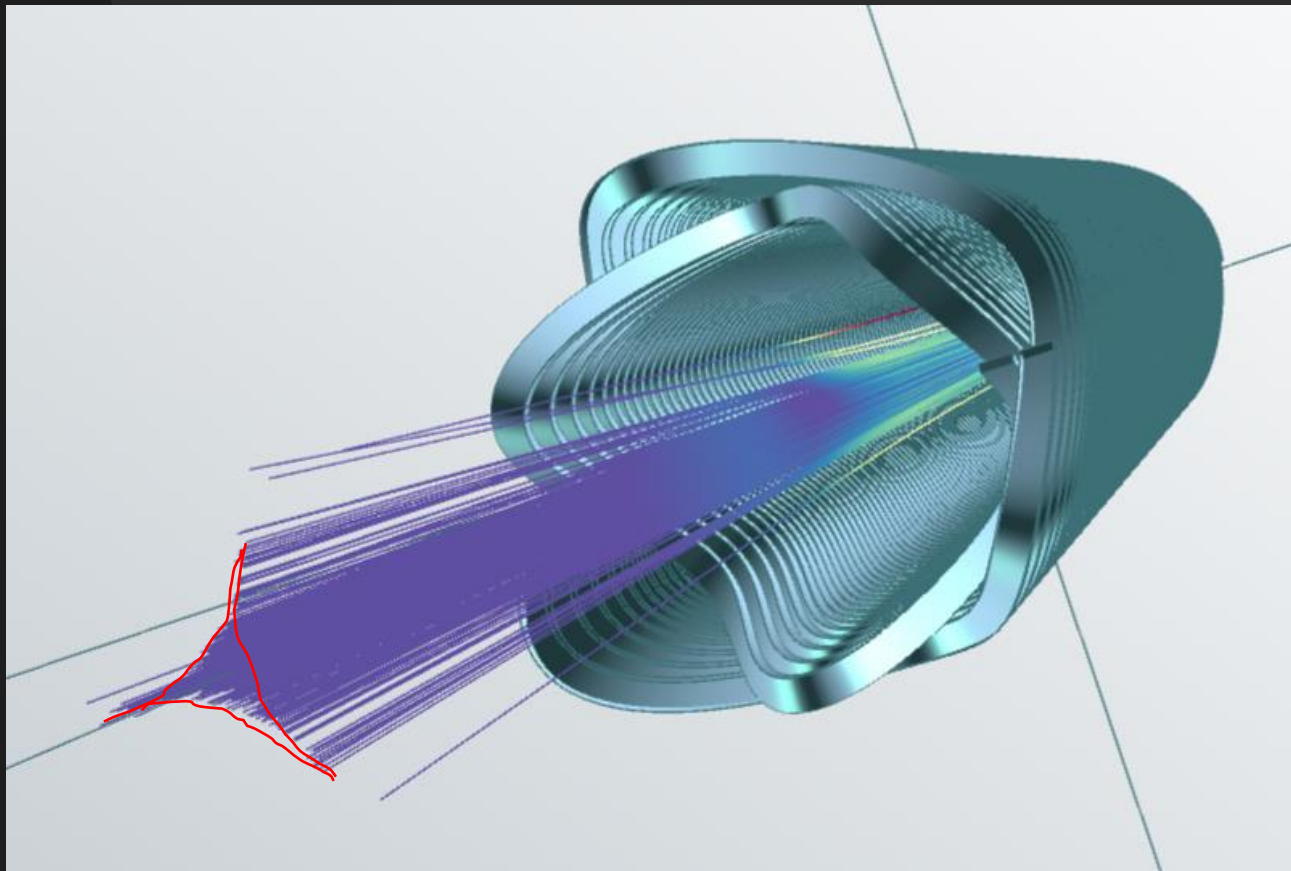
curvature adds other high order harmonics
quadrupole +

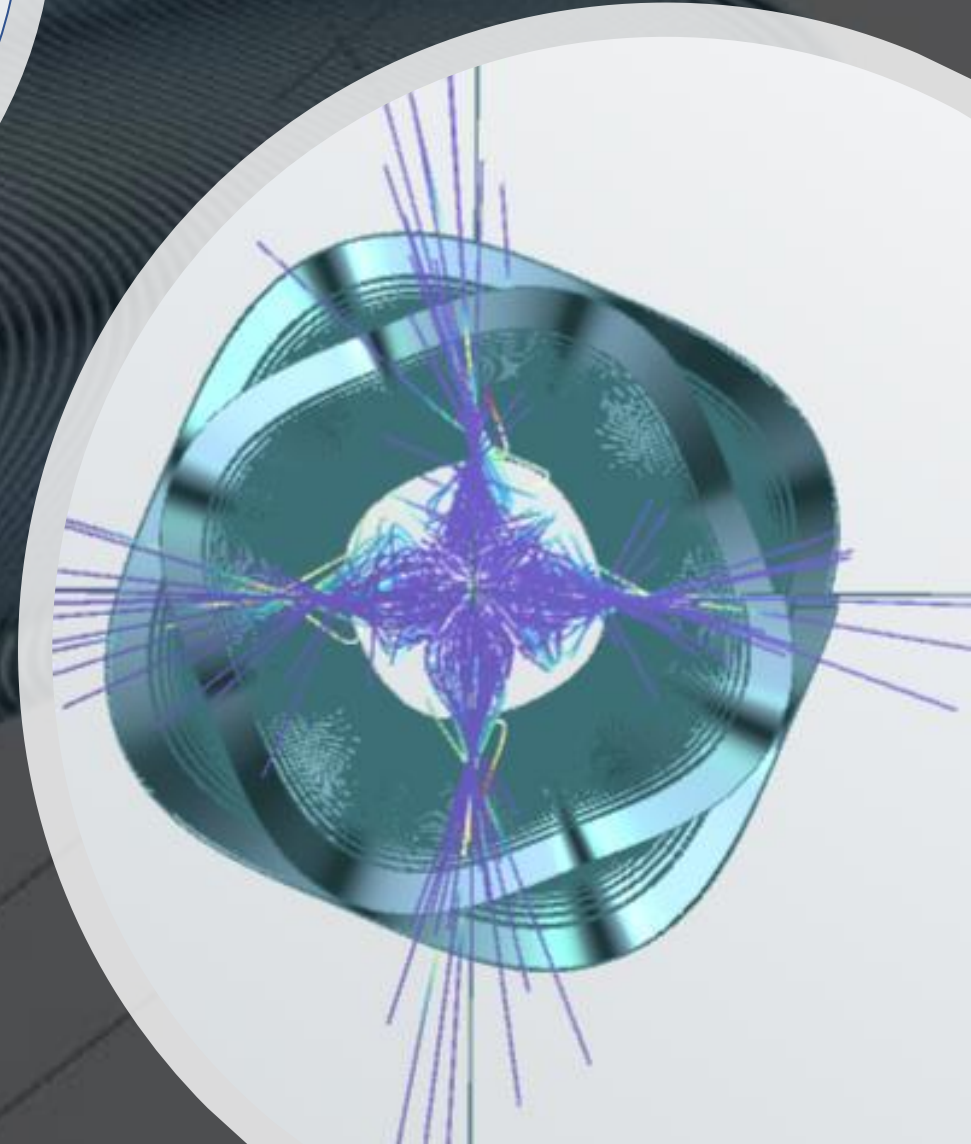
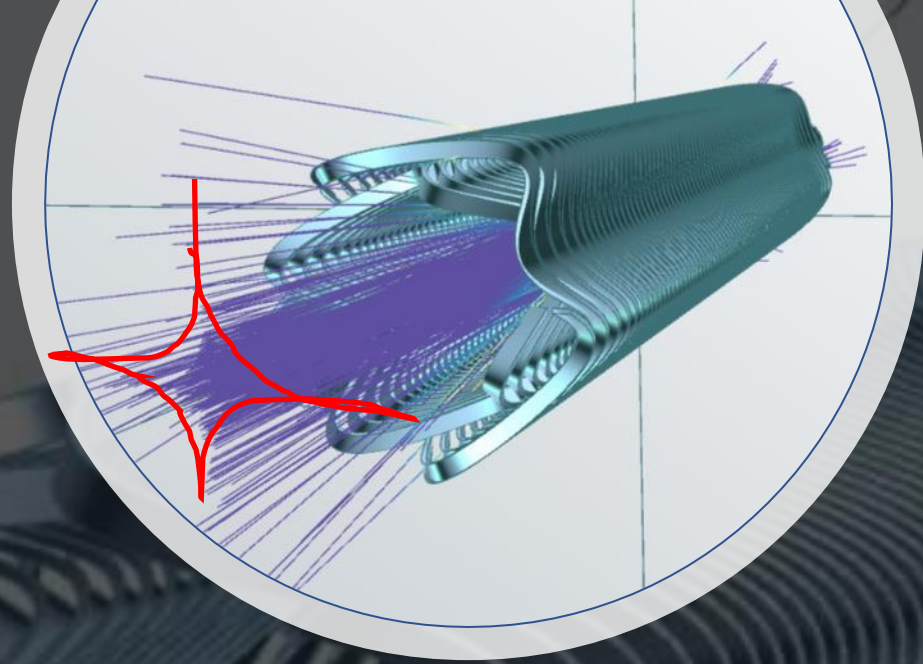


Quadrupole focuses in one plane
+ & - Current effect on beam rotates 90 deg.



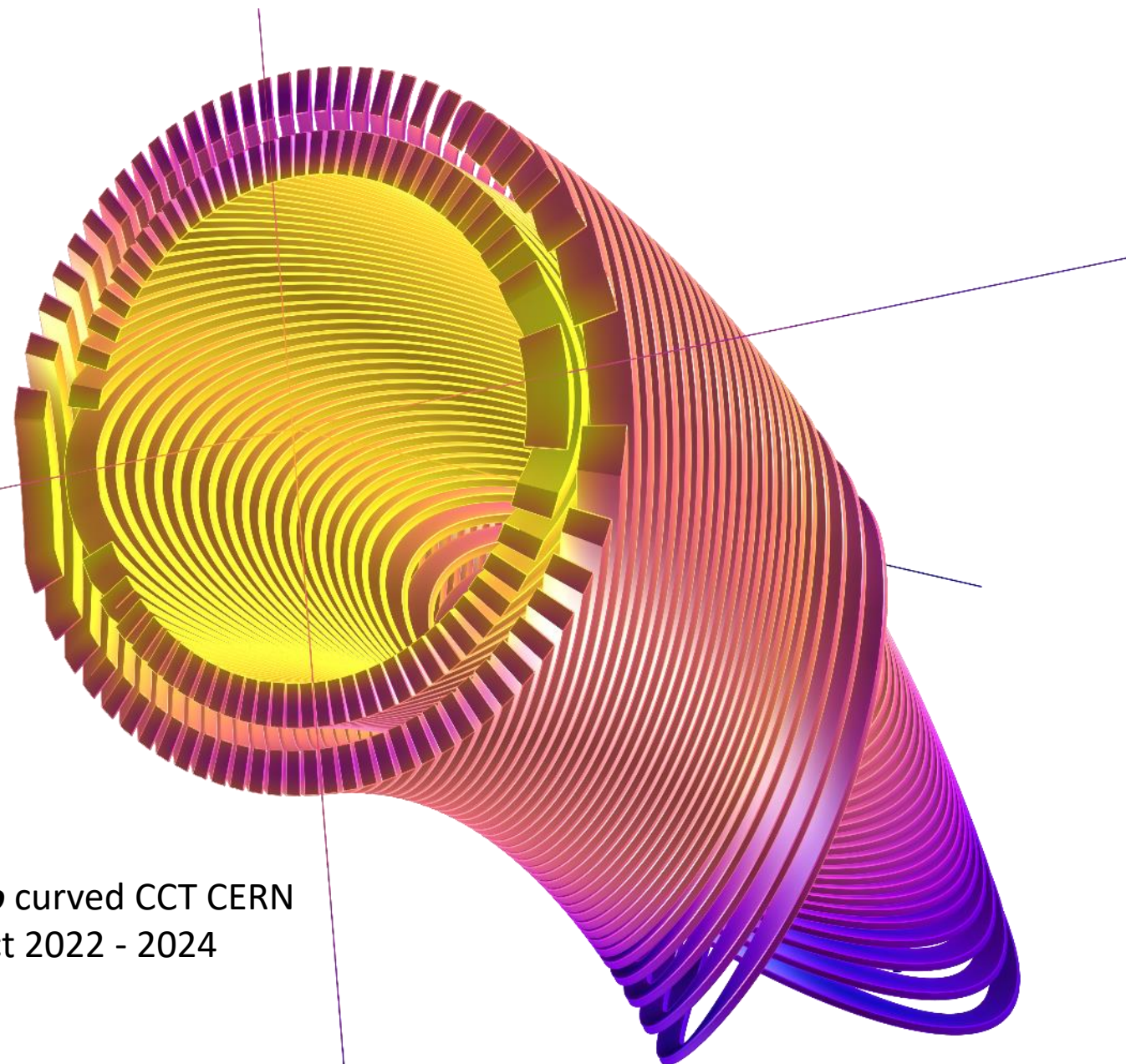
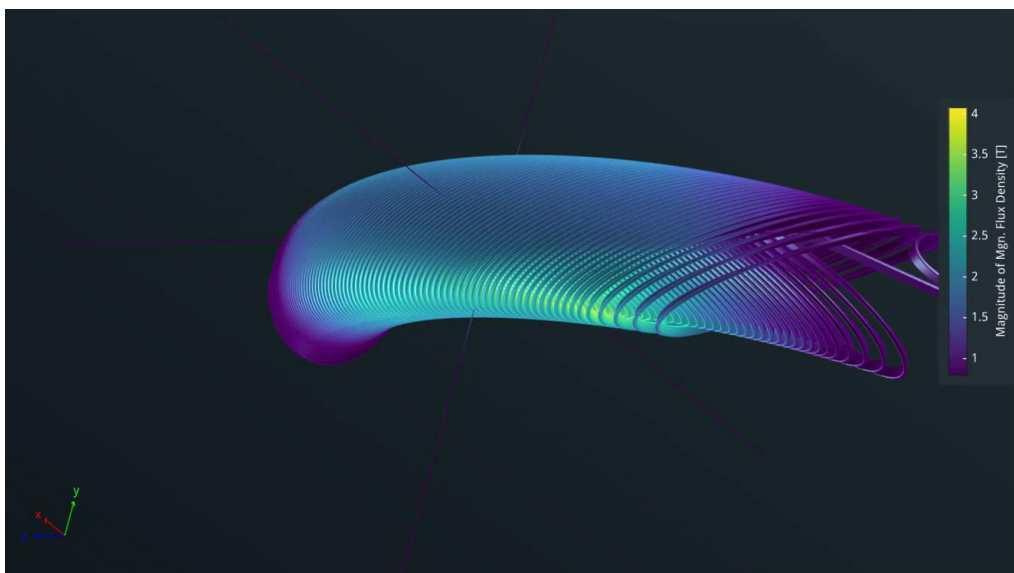
Sextupole beam manipulation





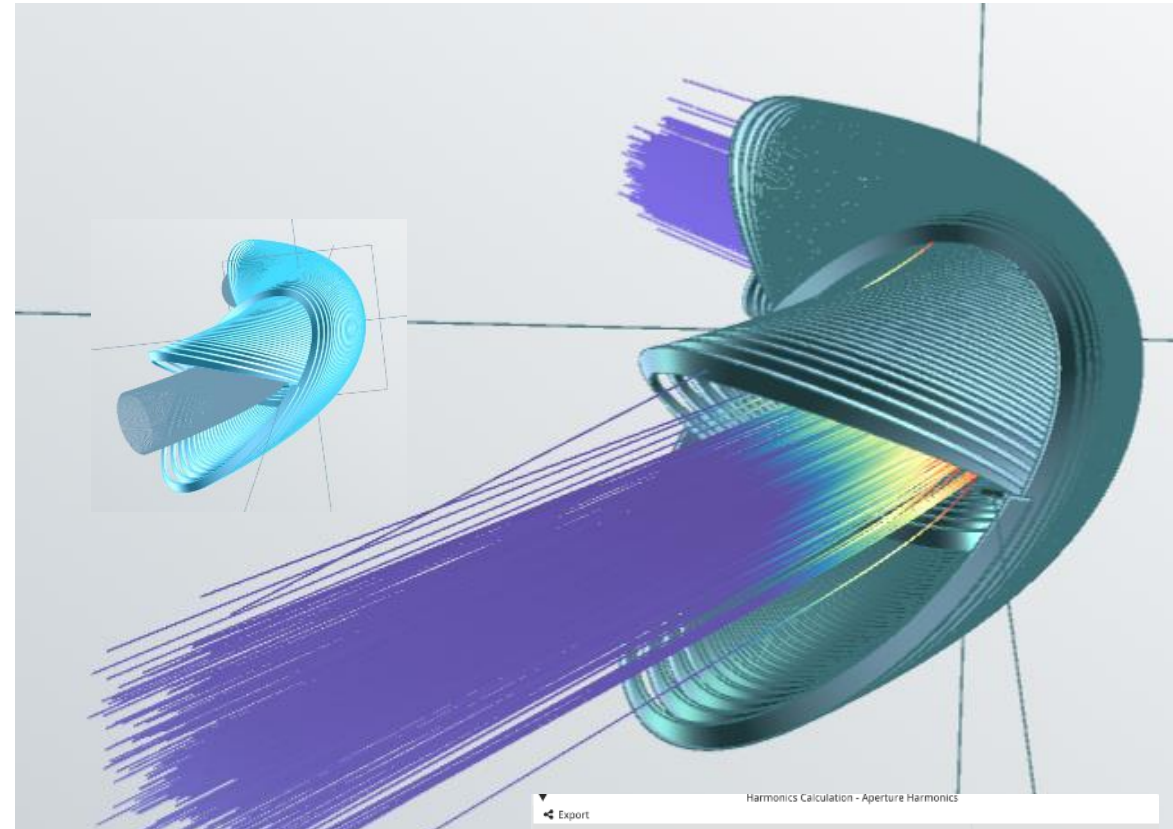
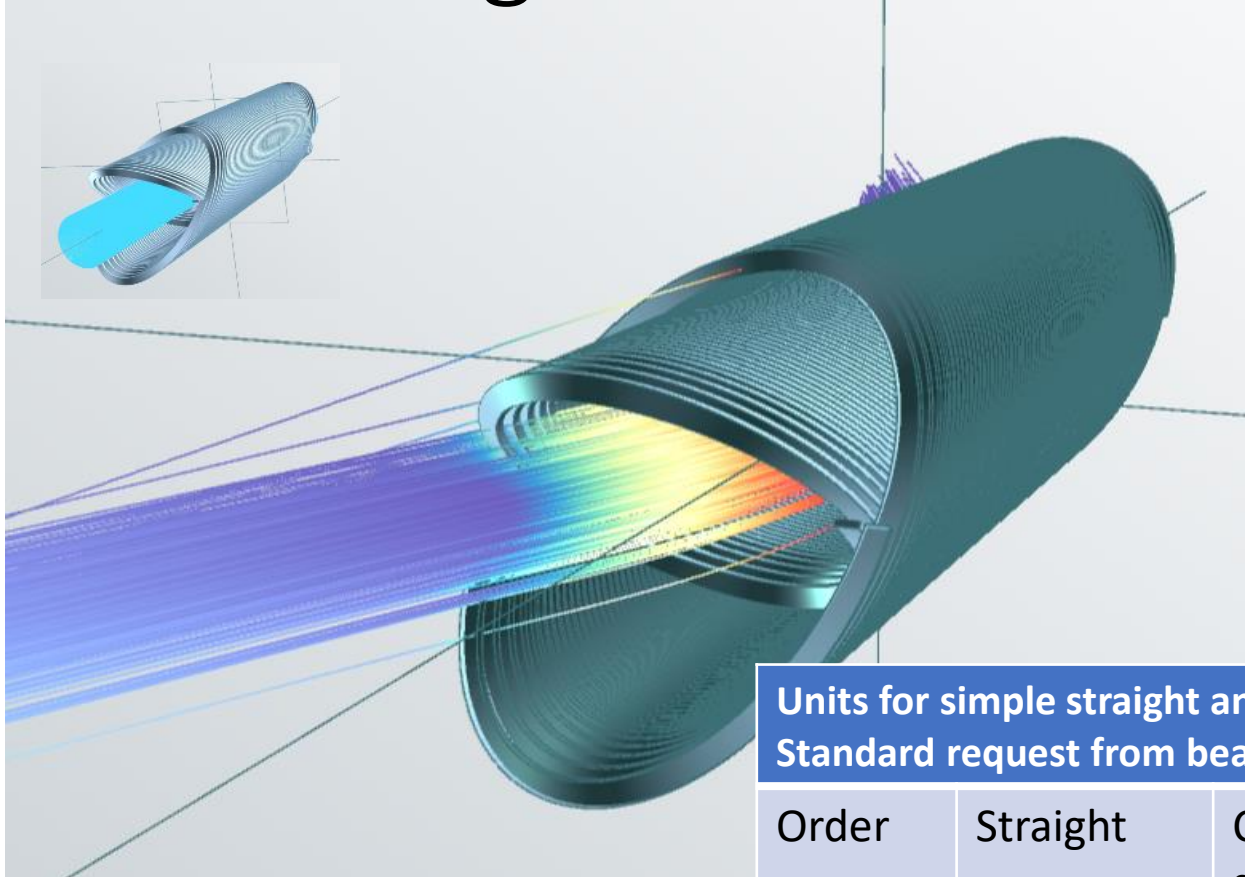
Octupole beam manipulation

Design features



Fusillo curved CCT CERN
project 2022 - 2024

Effect of tight curvature



Units for simple straight and curves coils 1571 mm
Standard request from beam dynamics is < 10 units

Order	Straight	Curved std calc	Curved compensated
B2	- 0.23	- 333	-1250
B3	-0.696	-3.36	7.66
B4	-0.0227	- 0.406	-0.294
B5		-0.0411	-0.029

Harmonics Calculation - Aperture Harmonics

Export

Main Harmonics			Skew harmonics			Axial Field					
Order	An [T.m]	an	Normalized Shape	Order	Bn [T.m]	bn	Normalized Shape	Order	Bn [T.m]	bn	Normalized Shape
A1	1.45e-07	0.00		B1	2.78e+03	10000.00					
A2	-3.26e-09	-0.00		B2	-1.25e-01	-449.92					
A3	1.72e-07	0.00		B3	7.66e-04	2.76					
A4	1.09e-07	0.00		B4	2.94e-05	0.11					
A5	1.13e-07	0.00		B5	-2.90e-06	-0.01					

Harmonics Calculation - Aperture Harmonics

Export

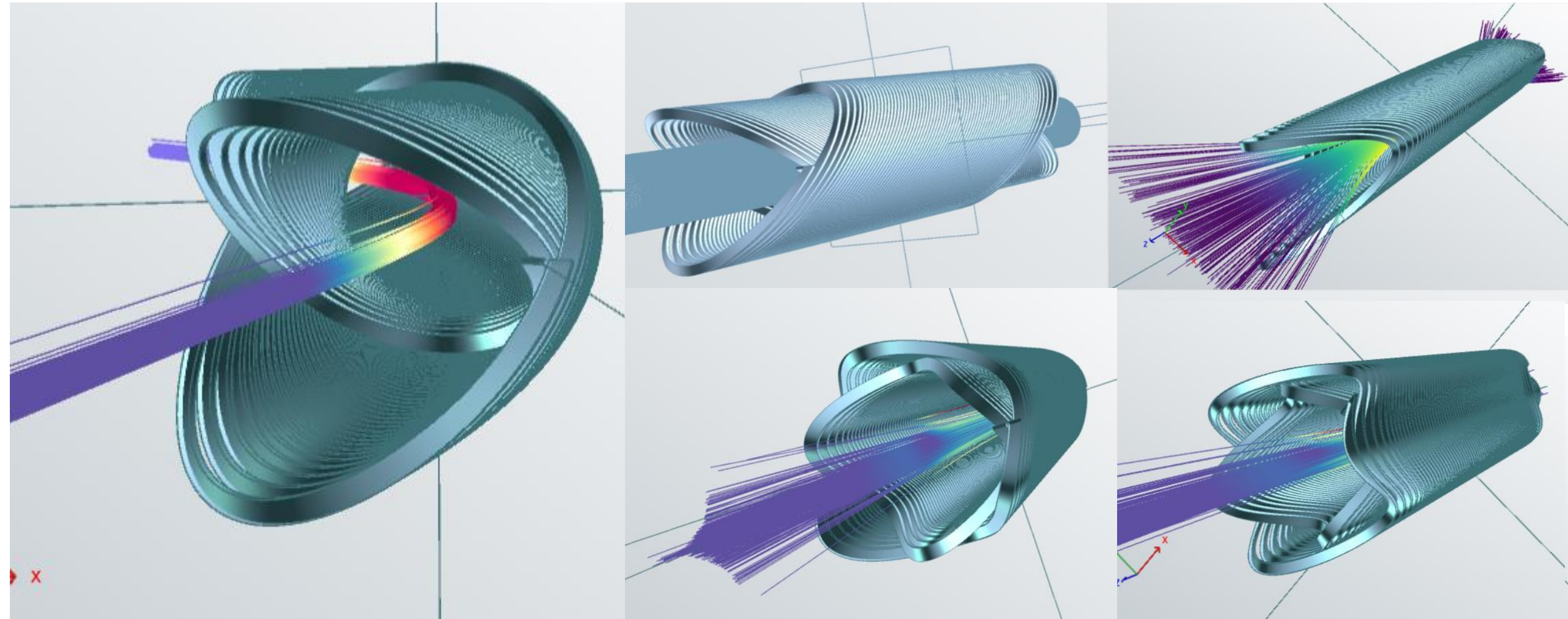
Main Harmonics			Skew harmonics			Axial Field					
Order	An [T.m]	an	Normalized Shape	Order	Bn [T.m]	bn	Normalized Shape	Order	Bn [T.m]	bn	Normalized Shape
A1	1.40e-07	0.00		B1	2.78e+03	10000.00					
A2	7.16e-09	0.00		B2	-3.33e-02	-120.14					
A3	1.76e-07	0.00		B3	-3.36e-04	-1.21					
A4	1.18e-07	0.00		B4	-4.06e-05	-0.15					
A5	1.17e-07	0.00		B5	-4.11e-06	-0.01					

Harmonics Calculation - Aperture Harmonics

Export

Main Harmonics			Skew harmonics			Axial Field					
Order	An [T.m]	an	Normalized Shape	Order	Bn [T.m]	bn	Normalized Shape	Order	Bn [T.m]	bn	Normalized Shape
A1	1.43e-09	0.00		B1	2.43e+00	10000.00					
A2	1.84e-08	0.00		B2	-1.23e-05	-0.05					
A3	-1.52e-09	-0.00		B3	-6.96e-05	-0.29					
A4	3.44e-08	0.00		B4	-2.27e-06	-0.01					

Adding all the coils shapes and more together into one optimized coil.



230 mm aperture , 1 m radii Curved CCT former weld and machining at CERN

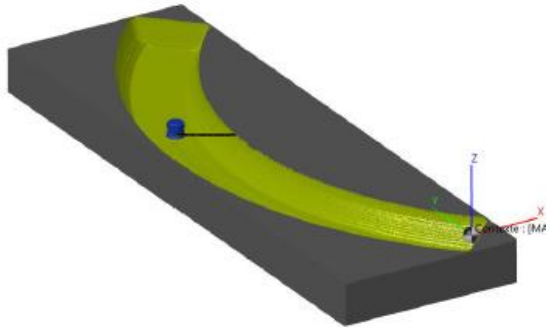


Figure 1 Half-shell interior roughing in bulk material

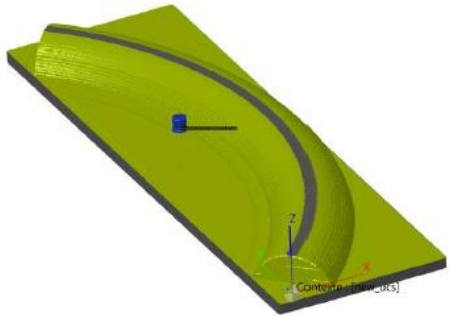


Figure 2 Half-shell exterior roughing

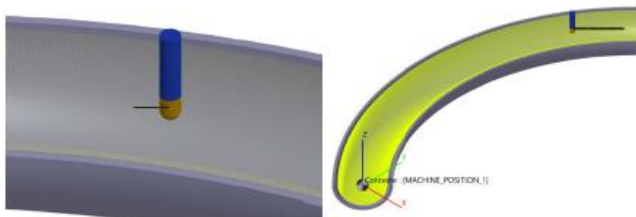


Figure 3 Interior finishing

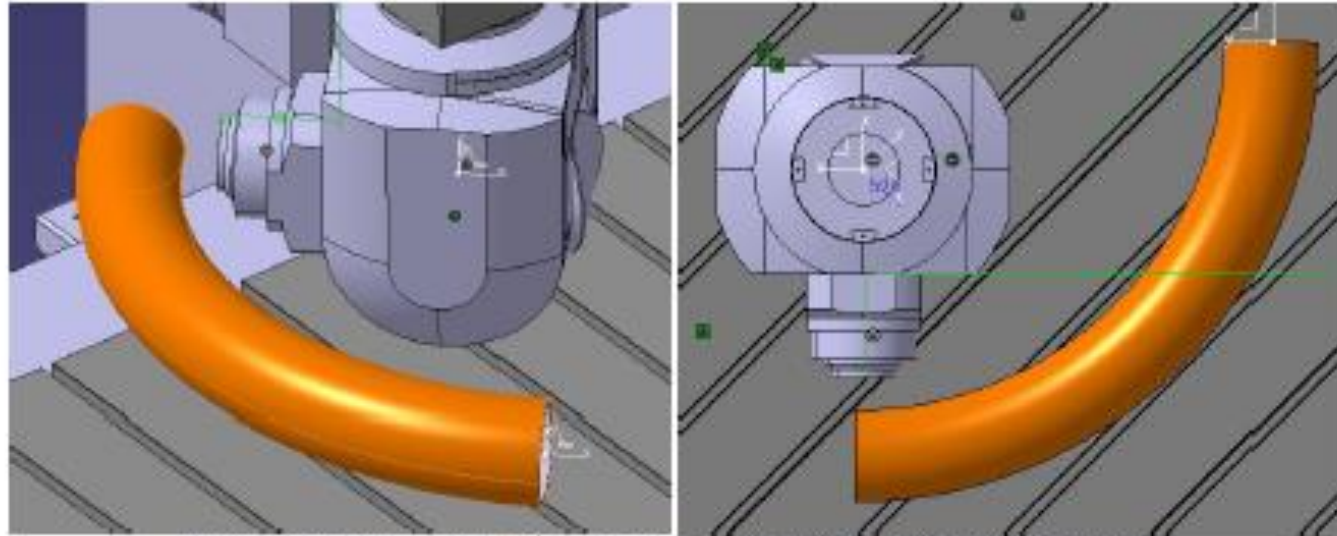
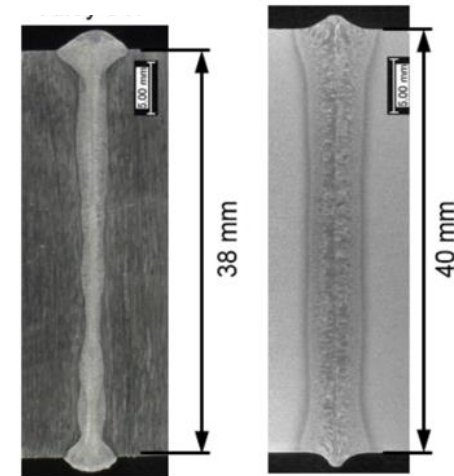
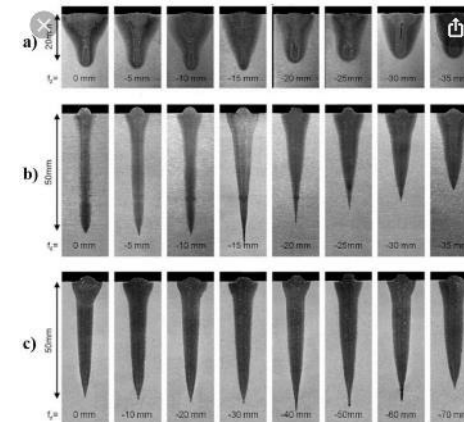
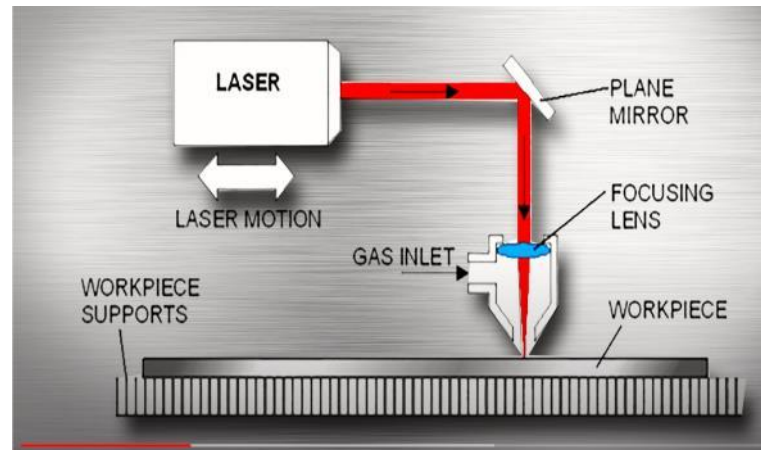


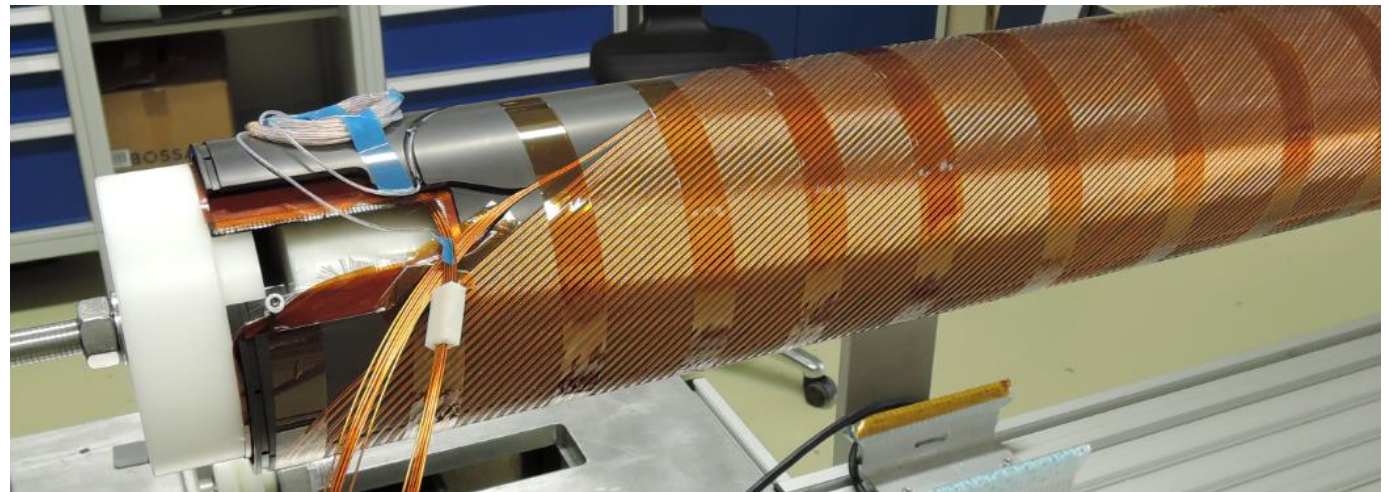
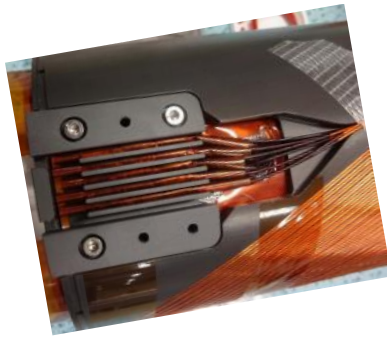
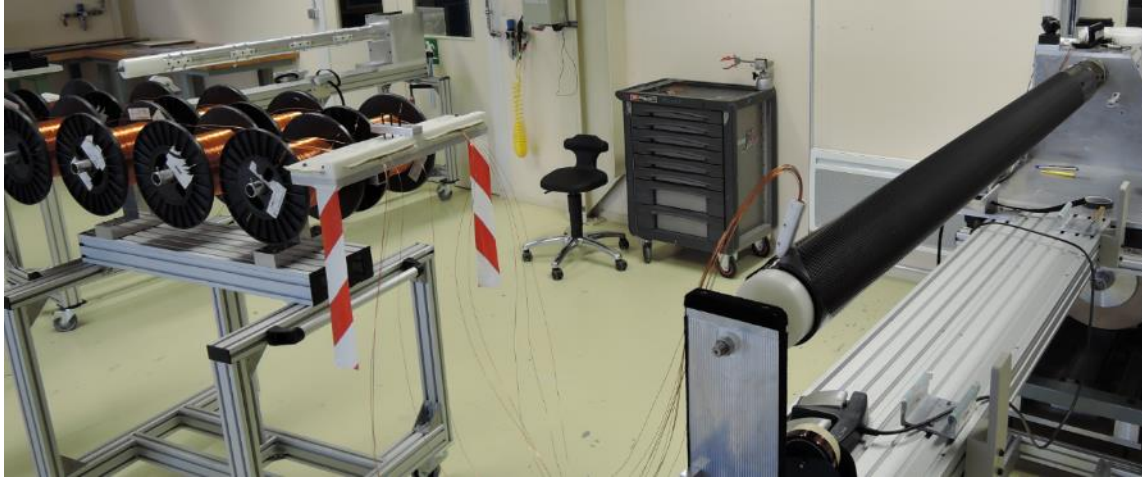
Figure 4 Configuration piece-machine spindle (Waldrich HF30 example)

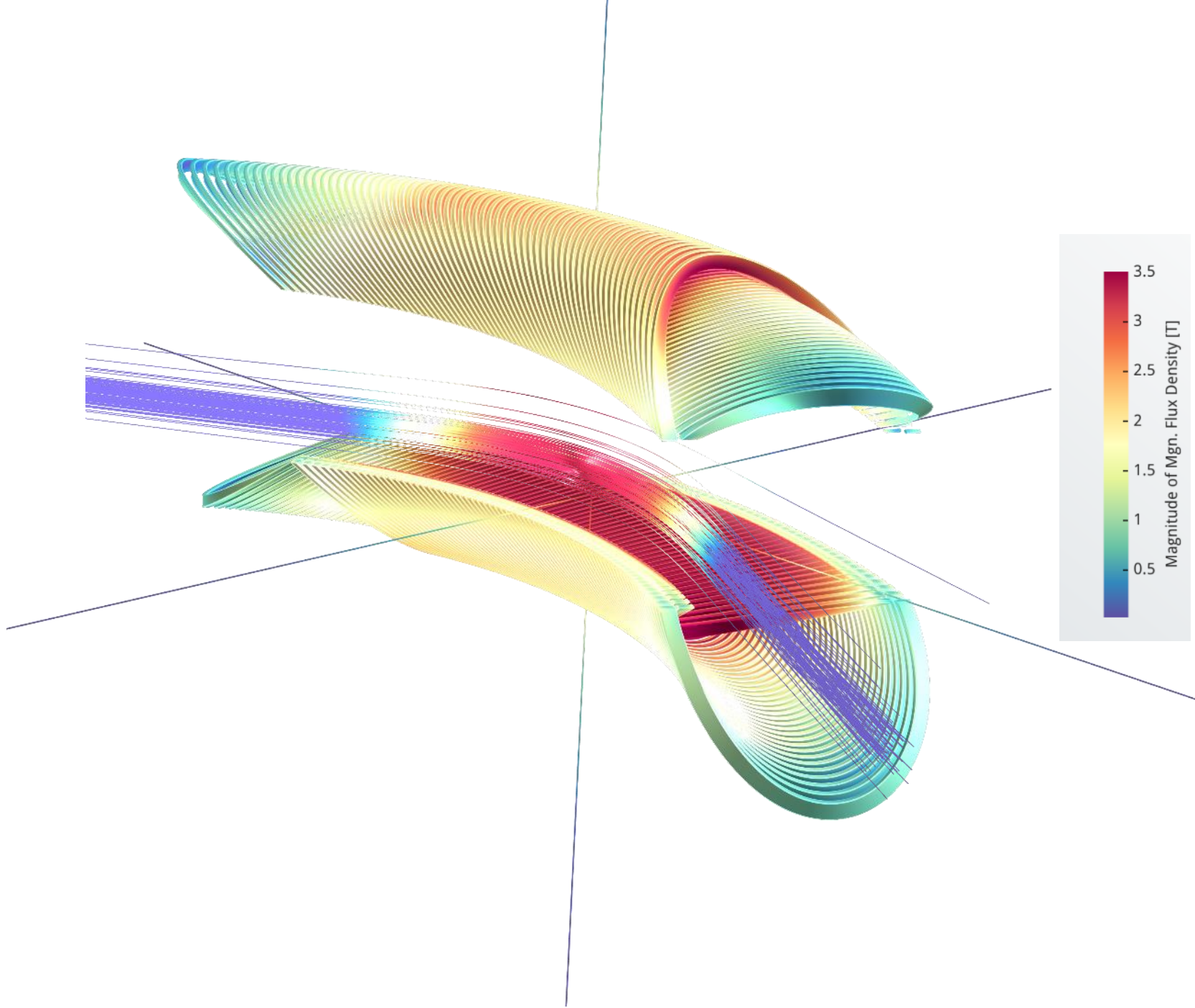


I. Winding

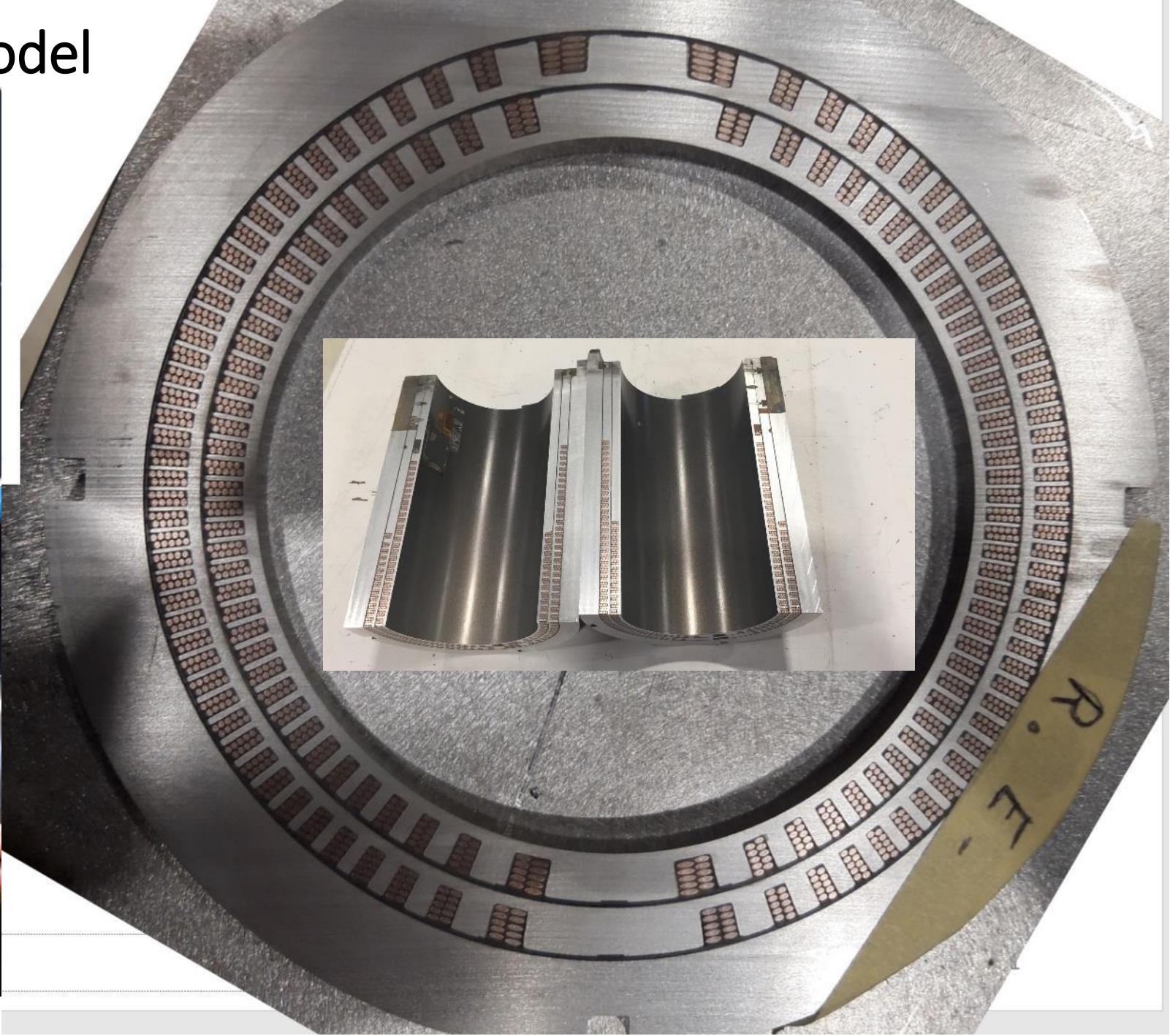
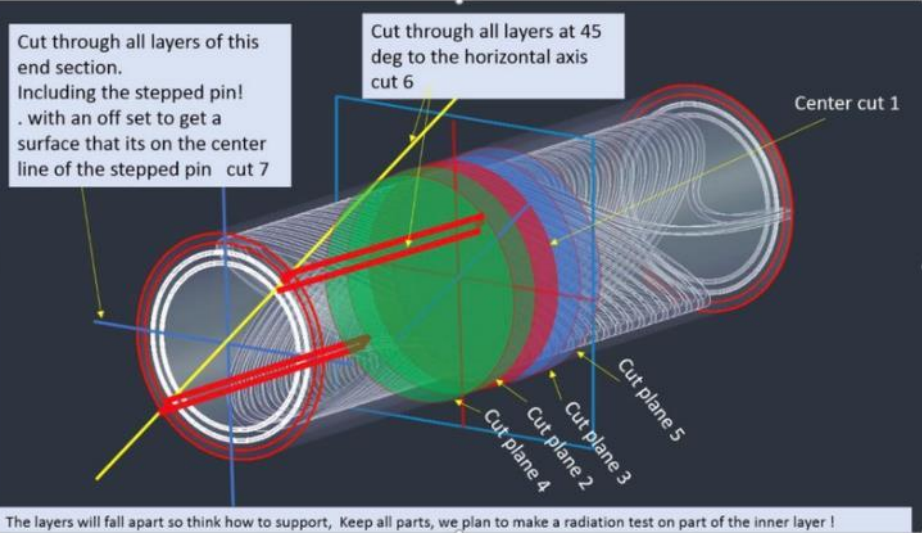
Winding- :

- Winding OUTER layer



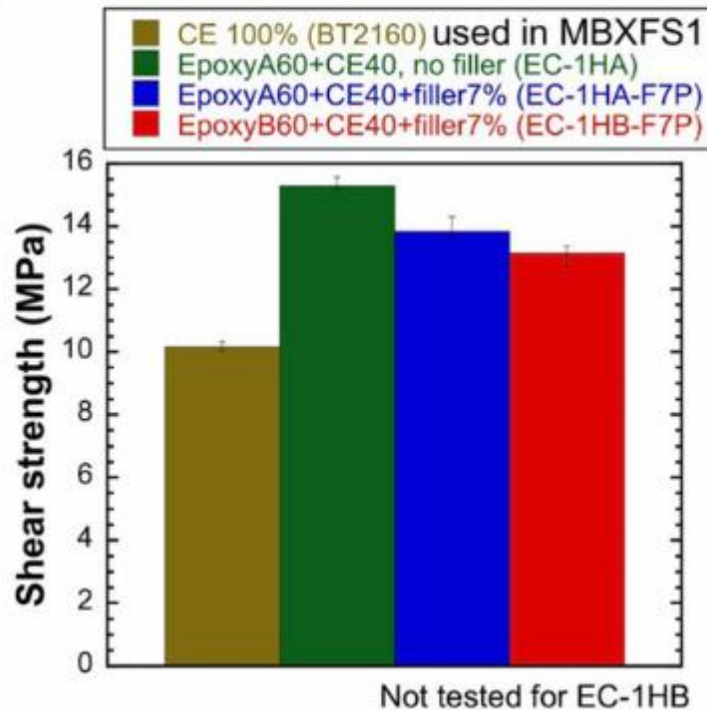


Looking inside the 0.5m model

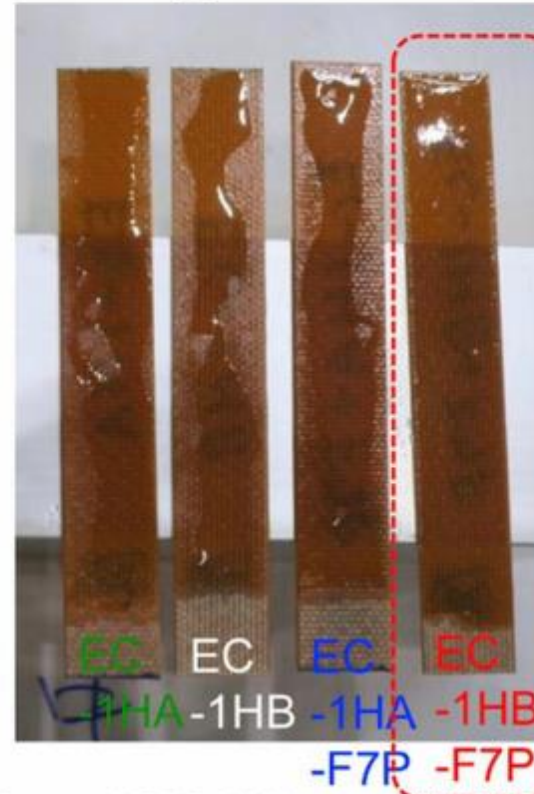


Wet-winding with epoxy-blended CE resin (A countermeasure against coil end deformation)

Shear strength

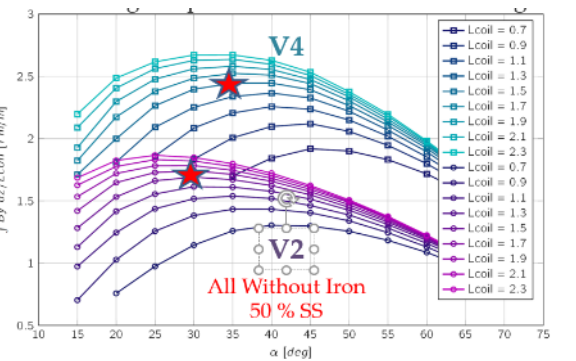
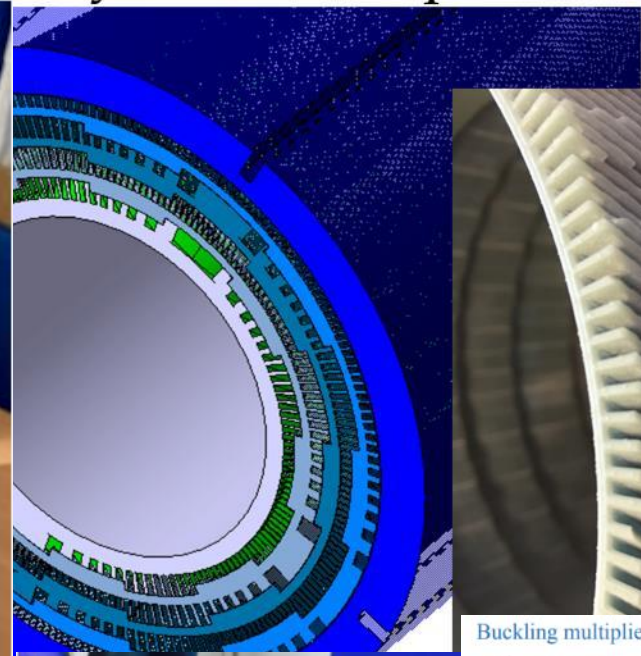
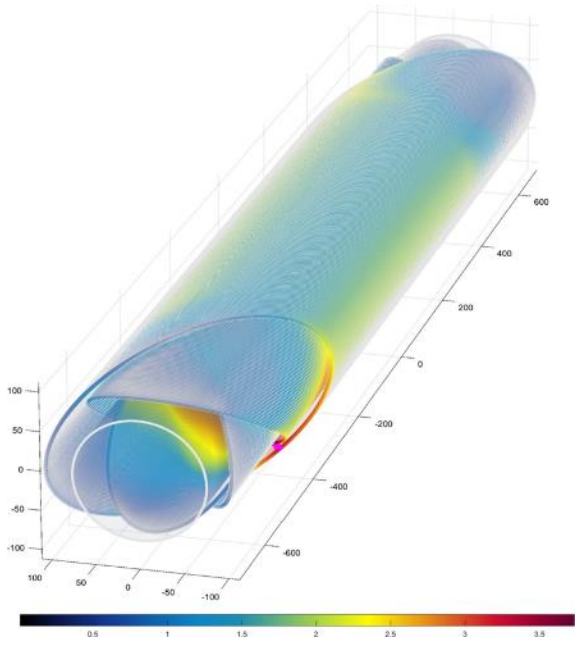


Painting test



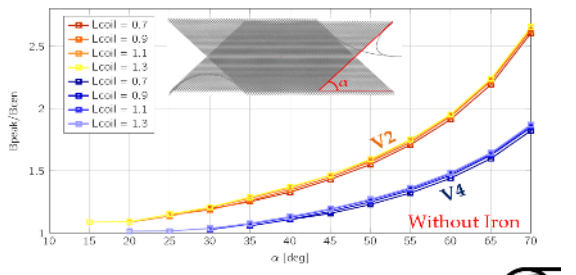
- Four kinds of epoxy-blended CE resins provided from ARISAWA were tested
 - Epoxy : CE = 60 : 40 for all resins
 - Viscosity: lower in epoxy A, higher in epoxy B
 - W or W/O filler (to control viscosity)
- **EC-1HB-F7P (Epoxy B + CE + 7wt% Silica filler)** was selected from acceptable bonding strength with highest viscosity

Nested CCT and Rad hard spacers ,



Skew Angle Influence

Ratio B_{peak}/B_{cen} depends on skew angle and # of layers

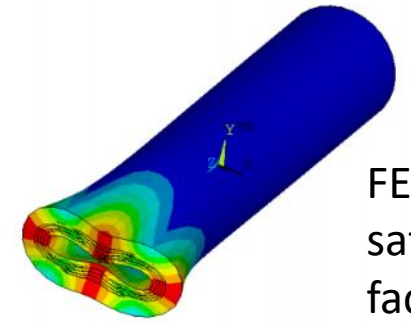


Buckling multipliers

SET	TIME/FREQ	LOAD STEP	SUBSTEP	CUMULATIVE
1	1.5556	1	1	1
2	1.7894	1	2	2
3	1.9806	1	3	3

1st buckling multiplier 1.55, so the structure is safe

1st buckling mode shape

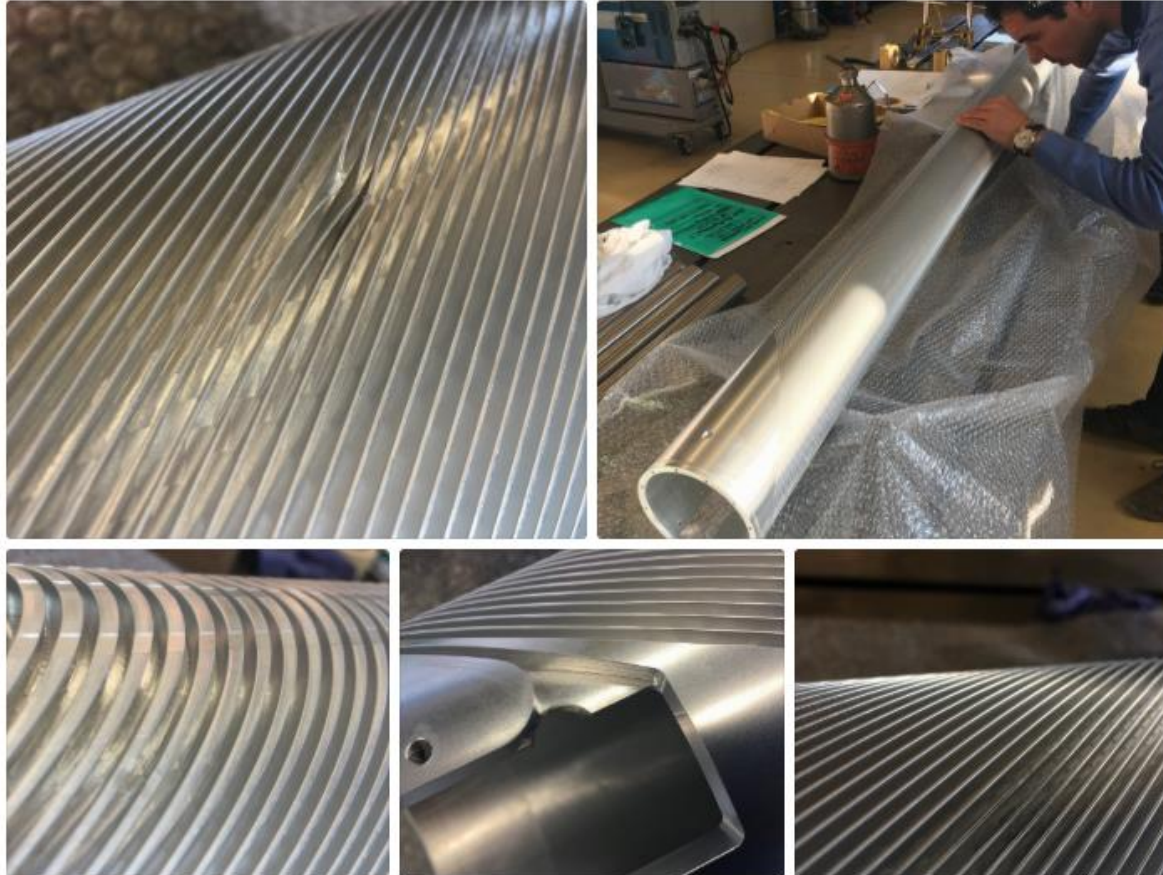


FEA safety factor 1.55



You added an **update**

Mar 22, 2018 ▾



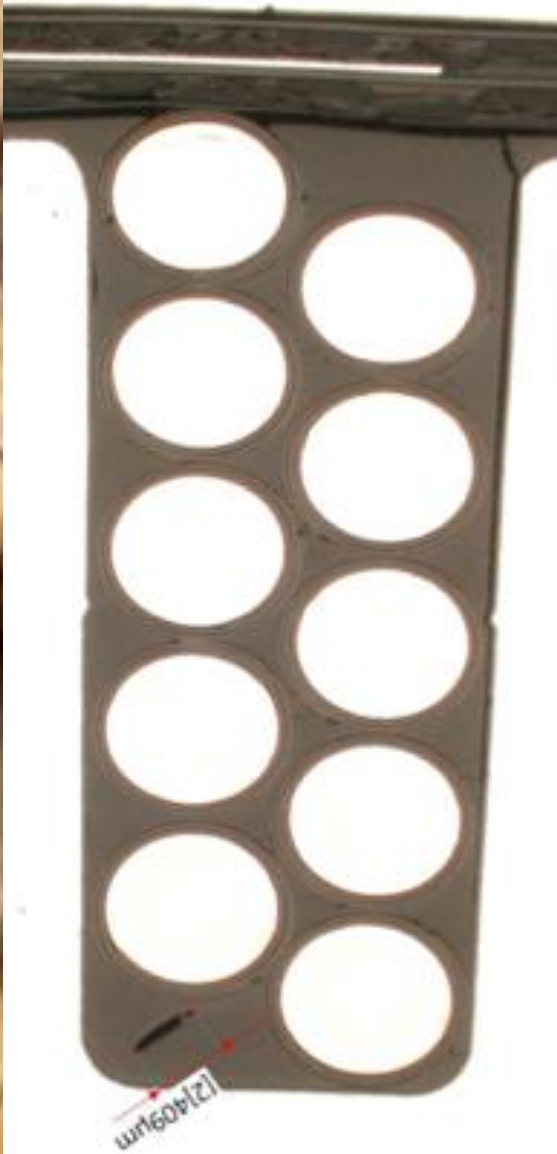
Damaged Former : (. and it's repair ! : j

One of the inner 2.2 m cct formers was damaged during mounting into the hard Anodization tank. A second problem was encountered when too high current melted the connection point.

We repaired the damaged channel section, thanks to the main cern machine shop team.

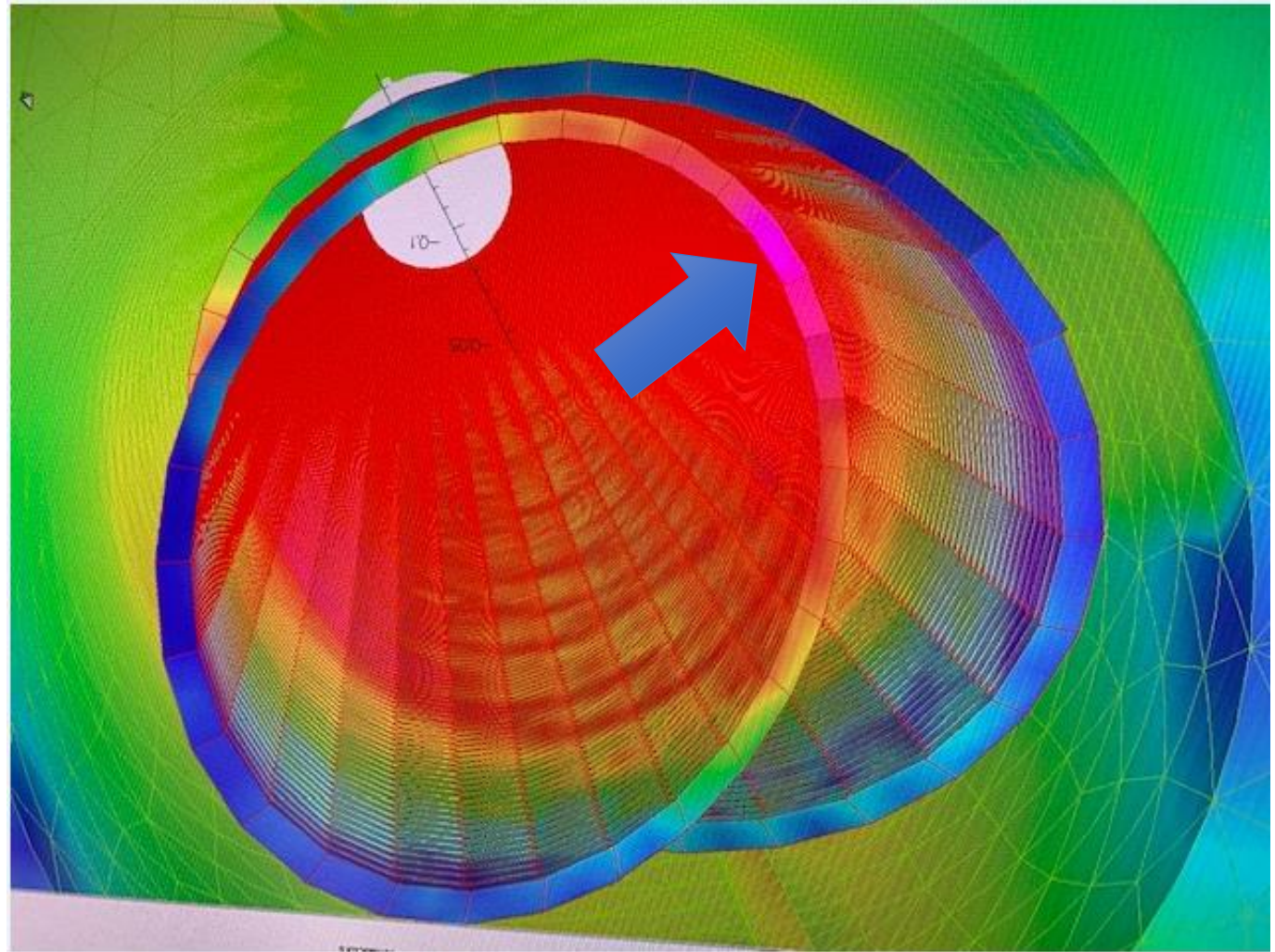
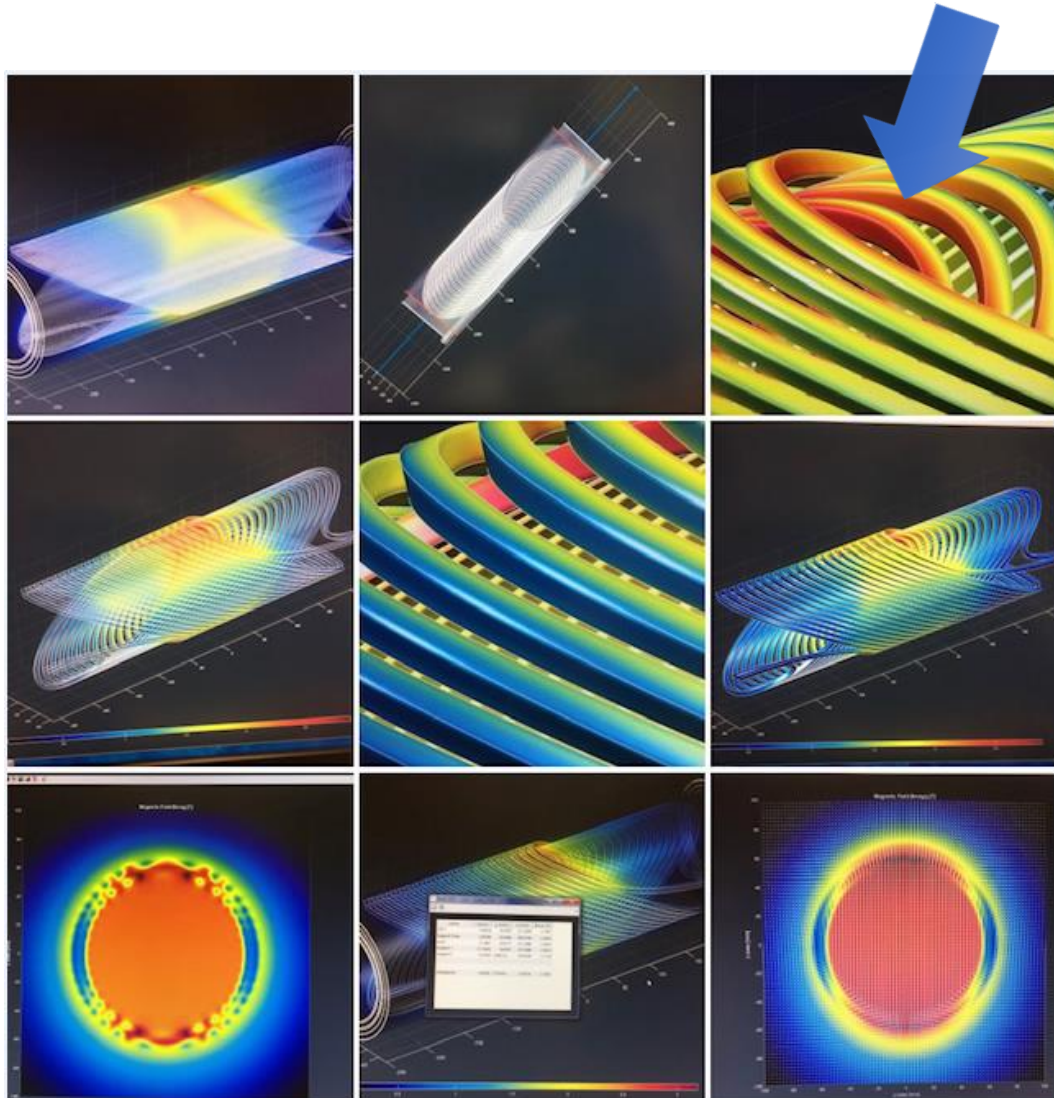
Look for the picture on the initial repair.

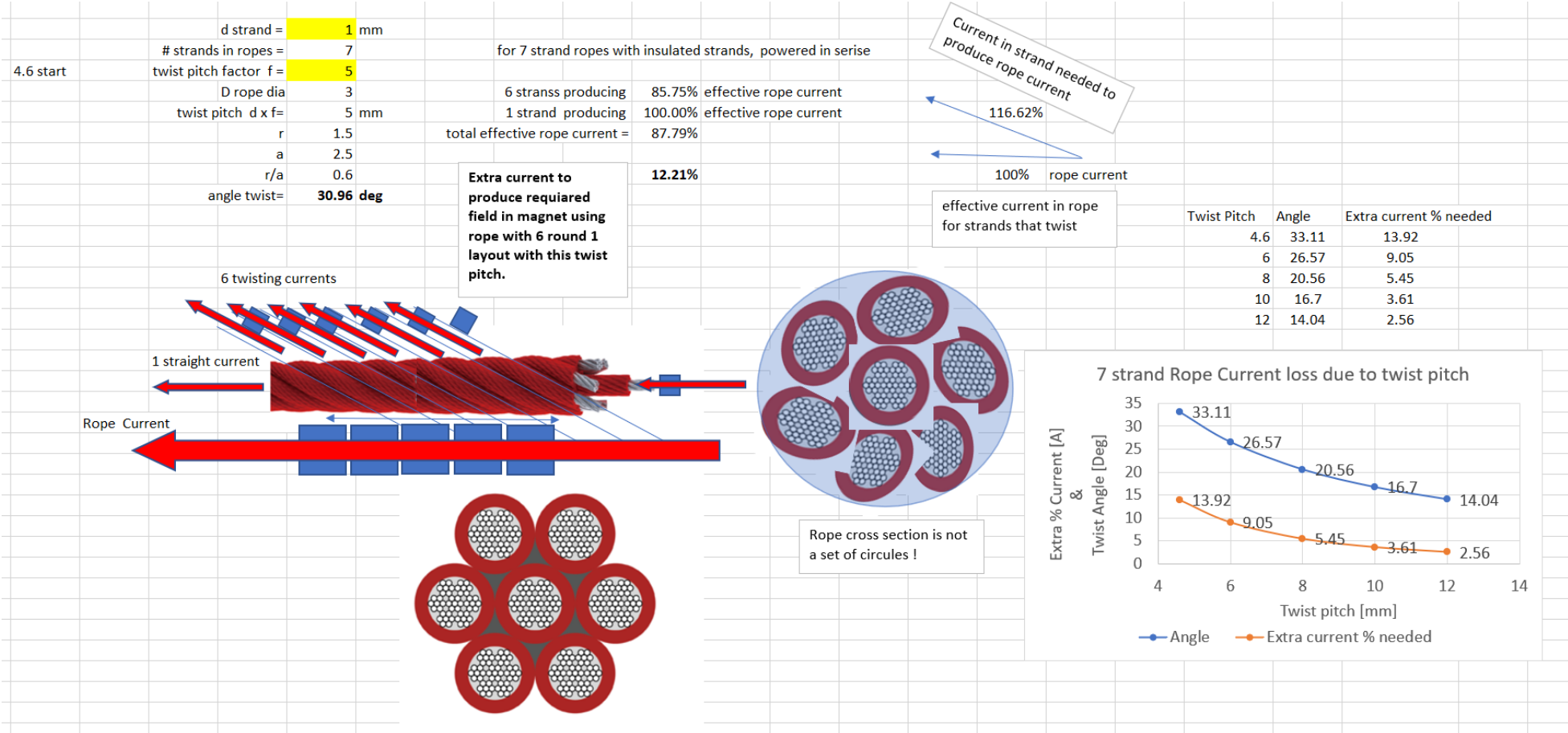
Stable Stacking



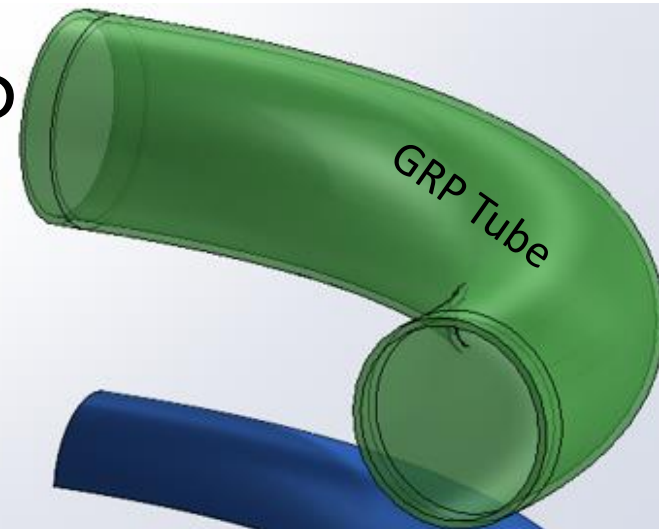
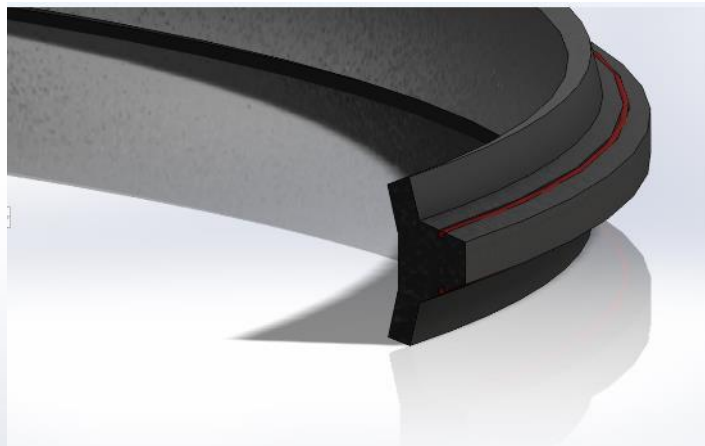
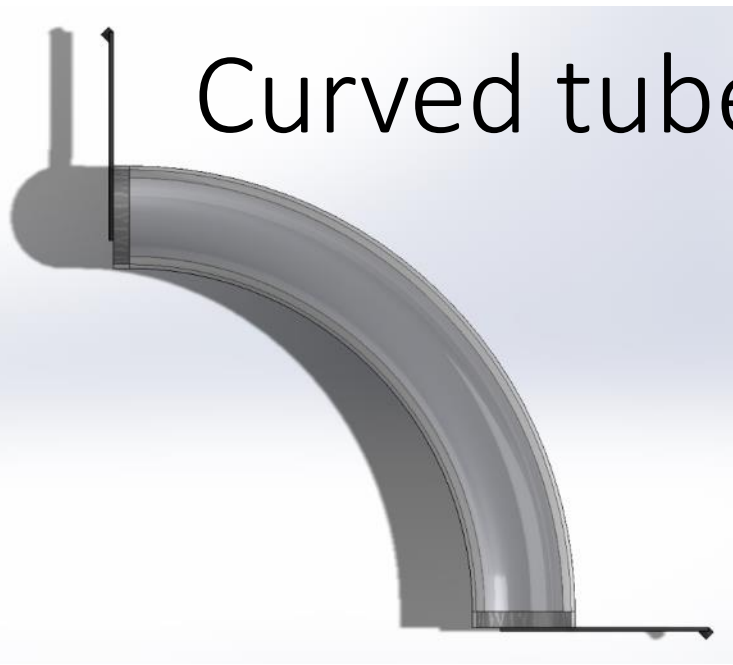
We should consider designing the coil to have an inherently stable stacks!

MCBRD CCT 2-layer Max Field is between layers at the ends





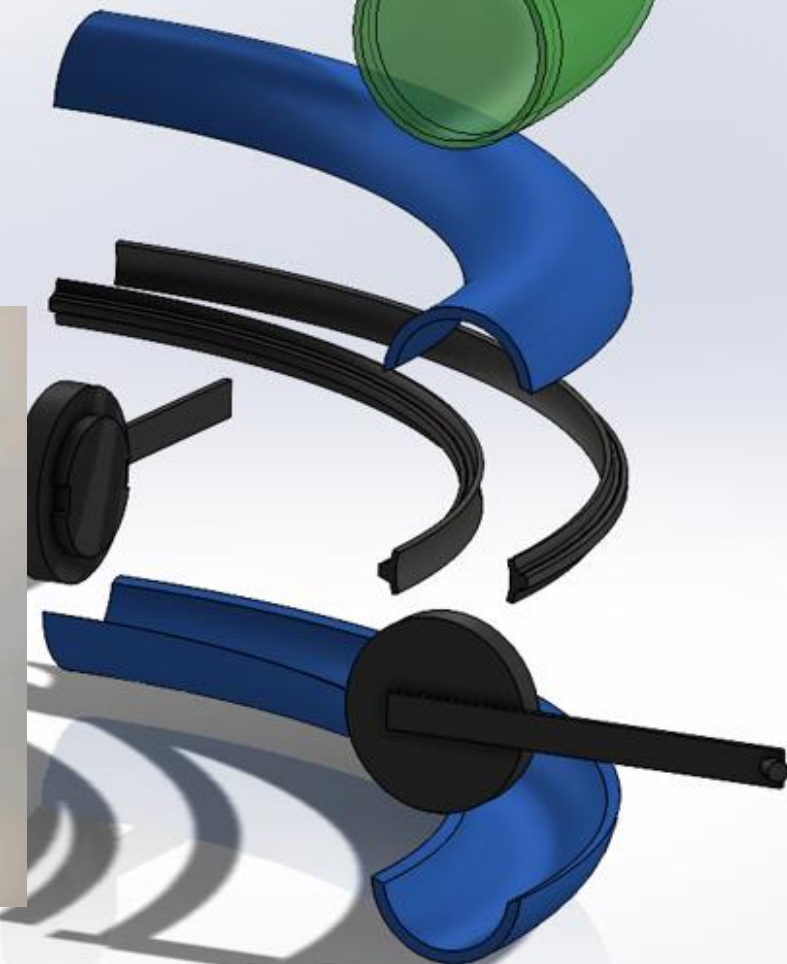
Curved tube manufacture in GRP



We can make curved GRP tubes on a reusable mandrel!

This produces an accurate inner tube surface!!

The magnet cost can be reduced significantly < \$\$\$
For subsequent magnets!



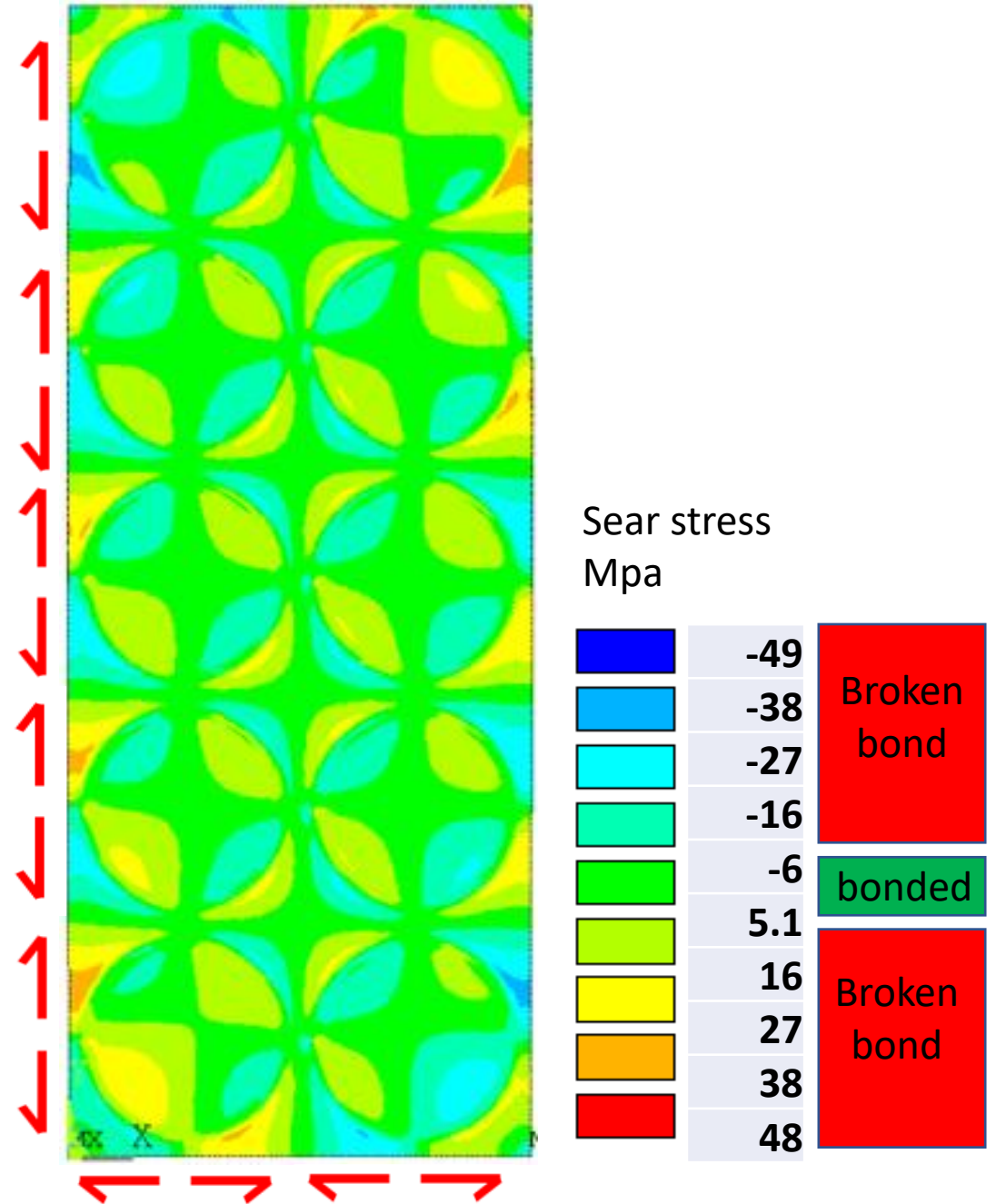
Shear Stress at 4 K

No magnetic stress yet

The bonds break, at the surfaces of the insulated wire and at the channel walls with ~ 5 MPa in shear

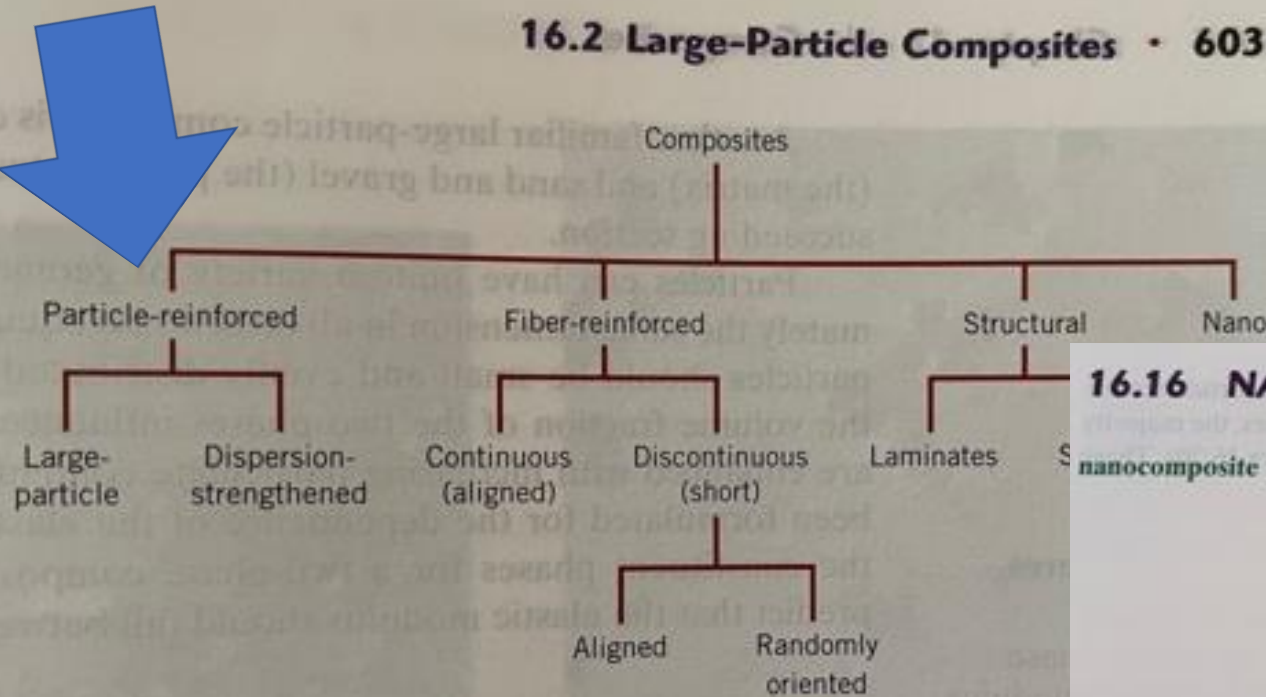
At 4 K with the CTD101K we see 20 to 30 MPa

Then we expect the bonds to start to be broken. In some places and not in others.



Composites family

16.2 Large-Particle Composites • 603



Development ideas

16.16 NANOCOMPOSITES

The materials world is experiencing a revolution with the development of a new class of composite materials—the **nanocomposites**. Nanocomposites are composed of nanosized particles (or *nanoparticles*)⁵ that are embedded in a matrix material. They can be designed to have mechanical, electrical, magnetic, optical, thermal, biological, and transport properties that are superior to conventional filler materials; these properties can be tailored for use in specific applications. For these reasons, nanocomposites are becoming infused in a number of modern technologies.⁶

An interesting and novel phenomenon accompanies the decrease in size of a nanoparticle—its physical and chemical properties experience dramatic changes; furthermore, the degree of change depends on particle size (i.e., number of atoms). For example, the permanent magnetic behavior of some materials [e.g., iron, cobalt, and iron oxide (Fe_3O_4)] disappears for particles having diameters smaller than about 50 nm.

Two factors account for these size-induced properties of nanoparticles: (1) increase in ratio of particle surface area to volume; and (2) particle size. As Section 16.1 notes, surface atoms behave differently than atoms located in the interior of a material. Consequently, as the size of a particle decreases, the relative ratio of surface atoms to bulk atoms increases; this means that surface phenomena begin to dominate. In extremely small particles, quantum effects begin to appear.

“

The roots of education are bitter, but the fruit is sweet.

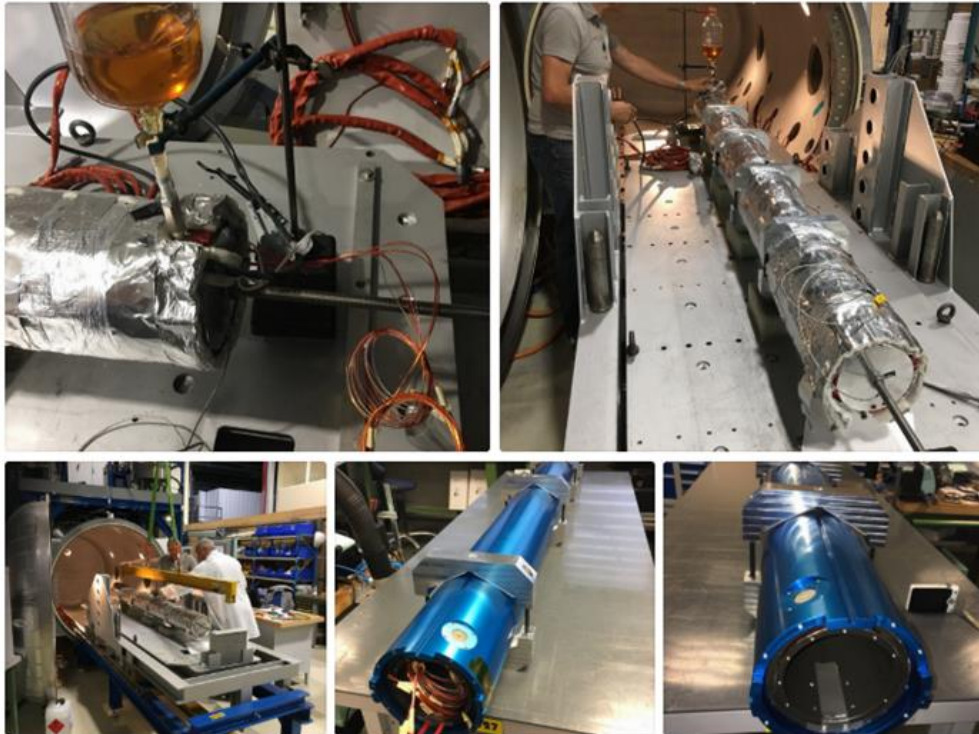


Aristotle

Impregnation 2 to 5 bar over pressure

You added an update

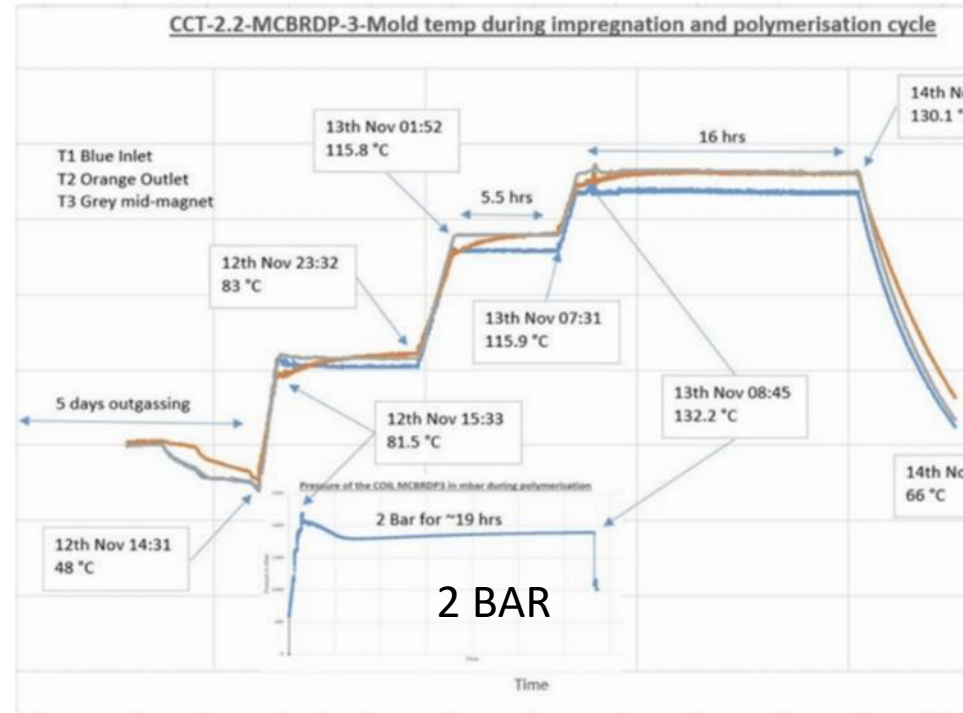
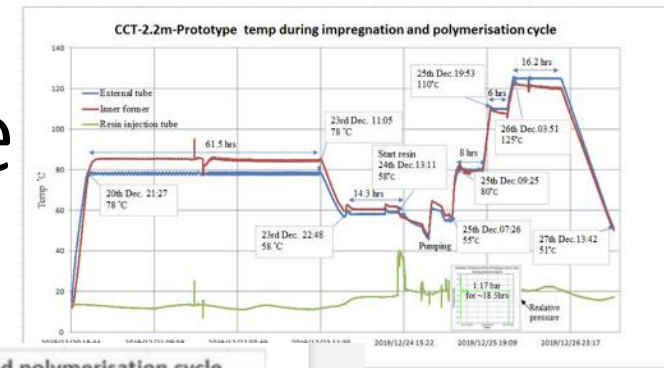
Jun 18, 2018



Impregnation of first long aperture & 2nd waiting

The resin filled the coil in 1hr 5 mins. A press of 2 bar was applied without any leak. 4 kg in total of resin was in the system. With about 3.5 kg in the magnet. We will increase the volume for the next aperture.

The 0.5 m model filled in 55mins.



CCT 3 Impregnation: Temperature and Pressure Plot.

The attached plot gives the overview of the temperature and pressure profile during impregnation.

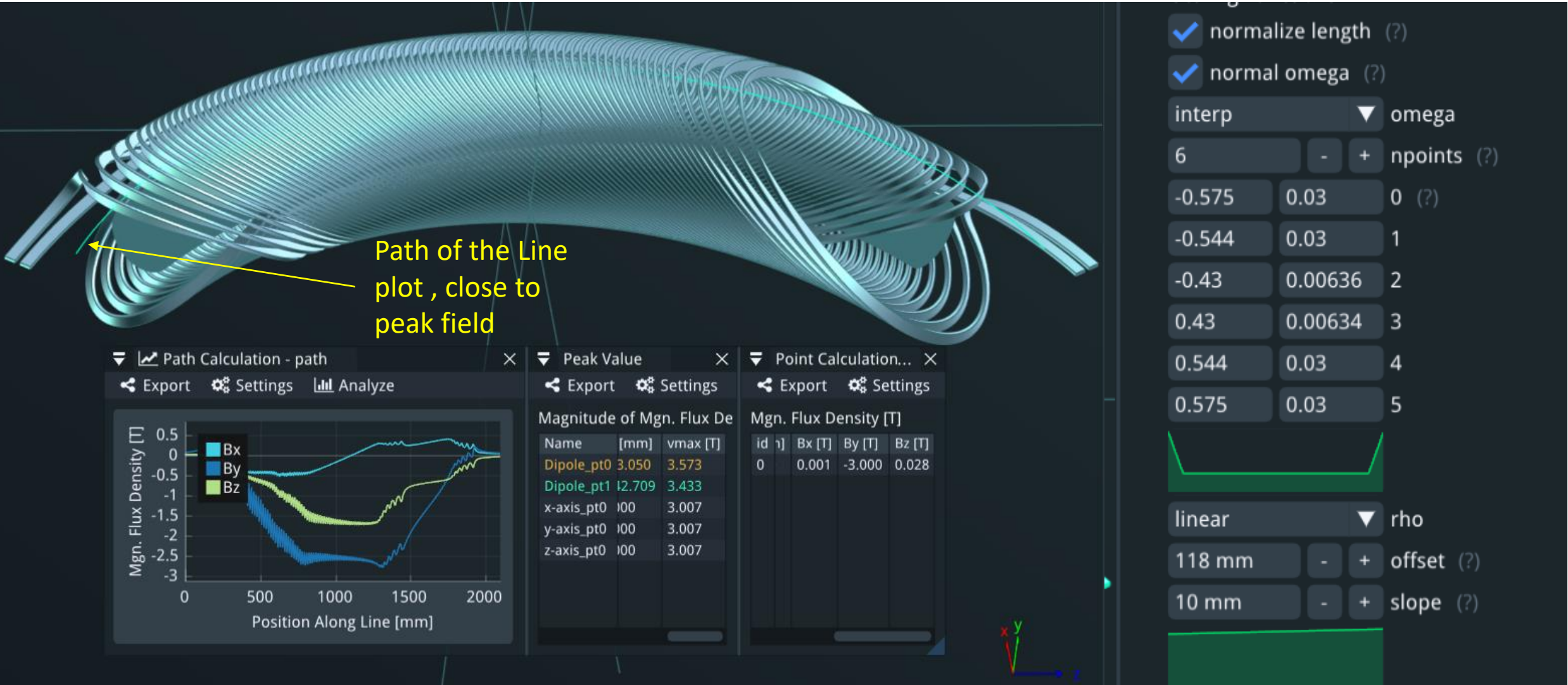
Cutting tool 5 deep to 1 wide ratio of channel

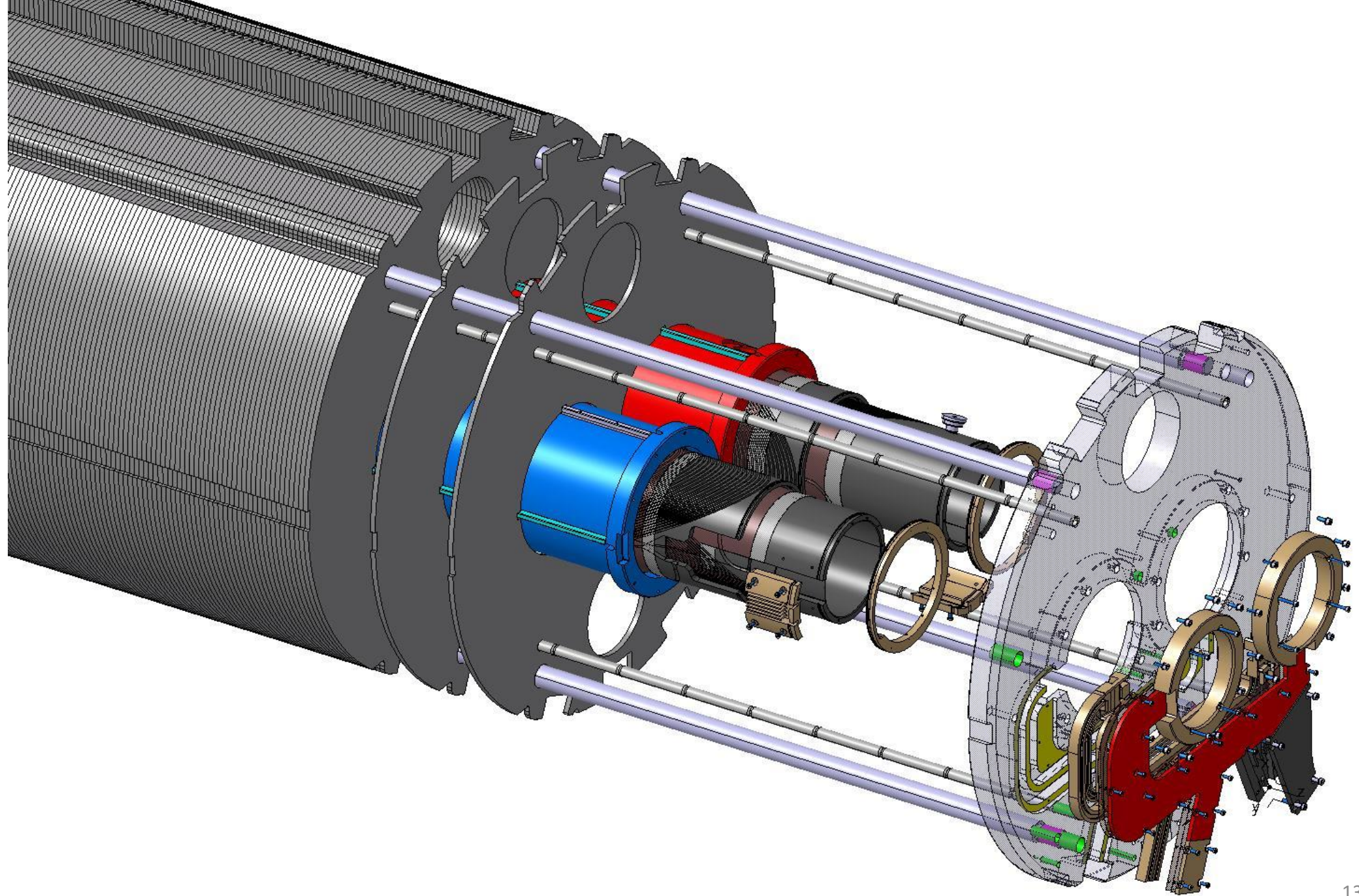


Min wall 0.3mm with 2mm wide channel



Peak field reduction at end in coil!!! *The important one!*
 By pitch increase in last few end turns ,





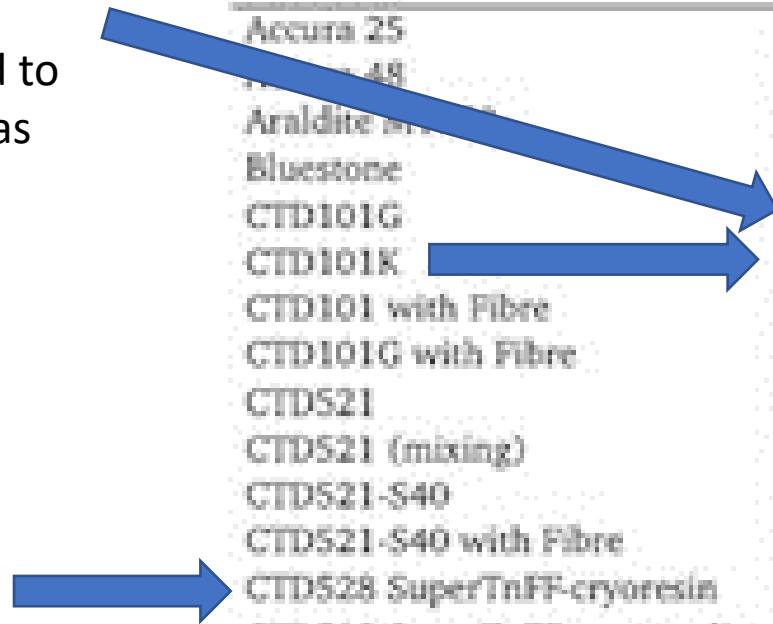
Some interesting resin data

TABLE II
FITTING COEFFICIENTS FOR EPOXIES

$$\frac{L - L_{293}}{L_{293}} = a + bT + cT^2 + dT^3 + eT^4 + fT^5$$

Substance	a	b	c	d	e	f
Accura 25	-12.70	4.43e-03	1.55e-04	-4.31e-07	2.35e-09	-3.89e-12
Accura 48	-11.30	7.07e-04	2.18e-04	-7.82e-07	2.63e-09	-3.41e-12
Araldite 502	-12.00	4.05e-04	2.37e-04	-8.51e-07	2.86e-09	-3.76e-12
Bluestone	-5.97	1.98e-03	1.11e-04	-5.42e-07	2.13e-09	-2.90e-12
CTD101G	-5.35	1.84e-03	7.26e-05	-7.17e-08	1.84e-10	-4.53e-13
CTD101K	-12.10	4.27e-03	1.90e-04	-2.90e-07	3.69e-10	-4.27e-13
CTD101 with Fibre	-1.94	1.49e-03	4.34e-05	-2.57e-07	9.26e-10	-1.19e-12
CTD101G with Fibre	-2.10	1.14e-03	4.21e-05	-2.11e-07	7.11e-10	-8.21e-13
CTD521	-11.60	2.25e-03	2.23e-04	-8.55e-07	2.91e-09	-3.76e-12
CTD521 (mixing)	-2.06	9.71e-04	4.12e-05	-7.20e-08	-7.52e-11	2.79e-13
CTD521-S40	-8.51	3.82e-03	1.48e-04	-6.33e-07	2.41e-09	-3.33e-12
CTD521-S40 with Fibre	-2.11	8.07e-04	4.34e-05	-1.40e-07	3.39e-10	-3.84e-13
CTD528 SuperTnFF-cryoresin	-2.42	1.09e-03	5.46e-05	-1.50e-07	1.65e-10	-7.53e-15
CTD528 SuperTnFF-cryo-applic	-11.90	1.03e-03	2.18e-04	-7.43e-07	2.58e-09	-3.44e-12
CTD-DP 5.1	-15.30	4.66e-03	2.55e-04	-1.67e-06	7.87e-09	-1.11e-11
CTD-DP 5.1 with Fibre	-1.78	4.61e-04	4.06e-05	3.56e-08	-6.99e-10	1.12e-12

CTD101G
But would need to
be wet wound as
Bama did !



CTD101K, 12.0 mm/m

3.8 CTD101K

description: Anhydride cured epoxy. Radiation resistant. Made by Composite Technology Development.

weblink: www.ctd-materials.com

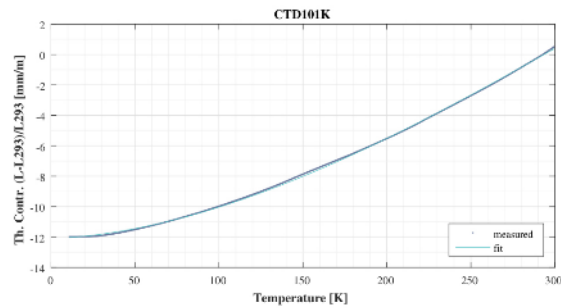
Thermal Contraction at 10K (mm/m)
-12.04

Start Temp (K)	End Temp (K)
10.9	299.5

$$\frac{L - L_{293}}{L_{293}} = a + bT + cT^2 + dT^3 + eT^4 + fT^5$$

Coeff	Value
a	-1.21e+01
b	4.27e-03
c	1.90e-04
d	-2.90e-07
e	3.69e-10
f	-4.27e-13

R Squared 0.999976



CTD101G 5.3 mm/m

3.7 CTD101G

description: Alumina filled, anhydride cured epoxy. Radiation resistant. Made by Composite Technology Development.

weblink: www.ctd-materials.com

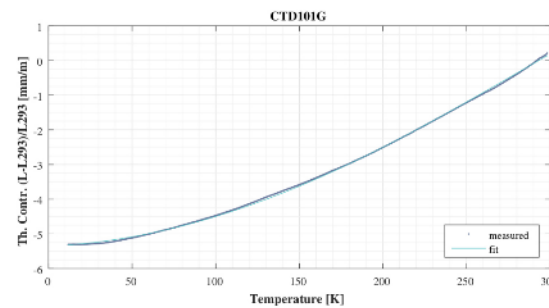
Thermal Contraction at 10K (mm/m)
-5.32

Start Temp (K)	End Temp (K)
11.7	298.2

$$\frac{L - L_{293}}{L_{293}} = a + bT + cT^2 + dT^3 + eT^4 + fT^5$$

Coeff	Value
a	-5.35e+00
b	1.84e-03
c	7.26e-05
d	-7.17e-08
e	1.84e-10
f	-4.53e-13

R Squared 0.999970



CTD528 Super 2.4 mm/m

3.15 CTD528 SuperTnFF-cryoresin

description: Epoxy made by Composite Technology Development for cryogenic uses.

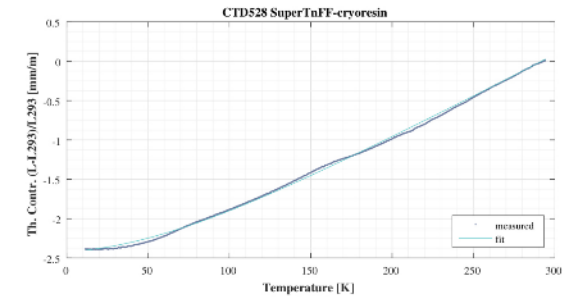
Thermal Contraction at 10K (mm/m)
-2.40

Start Temp (K)	End Temp (K)
11.5	294.1

$$\frac{L - L_{293}}{L_{293}} = a + bT + cT^2 + dT^3 + eT^4 + fT^5$$

Coeff	Value
a	-2.42e+00
b	1.09e-03
c	5.46e-05
d	-1.50e-07
e	1.65e-10
f	-7.53e-15

R Squared 0.999933



CERN 3m long ~ 0.5 m dia turning CNC milling m/c

m/c spec **7 um** over 3 m and achieves **~ 10 um** for our flexible tube! Very nice.

Target value under 50 um

lateral shift [mm] S	0.0686	0.085	0.0988	0.0824	0.0252
r [mm]	68.15	68.15	68.15	68.15	68.15
Angle in [mRad]	1.006603	1.247249	1.449743	1.209098	0.369773

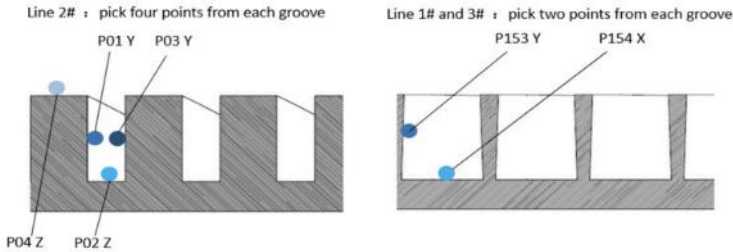
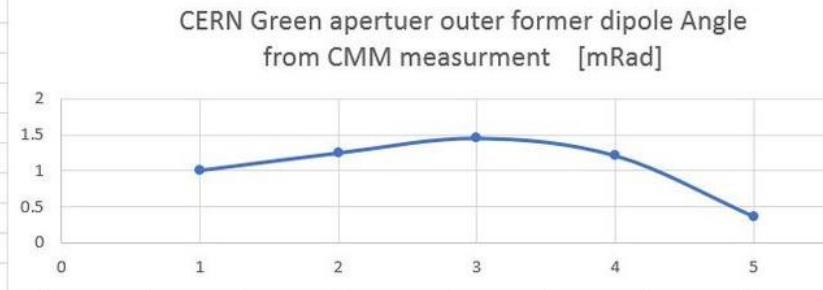
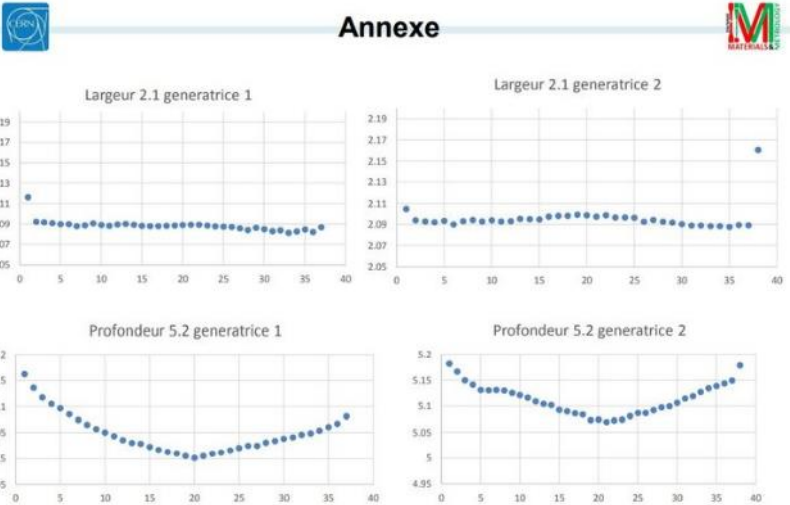


Fig3. Measuring Points of each Groove



Shipping from china to CERN 8 weeks

10th oct



21st Oct CERN

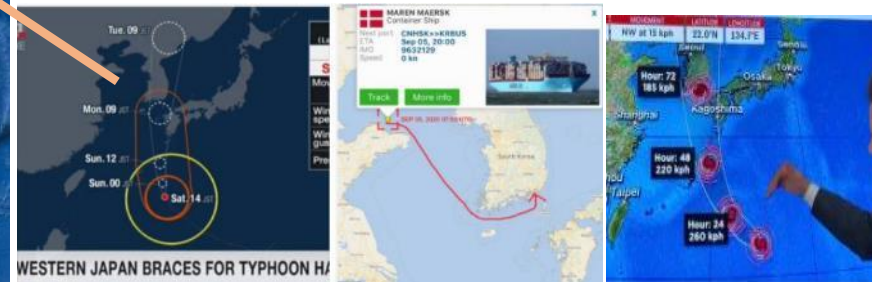
Suez 2nd Oct



16th Sep Hong Kong



IMP Lanzhou to Port of Tianjin ~ 1573 km by road



WESTERN JAPAN BRACES FOR TYPHOON H...



26th Sep

Our magnet is approaching a dangers area Last attack was in May 2020 this year



Measured Errors

Apertures without yoke



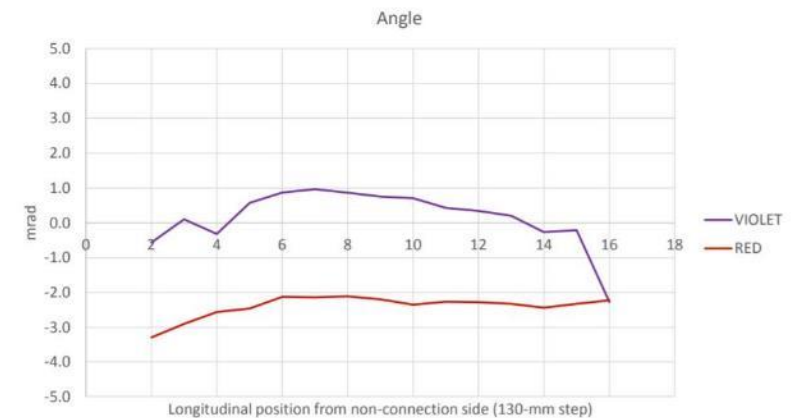
Multipoles within 2 units

Rref = 35 mm

Magnetic angle with respect to key slots



MCBRDP2 with yoke at room temperature



Angles within ± 3 mrad

Field errors in aperture ~ 2 units only !
 Field angle ± 3 mrad that's 0.05 mm tolerance in position of wires in m/c formers.

Transfer Function < 5 units

1st winding test with the rectangular wire

!!!!failed!!!!



The enamel rectangular wire rotated as we tried to wind and finally was impossible to wind into the slot!

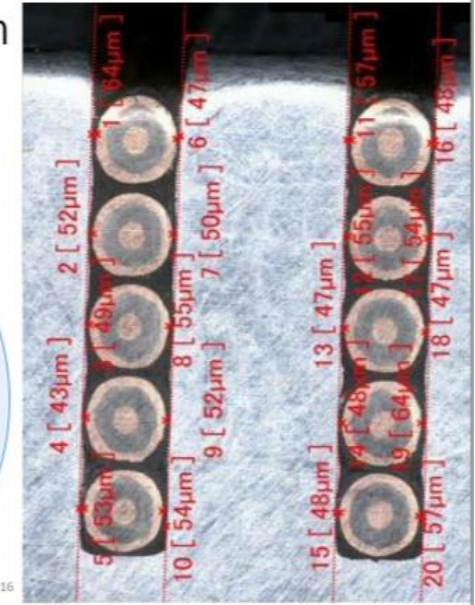


1mm x 5mm slot with 0.05mm glass impregnated insulation

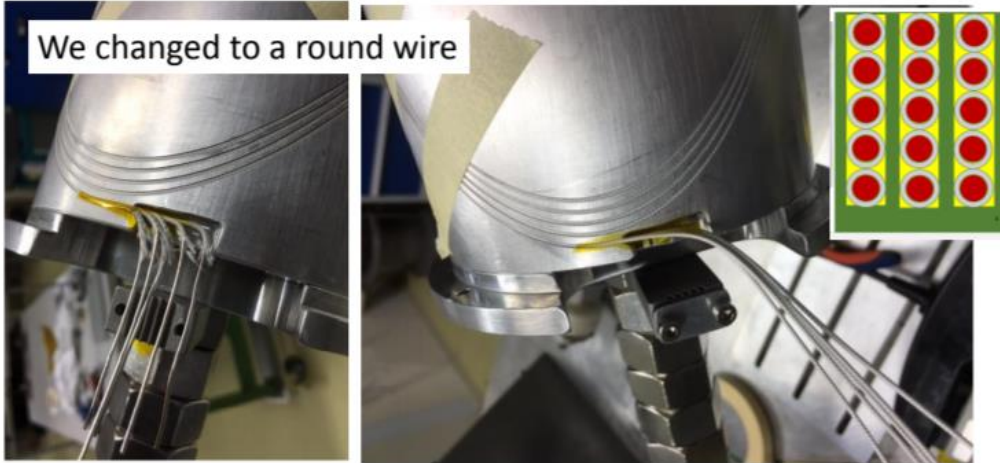


<https://edms.cern.ch/document/1760644/1/approvalAndComments>

Glyn A. Kirby CCT update Dec 2016



We changed to a round wire



Version 1, 1mm x 5mm deep winding test.
Tight to get glass insulated wire into slot without damaging the insulation but was achieved!
Former has some sharp edges. That will need removing on next models.

Glyn A. Kirby CCT

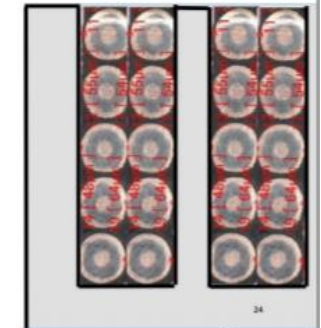
24

Version 2, Changing from 1x5 wires to 2x5 wires

- 1) Reduces machining time.
- 2) Increases machine tool size!
- 3) Increases number of joints

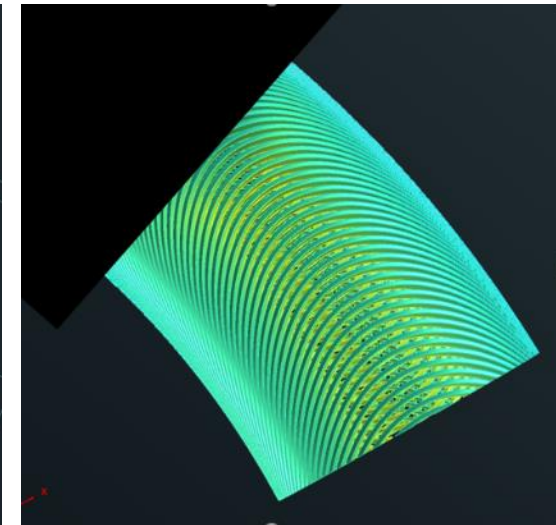
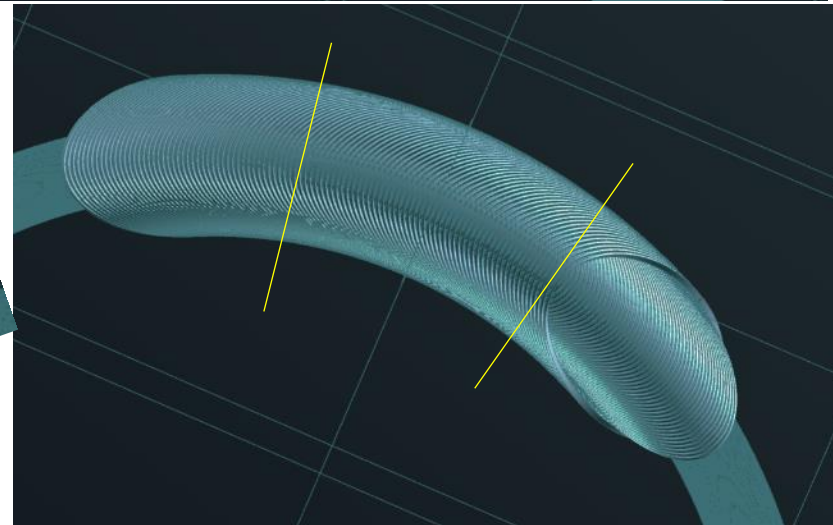
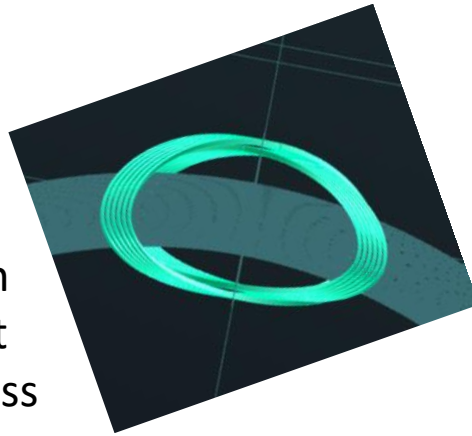
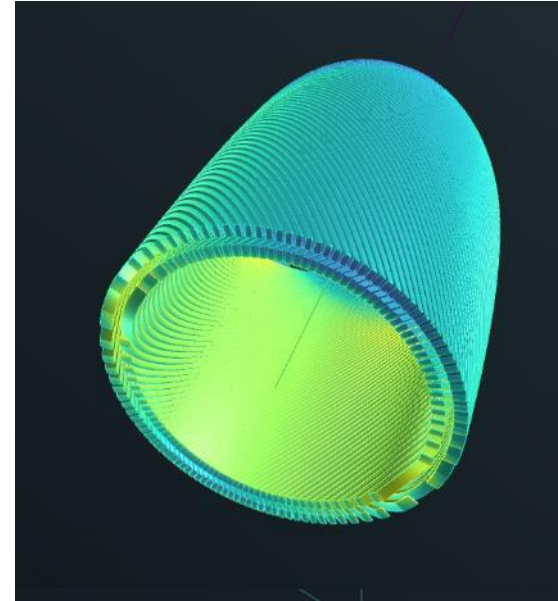
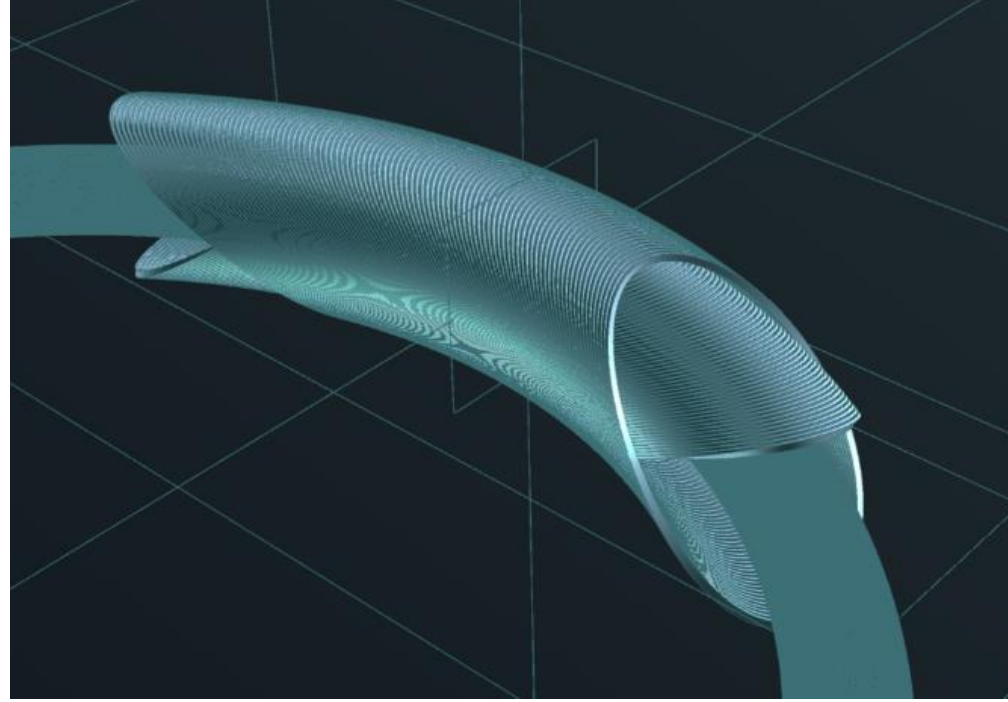
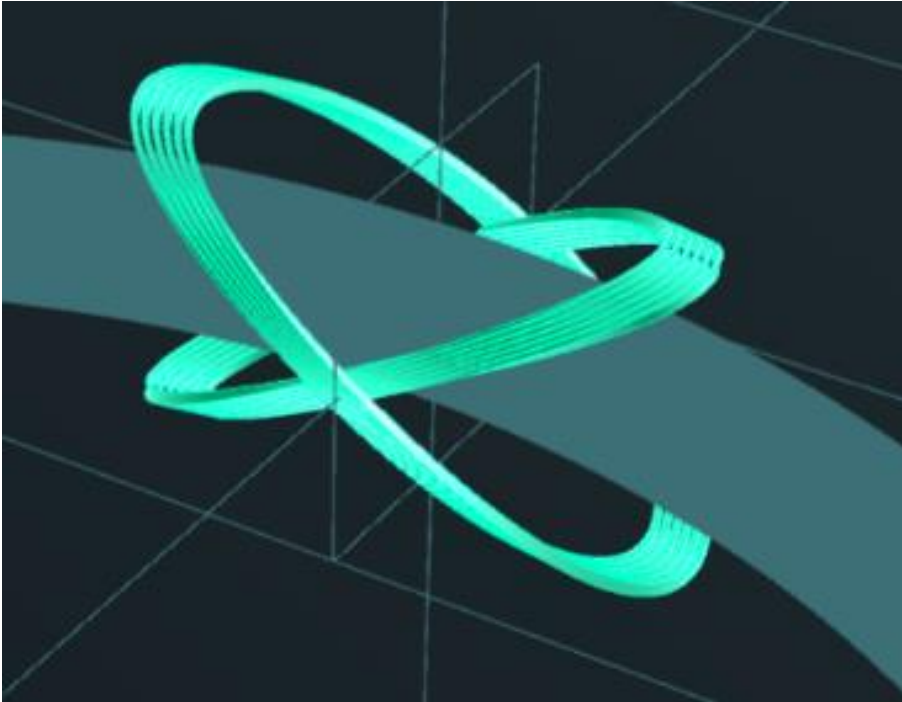


Glyn A. Kirby CCT update Dec 2016



25

Machining model



Two or three turns in a coil can be used to test the full magnet design to its full operating stress and conductor limits!